2005

Clinical Pharmacology of MS-275, A Histone Deacetylase Inhibitor

Milin R. Acharya
Virginia Commonwealth University

CLINICAL PHARMACOLOGY OF MS-275, A HISTONE DEACETYLASE INHIBITOR

A dissertation submitted in partial fulfillment of the requirements for the degree of Doctor of Philosophy at the Virginia Commonwealth University.

by

Milin R. Acharya, M.A. (Biochemistry), University of Scranton, Scranton, PA

Directors:

Jürgen Venitz, M.D., Ph.D., Associate Professor, Department of Pharmaceutics, Virginia Commonwealth University, Richmond, VA

&

William D. Figg, Pharm.D., MBA, Head, Clinical Pharmacology Research Core & Molecular Pharmacology Section, National Cancer Institute, National Institutes of Health, Bethesda, MD

Acknowledgment

I would like to acknowledge the contribution of the following individuals and organizations for their help and support in completion of this dissertation project:

Jurgen Venitz, my research co-advisor, who guided me during my stay at Virginia Commonwealth University and also through my research experience. His knowledgeable advice and continued support is highly appreciated.

William D. Figg, my research co-advisor, who provided me with a wonderful opportunity in allowing me to complete my dissertation work at the National Cancer Institute. The exposure to translational research at NCI will always be appreciated.

Alex Sparreboom, my immediate supervisor and a member of my dissertation committee, whose involvement and directions during this project were critical. His enthusiastic guidance, strong commitment to resolve scientific issues and an ever-inviting pleasant personality immensely helped during some trying times. His friendship and trust that was gained during scientific and non-scientific interactions will always be remembered and cherished.

Members of my dissertation committee, Dr. Patricia Slattum and Dr. John Roberts, for providing their valuable time in critically reviewing my research work.

I would also like to extend my gratitude towards all colleagues, fellow physicians, nurses, data managers and clinical support staff, and most importantly the cancer patients who volunteered to enroll in the clinical trials.

I would specially thank my colleagues at Virginia Commonwealth University and at National Cancer Institute for their friendship and support over these years.

Finally, I would like to express my continuing goodwill to all the friends, philosophers and guides, near or far, remembered or forgotten, for all the knowledge they imparted and for all the difference it makes in my life.

Table of Contents

List of Tables

Chapter 6

List of Figures

Abstract

CLINICAL PHARMACOLOGY OF MS-275, A HISTONE DEACETYLASE INHIBITOR

By Milin R. Acharya, M.A., Ph.D.

A dissertation submitted in partial fulfillment of the requirements for the degree of Doctor of Philosophy at Virginia Commonwealth University.

Virginia Commonwealth University, 2005

Directors: Jürgen Venitz, M.D., Ph.D., Associate Professor, Department of Pharmaceutics, Virginia Commonwealth University, Richmond, VA and William D. Figg, Pharm.D., MBA, Head, Clinical Pharmacology Research Core & Molecular Pharmacology Section, National Cancer Institute, National Institutes of Health, Bethesda, MD

The goal of this escalating single-dose phase I research study was to determine the safety, tolerability, pharmacokinetics, pharmacodynamics as well as *in vitro* metabolism and plasma protein binding of MS-275, a novel histone deacetylase inhibitor, in patients with solid tumors and lymphomas. A validated LC/MS assay was developed to quantitate MS-275 in plasma, human liver microsomes and urine. The pharmacokinetic (PK) evaluation was done using a non-compartmental approach. *In-vitro* plasma protein binding profile of MS-275 was characterized by a validated micro-equilibrium dialysis method. *In vitro* phase I and phase II hepatic metabolism of MS-275 were evaluated using human liver

microsomes. A correlative covariate analysis was performed in an effort to explain the wide inter-individual variability among patients.

Results from the study demonstrate that the validated LC-MS assay is specific, accurate, precise and sensitive. MS-275 demonstrates a substantial inter-individual PK variability in systemic exposure and clearance; exposures increase in near-proportion, while peak concentrations increase more than-proportionally with an increase in dose. Mean apparent oral clearance (CL/F) is independent of dose and exhibits apparent dose-independent PK behavior over the studied dose range. Oral absorption is highly variable. MS-275 has a 50-fold longer half-life in humans compared to pre-clinical species. PK/PD analysis showed significant correlation between occurrence of DLT and higher systemic exposures. Although there was an increase in the acetylation of histone H3 and H4 over time, preliminary analysis showed no significant correlation between PK parameters and change in % histone acetylation after 24 hours. MS-275 is moderately bound to plasma proteins. Hepatic phase I and II metabolic pathways are only minor routes of elimination, and MS-275 is neither a substrate for liver-specific organic anion transporting proteins, OATP1B1 and OATP1B3, nor a substrate for gastrointestinal efflux transporters ABCB1 (P-gp) or ABCG2. No significant correlation was found between CL/F and demographic, body measures and other clinical covariates, and inter-patient variability in CL/F remained similar in magnitude even after correcting dose for body surface area (BSA) or other body measures. BSA is not a significant predictor of MS-275 PK, and flat-fixed dosing can be used in the future.

CHAPTER 1

Introduction to Histone Deacetylase (HDAC) Inhibitors and MS-275

1.1 Background

In eukaryotic cells, DNA has been conserved throughout evolution in a condensed and densely packed higher order structure called chromatin. Chromatin, present in the interphase nucleus, comprises of regular repeating units of nucleosomes, which represent the principal protein-nucleic acid relationship. The major components of chromatin are nucleic acids (DNA and RNA) and associated proteins including histones, which are positively charged at neutral pH, and non-histone chromosomal proteins, which are acidic at neutral pH. Within the nucleus, chromatin can exists in two different forms; heterochromatin, which is highly compact and transcriptionally inactive form, or euchromatin, which is loosely packed and is accessible to RNA polymerases for involvement in transcriptional processes and gene expression. A nucleosome is a complex of 146 nucleotide base pairs of DNA wrapped around the core histone octamer that helps organize chromatin (Figure 1.1). The histone octamer is composed of two copies each of H2A, H2B, H3 and H4 proteins that are very basic mainly due to positively charged amino-terminal side chains rich in amino acid lysine. Post-translational and other changes in chromatin like acetylation/deacetylation at lysine residues, methylation at lysine or arginine residues, phosphorylation at serine resides,

ubiquitylation at lysines and/or ADP ribosylation are mediated by chemical modification of various sites on N-terminal tail (Figure 1.2).[1-3]

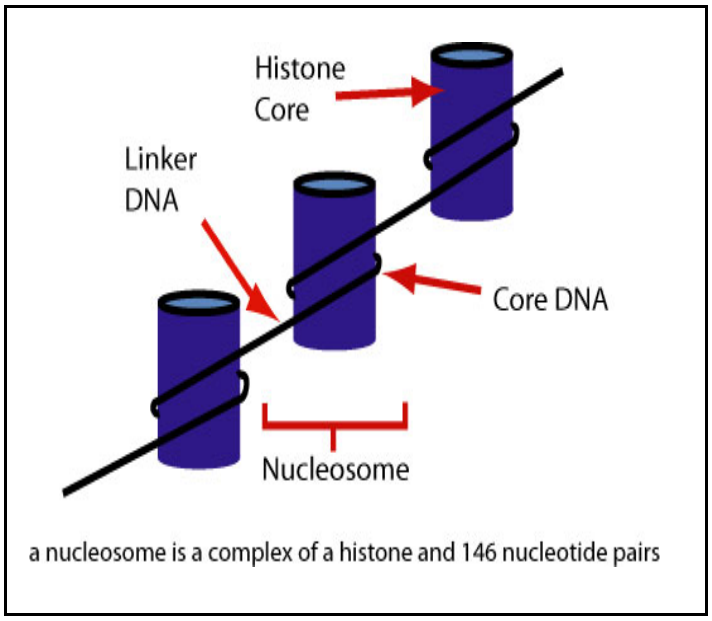

Figure 1.1 Organization of chromatin

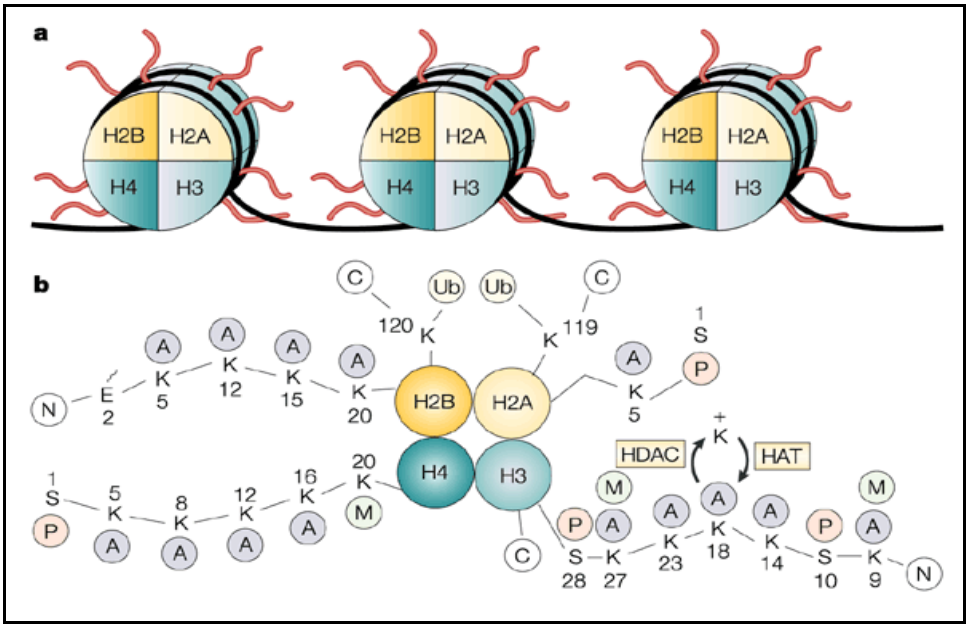

Adapted as is from [4]
a) Core proteins of nucleosomes are designated H2A (histone 2A), H2B (histone 2B), H3 (histone 3) and H4 (histone 4). Each histone is present in two copies, so the DNA wraps around an octamer of histones. **b)** Lysines (K) in the amino-terminal tails of histones are acetylation/deacetylation sites for HATs and HDACs. Acetylation neutralizes the charge on lysines. A, acetyl; C, carboxyl terminus; E, glutamic acid; M, methyl; N, amino terminus; P, phosphate; S, serine; Ub, ubiquitin.

Figure 1.2 Structure of histones in nucleosomes

The structural modification of histones is regulated mainly by acetylation/ deacetylation of N-terminal tail and is crucial in modulating gene expression, as it affects the interaction of DNA with transcription-regulatory, non-nucleosomal protein complexes. The balance between the acetylated/deacetylated states of histones is mediated by two different sets of enzymes; histone acetyltransferases (HATs) and histone deacetylases (HDACs). HATs preferentially acetylate specific lysine substrates among other non-histone protein substrates and transcription factors, impacting DNA-binding

properties and in turn, altering gene transcription. HDACs restore the positive charge on lysine residues by removing acetyl groups and thus are involved primarily in the repression of gene transcription by compacting chromatin structure (Figure 1.3). Thus, open lysine residues attach firmly to the phosphate backbone of the DNA, preventing transcription. In this tight conformation, transcription factors, regulatory complexes, and RNA polymerases cannot bind to the DNA. Acetylation relaxes the DNA conformation, making it accessible to the transcription machinery. High levels of acetylation of core histones are seen in chromatin-containing genes, which are highly transcribed genes; those genes that are silent are associated with low levels of acetylation. Since inappropriate silencing of critical genes can result in one or both hits of tumor suppressor gene (TSG) inactivation in cancer, theoretically, the reactivation of affected TSGs could have an enormous therapeutic value in preventing and treating cancer.[5]

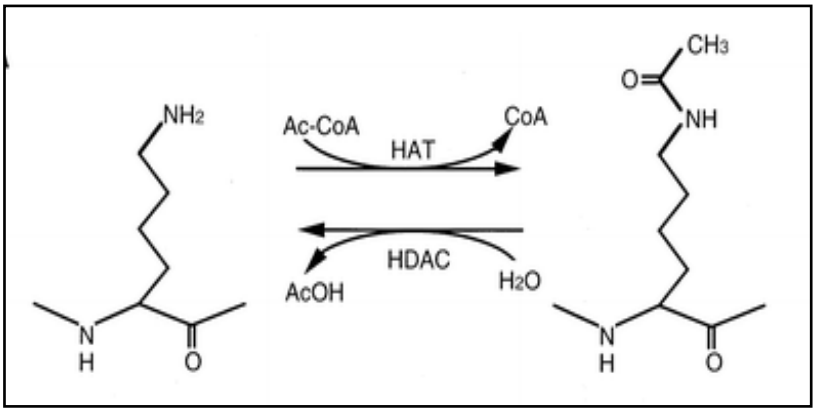

Adapted as is from [3]

Figure 1.3 Acetylation and deacetylation of lysine due to HAT and HDAC activity

1.2 Histone acetylases and deacetylases: classification and function

The equilibrium steady state level of acetylation is tightly controlled by the opposing effects of both HATs and HDACs, which in turn regulate the transcription status of not just histones but also of other substrates such as p53. [6] Several groups of proteins with HAT activity have been identified, including GNAT (Gcn5- related N-acetyl transferase) family, MYST (monocytic leukemia zinc finger protein) group, TIP60 (TAT-interactive protein) and the p300/CBP (CREB-binding protein) family. HATs act as large multiprotein complexes containing other HATs, co-activators for transcription factors, and co-repressors. [7-11] HATs, which bind non-histone protein substrates and transcription factors, have been called factor acetyltransferases. Acetylation of these transcription factors also affects their DNA binding properties and gene transcription. [12, 13] HAT genes may be over expressed, translocated, or mutated in both hematological and epithelial cancers. [14-16] Translocations of HATs, CREB-binding protein (CBP), and p300 acetyltransferases, in frame into genes have given rise to many hematological malignancies. [17, 18]

There are three major groups or classes of mammalian HDACs based on their structural homology to the three distinct yeast HDACs: Rpd3 (class I), Hda1 (class II), and Sir2/Hst (class III). Class III HDACs consist of the large family of sirtuins (silent information regulators) (SIRs) that are evolutionarily distinct, with a unique enzymatic mechanism dependent on the cofactor NAD+, and are virtually unaffected by all HDAC inhibitors in current development. [19, 20] Class I and II HDACs contain active site zinc as a

critical component of their enzymatic pocket, have been extensively described to have an association with cancers, and are thought to be comparably inhibited by all HDAC inhibitors currently in development. The Rpd3 homologous class I include HDACs 1, 2, 3 and 8, are widely expressed in tissues and are primarily localized in the nucleus. Hda1 homologous class II HDACs 4, 5, 6, 7, 9a, 9b and 10, are much larger in size, display limited tissue distribution and can shuttle between the nucleus and cytoplasm, suggesting different functions and cellular substrates from Class I HDACs. [21, 22] HDACs 6 and 10 are unique as they have two catalytic domains, while HDACs 4, 8 and 9 are expressed to greater extent in tumor tissues and have been shown to be specifically involved in differentiation. [23] There is some evidence that certain inhibitors display a variable degree of HDAC specificity, and hence it would be imperative to identify differences in HDAC functions to better target and tailor specific drugs compounds. [6, 24-26] HDACs usually interact as constituents of large protein complexes that downregulate genes through association with co-repressors; like nuclear receptor corepressor (NcoR), silencing mediator for retinoid and thyroid hormone receptor (SMRT), transcription factors, estrogen receptors (ER), p53, cell-cycle specific regulators like retinoblastoma (Rb), E2F and other HDACs, as well as histones, but they can also bind to their receptor directly.[20, 27, 28]

1.3 Chromatin Modification and Cancer

DNA gene expression is controlled by an assembly of nucleoproteins that includes histones and other architectural components of chromatin, non-histone DNA-bound regulators, and additional chromatin-bound polypeptides. Changes in growth and

differentiation leading to malignancy appear to occur by alterations in transcriptional control and gene silencing. It is becoming increasingly apparent that imbalances of both DNA methylation and histone acetylation may play an important role in cancer development and progression. [1, 4, 14, 29] Unlike normal cells, in cancer, changes in genome expression are associated with the remodeling of long regions of regulatory DNA, including promoters, enhancers, locus control regions, and insulators, into specific chromatin architecture. These specific changes in the DNA architecture result in a general molecular signature for a type of cancer and complement its DNA methylation-based component. The changes in the infrastructure of chromatin over a target promoter are more profound than those observed by these enzymes acting independently. [30, 31] Apart from acetylation, histone tails undergo other modifications including phosphorylation, ubiquitylation and adenosine diphosphate ribosylation. These other areas of modifications have not yet been explored enough to identify their roles in epigenetic modifications. [32]

Disruption of HAT and HDAC function is associated with the development of cancer and malignant cells target chromatin-remodeling pathways as a means of disrupting transcriptional regulation (Figure 1.4). [15] Of the various hypotheses describing deregulation mechanisms, the following three have been put forth frequently: i) disordered hyperacetylation could activate promoters that are normally repressed, leading to inappropriate expression of proteins, ii) abnormally decreased acetylation levels of promoter regions could repress the expression of genes necessary for a certain phenotype and iii) mistargeted or aberrant recruitment of HAT/HDAC activity could act as a

pathological trigger. Even though there have been no direct alterations in HDAC genes demonstrated in cancer, the association of HDACs with various oncogenes and tumor suppressor genes is now well-established, as is the potential for HDAC involvement in tumorigenesis. [33]

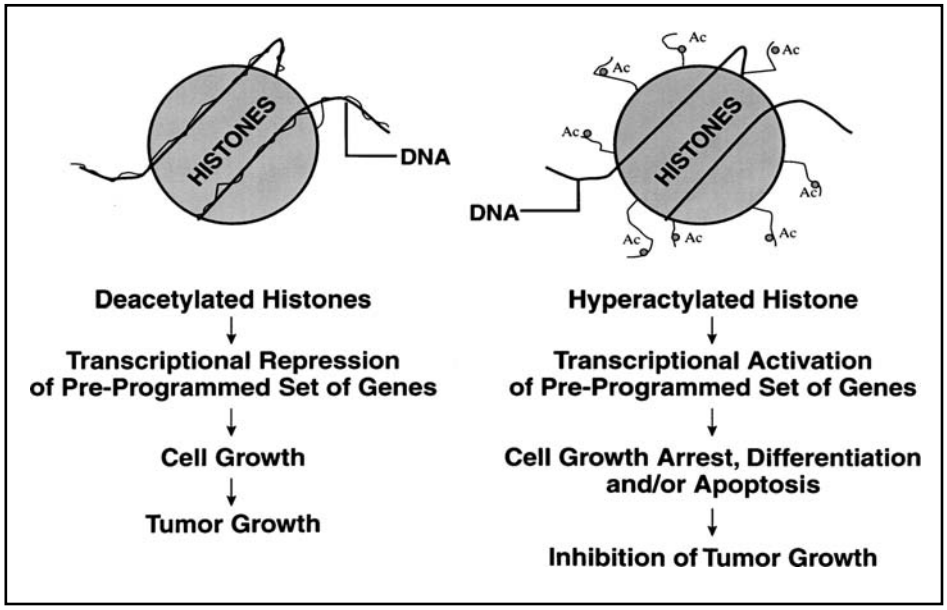

Adapted as is from [3]

Figure 1.4 Chromatin modifications and its role in cancer

1.4 Histone deacetylase inhibitors as anticancer agents

The findings of recruitment of HDAC enzymes in cancer have provided a rationale for using inhibition of HDAC activity to release transcriptional repression as a viable option towards achieving eventual therapeutic benefit. [16] Inhibition of HDAC function can release dysregulation of genes involved in cell cycle progression, differentiation and apoptosis. HDAC inhibitors block the deacetylation function, causing

cell cycle arrest, differentiation, and/or apoptosis of many tumors. [17] Several HDAC inhibitors have exhibited potent antitumor activity in human xenograft models, suggesting their usefulness as novel cancer therapeutic agents. Several are currently in phase I/II clinical trials, both in hematological malignancies and in solid tumors (Figure 1.5). Compared to agents used initially, some of the newer agents are effective *in-vitro* or *in-vivo* at nanomolar concentrations and are relatively less toxic. A wide range of structures inhibit activity of class I/II HDAC enzymes, and with a few exceptions these can be divided into structural classes including: (1) carboxylates (short chain fatty acids), (2) small-molecule hydroxamates, (3) electrophilic ketones (epoxides), (4) cyclic peptides and (5) benzamides and (6) other hybrid compounds. Table 1.1 describes the various compounds, their activities in cell lines and pre-clinical murine models and their current clinical status.

Table 1.1 Classes of HDAC inhibitors

Class	Short Name	Other name	*In-vitro* cell culture activity (concentration)	*In-vivo* pre-clinical activity (murine or human xenograft model)	Clinical trial status (Phase)
Carboxylates (Short chain fatty acids)	PA	phenylacetate	Yes (µM)	Leukemia, glioblastoma	I/II
	PB	sodium phenylbutyrate	Yes (µM)	Prostate, endometrial	I/II
	VA	valproic acid	Yes (mM)	Brain, melanoma	I/II
	AN-9	Pivanex, pivaloyl oxymethyl butyrate	Yes (µM)	NSCLC, leukemia	I/II
Hydroxamic acids (HA)	SAHA	suberonyl anilide hydroxamic acid	Yes (nM)	Lung, prostate, melanoma	I/II
	CBHA	m-carboxycinnamic acid bishydroxamic acid	Yes	Neuroblastoma	-
	SBHA	suberic bishydroxamic acid	Yes	Melanoma, sarcoma	-
	Pyroxamide	-	Yes (µM)	-	I
	TSA	trichostatin A	Yes (nM)	Cervical, hepatoma,	
	Oxamflatin	-	Yes (µM)	Melanoma	
	NVP-LAQ824	-	Yes (nM)	Colon, multiple myeloma	I
Electrophillic ketones (epoxides)	TPX	Trapoxin A & B	Yes (nM)	-	-
	AOE	2-amino 8-oxo-9,10-epoxy decanoic acid	-	-	-
	Depudecin	-	Yes (mM)	-	-
Cyclic peptides	Apicidin	-	Yes (nM)	Melanoma, leukemia	-
	FK-228, FR901228	Depsipeptide	Yes (nM)	Melanoma, colon, sarcoma, fibrosarcoma,	I/II

				lung, gastric	
Benzamides	**MS-275**	**MS-27-275**	**Yes (μM)**	**Leukemia, colorectal, gastric, pancreatic, lung, ovarian**	**I/II**
	CI-994	N-acetyl dinaline	Yes (indirect effect)	Colorectal, pancreatic, mammary, prostate, sarcoma, leukemia	I
Other hybrid compounds	CHAPs	cyclic HA-peptides (TPX-TSA analogues)	Yes (nM)	Melanoma, lung, stomach, breast	-
	Scriptaid	TPX-HA	Yes (nM)	-	-
	Tubacin	-	-	-	-
	JNJ1624 1199	-	-	-	-
	A-161906	-	Yes (nM)	-	-
	3-CI-UCHA	6- (3-chlorophenylureido)caproic hydroxamic acid	-	-	-
	PXD101	-	Yes (nM)	Breast, prostate, ovarian, colon, NSCLC	-

Comprehensive reviews on the structure, medicinal chemistry and structure-activity relationships of more than 80 different HDAC inhibitors and analogues have been previously published or reviewed. [26, 33-44] Despite the structural distinctiveness, all of these HDAC inhibitors can be broadly characterized by a common pharmacophore that includes key elements of inhibitor-enzyme interactions.[26] Most of these compounds were designed to have three basic components: a hydrophobic cap that blocks the entrance to active site, a polar site and a hydroxamic acid type zinc-binding active site separated by a

hydrophobic spacer that has optimal length spanning the hydrophobic pocket on the enzyme (Figure 1.5). [45]

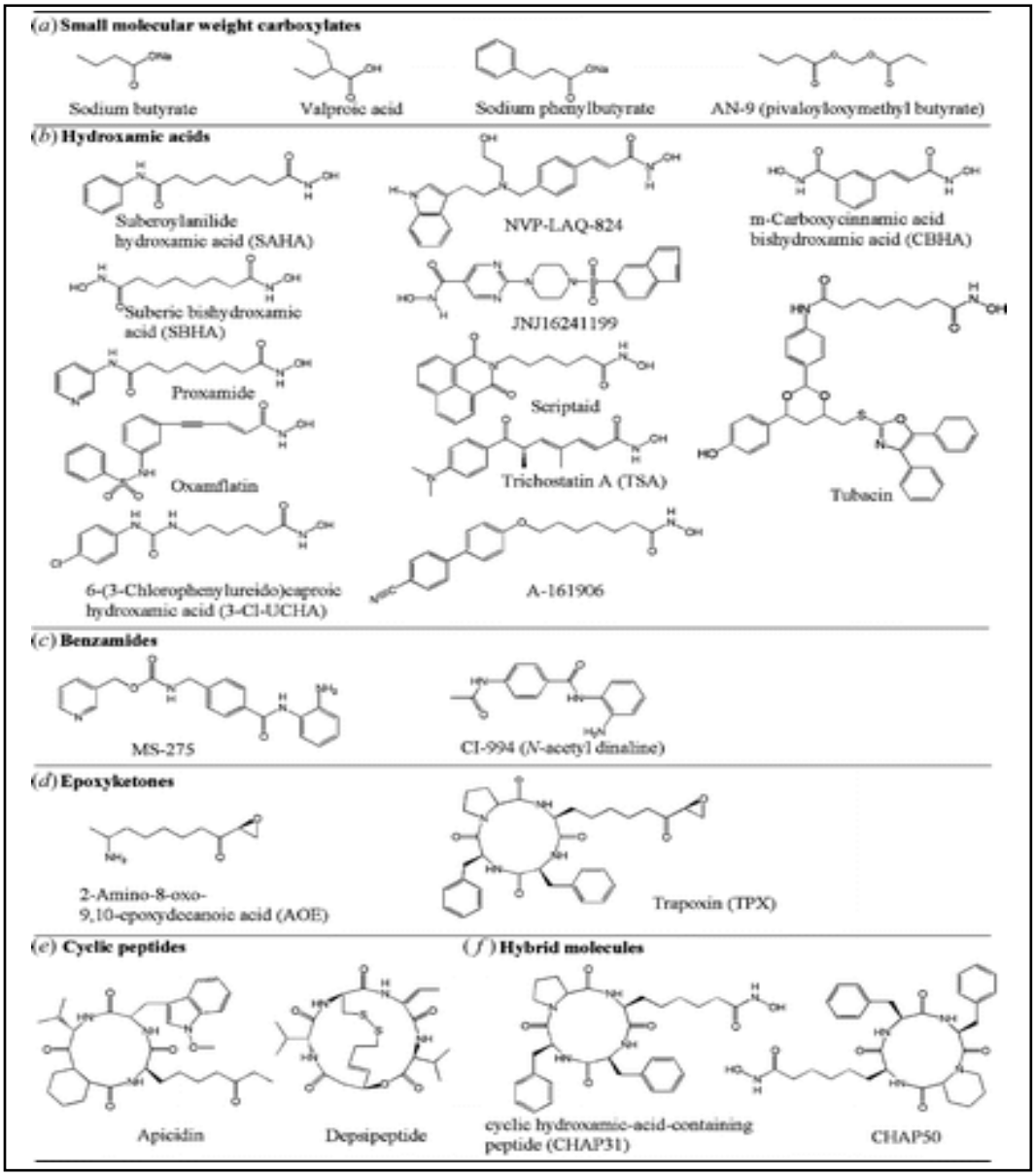

Adapted as is from [45]

Figure 1.5 Structures of various classes HDAC inhibitors

1.4.1 Short chain fatty acids

Dimethyl sulfoxide was one of the first compounds identified to be active in transformation and cell differentiation. As a result of this, several compounds were synthesized and screened for activity in differentiation, growth arrest and or apoptosis.[4] Valproic acid, a well-tolerated antiepileptic, is effective *in-vitro* as a HDAC inhibitor at relatively high (millimolar) concentrations and has much weaker affinity. It has been shown to selectively induce proteasomal degeneration of HDAC2 and is antiangiogenic *in-vitro* and *in-vivo*.[46-48] It also has been shown to have antigrowth activity of human endometrial cells and also to inhibit proliferation and induce apoptosis in acute myeloid leukemia cells expressing P-glycoprotein and multi-drug resistance protein MRP1. [49, 50 51] Valproic acid has been recently shown to inhibit angiogenesis *in-vitro* and *in-vivo* and markedly affects genes relevant in proliferation and apoptosis. [48, 52]

Phenylacetate (PA) can penetrate the CNS and when tested in solid tumors, showed antitumor effects mediated by histone acetylation. PA is a metabolite of phenylbutyrate (PB) after β-oxidation in the liver and kidney [53, 54]. PB, a well studied member of the short chain fatty acids, can arrest cells in G_1–G_0 by inducing $p21^{WAF1}$ and other cdk-2-associated cell cycle proteins, alter levels of expression of activation and chemotaxis proteins such as urokinase-plasminogen activator, induce apoptosis, inhibit telomerase, and increase MHC class I expression, in various tumor models. [55] However, the short chain fatty acids have a low potency due to their short side chains, limiting their contact with the catalytic pocket of HDACs. [56] In human CCRF-CEM, acute T-lymphoblastic leukemia cells, butyrate and other HDAC inhibitors caused G2/M cell

cycle arrest as well as apoptotic cell death. [57] Butyrates induce histone acetylation and granulocyte maturation in AML, selectively inhibiting growth in human prostate cancer and cervical carcinoma cells. [58-60] Butyrates have been under extensive clinical evaluation in both hematologic malignancies and solid tumors. Butanoic acid or its prodrug pivaloyl oxymethyl butyrate (AN-9) is currently undergoing phase I/II clinical trial after it showed 10-fold more potent activity than SB in leukemia tumor cell lines. [61-63] The antineoplastic activity of AN-9 stems from rapid hydrolysis and release of butyrate, permitting efficient delivery to subcellular targets. [64, 65] In spite of their overall weak activity of SCFA, several agents with known safety profile such as valproic acid have been studied clinically owing to their approved use for alternative medical conditions. [66-68]

1.4.2 Hydroxamic acids

This is the broadest class of inhibitors with high affinity for HDAC, which inhibit both HDAC I and II. Inhibitors containing hydroxamic acid (HA) residues bind with high affinity to the HDAC catalytic site, blocking the access of the substrate to the zinc ion. [69] The general structure of these substances consists of a hydrophobic linker that allows the hydroxamic acid moiety to chelate the cation at the bottom of the HDAC catalytic pocket, while the bulky part of the molecule acts as a cap for the tube. Most of the compounds in this group are very potent (functioning at nanomolar to micromolar concentrations *in-vitro*) but are reversible inhibitors of class I/II HDACs.

Trichostatin A (TSA) was one of the first HDAC inhibitors to be described and is widely used as a reference in research in this field. [70, 71] It was originally developed as an

antifungal agent but is relatively unstable and due to its toxicity to patients and lack of specificity for certain HDACs has been responsible for the search for other substances. [24, 72] The design of many synthetic drugs has been inspired by TSA structure (the aromatic "cap", hydroxamic acid functionality and hydrophobic linker between them). TSA blocks *in-vitro* proliferation and triggers apoptotis in hepatocellular carcinoma cells, blocks cell cycle progression in HeLa cells and differentiation in ovarian cancer cells by changing p21 tumor suppressor gene and DNA-binding Id1 protein. [73-75] TSA has also been shown *in-vivo* to suppress growth of pancreatic adenocarcinoma cells and ACHN renal cell carcinoma via cell cycle arrest in association with p27, or apoptosis. [76, 77] TSA is more sensitive in estrogen receptor alpha (ERα-) positive breast cancer cells in inhibiting HDAC.[78]

Simple hydroxamic acid derivatives such as suberoylanilide hydroxamic acid (SAHA) and pyroxamide have activity at submicromolar concentrations. [79-81] SAHA is a second-generation polar-planar compound that induces growth arrest, differentiation and/or apoptosis and is under clinical investigation in both hematological and non-hematological malignancies. [80, 82-84] In studies with breast cancer cells, SAHA inhibited clonogenic growth and induced apoptosis, while in malignant human hemotopeoitic cells, SAHA induced marked toxicity but showed relatively minor maturation activity. [85, 86] SAHA also showed antiproliferative and pro-apoptotic actions in several mouse xenografts and cancer cells including prostate, bladder carcinoma and myeloma. SAHA also induced CDK inhibitor p21WAF1/Cip1, and the inhibitory activity was independent of p53 status. [87-91] Pyroxamide is another compound in this class that induced terminal

differentiation in murine erythroleukemic cells and caused growth inhibition in prostate carcinoma, bladder and neuroblastoma cells via apoptosis. [41, 92, 93] In experiments with SAHA and butyrates, a model has been proposed in which induction of apoptosis in Bcr/Abl+ cells by HDIs involves coordinate inactivation of the cytoprotective Raf/MEK/ERK pathway in conjunction with the ROS-dependent activation of JNK. [94]

Oxamflatin is another compound in the same class which induces transcriptional activation of junD causing cell cycle arrest and morphological changes similar to TSA. [95] Scriptaid was found to be one of the most potent analogues in a search for substances that augment signal transduction pathways and when screened in human and animal tumor cells, showed similar antiproliferative effects as SAHA [35, 96] NVP-LAQ824, a cinnamic HA has been shown to inhibit HDAC *in-vitro* and to cause transcriptional activation of p21 promoter in reporter gene assays as submicromolar concentrations in multiple myeloma. [97] NVP-LAQ824 was selective in its action as it required longer exposure and higher concentrations to retard growth of normal human fibroblasts. [98] Another HA analogue, suberic bishydroxamate (SBHA) was shown to regulate expression of multiple apoptotic mediators and induce mitochondria-dependent apoptosis in melanoma cells. [99] PXD101 is a novel hydroxamate-type inhibitor of HDAC activity in nanomolar ranges in leukemia cells. It was shown to delay growth for xenografts of cisplatin-resistant ovarian tumor cells and had marked increase in acetylation of histone and showed good antitumor activity [100]

Newer compounds such as cyclic HA peptides (CHAPs), and a structural combination of HA like TSA and the cyclic tetrapeptides like trapoxin, inhibit isoform selective HDACs at nanomolar concentrations. [101, 102] One of the CHAP derivatives inhibited growth in four of five human tumor lines implanted into nude mice and shows great promise as therapeutic agent with higher selective inhibition of HDAC. [103]

1.4.3 Cyclic peptides

Cyclic peptides having epoxyketone (epoxides) may act by chemically modifying an active site nucleophile with the epoxy group and forming H-bonds with ketone. These chemicals are supposed to trap HDACs through the reaction of the epoxide moiety with the zinc cation or an amino acid (forming a covalent attachment) in the binding pocket. However, the lability of the epoxide functionality prevents significant *in-vivo* activity, which makes them of little pharmacologic interest. The only HDAC inhibitors in this set of compounds are a number of natural products with significant *in-vitro* activity, such as Trapoxin A, B (TPX), depudecin and 2-amino 8-oxo-9,10-epoxydecanoic acid (AOE). TPX is a hybrid molecule containing cyclic peptide (acts as hydrophobic cap) and epoxyketone moiety that has shown irreversible inhibition of mammalian HDACs at nanomolar ranges. [103-105] Cyclic tetrapeptides such as apicidin, which has an ethyl ketone moiety, as well as FK228 (also referred to as depsipeptide, FR901228) inhibit HDACs at nanomolar concentrations. Apicidin is a fungal metabolite that is able to inhibit HDACs and proliferation of tumor cells via induction of p21WAF1/Cip1 and gelsolin. [106] It is postulated that apicidin interacts with the catalytic site and has been shown to inhibit cell

proliferation in several human cancer cell lines due to its anti-invasive and anti-angiogenic activity. [107-111] FK228 is a natural product derived from *Chromobacterium violaceum* that exhibits potent antitumor activity through currently unknown mechanism of action. [112] One hypothesis proposes that the disulfide bridge is reduced inside the cell or organism and the 4-mercaptobut-1-enyl residue then fits inside the HDAC catalytic pocket, chelating Zn^{2+} in a manner similar to that of other inhibitors. In cultured cells, it is able to induce histone hyperacetylation and growth arrest at nanomolar concentrations. In human leukemia cells, FK228 had IC50 values at nanomolar concentrations and induced apoptosis *ex-vivo* in cells from patient with chronic lymphocytic leukemia. [113-116] In addition, FK228 has been shown to be antiangiogenic by modulating expression of c-myc and other regulatory genes. [117] FK228 is currently undergoing extensive evaluation in clinical trials. [117-120]

1.4.4 Benzamides

The synthetic benzamide derivatives include a structurally diverse group of compounds such as MS-275 and CI-994. CI-994 has shown efficacy in solid tumors in murine models but does not inhibit HDAC directly. The mechanism of its action is unknown, but it appears to inhibit both histone deacetylation and cellular proliferation at the G1–S transition phase. [121-123] MS-275 and some of its derivatives inhibit HDACs *in-vitro* at micromolar concentrations, but the mechanism is not clearly understood. It is believed that the diaminophenyl group is very important for the inhibitory behavior; probably, both amino functionalities chelate the metallic ion in the catalytic site. MS-275-

associated HDAC-inhibitory activity is accompanied by an increase in expression of cyclin dependent kinase inhibitor p21WAF1/Cip1 and accumulation in G1-phase. [124, 125] MS-275 displays anti-proliferative activity in several human cancer cell lines including breast, colorectal, leukemia, lung, ovary and pancreas. MS-275 suppressed growth of several pediatric cancer cell lines in dose-dependent manner, as well as tumors transplanted in nude mice. [126] MS-275 and CI-994 are undergoing clinical trials. There are reports of novel nonhydroxamate sulfonamide anilides similar in structure to MS-275 that have shown lower toxicity and comparable antiproliferative activity.[34, 127] Currently, focus is on development of novel compounds based on core structures of HA or benzamide platform, which may have better HDAC inhibitory profile and lower toxicity compared to parent compounds.

1.5 Mode of action of HDAC inhibitors in cancer cells

Even though a number of HDAC inhibitors have shown considerable promise in preclinical models, the mechanism of action has not been fully evaluated. The most widely accepted proposed mechanism of action is described in detail in Figure 1.6. HDAC inhibitors are effective in affecting cell cycle arrest, apoptosis, anti-angiogenesis and differentiation in cultured and transformed cells from both hematologic (leukemias, lymphomas and myelomas) and epithelial (breast, bladder, ovarian, prostate and lung) tumor sources. The change that occurs after treatment with HDAC inhibitors (growth arrest, terminal differentiation, or apoptosis) appears to be dependent upon the tumor cell line rather than the specific HDAC inhibitors used. [32] The HDAC family is divided into

the Zn-dependent (Class I and Class II) and Zn-independent, NAD-dependent (Class III) enzymes. The Zn-dependent enzymes have been the focus of intense research, whilst Class III enzymes have been recently implicated in acetylation and regulation of key cell cycle proteins such as p53. [128] [129] Interestingly, a number of studies have shown that HDAC inhibitors are relatively non-toxic to normal cells or tissues, but exhibit selective cytotoxicity against a wide range of cancer cells. [130, 131] It has been postulated that defective cell cycle checkpoint regulation of neoplastic cells may render them susceptible to HDAC inhibition-induced apoptosis. [16, 132]

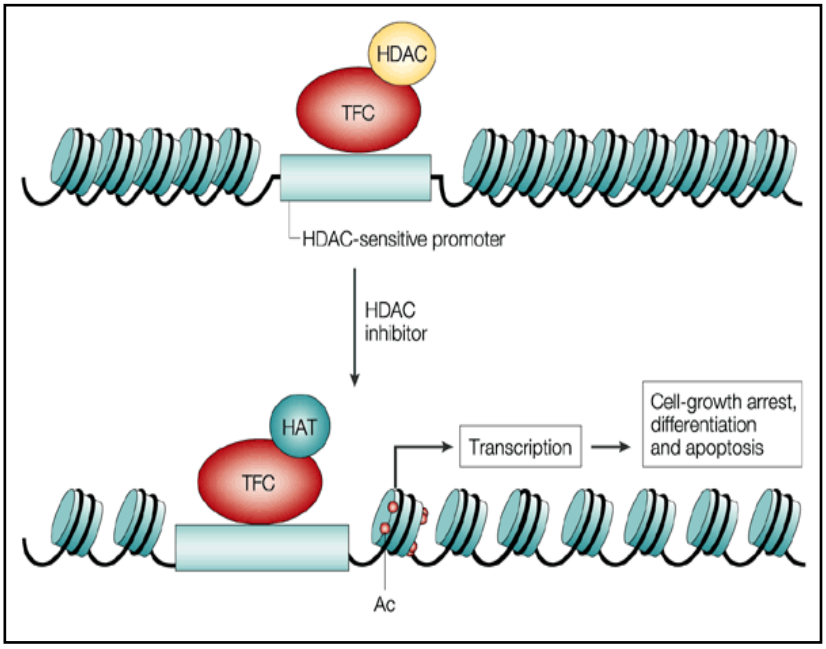

Adapted as is from [4]
When histones are acetylated, the DNA that is tightly wrapped around a deacetylated histone core relaxes. Specific sites in the promoter region of a subset of genes that recruit the transcription factor complex (TFC) with HDAC and that the accumulation of acetylated histones in nucleosomes leads to increased transcription of this subset of genes (for example, *CDKN1A*, which encodes WAF1), which, in turn, leads to downstream effects that result in cell-growth arrest, differentiation and/or apoptotic cell death and, as

a consequence, inhibition of tumor growth. Ac, acetyl group; HAT, histone acetyltranferase.

Figure 1.6 Proposed mechanism of action of HDAC inhibitors

As noted earlier, histone acetylation is known to precede gene transcription, and among the genes that are consistently upregulated because their promoters are associated with acetylated histones, is the cell cycle gene *CDKN1A*, which encodes cyclin-dependent kinase (CDK) inhibitor $p21^{WAF1}$. The CDK inhibitor WAF1 inhibits cell-cycle progression by blocking CDK activity and the arrest of the cell cycle in G1 stage. Most HDAC inhibitors namely, butyrates, TSA, depsipetide, oxamflatin, MS-275 and SAHA induce expression of p21. [86, 106, 125, 133-142] Some cDNA microarray studies have shown that treatment with TSA or SAHA alters the expression of a selective subset of approximately 2% of cellular genes that are either upregulated or downregulated. [143-145] The genes that are usually affected by these inhibitors are *CDKN1A* and *CDKN2A* where the latter encodes genes of cell cycle regulation such as p16, cyclin E and thioredoxin binding protein 2.[85, 146] Thus, gene promoters have specific sites, such as SP1, which bind HDAC containing transcription complexes and repress gene transcription. [147, 148] Inhibition of HDACs will activate these silenced genes, contributing to growth arrest, differentiation and/or apoptosis of transformed cells. Treatment with HDAC inhibitors triggers both the intrinsic and the extrinsic pathway of apoptosis by sensitizing tumor cells to the death ligands. [32] Several HDAC inhibitors, including SB, SAHA and MS-275 induce mitochondrial permeability where pro-apoptotic molecules such as cytochrome c, are released into the cytosol, resulting in eventual activation of caspase-dependent

apoptotic cascades (both receptor and mitochondria-mediated). [149-152] Upregulation and induction of a conformational change of the pro-apoptotic proteins are some of the HDAC inhibitor-induced upstream events that may trigger the mitochondrial pathway of apoptosis as is described for MS-275 and SB or as is proposed in case of SAHA, may not require key caspases such as caspase-8 and caspase-3. [153, 154] Recently, reactive oxygen species (ROS) have been identified as a major cell death mechanism of several HDAC inhibitors.[153, 155] There is some evidence that HDAC inhibitors may induce acetylation of non-histone proteins such as heat shock protein hsp90. Depsipeptide, SAHA and LAQ824 lower the threshold for apoptosis by inducing the acetylation hsp90 and thus affect oncoproteins such as Bcr-Abl and FLT-3. [156, 157] This eventually results in the inhibition of its chaperone association with important pro-survival client proteins such as Erk, Akt and c-Raf. [94] SAHA and oxamflatin were also shown to kill both ABCB1 positive and negative cells, whereas FK228 was shown to be substrate for ABCB1.[158] These data may provide insight into defining rational approaches to chemotherapy, where the genetic profile of tumor is matched with the functional profile to promote favorable clinical response.

Induction of the cell cycle inhibitor plays an important role in the induction of differentiation by HDAC inhibitors. SAHA and sodium butyrate were shown to induce differentiation of leukemia and breast cancer cells. [66, 67] Induction of the expression of other molecules involved in differentiation, such as gelsolin, an actin binding protein involved in cell morphology and structural changes was observed during treatment with HDAC inhibitors. [74, 106, 159, 160] In addition to pro-apoptotic and cytostatic activities,

another mode of tumor regression following treatment with HDAC inhibitors may be by indirect inhibition of angiogenesis. In *in-vitro* models, depsipeptide blocked potently the hypoxia-stimulated proliferation, invasion, migration, adhesion, and tube formation of bovine aortic endothelial cells. [117] Effective concentrations were comparable to cytotoxic concentrations, and there was an indication of possible modulation of gene transcription as evidenced by the expression of angiogenic-inhibiting factors such as von Hippel Lindau and neurofibromin 2 and the suppression of angiogenic-stimulating factors such as vascular endothelial growth factor (VEGF). [115, 161] Other HDAC inhibitors like apicidin, TSA, butyrate and newer analogue LAQ824 were all shown to inhibit angiogenesis through VEGF inhibition. [48, 110, 162-164]

Such insights into the mechanisms by which HDAC inhibitors interfere with cancer cell growth and survival has prompted the search for combination strategies to optimize therapy.

1.6 Combination therapy of HDAC inhibitors with other drugs *in-vitro*

Silencing of genes that affect growth and differentiation has been shown to occur by aberrant DNA methylation in the promoter region and by changes in chromatin structure that involve histone deacetylation. [165, 166] DNA methylation and histone deacetylation appear to act as synergistic layers for the transcriptional silencing of genes in cancer.[167-169] Such findings have great implication in development of combination therapies.

Epigenetic mechanisms, such as DNA methylation and histone deacetylation, may also play a role in loss of estrogen receptor alpha (ER) expression in ER negative human breast cancer cells. Previous studies showed that pharmacologic inhibition of these mechanisms using the DNA methyltransferase inhibitor, 5-aza-2'deoxycitidine (AZA), and TSA, resulted in expression of functional ER mRNA and protein.[170] Scriptaid, a novel TPX-HA analogue, inhibits tumor growth *in-vitro* and *in-vivo* and, in conjunction with AZA, acts to re-express functional ER.[171] In another study, TSA was shown to sensitize ER alpha negative antihormone-unresponsive breast cancer cells to tamoxifen treatment, by upregulating its activity.[172] The *in-vitro* antineoplastic activity of 5-aza-2'deoxycitidine (AZA), in combination with TSA or depsipeptide, on the human myeloid leukemic cell lines produced a greater inhibition of growth and DNA synthesis and a greater loss of clonogenicity than either agent alone.[173] Similar results were noted with PB and AZA combination in lymphoid leukemic cells.[174] Another study found that when AZA was combined with PB, murine lung tumor development was significantly reduced >50%, while no effect was observed with PB alone. [175]

Chromatin DNA is tightly packed, and hence accessibility to the drug target may reduce the efficiency of these anticancer drugs. When six cancer cell lines were pre-treated with TSA or SAHA followed by exposure to anticancer drugs like etoposide (VP-16), campothecin, cisplatin, doxorubicin, 5-fluorouracil, cyclophosphamide or ellipcitine, there was more than 10-fold sensitization of cells for VP-16. The data suggest that loosening-up the chromatin structure by histone acetylation can increase efficiency of several anticancer agents. [176] SAHA significantly potentiated the DNA damage by

topoisomerase II inhibitors; however, synergy was dependent on the sequence of drug administration and expression of target. Pre-exposure of cells to SAHA for 48h was synergistic, whereas shorter period of exposure abrogated synergy, and pre-treatment with topoisomerase II inhibitor showed antagonistic effects. [177]

Inhibition of cell survival signals and proliferation by inhibitors of tyrosine kinase activity, in combination with HDAC inhibitors is another mechanism to induce differentiation and/or apoptosis.[178] The cytotoxic effects following the introduction of SAHA with imatinib mesylate showed accumulation of acetylated histones H3 and H4, induction of p21 and p27, and, following SAHA treatment, there was a decline in the mRNA and protein levels of Bcr-Abl, resulting in G1 arrest and apoptosis of leukemic cells. Co-treatment with imatinib mesylate and SAHA caused significantly more down-regulation of tyrosine kinase activity of Bcr-Abl and apoptosis of these cells when compared to treatment with SAHA alone. These findings suggested that co-treatment with SAHA and imatinib mesylate or arsenic trioxide are cytotoxic to Bcr-Abl positive acute leukemia cells, and these agents may be a promising therapeutic strategy against imatinib mesylate-refractory Bcr-Abl positive acute leukemia. [179, 180] Similar results were achieved on combined exposure of Bcr/Abl positive human myeloid leukemia cells to imatinib (gleevec, STI571) and SAHA, leading to diverse perturbations in signaling and cell cycle-regulatory proteins, associated with a marked increase in mitochondrial damage and cell death. [179] SAHA and PB were also shown to synergistically induce apoptosis in human leukemic cells when co-treated with hsp90 antagonist 17-allylamino-17-demethoxygeldenamycin (17-AAG). [181] Similar cumulative inhibitory effects were

noted on combined treatment of SB and flavopiridol, where interruption of HDAC-mediated p21(WAF1/Cip1) induction by flavopiridol-potentiated apoptosis. [182, 183] Recently, the same group of researchers showed that MS-275 acts synergistically with fludarabine to increase the apoptotic activity in leukemia cells. [184] Moreover, proteasome inhibitor bortezomib interacts synergistically with SB or SAHA to cause oxidative injury and apoptosis in Bcr/Abl positive multiple myeloma and leukemia cells sensitive and resistant to imatinib. [185, 186]

LAQ824 lowers expression and promotes proteasomal degradation of Bcr-Abl and induces apoptosis of imatinib-sensitive or refractory chronic myelogenous leukemia-blast crisis cells.[187] Recent studies show that LAQ824 can also promote degradation of mutant FLT-3 and induce apoptosis of AML cells carrying the mutated FLT-3. The addition of the Flt-3 kinase inhibitor PKC412 had a synergistic effect on apoptosis in AML cells with mutant FLT-3.[188] The combination of SAHA or LAQ824 with various cytotoxic agents such as taxotere, trastuzumab, gemcitabine and epothilone B, enhanced the cytotoxic effects in breast cancer cells, while the combination of 5-fluorouracil and other chemotherapy agents with PB also enhanced the cytotoxic effects in colorectal cancer cells. [189-191] In two separate studies, SAHA also potentiated sensitizing melanoma cells to TNF-related apoptosis-inducing ligand (TRAIL) induced apoptosis by simultaneous activation of intrinsic and extrinsic pathways. [192, 193] In another study, VA was shown to increase cellular sensitivity to estrogens, progestins and other hormone nuclear ligands, by functioning as activator of p42/p44 mitogen-activated protein kinase (MAPk). [194] TSA upregulated RECK glycoprotein that negatively regulates matrix

metalloproteinases (MMPs) and inhibits tumor metastasis and angiogenesis by specifically inhibiting MMP-2.[195] Radiotherapy is an effective treatment for several cancers but causes cutaneous radiation syndrome. PB, TSA and VA were shown to decrease skin fibrosis and tumorigenesis by suppressing aberrant expression of TGF-beta and TNF-alpha. [196] In human gastric and colorectal cancer cells, depsipeptide, MS-275 and CBHA all augmented radiation-induced cell death. [197] Moreover, HDAC inhibitors have shown synergism when combined with all-trans retinoic acid (ATRA) to overcome the block in differentiation due to specific translocations associated with acute promyelocytic leukemia. [83, 198, 199]

1.7 HDAC inhibitors in clinical trials

Based on promising non-clinical data, several HDAC inhibitors are currently being investigated in early phase trials in humans, both as single agent and in combination with known cytotoxic compounds. HDAC inhibitors such as PA, PB, VA, AN-9, SAHA, LAQ824, pyroxamide, FK228, MS-275 and CI-994 are in clinical trials in patients with various metastatic or refractory solid tumors in advanced stages and those with hematologic malignancies like acute myeloid leukemia (AML), acute lymphocytic leukemia (CLL), chronic myeloid leukemia (CML), chronic lymphoid leukemia (CLL), or lymphomas.

Details about phase of development, major toxicities, pharmacokinetics and preliminary data on pharmacodynamics and clinical response of various HDAC inhibitors used as

single agents or given in combination with agents that are undergoing clinical development are summarized in Table 1.2 and Table 1.3 respectively.

1.8 Future direction

The concept of mechanism-based therapeutic development of novel anticancer agents is now being fully recognized, since targeting of abnormalities specific to cancer has shown to offer new directions. The first generation of HDAC inhibitors in clinical trials has shown encouraging antitumor effects, with acceptable safety profiles. There may be significant repercussions in success or failure of an anticancer agent, when targeting a specific subtype of HDAC without having a broader understanding of mechanism of action and the differential role each enzyme play in chromatin remodeling in cancer cells. Although, none of these agents in clinical trials were developed to be selective inhibitors of individual HDAC subtype, they do show some target selectivity. [129] For example, MS-275 showed *in-vitro* selective inhibition of HDAC1 and HDAC3, but was inactive against HDAC8. [200] Similarly, FK228 has activity against class I (HDAC1 and HDAC2) enzymes, but not against class II (HDAC4 and HDAC6). [201] The challenge remains to develop specific inhibitors of class I HDACs that are primarily located within the nucleus and class II HDACs that are known to shuttle between nucleus and cytoplasm [21, 56]. Recent findings using siRNA techniques to understand HDAC isotypes as potential targets, suggested that class I HDAC enzymes may be more relevant targets for intervention in oncology. [37] In any case, chromatin modifying enzymes have provided an

increasingly validated therapeutic target and there is now compelling evidence that these compounds exhibit efficacy in human diseases.

Phase I and phase II clinical trials with HDAC inhibitors have been completed, and others are being initiated. Most of these have been able to identify suitable doses for treatment with relatively low toxicity and reasonable efficacy in various cancers. Remission appeared to be transient in some of the patient trials, suggesting a need for determination of optimal dosing regimens.[32] Based on preliminary clinical data and the apparent cytostatic mechanism of action, most HDAC inhibitors, with the possibly exception of FK228 in the treatment of renal cell carcinoma, seem to fit more as combination treatment with existing chemotherapy regimens along with being used in other mechanism-based agents. Nonetheless, various questions still remain to be answered: 1) what role do altered HAT or HDAC activities have in conjunction with tumorigenesis? Is it a direct effect or is an epigenetic adaptive phenomenon?; 2) why are tumor cells more resistant to HDAC inhibitors than normal cells, and is there a possibility that there may be increased HAT/HDAC activity in tumors?; 3) is modification of histone(s) the only mechanism leading to anti-neoplastic effects or are there targets responsible that are yet undefined?; and 4) what is the target specificity of HDAC inhibitors? [112] Unraveling specific roles of HDAC isozymes during human tumorigenesis will provide further incentive for the development of more specific HDAC inhibitors, potentially those enhancing clinical activity as well as decreasing aspecific toxicities. Also, optimizing potential interactions with other rationally designed and integrated therapeutic agents remains a promising premise for exploration. In addition, there is a

general current lack of knowledge on the pharmacokinetics and biodistribution of various HDAC inhibitors studied clinically. Current evidence suggests that novel formulations and drug delivery strategies that allow better targeting may significantly enhance the therapeutic potential of HDAC inhibitors.[45]

1.9 Conclusion

A wealth of recent data has become available suggesting that histone modification is a promising therapeutic strategy affecting many of the hallmark traits of cancer. [202] Drugs such as HDAC inhibitors that have pleiotropic actions in modulating multiple genes, pathways and biological features of malignancy, might prove to be suited for dealing with multiple oncogenic abnormalities seen with most cancer types.[33] Although the clinical development of novel HDAC inhibitors seems certain, their actual value will greatly depend on identification of molecular and cellular predictors of toxicity and elucidation of their mechanism of action as anticancer agents.

Table 1.2 HDAC inhibitors in clinical trials as single agents

Name (Ref)	Phase	N	Tumor type	Route of administration / dosing regimen	DLT and adverse events	MTD/PK results	Clinical response/outcome
PA[203]	I	17	Solid tumors	IV bolus (60-150 mg/kg), target level 200-400g/ml x 2 weeks	CNS depression, emesis, confusion, lethargy	Non-linear PK, evidence of metabolic induction, 99% PA converted to PG and eliminated in urine, CNS penetration	3/9 SD x 2 months in HRPC, 1/6 SD >9 months in glioblastoma
PA[204]	I	18	Solid tumors	IV 1 h infusion b.i.d. 125 and 150 mg/kg x 2 weeks every 4 weeks	CNS depression	PA induced own clearance (27%), MTD 125 mg/kg, Cmax 2500 g/ml	1 PR glioblastoma, 1 HRPC with 50% post-therapy PSA decline
PA[205, 206]	II	43 & 9	Recurrent malignant gliomas	IV infusion 400mg/kg/day, comapared 2 schedules, 2weeks every 2 weeks or 12-day every 2 days Max 450 mg/mg/day	Fatigue, malaise, somnolence, disorientation, weakness, nausea, vomiting & granulocytopenia	No differences in plasma concentration between 2 treatments, no apparent induction of PA metabolism	For schedule 1, PR 3/40 (7.5%), SD in 7/40 patients (17.5%), PD < 2 months 30/40 patients , For schedule 2, 1/7 SD, 6/7 PD
PB[207]	I	24	Refractory solid tumors	IV infusion 120-h every 3 weeks, dose 150 – 515 mg/kg/day	Neurocortical somnolence, confusion, hypokalaemia, hyponatreamia, fatigue, nausea	MTD =410 mg/kg/day, plasma CL increased continuously after 24h, PA accumulated when Vmax was less than dosing rate	No CR, 2 SD, reduction in bone pain
PB[208]	I	28	Refractory solid tumors	Oral dose TID 9-45 g/day in 5 dose levels	Grade 1 – 2 dyspepsia, fatigue, neurocortical nausea, vomitting,	MTD 27 g/day, bioavailability 78%, biologically active concentrations (0.5mM)	No CR, PR, 7 patients (25%) with SD > 6 months

					hypocalcaemia		
PB[67]	I	27	Myeloid dysplesia, AML	IV infusion for 7 day every 28 days	Neurocortical somnolence, confusion,,slurred speech, hyperammonaemia	MTD 375 mg/kg/day	No CR, PR, hematological improvements, increased neutrophils in 3, decreased blasts in 3
AN-9[62]	I	28	Advanced solid tumors	IV infusion, 6 h x 5 days every 21 days at doses 0.047 - 3.3 g/m^2/day	No DLT, nausea, vomiting, fatigue, vision disturbance, anorexia, fever	MTD 3.3 g/m^2/day based on volume of maximum lipid formulation administerable	1 PR, no increase in fetal hemoglobin
AN-9[63]	II	47	Refractory NSCLC	IV infusion, 2.34 g/m^2/day over 6 h x 3 days every 21 days	Grade 1-2 fatigue (34%), nausea (17%), dysgeusia (11%)	-	3/47 PR, 14 patients with SD > 12 weeks (30%), median survival 6.2 months, 1-year survival of 26%
VA[209]	I	26	Progressive cancers	IV infusion 1 h split twice daily x 5 days every 2 weeks at 30-120 mg/kg/day	Grade 3/4 neurotoxicity, no severe hematological	MTD 60 mg/kg, PBMC showed hyperacetylation	Neurotoxicity is dose-limiting
SAHA[210]	I	37	Solid tumor and hematologic malignancy (B))	IV infusion, (A) 2 h x 3 days every 3 weeks, at 75-900 mg/ m^2/day (B) 2 h x 5 days every 1-3 weeks 300-900 mg/ m^2/day for 3-15 days	(A) No DLT in 8/8, (B) Grade 3/4 thrombocytopenia and neutropenia in hematological patients	MTD on (B), 300 mg/ m^2/day $t_{1/2}$ = 21-58 min, AUC increased with dose, accumulation of acetylated histones in PBMC after 4 h at all dose levels	1 PR in refractory Hodgkin's disease & SD > 6 months in 2 patients with bladder cancer
SAHA[211]	I	15	Advanced refractory leukemias	Orally TID x 14 days every 21 days at 100-250 mg	No DLT, nausea, vomiting, diarrhea,	Histone hyperacetylation at all dose levels	1 CR at dose level 3 after 2 courses, 2 AML, 1 MDS patient

			or MDS		anorexia, headache, fatigue, dyspepsia		had decrease in marrow blasts to < 10%
SAHA[212]	I	39	Advanced cancers	Oral, daily or BID at 200-600 mg	Thrombocytopenia, fatigue	Prolonged plasma concentrations <10 h with single dose	Prolonged duration of acetylated histones in PBMC (>10 h), objective response in patients with larynx, renal cancer and lymphoma
SAHA[213]	II	13	SCCHN (metastatic head and neck cancers)	Oral, daily at 400 mg	No DLT, grade 3-4 thrombocytopenia, anemia, anorexia	-	No PR or CR, 1 MR based on tumor shrinkage,
Depsipeptide[118]	I	33	Advanced cancers	IV infusion 4 h, weekly x 3 every with 1 week off at 1-17.7 mg/m^2	Grade 3 thrombocytopenia, fatigue, nausea, vomiting, anorexia at dose above 5 mg/ m^2, subtle ECG changes	MTD 13.3 mg/ m^2/day	No decrease in cardiac enzymes of ejection fraction
Depsipeptide[119, 214]	I	37	Advanced or refractory cancers	IV infusion 4 h on days 1 and 5 every 21 days at dose 1-24.9 mg/m^2	Grade 3 fatigue, nausea, vomiting, grade 4 thrombocytopenia, cardiac arrhythmia	MTD 17.8 mg/m^2 over 4 h over 4 h $t_{1/2}$(a) =0.42 h; elimination $t_{1/2}$(b) =8.1h, mean CL=11.6 L/h/m^2 , inhibition of cell cycle in PC-3 cells	Increased acetylation of histones in Sezary cells, no effect on histones after 7 h, 1PR in colon cancer x 6 months, 1 CR in peripheral T-cell lymphoma, 3 PR in CTCL

Depsipeptide[120]	I	20	CLL and AML	IV infusion on days 1, 8, 15 at 13 mg/m^2	Fatigue, nausea, progressive constitutional symptoms	Increases in histone acetylation by 100%, p21 promoter H4 acetylation, p21 protein	No cardiotoxicity, need to explore other schedules due to progressive toxicity
CI-994[123]	I	53	Solid tumors	Orally on schedule (A) x 2 weeks, (B) x 8 weeks followed by 2 weeks rest	Schedule (A) thrombocytopenia, neutropenia, increased LFT, creatinine, (B) thrombocytopenia, nausea, vomiting	Schedule (A) MTD 15 mg/m^2/day, no cumulative toxicities, (B) MTD 8 mg/m^2/day, $t_{1/2}$ = 7.4-14.1 h, inverse relationship between platelet nadir and AUC, low effect of food on absorption	Both schedules, 1 PR in NSCLC x 2years, 3 SD in NSCLC, colorectal and renal cancer
MS-275[215]	I	30	Solid tumors and lymphomas	Orally on schedule (A) daily x 28 days every 6 weeks, (B) weekly x 4, every 6 weeks at 2-12 mg/m^2	Schedule (A) severe GI toxicity, (B) and (C) fatigue, nausea, vomiting, anxiety thrombocytopenia, headache	MTD on (A) 2 mg/m^2, (B) 10 mg/m^2, histone acetylation at all dose levels	Schedule (A) intolerable, 15 SD on (B),
MS-275	I	33	Hematologic malignancy	Orally q7 day for 4 weeks every at 4-10 mg/m^2	Sepsis, severe line infections at 10 mg/m^2 , neutropenia, GI toxicity	MTD at 8 mg/m^2	1 PR in patient with AML
MS-275[216]	I	17	Solid tumors and lymphomas	Orally on schedule (A) 2-6 mg/m^2 biweekly, (B) 2 mg/m^2 twice weekly x 3 weeks with 1 week off, (C) 4 mg/m^2 weekly for 3	No drug related DLT, grade 1-3 hypohosphatemia, asthenia, nausea, anorexia	MTD not reached on (A), (B) not pursued, rapid absorption with Tmax 0.5- 2h, dose-dependent increase in exposure, biphasic elimination with t12=100h	1 PR on (A) in melanoma, 3 SD in Ewing's sarcoma, rectal carcinoma and melanoma

				weeks with 1 week off			
LAQ824[217]	I	21	ALL, AML, CLL, CML, MDS	IV infusion, 3h on days 1-3 of 21 day cycle at 6-80 mg/m^2 in 6 dose levels	Thrombocytopenia (cerebral bleeding), grade 2 hyperbilirubinemia	MTD 36 mg/m^2 ,dose-proportional increase in exposure, $t_{1/2}$=9-18 h, 1.5 fold accumulation at day 3, Cmax after 1.5h , not at end of infusion in >50% patients, indicates non-linear PK	No QTc prolongation, ECG <400 msec, 1CR in M1 AML, 6 SD, histone acetylation at >12 mg/m^2 doses
LAQ824[218]	I	28	Advanced solid tumors	IV infusion, 3h on days 1-3 of 21 day cycle at 6-100 mg/m^2 in 7 dose levels	Grade 3/4 transient transaminitis, fatigue, hyperbilirubinemia, nausea, thrombocytopenia,	Dose-proportional increase in exposure,$t_{1/2}$=8-14 h, Cmax after 1.5h , not at end of infusion in >50% patients, indicates non-linear PK	1 ECG > 500msec, 3 SD, histone acetylation at > 12 mg/m^2 doses
LBH589[219]	I	13	Advanced solid tumors	IV infusion, 30 min either on (A) days 1-3 and 8-10 of 21 day cycle at 1.2 -7.2 mg/m^2, (B) days 1-3 or 15-17 of 28 day cycle at 2.4-4.8 mg/m^2	Prolonged grade 2 thrombocytopenia in (A), grade 3 neutropenia, anemia, hypoglycemia	Exposure increased proportionally with dose, $t_{1/2}$ =15-20 h	6 SD, increased histone acetylation after first dose

Table 1.3 HDAC inhibitors in combination therapy with other agents

Name (Ref)	Phase	N	Tumor type	Route of administration / dosing regimen	DLT and adverse events	MTD/PK results	Clinical response/outcome
CI-994 + gemcitabine[220]	I	20	Advanced cancers	Gemcitabine IV infusion weekly x 3 with 1 week off at 1000 mg/m^2, CI-994 orally daily x 21 days escalating at 2-8 mg/m^2	Grade 4 thrombocytopenia (30%) at 8 mg/m^2	MTD 6 mg/m^2 oral x 21days with 1000 mg/m^2 gemcitabine, rapid absorption, Cmax within 2 hours of dosing	2 MR, 12 SD with median 105 days, 4 PD
CI-994 + capecitabine[221]	I	54	Advanced cancers	Schedule (A) IV capecitabine twice daily at 1650 mg/m^2/day, CI-994, 2-10 mg/m^2 orally x 2 of 3 weeks, (B) CI-994 x 5 of 6 week , (C) capecitabine 2000 mg/m^2/day, CI-994 orally x 2 of 3 weeks	Thrombocytopenia,	MTD 6 mg/m^2 (10 mg) with capecitabine 2000 mg/m^2/day, PK of CI-994 unaltered by capecitabine	No correlation between BSA and PK parameters, platelet nadir best predicted by Cmax
CI-994[222]	II	32	NSCLC	Orally, daily at 8 mg/m^2	Thrombocytopenia, fatigue,anorexia , nausea, vomiting, paresthesia	-	2 PR, 8 SD > 8 weeks, median survival 30 weeks
CI-994[223]	II	48	Renal cell carcinoma	Orally, daily at 8 mg/m^2	Thrombocytopenia, fatigue,anorexia , nausea, vomiting,	-	26 SD for >8 weeks, median survival = 48 weeks

					paresthesia		
CI-994[224]	II	17	Advanced pancreatic cancer	Orally, daily at 8 mg/m^2	Thrombocytopenia, asthenia, anorexia	-	2 SD for 6 weeks, No objective response, cytostatic mechanism
CI-994 + carboplatin or paclitaxel [225]	I	21	Refractory solid tumors	Oral CI-994 daily x 7 or 14 days every 21 days (4-6 mg/m^2/day), Carboplatin every 21 days Paclitaxel 175-225 mg/ m^2 every 21 days	DLT=neutropenia,thrombocytopenia diarrhea & weakness	MTD; CI-994 4 mg/ m^2/day with paclitaxel 200 mg/m^2. carboplatin	1 CR bladder 2 PR NSCLC, 6 SD
PB+AC	I	6	Solid tumors	AC 25 mg/m2 o.d.days 1 –14 PB 400 mg/kg/day Cl days 6 and 13 every 5 weeks	ND	ND	No change in pre or post – tumor specimens for methyltransferase or GST
PB+ RA	-	5	APL	RA(30-90 mg/ m^2/day)+PB (150-400 mg/kg/day)	ND	ND	1/5 cytological CR
AN-9 + docetaxel [226]	II	12	Advanced NSCLC	AN-9 IV infusion 6h/ day for days 1-3 at 1.5-2.5 g/m^2, docetaxel on day 4 at 75 mg/m^2, regimen repeated every 3 weeks	No DLT, adverse events unrelated to AN-9, grade 3 neutropenia due to docetaxel in 9 (75%) patients	MTD 2.5 g/m^2 with 75 mg/m^2 docetaxel	3 PR, decrease in tumor size,

1.10 MS-275

A series of synthetic benzamide derivatives with HDAC-inhibitory activity both *in-vitro* and *in-vivo* were discovered by Mitsui pharmaceuticals (now, Schering AG). One of these, MS-275, a pyridyl carbamate, induces chromatin and protein hyperacetylation and antitumor activity through its two HDAC interaction sites. MS-275 is structurally and functionally unique, particularly with respect to its ability to induce cytotoxicity (Figure 1.7). The hypothesis is that MS-275's unique inhibition of HDAC activity modulates expression of a specific set of genes in malignant cells resulting in differentiation, growth arrest, and/or apoptotic cell death. The information obtained from translational research in clinical trials may help to identify critical targets of HDAC inhibitors in solid tumors. Limited toxicity observed in animal studies, especially during the 28-day dosing schedule, gave initial hope for MS-275 to be a potentially well-tolerated chemotherapeutic agent.

Preclinical pharmacology studies with MS-275 indicated a peak plasma concentration within 10 minutes when administered IV bolus, and 30 to 40 mins when administered orally. The MS-275 half-life ($T_{1/2}$) in plasma of approximately 1 hr was similar in rats, mice and dogs, irrespective of administration route. Approximately 81% of drug was bioavailable with oral administration, and preclinical toxicity was minimal to the parenchymal organs. The dose limiting toxicity (DLT) was myelosuppression in all species. In an oral daily schedule over 28 days, the maximal tolerated dose (MTD) was 6 mg/m^2 for dogs and 18 mg/m^2 for rats. Adverse events, mostly gastrointestinal

disturbances, fatigue, nausea and vomiting were usually observed during the 3rd and 4th week of dosing. *In-vitro*, human bone marrow sensitivity to MS-275 was similar to rats.

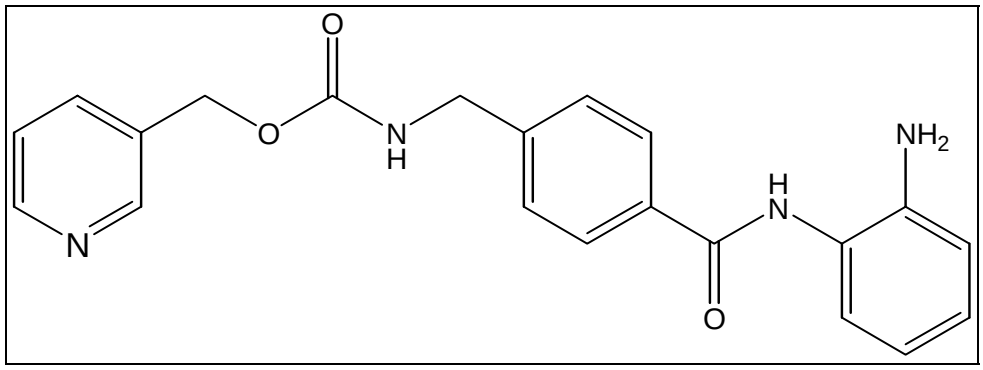

Figure 1.7 Structure of MS-275

1.10.1 Physico-chemical properties

Structure: Figure 1.7 depicts the structure of MS-275

Names: MS-275, MS-27-275 (NSC 706995),

Molecular Formula: $C_{21}H_{20}N_4O_3$

Molecular Weight: 376.41

Route of administration: Oral (by mouth). MS-275 exhibits good oral bioavailability, with comparable absorption as a tablet and a capsule (bulk powder). Dogs pretreated with pentagastrin to reduce gastric pH exhibited enhanced absorption and a decrease in individual variations of C_{max} and area under the curve (AUC).

Dose formulation: MS-275 is supplied as round orange (0.1 mg), light brown (1.0 mg), or intense yellow (5 mg) coated tablets. The film coating is an aqueous solution consisting of

hydroxypropylmethyl cellulose, talc, titanium dioxide, and one or two ferric oxide pigments as coloring. Each tablet contains mannitol, carboxymethylstarch sodium, hydroxypropyl cellulose, potassium bicarbonate and magnesium stearate.

1.10.2 Mechanism of action

MS-275, by inhibiting histone deacetylation, plays a major role in acetylation/deacetylation of histone proteins within the nucleosome. Inhibition of histone deacetylases induces histone hyperacetylation that, in turn, leads to gene expression in diverse hematopoietic and malignant cell lines *in-vitro* and *in-vivo* (Figure 1.8). Among the genes whose expression is induced by MS-275 is p21WAF-1/CIP-1, independent of p53 activity. The induction of p21, in turn, is thought to be responsible for the cell cycle arrest (at least in part through reduction of retinoblastoma protein phosphorylation) and antiproliferative activities of MS-275 seen in multiple malignant cell types. In addition to its ability to bypass p53-dependent pathways, MS-275 also appears to be independent of the presence and magnitude of multidrug resistance–1 (MDR1) gene/protein expression. There have been numerous *in-vitro* and *in-vivo* studies that have shown that MS-275 possesses antitumor activity.[35, 124-127, 227, 228] It has been recently shown that MS-275 preferentially inhibits HDAC1 but not HDAC6 which is reported to be responsible for tubulin deacetylation and for which a specific inhibitor has been recently reported in literature.[229] A structural analogue with 3-aminophenyl substitution showed none of the activities found for MS-275, indicating that the binding of 2-aminophenyl group of MS-275 to an unidentified site on HDAC molecules is important for its HDAC inhibitory function.[124] As shown in Figure 1.8, there was a dose-dependent decrease in radiolabelled

acetic acid released relative to control or 3'-aminophenyl substituted compound, indicating higher acetylation activity due to inhibition of HDACs.

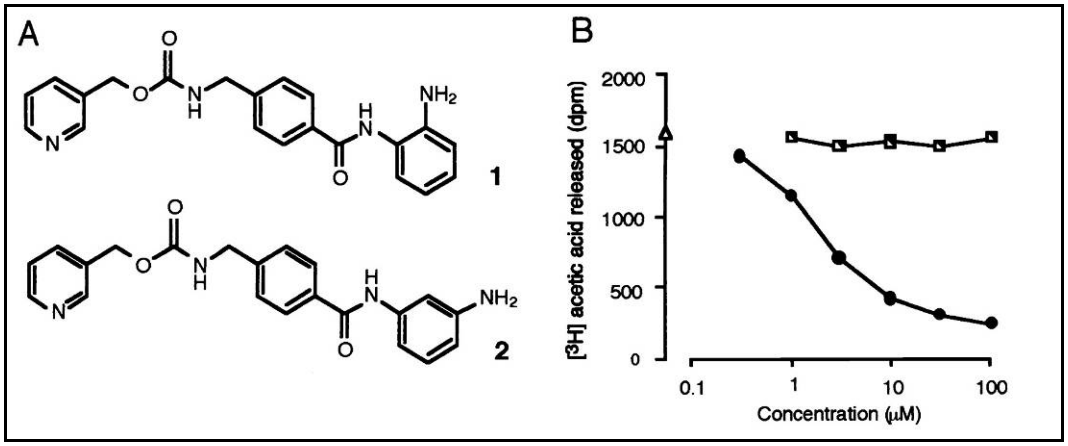

Data and figure adapted from [125]
A) Compound 1 is 2'-aminophenyl substituted MS-275 and compound 2 is 3'-amino derivative. B) Inhibition of human histone deacetylase by MS-275 when activity was measured using radiolabelled acetic acid either in the presence of MS-275 (●) or compound 2 (◥) or in the absence of the agent (△).

Figure 1.8 Hyperacetylation of histones on treatment with MS-275

1.10.3 In-vitro activity (molecular and cellular)

In National Cancer Institute's (NCI) 60 cell-line screen, MS-275 displayed a unique pattern of cytotoxicity in comparison to available anticancer agents, and displayed potent anti-proliferative activity.[230] Furthermore, cDNA microarray analysis suggested MS-275 promotes gene expression which subsequently favors growth arrest and differentiation. In addition, antitumor activity has been observed in myeloma, promyelocytic leukemia and SCLC models in studies at NCI. MS-275 may achieve its

antiproliferative effect through increased expression of p21 and TGF-beta type II receptor and may also promote differentiation in some cells as indicated by induction of the maturation marker gelsolin.[125, 228, 231]

Analysis of p53 and p21 (WAF1/CIP1) by Western blot indicated that when sensitive cell lines were exposed to MS-275, the accumulation of p21 was directly proportional to the cell line sensitivity and was independent of p53 levels. MS-275 also showed properties similar to the HDAC inhibitors sodium butyrate and trichostatin-A since it causes growth arrest with altered cell cycle distribution. Such modulation results in decreased S-Phase fraction, with concomitant induction of the actin-modulating protein, gelsolin, in PC3M cells. To identify differential mechanism of HDAC inhibitors to target the same genes, a cDNA microarray analysis was used to generate global gene expression profiles in prostate carcinoma (PC3M) cells in response to TSA and MS-275. These studies demonstrated that MS-275 has its own unique targets and HDAC binding site affinity. MS-275 was observed to have exposure time-dependent antitumor activities in 11 cell lines. The IC_{50} (concentration at which 50% growth inhibition occurs) for MS-275 was 2.0-4.8 μM (1.5-3.6 ng/ml) in human leukemia cell lines. Exposure to MS-275 at concentrations of 0.3 and 1 μM resulted in accumulation of hyperacetylated histones in tumor cell cultures. The levels of acetylation were identical in different cell lines (K562, HL-60, A2780, KB-3-1 and HCT-15).[124, 125]

MS-275 induced increased transcription of $p21^{WAF1/Cip1}$ and gelsolin, both of which are considered tumor suppressors. Accumulation of $p21^{WAF1/Cip1}$ in tumor cells with lower antiproliferative IC_{50} values (Table 1.4) tended to be faster and greater than in

tumor cells with higher IC_{50} values, while induction of gelsolin did not appear to correlate with the antiproliferative sensitivity of cells to MS-275. [125] However, when cells were inoculated in mice, there was decreased tumorigenicity due to overexpression of gelsolin, and hence investigators believe that gelsolin may function as a tumor suppressor *in-vivo* but not *in-vitro*. [232]

Table 1.4 *In-vitro* antiproliferative sensitivity of human tumor cell lines to MS-275

Cell line	Tumor type	IC_{50} (µM)
A2780	human ovarian cancer	0.0415
Calu-3	Human lung cancer	0.195
HL-60	Human leukemia	0.212
K562	Human leukemia	0.589
St-4	Human gastric cancer	0.820
HT-29	Human colorectal cancer	1.29
KB-3-1	Human oral cancer	1.46
Capan-1	Human pancreatic cancer	1.70
HCT-15	Human colorectal cancer	4.71

Data from MS-275 Investigator's Brochure

1.10.4 In-vivo activity

MS-275 has been tested on human tumor xenograft models prepared by subcutaneously injecting suspension of cancer cell lines into nude mice. Mice were then treated orally with daily doses (12.3, 24.5, or 49 mg/kg/day) of MS-275 on a 5 day/week dosing schedule repeated for 4 weeks. Compared with untreated and 5-FU-treated control groups, an anti-tumor activity of MS-275 was observed against the following carcinoma mouse models: 4-IST and St-4 Gastric, KB-3-1 epidermoid, Ca-pan-1 pancreatic, HT-29

colon, A2780 ovarian, and Calu-3 lung. The activity of MS-275 was superior to that observed with 5-FU in most cases. *In-vivo* efficacy was also examined in xenografts with human myeloma, RPMI-8226. SCID mice bearing subcutaneous RPMI-8226 xenografts were treated with MS-275 orally on a 5 day/week schedule repeated for 3 weeks at doses of 20, 30, and 45 mg/kg/day. The hollow-fiber assay indicated that MS-275 therapy was relatively ineffective after a short (~ 4 day) exposure, and these findings have lead investigators to further test a longer treatment regimen. Extended *in-vivo* studies of MS-275 showed good efficacy compared to irinotecan in the colon carcinoma model or paclitaxel in the lung carcinoma model. The best antitumor activity of MS-275 in human tumor xenografts was observed on a 4-week long oral, once daily schedule.[105]

1.11 Pharmacological and toxicological studies

Preclinical pharmacokinetic studies of MS-275 were performed in mice, rats, and dogs (data on file, Schering AG). In rodents, MS-275 was administered intravenously and orally in order to characterize the plasma concentration-time profiles and to determine bioavailability. Studies in dogs were more extensive and included assessment of oral bioavailability in fasted and fed animals; investigation of the effects of gastric pH on the absorption of MS-275; comparison of the pharmacokinetics of two different crystal forms of the compound; and evaluation of oral absorption following administration of MS-275 in tablets prepared for clinical use.

1.11.1 Pharmacokinetics in mice and rats

In mice, after a single intravenous bolus dose of 49 mg/kg, MS-275 achieved peak level (10 min) of 110 μM in plasma, followed by a biphasic decline with distribution and elimination half-lives of 0.16 hr and 1.3 hr, respectively. After oral gavage of 49 mg/kg, peak plasma levels of 67 μM were observed at 10 minutes. Elimination was monophasic, with a half-life of 1.1 hr. Calculation of AUC values of oral and intravenous administration yielded an estimated oral bioavailability of 81%. In rats, after a single intravenous bolus dose of 24.5 mg/kg, MS-275 achieved peak level (10 min) of 24.5 μM in plasma, followed by a biphasic decline with distribution and elimination half-lives of 0.31 hr and 2.1 hr, respectively. After oral gavage at 24.5 mg/kg, peak plasma levels of 14.9 μM were observed at 10 minutes. Elimination was monophasic, with a half-life of 1.7 hr. Calculation of AUC values of oral and intravenous administration yielded an estimated oral bioavailability of 75%. Initially, for quantification of MS-275 in mouse, rat and dog plasma, a reversed phase HPLC assay with UV detection at 230 nm was developed using an internal standard (4,4'-diaminobenzanilide) using solid phase extraction. Calibration curves were linear for MS-275 concentrations from 0.01 to 50 μM.

1.11.2 Pharmacokinetics in Dogs

Following administration of MS-275 to fasting dogs, the plasma concentration in each individual varied considerably (data on file, Schering AG). The standard deviations for Cmax, AUC, and bioavailability were relatively large (>50%) in the fasting group. However, the elimination was monophasic with a half-life of ~1 hr, similar to that observed after intravenous administration, so the variability was believed related to

individual differences in absorption. It was further postulated that these differences might be related to the effect of gastric pH on the solubility of MS-275. When gastric pH was lowered by prior administration of pentagastrin, the mean bioavailability was increased (from mean value of 30% to 55%), and the overall variability of the plasma concentration-time curves and derived pharmacokinetic parameters was reduced (Table 1.5). When animals were fed prior to MS-275 administration, mean C_{max}, and $AUC_{0\text{-}max}$ values were similar to those obtained in the fasting state, but the variability was considerably lower. The fed condition resulted in approximately 50% lower C_{max} and $AUC_{0\text{-}max}$ values compared with fasted + pentagastrin, but both interventions reduced the observed variability of MS-275 absorption. Food intake also appeared to delay T_{max} by approximately 20 min. Studies have demonstrated that MS-275 is reasonably well absorbed following oral administration to dogs (bioavailability 28-55%), but that absorption is substantially dependent on gastric pH and/or food intake. Sequential administration of MS-275 tablets observed higher C_{max} and AUC values than that of the powdered form. These results indicated that MS-275 tablets have higher bioavailability.

Table 1.5 Mean plasma pharmacokinetic parameters for oral administration of MS-275 (1.5 mg/kg = 30 mg/m^2) in beagle dogs

Study group	Cmax (µg/ml), (µM)	Tmax (h)	$t_{1/2}$ (h)	$AUC_{0\text{-max}}$ (µg*h/ml)	F (%)
IV	2.35 ± 0.28, (6.24 ± 0.73)	-	0.17 ± 0.07 (α) 0.96 ± 0.19 (β)	2.01 ± 0.23	-
Oral (fasted)	0.43 ± 0.32, (1.14 ± 0.85)	0.45 ± 0.21	0.90 ± 0.14	0.61 ± 0.49	30 ± 22
Oral (fasted + Pentagastrin)	0.87 ± 0.33, (2.31 ± 0.88)	0.50 ± 0.18	0.91 ± 0.10	1.11 ± 0.24	55 ± 9
Oral (fed)	0.40 ± 0.14, (1.06 ± 0.37)	0.81 ± 0.24	0.64 ± 0.08	0.56 ± 0.09	27 ± 3

Data is from MS-275 investigator's brochure. All values are mean ± SD. Pentagastrin was administered intramuscular (10 µg/kg) 15 mins prior to MS-275 dosing.

Oral absorption of MS-275 tablets was evaluated in four male beagle dogs by administering a total dose of 20 mg: 4 x 5mg tablets or 2 x 10mg tablets orally with 20 ml water. There were no significant differences in PK parameters between two combinations (Table 1.6). AUC and Cmax values (after correction for dose/body weight differences) were 1.45-2.29 fold and 0.83 to 3.29-fold higher, respectively, when administered as tablet compared to bulk powder. Hence, there was higher bioavailability in dogs for tablets indicating suitability for use clinical use.

Table 1.6 Mean plasma pharmacokinetic parameters for oral administration of MS-275 tablets at two different schedules in dogs

Dose regimen	Cmax (µg/ml), (µM)	Tmax (h)	$T_{1/2}$ (h)	$AUC_{0\text{-max}}$ (µg*h/ml)
4 x 5mg tablets	0.75 ± 0.17, (2.00 ± 0.45)	0.75 ± 0.20	0.73 ± 0.99	1.10 ± 0.11
2 x 10mg tablets	0.64 ± 0.30, (1.70 ± 0.80)	0.69 ± 0.13	0.64 ± 0.03	0.94 ± 0.43

Data from MS-275 Investigator's Brochure

1.11.3 In-vitro and in-vivo toxicity

Murine and human bone marrow progenitor cells (CFU_{GM}) were continuously exposed *in-vitro* to 0.001, 0.1, 1, 10 and 100 µM concentrations of MS-275. The IC_{90} values calculated from the second order regression analysis were 24, 5.8, and 15.1 µM for murine, canine, and human CFU_{GM}. The dog CFU_{GM} appeared to be more sensitive to the toxic effects of MS-275 than either human or mouse cells. The *in-vivo* MTD was 40 mg/kg/day when 240 mg/m2 of MS-275 was given to rats on a daily basis for 5 days (24). The MTD of MS-275 was 15 mg/kg/day (90 mg/m^2/day) and 3 mg/kg/day (18 mg/ m^2/day) for 14 and 28 days, respectively in mice. Bone marrow toxicity appeared to be a dose-limiting factor in the rat. The MTD of MS-275 given orally to dogs for 5 days was 2 mg/kg/day (40 mg/m^2/day). The MTD of MS-275 was less than 0.7 mg/kg/day (14 mg/m^2/day). Bone marrow and gastrointestinal toxicity also appeared to be DLT in dogs. Therefore, the maximally tolerated dose of MS-275 given orally once a day for 28 days in dogs was >0.3 mg/kg/day (6 mg/ m^2/day) (data on file, Schering AG).

Based on these promising pre-clinical data, several early phase clinical trials were initiated mainly to identify MTD, dose-limiting toxicities and a dosing regimen for further efficacy studies.

Hypothesis and Objectives

The hypotheses were tested and the objectives of the study were as follows:

1) Hypotheses

1. MS-275 will be well tolerated in the clinic when given orally at the proposed doses.
2. MS-275 will have quantifiable effects on the *in-vivo* biomarkers of anti-proliferation and apoptosis in the tumor cells.
3. The *in-vitro* and *ex-vivo* plasma protein binding will be extensive and linear in the clinically achievable concentration range.
4. Metabolism by transporters and phase II enzymes will be the major metabolic pathway for MS-275.
5. MS-275 will exhibit linear pharmacokinetics and single-dose pharmacokinetics will be useful in predicting steady state concentrations.
6. The relevant pharmacokinetic parameters of MS-275 absorption and disposition will be calculated, which may possibly explain inter-individual variability.

2) Objectives

1. To develop and validate an LC/MS assay that will quantitate MS-275 in human plasma or other matrix such as human liver microsomes.

2. To characterize the pharmacokinetics of oral MS-275 in plasma of patients with solid tumors and lymphomas.
3. To make pharmacodynamic correlations, if any, with the *in-vivo* anti-proliferative and apoptotic markers of biological effect and/toxicity.
4. To assess the *in-vitro* plasma protein binding of MS-275.
5. To characterize *in-vitro* the metabolic fate of MS-275.

CHAPTER 2

Detection and Quantitation of MS-275, a Histone Deacetylase Inhibitor, in Human Plasma, Liver Microsomes and Urine by High-Performance Liquid Chromatography-Electrospray Mass Spectrometry

2.1 Introduction

A validated analytical method is required for measuring the plasma concentrations of MS-275 in patients receiving the drug. Hence, a rapid method was developed for the quantitative determination of MS-275, in human plasma. The method was also applied and slightly modified to quantify concentration of MS-275 in different matrices, namely, urine and human liver microsomes. For the plasma matrix, calibration curves were constructed in the range of 1 to 100 ng/ml, and were analyzed using a weight factor proportional to the nominal concentration. Sample pretreatment involved a one-step protein precipitation with acetonitrile of 0.1-ml samples. The analysis was performed on a column (75 × 4.6 mm I.D.) packed with 3.5-μm Phenyl-SB material, using methanol – 10 mM ammonium formate (55:45, vol/vol) as the mobile phase. The column effluent was monitored by an UV detector at wavelength of 205nm and mass spectrometry with positive electrospray ionization. The values for precision and accuracy were always ≤ 5.58% and < 11.4% relative error, respectively. This validated method was then successfully applied to examine the pharmacokinetics of MS-275 in cancer patients.

2.2 Experimental details

2.2.1 Chemicals and materials

MS-275 (batch number: 81300002; HPLC purity, 99.82%) was supplied as a crystalline white powder by Schering AG (Berlin, Germany). HPLC-grade methanol and acetonitrile were obtained from J.T. Baker (Phillipsburg, NJ, USA). Ammonium formate and formic acid were purchased from Sigma (St. Louis, MO, USA). Deionized water was generated with a Hydro-Reverse Osmosis system (Durham, NC, USA) connected to a Milli-Q UV Plus purifying system (Malbourough, MA, USA). Drug-free heparinized human plasma was obtained from the National Institutes of Health Clinical Center Blood Bank (Bethesda, MD, USA).

2.2.2 Equipment and instrumentation

The experiments were carried out with a HP1100 system (Agilent Technology, Palo Alto, CA, USA). The system consisted of a G1312A binary pump, a mobile phase vacuum degassing unit, a G1329A autosampler, a temperature-controlled column compartment, and a HP1100 single-quadrupole mass-spectrometric (MS) detector equipped with an electrospray source. The autosampler seat and needle sets consisted of a polyether-ether-ketone-based needle seat and assembly, and a Tefzel seal (Agilent Technology) was used in the injector valve to avoid carry-over. Data were acquired and integrated by the ChemStation software run on a HP Vectra 150/PC with a Windows NT operating system. The stationary phase was composed of Phenyl-SB material (Agilent Technology) packed in a stainless steel column (75 × 4.6 mm I.D. with 3.5 μm particle

size), and a Phenyl-SB guard column (12.5 × 4.6 mm I.D. with 5 μm particle size) attached to a column-inlet filter (3 mm × 0.5 μm; Varian, Walnut Creek, CA, USA). PEEK tubing of 0.127 mm I.D. (Upchurch Scientific, Oak Harbor, WA, USA) was used to connect the column to the pump and the MS detector with minimal tubing length to avoid an excessive post-column volume.

2.2.3 Chromatographic and MS conditions

Chromatographic separations were achieved using a mobile phase consisting of methanol and 10 mM ammonium formate (pH 3, adjusted with formic acid) (55:45, vol/vol), with a flow rate set at 0.8 ml/min. The analytical column was kept at ambient temperature. The column effluent was connected to an electrospray ionization MS interface without splitting. The MS detector was operated in the positive ion mode, with single ion monitoring at a fragmentor setting of 65 V and a multiplier gain of 2. Nitrogen was used as the nebulizer gas at a pressure of 55 PSI and as drying gas at a flow rate of 13 l/min and a temperature of 350°C. The capillary voltage was set at 2200 V, and selected-ion monitoring was accomplished at m/z 377 for the protonated molecular ion of MS-275. Monitoring was performed using a dwell time of 578 ms and was monitored in the high-resolution mode. Simultaneously, UV detection was done at 230 nm and 280 nm to detect possible metabolites in clinical samples. After data acquisition, the selected-ion monitoring chromatograms were integrated using the HP ChemStation software and used for quantitation.

2.2.4 Preparation of standards

Stock solutions were prepared in triplicate by accurately weighting, after correction for purity, an appropriate amount of MS-275 and dissolving in methanol. The final concentration of the stock solutions was 1 mg/ml, and these were stored at -20^{o}C. Working standard solutions were prepared over a range of 0.02 to 40 µg/ml by serial dilution of the stock solution with methanol, and then stored at -80^{o}C. Plasma calibration standards of 1, 5, 10, 20, 50 and 100 ng/ml were prepared fresh as needed by mixing 30 µl working standard solution with 570 µl blank human plasma. Quality control (QC) samples were prepared from an independent stock solution at concentrations of 3, 40, and 80 ng/ml by dilution of the working stock solution with blank human plasma. These QC samples were subdivided into 0.1-ml aliquots, and stored at –80^{o}C. Standard and QC solutions were prepared as shown in Table 2.1 and Table 2.2 respectively.

Table 2.1 Preparation of standards

QC	Concentration	Mixture
A	1mg/ml	10mg/10ml(MeOH)
B	40µg/ml	1ml of A solution/25ml(MeOH)
C	10µg/ml	1ml of B solution + 3ml of MeOH
D	2µg/ml	1ml of C solution + 4ml of MeOH
E	0.2µg/ml	0.5ml of D solution + 4.5ml of MeOH

Working standards		Spiking solution	Spiking solution (µl)	MeOH (µl)
F	**2000**	C	200	800
G	**1000**	C	100	900
H	**400**	D	200	800
I	**200**	D	100	900
G	**100**	D	50	950
K	**20**	E	100	900

Standard solutions	Spiking solution	Spiking solution (µl)	Plasma (µl)
100	F	30	570
50	G	30	570
20	H	30	570
10	I	30	570
5	G	30	570
1	K	30	570

Table 2.2 Preparation of quality controls

QC	Concentration	Mixture
I	1mg/ml	10mg/10ml(MeOH)
II	40µg/ml	1ml of I solution/25ml(MeOH)
III	8µg/ml	1ml of II solution + 4ml of MeOH

Working QC solutions		Spiking solution	Spiking solution (µl)	MeOH (µl)
IV	**1600**	III	200	800
V	**800**	III	100	900
VI	**60**	V	75	925

QC solutions	Spiking solution	Spiking solution (µl)	Plasma (µl)
80	IV	200	3800
40	V	200	3800
3	VI	200	3800

2.2.5 Sample preparation

Standards, QCs samples, and patient samples were allowed to thaw at room temperature. A 0.1-ml aliquot of each was transferred to a 1.5-ml Eppendorf tube (Hamburg, Germany) and 500 µl of acetonitrile were added to precipitate plasma proteins. The mixture was vortex-mixed for 30 seconds, and then centrifuged for 5 minutes at 13,000 rpm. A volume of 500 µl of the clear supernatant was transferred to a glass tube and evaporated to dryness under desiccated air in a water bath at 45^{o}C in a Zymark TurboVap LV (Hopkinton, MA, USA). The residue was reconstituted in 200 µl

of a mixture of methanol and water (50:50, vol/vol), followed by vortex-mixing. A 50-µl volume of the reconstituted sample was injected into the chromatographic system.

2.2.6 Validation characteristics

To evaluate the specificity of the analytical procedure, blank human plasma samples obtained from 6 different individuals were extracted and analyzed for the presence of interfering endogenous substances. In addition, plasma samples containing mixtures of several commonly administered drugs were tested for potential chromatographic interference with MS-275.

Calibration curves were constructed by plotting the peak area of the analyte versus the nominal concentration (x) of the calibration standards. The regression parameters of slope, intercept and correlation coefficient were calculated by a weighted ($1/x^2$) least-squares linear regression analysis. The linearity was evaluated by comparing the correlation coefficient (r^2), residuals and errors between theoretical and back calculated concentrations of calibration standard samples.

The accuracy and precision were assessed by analyzing QC samples prepared at 3 different concentrations equally distributed over the tested range (i.e., spiked at 3, 40, and 80 ng/ml) in 6 replicates on 3 different days. The accuracy of the assay was evaluated by the percentage deviation (DEV) from the theoretical concentration (TC) using the formula:

$$DEV = 100\% \times (\text{mean back calculated concentration} - TC) / TC$$

Within- and between-assay precision were obtained by one-way analysis of variance (ANOVA) testing, and reported as relative standard deviation for each QC concentration. The extraction recovery for MS-275 in human plasma was determined at 3 concentration levels in triplicate using samples spiked to contain 3, 40, and 80 ng/ml, using comparison with samples prepared in 50% (vol/vol) methanol in water injected without extraction.

The stability of MS-275 in human plasma was assessed during three freeze-thaw cycles and at room temperature for up to 24 hours. Four aliquots of QC samples of three different concentrations were thawed at room temperature, and kept at this temperature for 0, 12, and 24 hours, and immediately analyzed. For the freeze-thaw stability study, QC samples at three different concentrations in quadruplicate, and stored at -80^{o}C for 24 hours. Next, the samples were thawed at room temperature, and were refrozen for 12 hours under the same conditions. The freeze-thaw cycle was repeated two more times, and then analyzed on the third cycle.

2.2.7 Clinical experiment

To demonstrate the applicability of the final analytical procedure, samples were obtained from a cancer patient, who participated in the ongoing multi-dose Phase I clinical trial with MS-275 tablets as single-agent therapy. The drug was administered orally with a meal at a dose of 10 mg/m^2. The current experiment was approved by the local Institutional Review Board, and the patient signed informed consent before study entry for the blood sampling procedure. A total of 11 blood samples (7 ml each) were

obtained and collected in 10-ml glass tubes containing heparin as an anticoagulant. These samples were obtained before drug administration and at approximately 0.5, 1, 2, 6, 12, 24, 36, 48, 60 and 72 hours after drug administration. Specimens were immediately centrifuged at 3,000 g for 5 minutes to separate the plasma supernatant, which was stored at -70°C until the time of analysis. Plasma concentration-time data of MS-275 were analyzed by noncompartmental methods using the software package WinNonlin v4.0 (Pharsight Corp., Mountain View, CA) using equal weighting.

2.3 Results and discussion

2.3.1 Chromatography

The mass spectrum of MS-275 showed a protonated molecular ion (MH^+) at m/z 377, in accordance with the NTP chemical repository database, a sodium adduct at m/z 399 ($MH^+ + Na$), and a prominent fragment ion peak at m/z 359 ($MH^+ - H_2O$) (Figure 2.1).

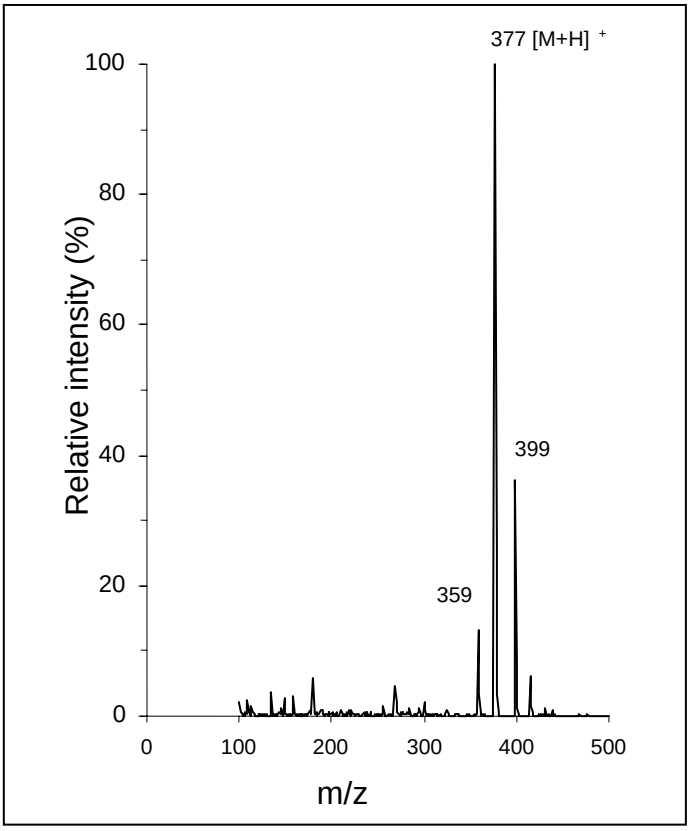

Figure 2.1 Liquid chromatographic-electrospray mass spectrum of MS-275

Sample pretreatment was initially performed by a solvent extraction (e.g., using ethyl acetate) or by solid phase-extraction (e.g., using C18 micro-extraction columns). However, these procedures resulted in poor extraction recovery, particularly at the upper limit of the expected concentration range (i.e., around 100 ng/ml). This is likely the result of the hydrophilic nature of MS-275, which is highly soluble in water (approximately 20 mg/ml at 20°C in acidic buffers). Among various alternative procedures tested, MS-275 was eventually efficiently extracted with adequate elimination of endogenous interfering compounds using a single protein precipitation step with acetonitrile. In the final

procedure, only a small fraction of the sample after extraction was injected (i.e., 50 µl of 200 µL used for reconstitution) on the column to maintain high efficiency and resolution, and assay sensitivity was thus compromised. Although increased injection volumes could achieve higher response factors, overloading of the small column resulted in asymmetric sample bands. The presence of 10 mM ammonium formate (pH 3) in the reconstitution mixture was found to induce a distorted separation artifact, which resulted in unstable response factors over time following repeat injections of extracted patient samples (not shown). In the final procedure, therefore, reconstitution of samples was performed with a mixture of methanol and water (50:50, vol/vol). Out of various chemicals that were tested, 4, 4'-diaminebenzanilide was initially selected for use as internal standard. But, we were unable to use 4, 4'-diaminebenzanilide due to incidences of variability in extraction when plasma from different sources was used.

2.3.2 Validation characteristics

Figure 2.2 displays chromatograms of an extract of blank human plasma sample (**A**), and an extract of a plasma sample spiked with MS-275 at a concentration of 1.0 ng/ml (LLOQ) (**B**). The mean retention time for MS-275 during the method validation was 4.3 minutes, and the overall chromatographic run time was established at 8 minutes.

Several different drugs were tested for potential interference with MS-275 (Table 2.3), and none of these drugs was found to give an interfering peak during the analysis around the retention time of MS-275. Plasma samples were acquired from patients who were currently taking these medications.

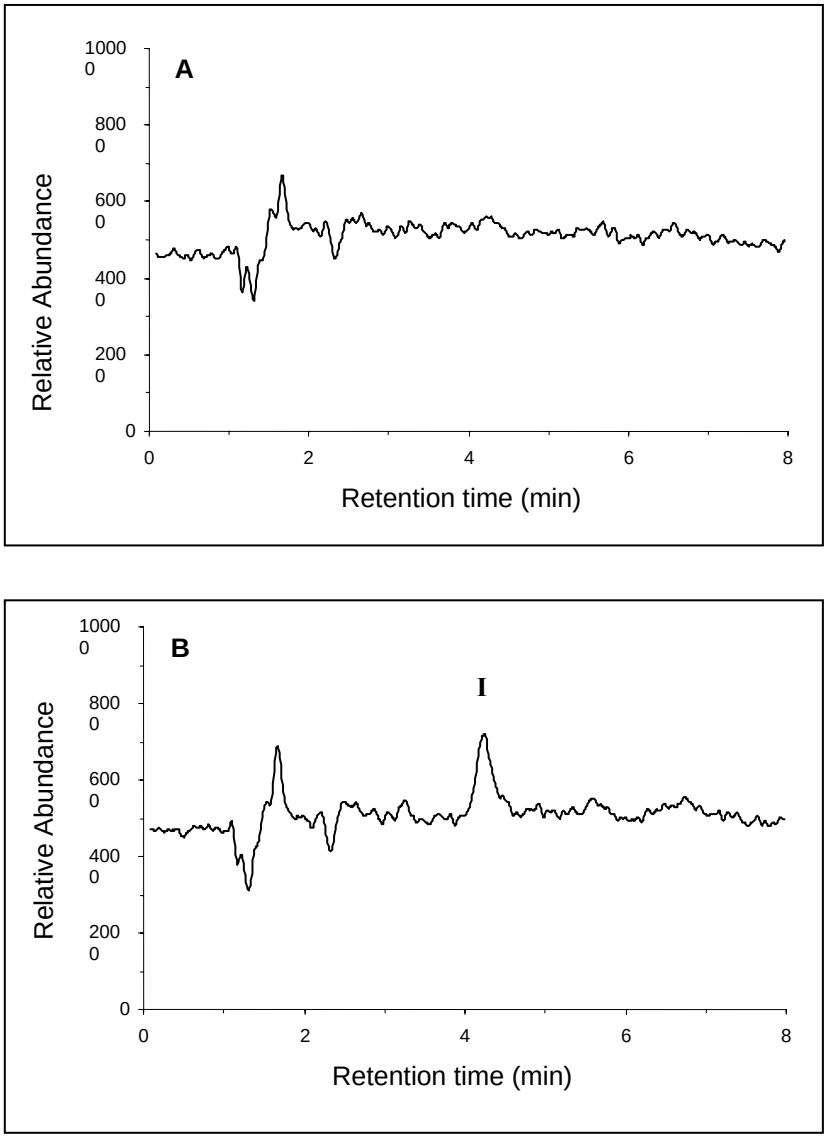

Figure 2.2 Typical chromatogram of reversed-phase liquid chromatographic analysis of a blank human plasma sample (A), and a human plasma sample spiked with MS-275 at a concentration of 1 ng/ml (B). The labeled chromatographic peak indicates MS-275 (I).

Table 2.3 Interference analysis of various commonly administered drugs

Amlodipine mesylate	Glucosamine sulfate	Palmidronate disodium
Atenolol	Hydromorphone	Phenytoin
Ciprofloxacin	Hydroxyzine	Pseudephedrine
Clotrimazole	Ketoconazole	Pyridoxine hydrochloride
Cyanocobalamine	Levofloxacin	Raloxifene
Dexamethasone	Levothyroxine	Ranitidine
Diazepam	Loperamide	Rofecoxib
Diphenhydramine	Metronidazole	Sertraline hydrochloride
Docusate sodium	Morphine sulfate	Verapamil
Epoetin alpha	Omeprazole	Warfarin
Fluticasone propionate	Ondansetron	Zolpidem tartarate
Folic acid	Oxycodone	

The assay for MS-275 analysis in plasma was found to be linear over the range of 1.0 to 100 ng/ml, applying the peak area in combination with a weighting factor of $1/x^2$, as indicated by the mean linear-regression correlation coefficient of 0.998 (n = 3). A comparative evaluation of accuracy between unweighted and $1/x^2$ weighted analysis is provided in Figure 2.3.

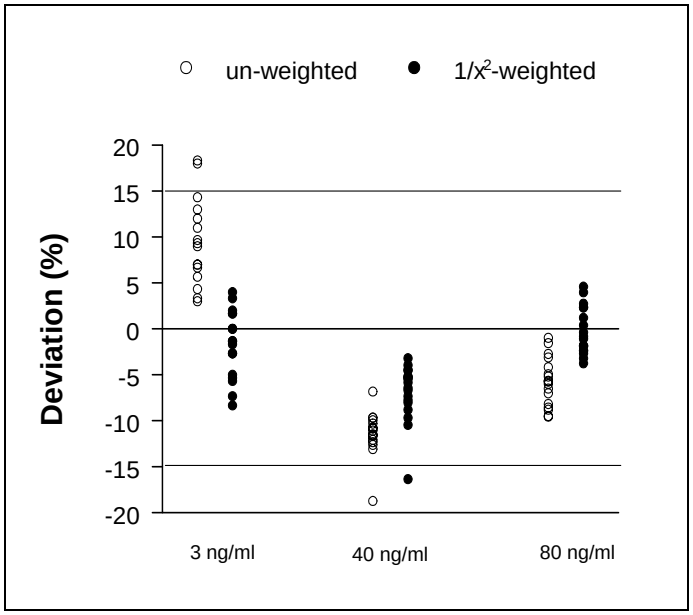

The horizontal dotted lines indicate the acceptable ± 15% deviation range

Figure 2.3 Comparison of accuracy (percent deviation from nominal) for unweighted versus $1/x^2$ weighted analysis of MS-275 in human plasma at 3 different concentrations

In blank human plasma spiked with MS-275 at 1.0 ng/ml, the mean percentage deviation from the nominal concentration and the within-run variability were both less than 20% [233]. Based on these results, the lower limit of quantitation for MS-275 in human plasma was determined to be 1.0 ng/ml, using 0.1-ml sample volumes. The limit of detection was determined to be 0.5 ng/ml but due to lack of reproducibility and high within-run variability, the lower limit of quantitation was confirmed to be at 1 ng/ml.

Validation data of the analytical method in terms of accuracy (percent deviation) and precision are shown in Table 2.4. The mean (± SE) equation was: Y = 7388 (±335) * X - 2091 (±571). At the upper limit of quantitation (i.e., 100 ng/ml), the mean percentage deviation and the within-run variability were less than 15%. The method was shown to be accurate, with an average accuracy at the three tested concentrations within ± 7% of nominal values, and precise with a within-run and between-run variability of less than 3.75%. The mean overall extraction recovery, determined at three different concentrations, was 37.9% (standard effect, 0.126%). A non-parametric Kruskal-Wallis one-way ANOVA indicated a minor concentration-dependence (p = 0.027), as determined by a Tukey-Kramer multiple comparison test for all pairwise differences between the means (Table 2.5).

Table 2.4 Validation summary for the analysis of MS-275 in spiked human plasma samples

Parameter	**Nominal concentration (ng/ml)**		
	3	40	80
Accuracy			
Mean observed (ng/ml)	2.95	37.2	79.8
Deviation (%; n = 18)	-1.69	-6.92	-0.26
Precision			
Intraday (%; n = 6)	4.58	1.13	1.56
Interday (%; n = 18)	3.75	3.31	2.56

Table 2.5 Recovery of MS-275 in human plasma (data expressed as chromatographic peak area of MS-275)

Nominal (ng/ml)	Plasma peak area	Methanol peak area	Relative recovery (%)
3	76984	181773	41.7
3	76783	187090	
3	77369	185003	
40	1152760	3269960	34.8
40	1133914	3248894	
40	1123663	3279752	
80	2419225	6517666	37.0
80	2433135	6522078	
80	2401394	6560018	

However, this effect is presumably due to normal analytical variability rather than reflecting a concentration-dependent extraction recovery. An improvement in recovery could be accomplished by using increased volumes of acetonitrile for primary isolation, followed by a repeat of the entire extraction procedure. However, in view of the relative consistency in the generated data, and the rapidity and ease of use, all experiments were performed using a one-step protein precipitation. Repeated freeze-thawing cycles had no influence on the stability. In addition, plasma samples spiked with MS-275 and stored for variable time periods at ambient temperature were also stable (Table 2.6 and Figure 2.4). On the basis of the generated validation parameters, the method was considered acceptable for the analysis of plasma samples in support of clinical pharmacokinetic studies. [233]

Table 2.6 Short-term temperature stability of MS-275 in plasma

Time (h)	Nominal (ng/ml)	Recovered mean ± SD (ng/ml)	Deviation (%)
0	3	3.00 ± 0.07	-0.08
0	40	40.5 ± 0.73	1.29
0	80	81.5 ± 0.86	1.83
12	3	2.55 ± 0.05	-15.0
12	40	39.9 ± 0.53	-0.33
12	80	78.0 ± 2.77	-2.50
24	3	2.71 ± 0.08	-9.75
24	40	39.8 ± 1.89	-0.47
24	80	78.9 ± 0.71	-1.37

Figure 2.4 Short-term temperature stability of MS-275 in plasma

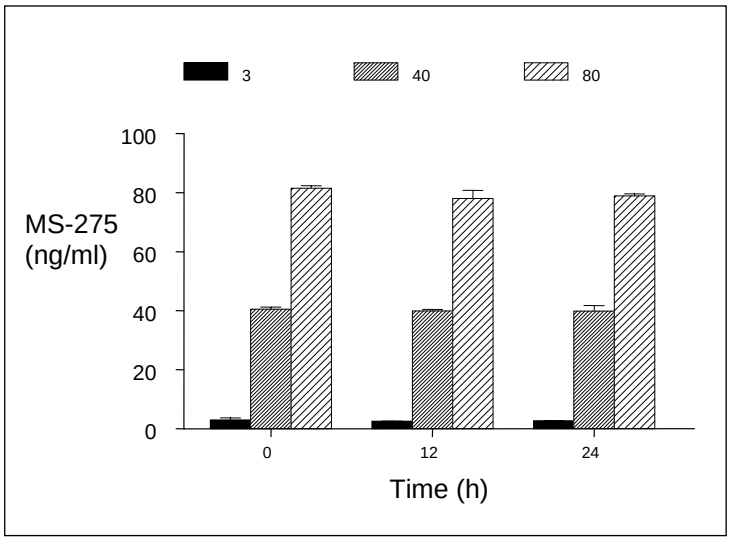

2.3.3 Clinical application of analytical method

The described analytical method was applied to a pharmacokinetic pilot study of MS-275 given orally to a single cancer patient. The observed concentration-time profile

of MS-275 is shown in Figure 5. The time to peak concentration occurred before the first sampling time point, and hence the initial absorption phase of MS-275 was not observed in this patient. The peak concentration of MS-275 was 41.7 ng/ml, and the area under the concentration-time curve amounted to 400 ng·h/ml, with an apparent oral clearance value of approximately 42 l/h/m^2. Ultraviolet detection was also carried out on all samples, but no additional peaks that might represent metabolites of MS-275 were detected.

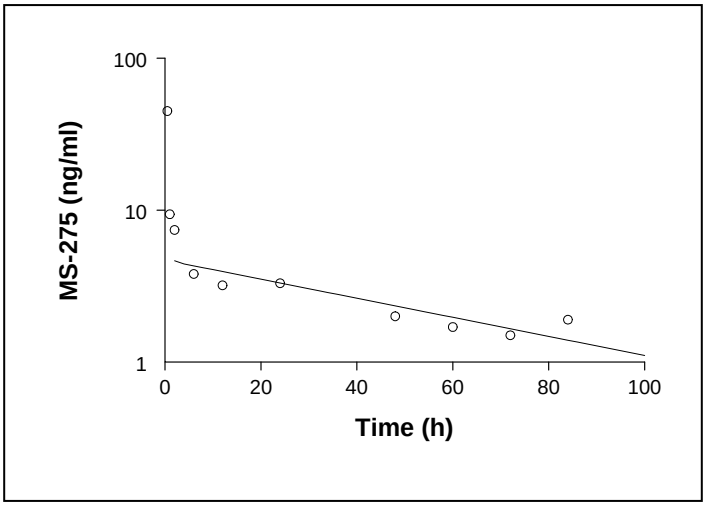

Figure 2.5 Plasma concentration-time profile of MS-275 in a patient with cancer after a single oral administration of the drug at a dose of 10 mg/m^2

2.4 Conclusion

In conclusion, the method presented for the determination of MS-275 in human plasma is specific, accurate and precise, and is selective and sensitive enough to be used

in clinical trials. The method permits the analysis of patient samples with low concentrations of MS-275, and is currently being used in various Phase I clinical trials in patients with hematological malignancies or solid tumors to further investigate the clinical pharmacologic profile of this agent.

CHAPTER 3

In-vitro and *In-vivo* Characterization of Plasma Protein Binding Profile of MS-275

3.1 Introduction

A preliminary pharmacokinetic evaluation of MS-275 given orally to cancer patients indicated that the terminal half-life of MS-275 in plasma (approximately 50 hours) is substantially longer than that observed in laboratory animals (approximately 1 hour). The basis for this long half-life in humans, at least as a speculation, is possibly related to enterohepatic recirculation processes. However, a variety of other factors may influence the prolonged circulation of MS-275 in humans, including binding of the compound to plasma proteins. Indeed, drugs with high affinity for plasma proteins often demonstrate a relatively slow distribution and elimination of drug from the central compartment, which may prolong the apparent half-life [234]. The purpose of this study was to characterize the binding properties of MS-275 to human plasma and individual proteins using a novel microequilibrium dialysis method, and to evaluate potential interspecies differences in binding affinity that might help explain the apparent pharmacokinetic discrepancy between humans and laboratory animals.

3.2 Materials and methods

3.2.1 Chemicals and reagents

MS-275 (batch number: 81300002; chromatographic purity, 99.82%) and [*G*-^{3}H] MS-275 (specific activity, 1543.6 MBq/mg, 17.5 MBq/ml) were kindly supplied by

Schering AG (Berlin, Germany). The final concentration of MS-275 in the radiolabelled vial was determined to be 11.3µg/ml (29.1 µM). HPLC-grade methanol and acetonitrile were obtained from J. T. Baker (Phillipsburg, NJ, USA). Ammonium formate and formic acid were purchased from Sigma (St. Louis, MO, USA). Deionized water was generated with a Hydro-Reverse Osmosis system (Durham, NC, USA) connected to a Milli-Q UV Plus purifying system (Marlborough, MA, USA). Bio-Safe II scintillation fluid was obtained from Research Products International (Mount Prospect, IL, USA). Purified human proteins, including albumin, α1-acid glycoprotein (AAG), α- , β-, and γ-globulin, fibrinogen, and lipoproteins, as well as mouse, rat, rabbit, dog, and pig plasma were obtained from Sigma. Other chemicals were of reagent grade or better. Pure protein solutions at respective physiological concentrations in healthy individuals were prepared in 0.01 M phosphate buffer (pH 7.4). The stock solutions of all test substances were made in dimethylsulfoxide. Human blood was obtained from healthy volunteers or cancer patients receiving MS-275, and the plasma fraction was separated by centrifugation (3000 × *g* for 5 min at 37 °C), and used within 1 hour after collection. Frozen, drug-free heparinized human plasma was obtained from the National Institutes of Health Clinical Center Blood Bank (Bethesda, MD, USA).

3.2.2 Development and validation of dialysis method

Initially this method was developed to characterize protein binding of docetaxel and several parameters were optimized as shown below (Table 3.1). Most of these

selected parameters were then incorporated in optimization of a standardized method for characterizing protein binding of several other drugs including MS-275.

Table 3.1 Details of the parameter optimization for micro-equilibrium dialysis method

Parameters	Tested values	Selected values
Molecular weight cut-off of plate membranes	5kDa, 10kDa	5kDa
Reaction time (to reach equilibrium) range	0.5, 1, 2, 3, 4, 6, 8, 16, 24, 48 h	5 hour
Wait time after mixing and before counting	1', 5', 30', 1h, 24h	5'
Scintillation counting time	1', 20'	1'
Spiking effects of [^{3}H] drug	Plasma chamber, PBS chamber	Plasma
Volume of dialysate used for counting	1/4th, 1/3rd, 1/2 and 3/4th of reaction volume	1/2
Total volume of reaction for plasma and PBS	200 µl, 250 µl , 300 µl	250 µl
Effect of cold drug on changes in fu using [^{3}H] drug	10, 100, 1000, 10000 ng/ml	No effect
Quenching in plasma on scintillation counting	2h, 4h, 6h, 8h, 24h, 48h	No effect till 8h

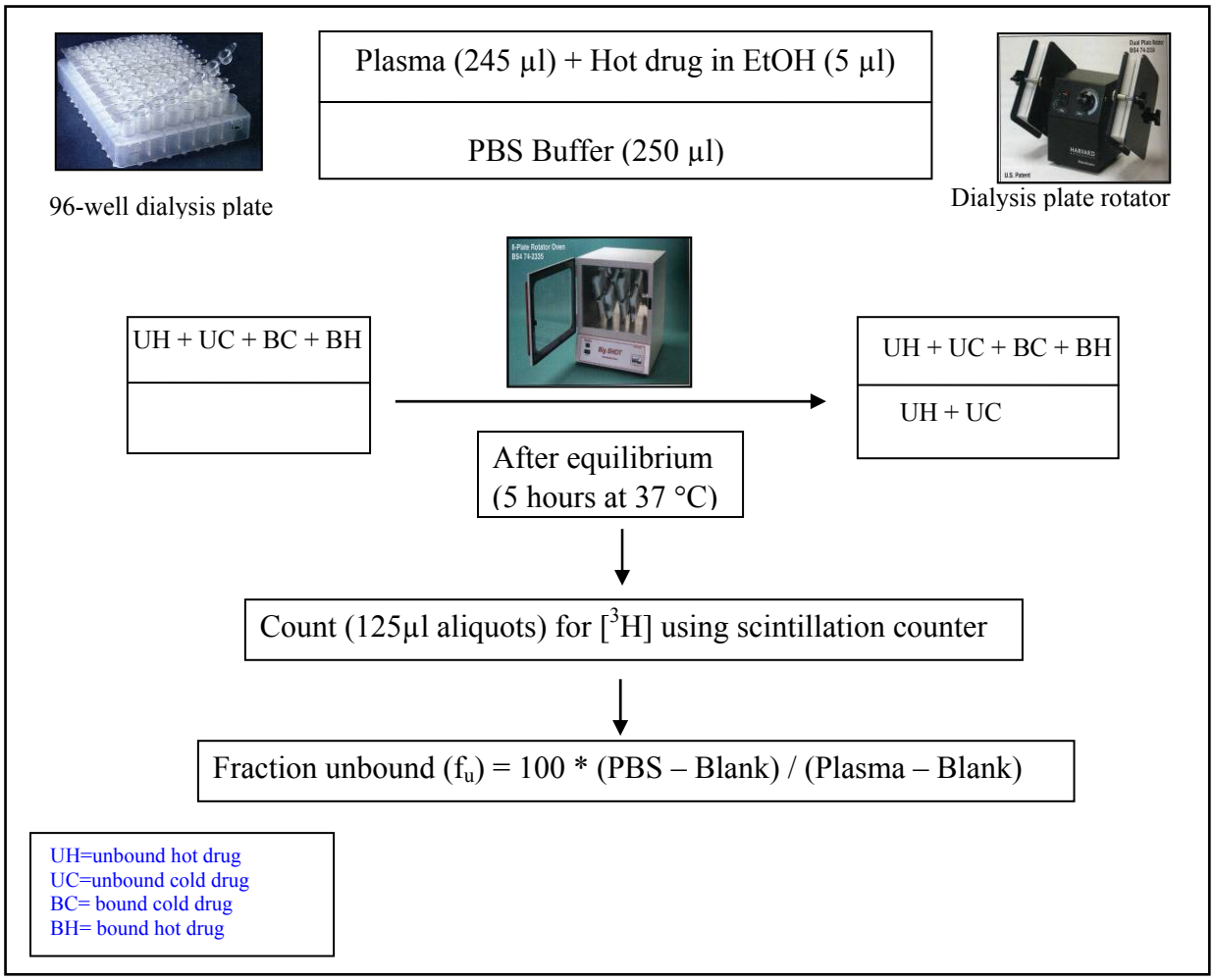

Figure 3.1 Layout of equilibrium dialysis method

For MS-275, equilibrium dialysis was performed on a plate rotator (Model # 74-2334, Harvard Apparatus, Holliston, MA, USA) at 37°C in a humidified atmosphere of 5% CO_2 using 96-wells micro-dialysis plates (Harvard Apparatus) [235]. The dialysis compartments in each well are separated by a regenerated cellulose membrane with a 5-kDa cut-off. Experiments were carried out with 250-µl aliquots of plasma containing a

tracer amount of [*G*-^{3}H] MS-275 against an equal volume of 0.01 M phosphate buffer (pH 7.4). Drug concentrations in 125 µl-aliquots of both compartments were measured by liquid scintillation counting for 1 minute following the addition of Bio-Safe II scintillation fluid on a Model LS6000IC counter (Beckman Instruments, Inc., Columbia, MD).

To evaluate the specificity of this procedure and check for displacement effect of other drugs on protein binding of MS-275, blank human plasma was spiked with 19 different commonly administered drugs at a concentration of 1 µg/ml and was analyzed for changes in the fraction unbound drug (f_u). The accuracy and precision were assessed by analyzing quadruplicate samples prepared from 5 different plasma sources in quintuplicate on 5 separate occasions. Within- and between-assay precision estimates were obtained by one-way analysis of variance, and reported as relative standard deviation. The impact of stability of MS-275 protein binding in human plasma was assessed during a freeze-thaw cycle at room temperature after 24 hours.

3.2.3 In-vitro binding experiments

Preliminary experiments indicated that volume shifts during the dialysis period were negligible (< 10%), and hence the results were used directly without applying a correction factor. The time course of equilibrium was assessed in quadruplicate at 15 and 30 minutes, and at 1, 2, 3, 4, 5, 6, 22, 24 and 28 hours after start of the experiment. Since f_u measurements were to be made on patient samples that contained variable amounts of

drug, f_u was also determined in plasma samples over the anticipated clinically relevant concentration range of MS-275 (i.e., 0, 1, 5, 10, 50, 100 and 500 ng/ml).

3.2.4 Estimation of binding parameters

The drug concentration ratio in the buffer and plasma or protein solution after dialysis was calculated for each paired observation, and was taken as an estimate of the unbound drug fraction (f_u). The bound drug fraction (f_{bd}) was calculated as $f_{bd} = (1 - f_u) \times 100\%$.

Modified Scatchard plots were constructed using the bound drug concentration (C_{bd}) and the unbound drug concentration (C_u), and initial estimates of binding parameters were obtained using an automated-model selection procedure implemented in the Siphar v4.0 software package (InnaPhase, Philadelphia, PA, USA). For human albumin and AAG, the observed data were described by equations for saturable [$C_{bd} = {}^{m}\Sigma_{I=1} (n_i P \times K_i \times C_u) / (1 + K_i \times C_u)$] and non-saturable binding [$C_{bd} = (nK) \times C_u$]. In these equations, C_{bd} and C_u are expressed as molar concentrations, m is the number of binding site classes, n the number of saturable binding sites per mole of protein in the i-th class (1, 2, or 3), P the molar concentration of protein binding, K the association constant, and nK the contribution constant of nonspecific, non-saturable binding on one site (per molar concentration of protein). Binding parameters were calculated by an iterative nonlinear regression analysis using the Powell minimization algorithm and weighted least squares with a weight equal to 1/*y*. The models were evaluated by the Akaike Information

Criterion, weighted sum of squared deviations and the coefficient of variation for each parameter estimate.

3.2.5 Patients and treatment

Blood samples were available from 5 patients, who were enrolled onto a Phase I clinical study with MS-275 as single-agent therapy [236]. Individual drug doses were normalized to body-surface area, and were administered orally as capsules (Schering AG) with food at a dose of 10 mg/m^2. Trial design, inclusion and exclusion criteria, premedication regimens, and detailed clinical profiles are documented elsewhere. The clinical protocol was approved by the National Cancer Institute review board (Bethesda, MD, USA), and all patients provided written informed consent before entering the study. From each patient, serial plasma samples were obtained during the first course of treatment at the following time points: (i) immediately before drug administration (pre-dose), and (ii) at 0.5, 1, 2, 6, 12, 24, 48, 60, 72, and 84 hours after the first drug administration. All blood samples were immediately placed in an ice-water bath, centrifuged within 30 minutes of collection at 1000 × *g* for 10 min at 4°C, and were stored at or below –70 °C until analysis (see below).

3.2.6 Measurement of total drug concentrations

Total MS-275 concentrations were determined using previously validated analytical method based on liquid chromatography coupled with mass spectrometric detection [237]. Chromatography was carried out with a HP1100 system (Agilent

Technology, Palo Alto, CA, USA). Data were acquired and integrated by the ChemStation software run on a HP Vectra 150/PC with a Windows NT operating system. Calibration curves ranged from 1 to 100 ng/ml, and were analyzed using a weight factor proportional to the nominal concentration. Sample pretreatment involved a one-step protein precipitation with acetonitrile of 0.1-ml samples. The analysis was performed on a stainless steel column (75 × 4.6 mm I.D.) packed with 3.5-µm Phenyl-SB material (Agilent Technology), using methanol – 10 mM ammonium formate (pH=3) (55:45, vol/vol) as the mobile phase. The lowest limit of quantitation was 1 ng/ml and the values for precision and accuracy were always ≤ 5.58% and < 11.4% relative error, respectively. The method was successfully applied to examine the pharmacokinetics of MS-275 in cancer patients.

3.2.7 Measurement of unbound drug concentrations

The fraction unbound (f_u) MS-275 in each individual patient plasma sample was determined using equilibrium dialysis, and samples were analyzed for total radioactivity (i.e., [*G*-^{3}H] MS-275) by liquid-scintillation counting as described above. The unbound drug concentrations (C_u) were calculated from the fraction unbound drug (f_u) and the total drug concentration in plasma (C_p) (i.e., the total of unbound and protein bound), as $C_u = f_u \times C_p$.

3.2.8 Pharmacokinetic analysis

Estimates of pharmacokinetic parameters for total and unbound MS-275 in plasma were derived from individual concentration-time data sets by noncompartmental analysis using the software package WinNonlin v4.0 (Pharsight Corporation, Mountain View, CA, USA). The area under the plasma concentration-time curve (AUC) was calculated using the linear trapezoidal method from time zero to the time of the final quantifiable concentration ($AUC_{[tf]}$). The AUC was extrapolated to infinity by dividing the last measured concentration by the rate constant of the terminal phase (k), determined by log-linear regression analysis. The apparent oral clearance of MS-275 (CL/F) was calculated by dividing the administered dose by the observed $AUC_{[inf]}$, and the terminal half-life was calculated as $ln2 / k$.

3.2.9 Statistical considerations

All experiments were performed in triplicate on at least 3 separate occasions, and statistical analyses were carried out using NCSS v2001 (J. L. Hintze, Kaysville, UT, USA). The effects of MS-275 concentration, concomitant drugs, and protein source on drug binding were estimated by a one-way ANOVA, and if overall $p < 0.05$, then followed by the Tukey-Kramer *post-hoc* test. All data are presented as mean values ± standard deviation (SD), unless stated otherwise, and for all tests the *a priori* cutoff for statistical significance was taken at p-value < 0.05.

3.3 Results

3.3.1 Validation of dialysis method for MS-275

Preliminary experiments revealed that the time to equilibrium was attained around 5 hours (Figure 3.2). All data were fitted to a sigmoidal maximum effect (Emax) model based on modified Hill equation, as follows: $E = Eo + Emax * [(KP^{\gamma})/(KP^{\gamma} + KP_{50}^{\gamma})]$. In this equation, Eo is the minimum reduction possible, fixed at a value of 0, Emax is the maximum response, fixed at 100, KP is the pharmacokinetic parameter of interest, KP_{50} is the value of parameter predicted to result in half of the maximum response, and γ is the Hill constant describing the sigmoidicity of the curve. It was confirmed in all equilibrium dialysis experiments that the total drug recovery from the fractions was equal to the amount of [*G*-^{3}H]MS-275 added to the plasma samples (mean recovery, 98%; $P > 0.05$ *versus* hypothesized mean of initial value = 100%). The mean relative SD of all sample values was less than 10%, assuring high discriminatory power in the detection of changes in MS-275 f_u in patient samples. With the final method, the within-run and between-run variability were always less than 6.4% and 9.8%, respectively.

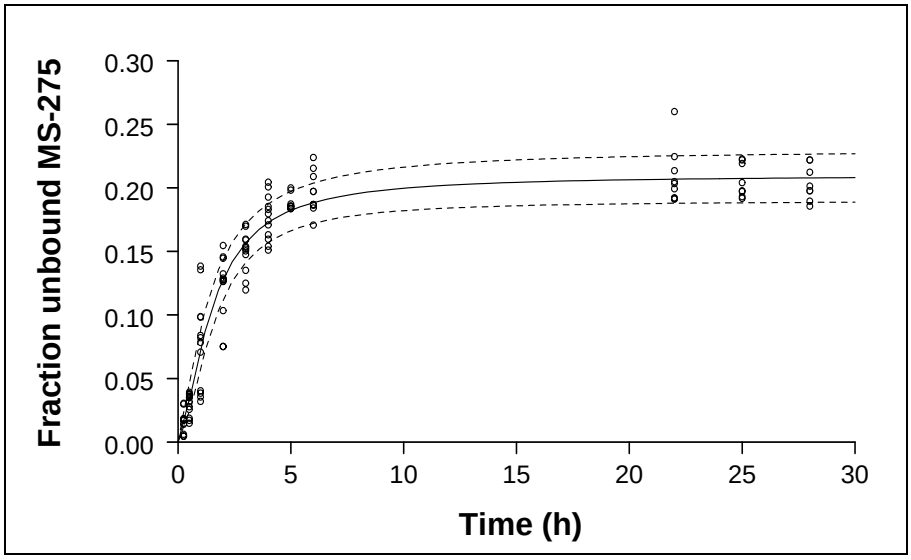

Data are presented as individual observations (symbols) and a predicted model fit according to a modified Hill function ($R^2 = 0.930$) (solid lines) with 95% prediction intervals (dotted lines).

Figure 3.2 Time course to reach equilibrium for determining optimal fraction unbound MS-275

Fresh plasma from 5 different sources was analyzed for f_u in triplicate, and then the same samples were frozen and thawed at room temperature on the next day and immediately analyzed to determine f_u. The mean f_u values were 0.188 and 0.206, respectively, before and after the freeze-thaw cycle ($P > 0.05$), suggesting no significant influence. In separate experiments using the LC-MS assay, the chemical stability of MS-275 during the dialysis was confirmed by analysis of plasma samples spiked with 100 ng/mL of MS-275 in dialysis plates after incubation for 5 hours at 37 °C.

3.3.2 In-vitro binding interactions with MS-275

MS-275 was found to bind moderately to human plasma (mean, 81.2 ± 3.2%), with a free drug fraction of 0.188 ± 0.008. There was no significant source difference in f_u when plasma was used from different healthy individuals (mean f_u, 0.185; p = 0.0938). The f_u obtained in previously frozen plasma from healthy volunteers was found to be slightly higher than that observed in the plasma from six cancer patient (mean f_u, 0.188 *versus* 0.168; p = 0.113).

At clinically relevant concentrations of MS-275 (1 to 500 ng/ml), the binding was concentration independent (P > 0.05), indicating a low-affinity, possibly non-specific and non-saturable process. MS-275 binding to physiological levels of albumin (3.5 – 4.5 g/dL; f_u, 0.27 ± 0.042) and AAG (0.04 – 0.1 g/dL; f_u, 0.19 ± 0.0037) was similar, drug-concentration independent (p = 0.53 and p = 0.80, respectively), and similar to the binding to patient plasma (Figure 3.3). When albumin and AAG were combined in the same buffer, the mean f_u was 0.146 ± 0.0010, suggesting that albumin and AAG contribute to the majority of binding of MS-275 in human plasma. Regression modeling based on plots of bound concentration vs. unbound concentration revealed that the weak binding to albumin and AAG was non-saturable on a single site in the concentration range studied, with the bound concentration linearly related to unbound drug ($R^2 > 0.99$). Binding affinity to AAG, as described by the slope, was about 4.7-fold higher than that of albumin, with association constants for non-saturable binding (nK) of 0.0247 ± 0.0003 μM^{-1} and 0.116 ± 0.020 μM^{-1} for albumin and AAG, respectively. Subsequent

experiments indicated that MS-275 also had weak binding affinity for globulins (α, β, γ), fibrinogen, and high and low-density lipoproteins (Fig 3.3).

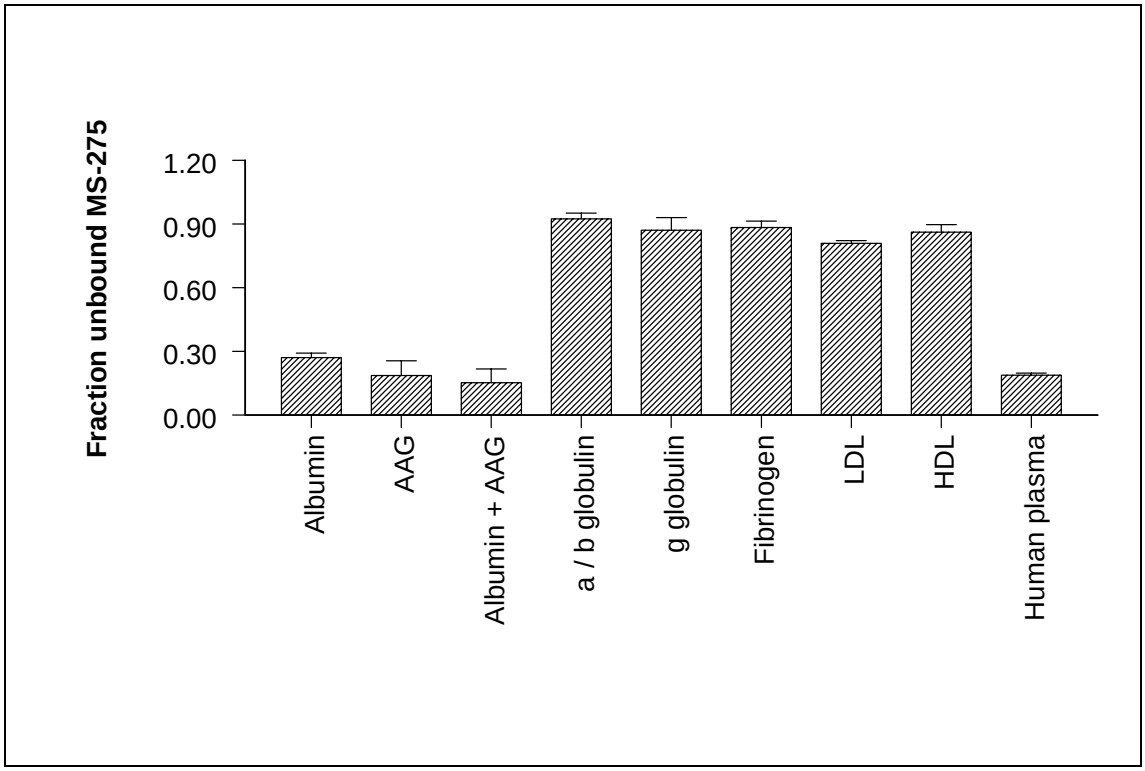

Data are presented as mean values (bars) ± SD (error bars). AAG, α_1-acid glycoprotein (0.04 – 0.1 g/dL); LDL, low-density lipoprotein (0.06 – 0.13 g/dL); HDL, high-density lipoprotein (0.04 – 0.14 g/dL); Fibrinogen (3 – 4 g/dL); α, β-globulins (0.3 – 0.9 g/dL); γ-globulin (0.7 - 1.5 g/dL); All, combined mixture of all tested proteins.

Figure 3.3 Binding of MS-275 to human plasma proteins.

3.3.3 Displacement interactions on binding sites

A slightly increased f_u was observed in the presence of ibuprofen (f_u, 0.236 ± 0.001) and metoclopramide (f_u, 0.270 ± 0.042), suggesting a weak displacement from

protein-binding sites (p = 0.00012, one-way ANOVA) (Table 3.2). The other tested drugs did not significantly alter the protein binding of MS-275.

Table 3.2 Effect of potentially co-administered drugs on plasma binding of MS-275

Drug name (1 µg/ml)	Fraction unbound MS-275		% change vs. control (p-value*)
	Mean	SD	
Acetylsalicylic acid	0.187	0.0163	+6.58 ± 5.35 (NS)
Alendronate	0.159	0.0124	-9.33 ± 4.06 (NS)
5-Azacytidine	0.178	0.0163	+1.40 ± 5.36 (NS)
Caffeine	0.221	0.0185	+25.8 ± 6.07 (NS)
Celecoxib	0.162	0.0447	-22.4 ± 14.7 (NS)
Cyclosporin A	0.178	0.0087	-0.389 ± 2.87 (NS)
Dexamethasone	0.182	0.0327	+14.1 ± 10.7 (NS)
Docetaxel	0.168	0.0099	-4.16 ± 3.26 (NS)
Erythromycin	0.164	0.0113	-6.48 ± 3.72 (NS)
Fludarabine	0.163	0.0095	-7.10 ± 3.13 (NS)
Hydrocortisone	0.170	0.0038	-3.18 ± 1.24 (NS)
Ibuprofen	0.236	0.0013	+34.6 ± 0.443 (0.00162)
Ketoconazole	0.173	0.0075	-1.83 ± 2.47 (NS)
Metoclopramide	0.247	0.0243	+40.8 ± 8.00 (0.00327)
Midazolam	0.174	0.0082	-0.808 ± 2.70 (NS)
Nifedipine	0.178	0.0139	+1.19 ± 4.57 (NS)
Paclitaxel	0.168	0.0083	-7.11 ± 2.74 (NS)
Ritonavir	0.177	0.0010	+0.817 ± 0.00 (NS)
UCN-01	0.169	0.0035	-3.94 ± 1.14 (NS)

*NS= not significant

3.3.4 Interspecies differences in MS-275 binding

MS-275 demonstrated a striking interspecies difference in plasma protein binding (p= 0.00846, one-way ANOVA) (Figure 3.4); compared to human plasma, the binding of MS-275 was significantly reduced in the mouse (f_u, 0.378 ± 0.101), rat (f_u, 0.393 ± 0.0070), rabbit (f_u, 0.375 ± 0.0416), dog (f_u, 0.436 ± 0.0159), and pig plasma (f_u, 0.439 ± 0.0116).

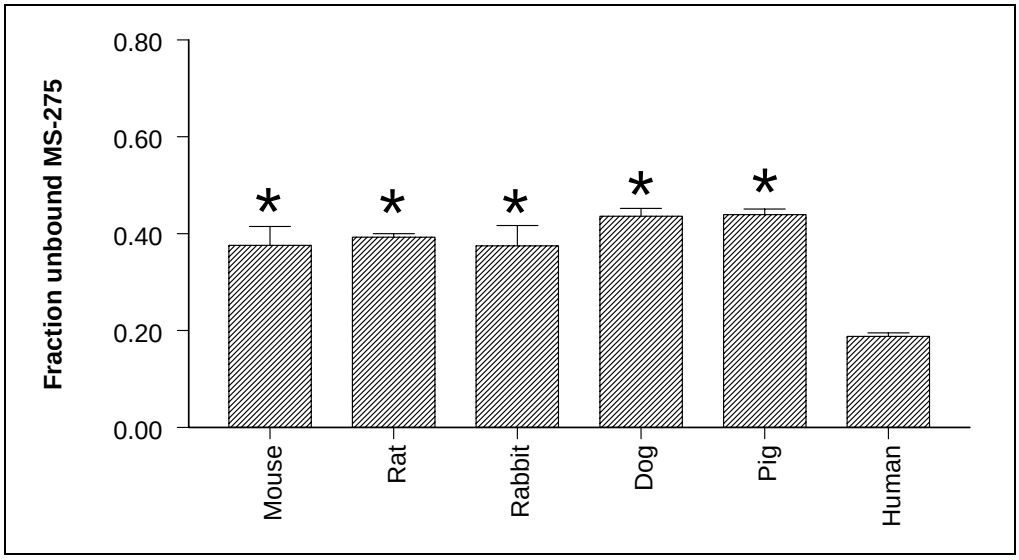

Data are presented as mean values (bars) ± SD (error bars), and the star (*) indicates p < 0.05 versus human plasma

Figure 3.4 Interspecies comparison of MS-275 binding to plasma

3.3.5 Clinical pharmacokinetics of unbound MS-275

The developed equilibrium dialysis method was applied to prospectively define the concentration-time profiles of total and unbound MS-275 in 5 patients with cancer receiving single-agent MS-275, which was administered orally at a dose of 10 mg/m^2. The mean plasma concentration-time profiles for total and unbound MS-275 are shown in Fig 3.5A. A summary of the pharmacokinetic parameters for total and unbound MS-275 is provided in Table 3.3. Moderate inter-individual variability in unbound MS-275 pharmacokinetic parameters was noted at the 10 mg/m^2 dose level, with a coefficient of variation for the apparent oral clearance of 36%. *In-vivo*, there were no significant changes in extent of MS-275 binding with 79.7 ± 5.9% (n = 56) drug bound based on data obtained at individual sampling time-points (Fig 3.5B).

Table 3.3 Summary of total and unbound pharmacokinetic parameters*

Parameter	Total MS-275	Unbound MS-275
Cmax (ng/ml)	50.6 ± 64.6 (9.41 – 163)	7.25 ± 7.18 (1.75 – 19.1)
Tmax (h)	1.0 (0.50 – 2.0)	1.0 (0.50 – 2.0)
AUC (ng·h/ml)	476 ± 155 (360 – 747)	96.6 ± 41.7 (56.2 – 167)
CL/F (l/h/m^2)	22.4 ± 5.43 (13.4 – 27.8)	117 ± 42.1 (59.8 – 178)
$T_{1/2}$ (h)	46.4 ± 12.6 (27.7 – 60.3)	52.4 ± 18.8 (30.3 – 80.5)
AUC ratio C_u/C_p	N/A	0.20 ± 0.042 (0.14 – 0.25)

* Data were obtained from 5 patients receiving MS-275 orally at a dose of 10 mg/m^2, and are presented in the table as mean values ± SD with range in parentheses, except for Tmax (median)
Abbreviations: Cmax, peak plasma concentration; Tmax, time to peak concentration; AUC, area under the plasma concentration-time curve; CL/F, apparent oral clearance; $T_{1/2}$, half-life of the terminal phase; C_u, unbound drug concentration; C_p, total drug concentration in plasma.

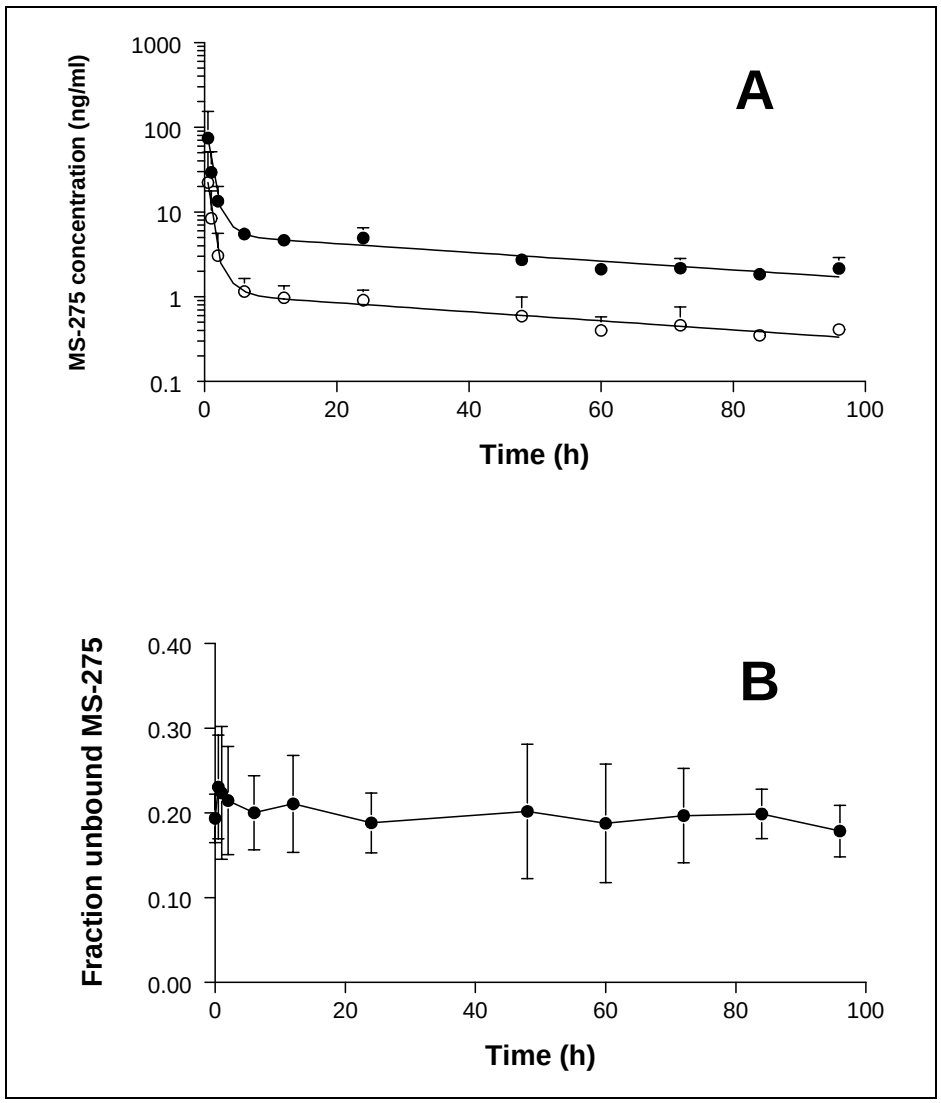

Data are presented as mean values (symbols) ± SD (error bars), and were obtained from 5 patients with cancer treated with MS-275 given orally at a dose of 10 mg/m^2.

Figure 3.5 Concentration-time profiles of total MS-275 (ng/ml) (closed circle) and unbound MS-275 (ng/ml) (open circle) in plasma (panel A) and the fraction unbound MS-275 in plasma versus time profiles (panel B).

3.4 Discussion

In the present study we have described the *in-vitro* and *ex vivo* plasma protein binding of MS-275, an investigational histone-deacetylase inhibitor. The binding of MS-275 to human plasma was approximately 81% and independent of drug concentration over the presumed clinically relevant range. When binding studies were extended to individual plasma proteins, it was found that AAG and human serum albumin contributed to about an equal extent to drug binding, with an association constant for nonspecific, nonsaturable binding of 0.116 μM^{-1} and 0.0247 μM^{-1} for AAG and albumin, respectively. There was a slight increase in value of f_u obtained from healthy volunteer plasma compared to plasma from six cancer patients. Even though this difference was not statistically significant, the decrease in overall f_u may be due to the plasma protein level changes that occur in cancer patients, including decreased albumin [238] and increased AAG [239].

In cancer patients, AAG concentrations vary approximately 5-fold between patients, and these variations may contribute to differences in protein binding and systemic drug clearance.[240] Albumin levels are lower in most cancer patient population due to adverse effects from chemotherapeutic regimen. AAG has been identified as a significant predictor of clearance of certain drugs (e.g. docetaxel), with high AAG levels being associated with reduced clearance. [241] Plasma binding of certain drugs may be further influenced by the presence of its formulation vehicles, such that there is an increase in its unbound fraction.[242] This time-dependent change in unbound fraction may result in unwanted toxicity if there is a correlation between exposure to unbound drug and

dose-limiting toxicities. In case of MS-275, because it is only moderately bound, there will be minor influence of plasma protein binding on pharmacokinetic profile.

Since treatment with MS-275 commonly involves numerous other drugs, interactions of bound MS-275 by these agents might occur, particularly in view of the relatively weak associations with its main binding proteins, AAG and albumin. The effect of 19 potentially co-administered drugs with MS-275 on its binding to plasma was performed with the maximum reported clinical concentrations of these drugs. It was found that only ibuprofen and metoclopramide at relevant clinical concentrations, significantly increased f_u of MS-275. Previous investigations have shown that albumin is the major binding protein in plasma for ibuprofen [243]. Furthermore, statistically significant interactions involving displacement of drugs from binding sites on albumin by ibuprofen have been described for various drugs [244]. However, based on theoretical considerations outlined in detail elsewhere [245], it is unlikely that changes in the protein binding of MS-275 as a result of co-administration of ibuprofen *in-vivo* will significantly influence the systemic exposure to MS-275. Nonetheless, since preliminary data seem to indicate that MS-275 might have a rather narrow therapeutic concentration range [236], the combined use of MS-275 with high doses of ibuprofen should be carefully monitored. The increase in f_u in the presence of metoclopramide is less well understood. The main binding protein for metoclopramide in human plasma is AAG [246], but its affinity is less than that of UCN-01 [247], which does not substantially interfere with the binding properties of MS-275. Given the structural similarities of metoclopramide and MS-275, it is possible that the observed interaction involves competition for the same site on an as

yet unidentified plasma protein. The other tested agents had no substantial influence on the binding of MS-275, even at relatively high concentrations, and are thus unlikely to modulate the pharmacokinetic profile of MS-275 *in-vivo*.

The present study demonstrated a striking species-dependence of plasma protein binding of MS-275. There was a remarkable two-fold difference in plasma protein binding of MS-275 to human plasma as compared to plasma from a variety of other species that are commonly used for pre-clinical studies. The reasons for the large differences in binding of MS-275 between the test species are currently unknown, although one possibility is species-dependent binding of MS-275 to AAG, as has been described previously for various xenobiotic ligands [248], including the staurosporine analogue UCN-01 [247]. Regardless of the underlying mechanism, this species dependent binding of MS-275 should be taken in consideration when attempting to extrapolate data obtained in tumor-bearing animals to the clinical situation. Because only unbound drug is involved in distribution and systemic elimination [234], the differential binding of MS-275 might explain, at least in part, the relatively slow apparent oral clearance and the long terminal half-life of observed in humans (~50 hours) [236], in comparison with the laboratory animals (mice 1.1 h, rats 2.1 h, dogs <1 h) (Schering AG, data on file).

There was moderate inter-individual variability in unbound MS-275 pharmacokinetic parameters at the dose level tested, with a relatively lower variability for the apparent oral clearance, which suggests that the inter-individual variation in plasma protein binding of MS-275 is relatively small in metabolically normal individuals. Consistent with the *in-vitro* data, almost 80% of drug was bound within the circulation

without any trend over time. Therefore, protein binding does not seem to be an important factor in pharmacokinetic monitoring for MS-275 in cancer patients, and that the more easily measured total MS-275 concentrations provide a consistent and accurate reflection of the unbound concentrations with relatively lower interpatient variability (i.e., the binding is concentration independent and reversible).

3.5 Conclusions

In conclusion, a reliable and reproducible equilibrium dialysis method for the determination of the fraction unbound MS-275 in plasma was developed and validated. MS-275 was found to bind with a moderate degree of affinity to several human plasma proteins, including AAG and albumin. This clearly signifies the importance to account for differences in the fraction unbound drug when attempting to extrapolate data obtained in *in-vitro* model systems in protein-free media to the clinical situation. The plasma binding of MS-275 was also found to be significantly species-dependent. Indeed, whereas in humans the major fraction of the administered drug is sequestered by AAG and albumin, thereby restricting the unbound concentration and affecting distribution and elimination pathways, in the other test species binding of MS-275 to plasma proteins was relatively insignificant. This not only provides a mechanistic explanation for the observed species differences in pharmacokinetic parameters of MS-275 noted previously, but also suggests that interspecies relationships between drug exposure measures and pharmacodynamic outcome of treatment should be based on unbound MS-275 concentrations.

CHAPTER 4

In-vitro Characterization of Absorption and Elimination Pathways of MS-275

4.1 Introduction

Interindividual variability in MS-275 pharmacokinetics, toxicity and response is extensive, and largely unexplained. We hypothesized that this is due to affinity of MS-275 for an uptake transporter that indirectly regulates elimination pathways. Here, we studied accumulation of [^{3}H] MS-275 in *Xenopus laevis* oocytes injected with cRNA of the liver-specific organic anion transporting polypeptide (OATP) family members OATP1B1 (OATP2) or OATP1B3 (OATP8).

Based on our data from similar experiments with paclitaxel, it was found that paclitaxel transport by OATP1B1 expressing oocytes was not significantly different from that of controls, whereas uptake by OATP1B3 was 3.25-fold higher ($P<0.0001$). OATP1B3-mediated paclitaxel transport was saturable (Michaelis-Menten constant, 6.79 μM), time-dependent, and highly sensitive to chemical inhibition. Furthermore, uptake was inhibited by the formulation excipient Cremophor EL (74.4% inhibition, $P<0.0001$, concentration = 10 μl/ml = 15 v/v), cyclosporin A (25.2%, $P=0.005$), glycyrrhizic acid (24.6%, $P=0.012$), and hyperforin (28.4%, $P=0.003$) at their clinically relevant concentrations. These data indicated that OATP1B3 is a key regulator of hepatic uptake, and suggested that this transporter has a role in the variable response to paclitaxel treatment.

Similar to paclitaxel, substantial interindividual differences in MS-275 pharmacokinetics, toxicity and response have been observed. However, the reasons for this variability are not well understood, but can be hypothesized to be due to disposition profile of MS-275. MS-275 is a novel compound under clinical development, and currently there are no published data in literature about metabolic pathways. The initial hypothesis is that MS-275 will be a substrate to hepatic CYP450 enzymes that play a role in metabolism and elimination of approximately 70% of drugs. It is increasingly recognized that drug disposition is highly dependent on the interplay between drug metabolizing enzymes and transporters [249]. There is a possibility that MS-275 is a substrate of the efflux transporters such as ABCB1 (P-glycoprotein) and/or ABCG2 (MDR1), and the mechanisms by which MS-275 may be taken up into hepatocytes also remain unknown.

Members of the organic anion transporting polypeptide (OATP) family mediate the cellular uptake of a large number of structurally diverse endogenous compounds and xenobiotics [250, 251]. The expression of OATP1B1 (formerly OATP2, OATP-C or LST-1) and OATP1B3 (formerly OATP8 or LST-2) is restricted to the basolateral membrane of hepatocytes [252, 253]. Consequently, these transporters facilitate the hepatocellular accumulation of compounds prior to metabolism and biliary secretion, and thus are likely to play an important role in governing drug disposition. Genetic polymorphisms in several members of the OATP family have been described [251], and there is accumulating evidence that these can result in interindividual variability in the pharmacokinetics of certain substrate drugs [254-256].

Hepatic phase I metabolic studies were performed using incubations with human liver microsomes, Tris Buffer, $MgCl_2$ and NADPH generating system. Both heat-inactivated microsomes and microsomes without NADPH generating system were used as negative controls. Incubations were terminated with the addition of acetonitrile and the supernatant was removed and evaporated to dryness and reconstituted samples were analyzed using the validated LC-MS assay.

Hepatic phase II metabolism for glucuronidation was also studied using an incubation of human liver microsomes with MS-275 (at different concentrations) along with UDPGA, magnesium chloride, 1-4 saccharolactone, alamethicin and Tris buffer. The urinary excretion data, if available, will be used to determine the 'total' MS-275 excreted in urine and the glucuronidated MS-275 which will be obtained by subtracting the amount of 'parent' compound from the 'total' MS-275 amount.

Based on the data available from the clinical trial on patients taking MS-275 on a biweekly schedule, a more-than proportional increase in mean or median peak concentrations (Cmax) with increasing dose, particularly at higher dose level was noticed (Appendix Figures 4.5 and 4.6). This may, in part, be due to the lower cohort size (n=3 patients) at these dose levels which may have increased the observed variability. Alternatively, there is a possibility that MS-275 may be a substrate for gastrointestinal efflux transporters such as P-glycoprotein (P-gp, ABCB1) or multi-drug resistance proteins such as ABCG2 (MDR1), commonly present in intestinal membranes. If MS-275 were a substrate, then at higher dose levels, it may be saturate these transporters and

hence peak concentrations measured in plasma compartment would increase more than proportional with dose.

ABCB1 (P-gp) as well as ABCG2 are the most prominent efflux transporters in the human intestine.[257] It is widely recognized that most compounds that are substrates of P-gp are also known to be metabolized by CYP3A4 (except for digoxin, fexofenadine, and possibly topotecan).[258-260] We have shown that MS-275 is not metabolized by CYP3A4 (from phase I experiments) and hence MS-275 may not be a substrate or an inhibitor of this transporter. This, of course, does not rule out possible role of other intestinal uptake and absorption transporters. Also, based on the new Biopharmaceutics Drug Disposition Classification System, MS-275 can be considered to fall under Class 3 compounds (high solubility, low permeability) and thus, absorptive transporter effects may predominate as compared to efflux transporter effects.[261] Also, the amount of drug administered as a single dose may not be high enough to saturate such transporters. To confirm the hypothesis of such substrate specificity, cellular accumulation experiments were performed using cell-lines transfected with genes that will specifically express P-gp or ABCG2.

4.2 Materials and methods

4.2.1 In-vitro uptake studies

Uptake of MS-275 was studied using *Xenopus laevis* oocytes specifically expressing human liver organic anion transporting proteins (OATPs). *Xenopus laevis* oocytes injected with water, OATP1B1 or OATP1B3 cRNA were purchased from BD

Biosciences (Woburn, MA). Studies were performed in sodium buffer containing 10 mM HEPES/Tris, 100 mM NaCl, 1 mM $MgCl_2$, 2 mM KCl and 1 mM $CaCl_2$, adjusted to pH 7.4 (BD Biosciences). [^{3}H]Paclitaxel (5 Ci/mmol), which was used as a positive control was obtained from Moravek Biochemicals Inc., (Brea, CA). The oocytes were washed and 8 to 12 were incubated at room temperature in 100 µL buffer containing 1µM of [*G*-^{3}H] MS-275 (Schering AG, Germany; purity, >99%) and 20 nM paclitaxel (final ethanol concentration 1%). After 90 minutes, the oocytes were washed four times with 3 ml of ice-cold buffer. The oocytes were then placed in individual scintillation vials and lysed by the addition of 150 µL 10% SDS (BD Biosciences) and agitation for 10 minutes. Following the addition of 5 ml scintillation fluid, radioactivity was measured using a LS 6000IC scintillation counter (Beckman Coulter, Inc. Fullerton, CA). Data represent the mean uptake and are presented as percent of control with error bars showing standard deviation. A two-tailed unpaired Student's *t* test was used to compare means. The uptake of [*G*-^{3}H] MS-275 and [^{3}H] paclitaxel is expressed as a percentage relative to uptake in the water-injected controls.

4.2.2 In-vitro phase I hepatic metabolism studies

Cytochrome P450-mediated metabolism of MS-275 was evaluated using human liver microsomes obtained from Xenotech (Lenexa, KS). Experiments were performed using 1 mg/ml of protein with incubations at 37°C in a Tris-HCl buffer (100 mM, pH 7.4) containing magnesium chloride (4 mM), and an NADPH-generating system consisting of 500 µL of $NADP^+$ (10 mM), 30 µL of glucose-6-phosphate dehydrogenase (1300 U/mL),

1000 µL of D-glucuose-6-phosphate (0.1 M), 870 µL of distilled water, and 100 µL of magnesium chloride (1 M). Heat-inactivated microsomes and microsomal incubations in the absence of the NADPH-generating system were used as negative controls (Table 4.1 A & B).

Table 4.1 Reaction mixture and details for hepatic phase I metabolism using human liver microsomes

(A)

Name	Buffer (µl)	Enzyme (µl)	NADPH (µl)	Drug (µl)	Control (µl)	Sample (µl)
Tris Buffer + $MgCl_2$ (24:1)	50	0	0	0	50	50
Enzyme	0	25	0	0	25	25
Drug	0	0	0	5	5	5
NADPH GS	0	0	100	0	0	100
Water	450	475	400	495	420	320
Total	500	500	500	500	500	500

(B)

Name	Original Conc.	Final Conc.
Tris buffer	1 M	100 mM
$MgCl_2$ (24:1)	1 M	4 mM
Enzyme	20 mg/ml	1 mg/ml
Drug	5 mg/ml (13.25 mM)	0.05 mg/ml (132.5 µM)
NADPH GS	10 mM	2 mM

Incubations were terminated with the addition of (twice the reaction volume) acetonitrile. After centrifuging the reaction mixture, the supernatant was removed and evaporated to dryness under desiccated air at 40°C in a Zymark Turbo Vap LV evaporator (Hopkinton, MA). Samples were reconstituted in mobile phase and analyzed by liquid chromatography-mass spectrometry as described previously [237]. Peak areas were quantified to determine loss of the parent compound. The assay was also modified by changing mobile phase and enabling UV detection at 205nm and 230nm for identification and quantitation of potential metabolite peaks. 2-methoxyestradiol (2ME2), an analogue of estradiol, which has been shown to be metabolized in hepatic microsomal system, was used as a positive control. Once the metabolite/s is/are detected, isozyme identification would be done using individual CYP450 enzymes to identify the specific enzymes subtypes involved in metabolism.

4.2.3 In-vitro hepatic phase II metabolism studies

Hepatic phase II metabolism for glucuronidation was studied by a two-fold approach; measuring decrease in parent peak (and formation of metabolites) using UDPGA and by measuring increase in parent peak after enzyme digestion using B-glucuronidase. First, glucuronidation was studied by measuring a decrease in parent peak area related to concentration of MS-275, using human liver microsomes and UDPGA. For identification of potential metabolites, the analytical method was modified to use gradient elution and also detect peaks at UV wavelengths of 205nm and 230nm. Similar

experimental conditions as described for phase I studies were used for characterizing phase II metabolic pathway of MS-275. Pooled human liver microsomes were used as a source of uridyl glucuronyl transferases (UGTs) and uridine diphosphate glucuronic acid (UDPGA) was added to the reaction mixture as a cofactor. Alamethicin, which acts as a detergent to make the cellular membrane porous for better transport of cofactors as well as 1-4 saccharolactone, which diminishes β-glucuronidase activity were added (Table 4.2). As a positive control, the phase II conjugation of 2-methoxyestradiol was assessed to verify glucuronidation activity.

Table 4.2 Reaction mixture and details for hepatic phase II metabolism using human liver microsomes

(A)

Name	Matrix (µl)	Drug (µl)	Control (µl)	Sample (µl)
Tris Buffer + $MgCl_2$ (24:1)	50	0	50	50
Enzyme	25	0	25	25
Drug	0	5	5	5
UDPGA	0	0	0	25
Alamethicin	12.5	0	0	12.5
Saccharolactone	25	0	25	25
Water	385.8	495	380.5	355.5
Total	500	500	500	500

(B)

Name	Original Conc.	Final Conc.
Tris buffer	1 M	100 mM
$MgCl_2$ (24:1)	1 M	4 mM
Enzyme	20 mg/ml	1 mg/ml
Drug	5 mg/ml (13.25 mM)	0.05 mg/ml (132.5 µM)
Alamethicin	2 mg/ml	50 µg/ml
Saccharolactone	100 mM	5 mM
UDPGA	100 mM	5 mM

With the second approach, 0.1 ml plasma samples from three patients at time-points where peak concentration were observed earlier, were treated with 200 units β-

glucuronidase enzyme for 2 hours at 37 ^{0}C. The main stock of β-glucuronidase (105,000 units/ml) was diluted such that a working stock with 200 units/20 µl can be used for the experiments. The increase in peak area of parent compound was measured using UV and LC-MS detections. The amount of glucuronidation can then be quantified by taking a ratio of increase in total MS-275 concentration and the parent concentration.

All incubations were terminated with the addition of acetonitrile. After centrifuging the reaction mixture, the supernatant was removed and evaporated to dryness under desiccated air at 40°C in a Zymark Turbo Vap LV evaporator (Hopkinton, MA). Samples were reconstituted in mobile phase and analyzed by liquid chromatography-mass spectrometry as described previously.[237] The ultraviolet (UV) spectrum at 205 nm was also recorded in order to further evaluate the presence of potential metabolites. Moreover, the chromatographic run-time was extended to 20 minutes, and a gradient elution was used in order to allow for slow eluting potential metabolites to be detected.

4.2.4 Preliminary urinary excretion information

In an effort to identify potential *in-vivo* glucuronidated metabolites in urine and the role of renal elimination, MS-275 concentration was measured in three patient urine samples, who received 2 mg/m^2 dose of MS-275. Calibration samples containing MS-275 were prepared by addition of aliquots of the working solutions to drug-free human urine. Calibration standards were prepared within the concentration range of 1 ng/mL to 1 µg/mL. The urine matrix had less interferences compared to plasma and the LC-MS method as described in Chapter 2 was modified and used for analysis.

Urine analysis for MS-275 was performed in three patients (24-hour urine, known volume), and fraction excreted unchanged in urine was estimated. Also, urine samples were digested with ß-glucuronidase (similar experimental conditions and conc. of enzyme as used for plasma experiments, see Chapter 2) and final concentrations were compared to look for an increase in parent compound concentration.

4.2.5 Cellular accumulation experiments to determine substrate specificity to efflux transporters

Human embryonic kidney (HEK-293) cells were transfected with either the empty vector (PC) (control), ABCG2 expressing (R2) or P-gp expressing (MDR-19) gene and were cultured and harvested and made available to us (courtesy of Dr. Bates, NCI). In preparing the cell monolayers, 2 mL of a cell suspension containing at least 1 x 10^6 cells in EMEM with 10% FCS was seeded in six-well tissue culture plates. 90% confluent cells were used for the experiment. On the day of experiment, cells were washed once with Hank's balanced salt solution (HBSS) (containing 10 mM HEPES buffer, pH 7.4), which is called transport buffer. 2 mL of transport buffer containing trace [*G*-^{3}H]MS-275 (0.5 µCi/ml) at a final concentrations of 30 nM and 300 nM (clinically relevant range) were added to each well. [*G*-^{3}H]Docetaxel was used as a positive control.[262, 263] The cells were incubated in drug containing transport medium for 2 h, after which the reaction was terminated by removing the medium and rinsed twice with 5 mL ice-cold transport buffer. Cells were lysed in 0.5 mL of 1 N NaOH, neutralized with 0.25 mL of 2 N HCl, and transferred to scintillation vials. 5 mL of scintillation cocktail was added to each vial,

and the total radioactivity was measured by liquid scintillation counter. All samples were done in triplicate. The cellular accumulation of radiolabelled drug was determined and amount of cellular uptake is presented as % change of control. A decrease in amount taken up would suggest active efflux transporter activity and substrate specificity.

In a separate experiment under similar conditions, cells were divided based on volume (approximately 500000/vial) and then treated with equal amount of radiolabelled drug in transport buffer. The cells were lysed as described above and were counted and results expressed as % change of control.

4.3 Results

4.3.1 General experimental optimizations

Preliminary experiments focused on determining the need to use an NADPH-generating system using glucose-6-phosphate (G6P) and glucose-6-phosphate dehydrogenase (G6PDH) using nicotine adenine dinucleotide phosphate (NADP+) as a cofactor versus simply using readily available NADPH (Sigma). The results were confirmed to be better when the generating system was used and hence for all phase I metabolism experiments, the NADPH generating system was prepared fresh for use (Table 4.3).

Table 4.3 Preparation of NADPH-generating system

Name	Mixture (µl)	Original Conc.	Stock solution
NADP+	500	10 mM	7.65 mg/ml
G6PDH	30	100 units	32 mg/ml
G6P	1000	100 mM	34 mg/ml
MgCl2	100	1 M	95.2 mg/ml
Water	900		
Total	2530		

Initial experiments focused on optimization of various parameters. Ideal substrate concentration for MS-275 was selected at 132.5 µM (= 50 µg/ml) after testing 5.3, 10.6, 15.9, 21.2, 26.5, 53, 106, 159, 212 and 265 µM. For MS-275, 1 mg/ml converts to approximately 2.65 mM. Incubation time was selected to be 90 minutes after testing 0, 15, 30, 45, 60, 75, 90 and 120 minutes. Human liver microsome enzyme concentration was selected to be at 1 mg/ml after testing for 0.5, 1 and 2 mg/ml. NADPH concentration was selected to be at 2 mM after testing 0.5, 1 and 2 mM. These set of conditions were kept constant for most other experiments.

4.3.2 In-vitro uptake and transport

Accumulation of [*G*-^{3}H] MS-275 by oocytes expressing OATP1B1 or OATP1B3 was not significantly different from that by water-injected controls ($p = 0.82$). Water-injected oocytes were used as a control for non-specific uptake and binding of MS-275 and paclitaxel. The uptake of [*G*-^{3}H] MS-275 and [*G*-^{3}H] paclitaxel by oocytes injected with OATP1B1 cRNA was measured and was found to be not significantly different from that by water injected oocytes. However, OATP1B3 expressing oocytes accumulated [*G*-^{3}H] paclitaxel 3.25-fold over controls ($p < 0.0001$, unpaired Student's *t* test), but not [*G*-^{3}H] MS-275 (Figure 4.1). This suggests that MS-275 is not a (high-affinity) substrate for the two main liver-specific isoforms of the family of organic anion transporting polypeptides, and is not supportive of active, transporter-mediated uptake of MS-275 into hepatocytes.

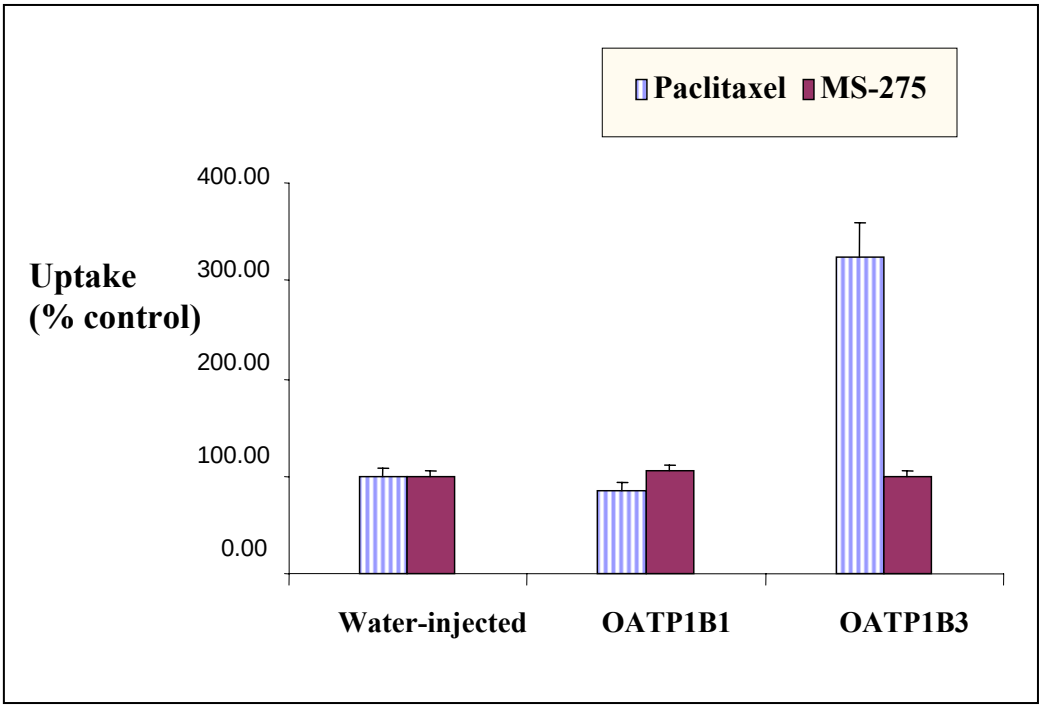

Figure 4.1 Uptake of radiolabelled MS-275 and paclitaxel into OATP expressing oocytes

4.3.3 In-vitro phase I metabolism

There was no apparent loss in parent compound concentration after incubations of MS-275 with human liver microsomes under the various conditions applied when assessed by LC-MS detection (Figure 4.2). The UV spectra of reaction mixture incubated with MS-275 at various concentrations in the clinically relevant range also did not show any evidence of oxidated metabolite(s) of MS-275 (Figure 4.3). These experiments were repeated several times in order to discount experimental errors. These results are consistent with the notion that hepatic phase I metabolism is a minor pathway of

elimination for MS-275, and likely does not contribute substantially to explaining inter-individual pharmacokinetic variability of MS-275.

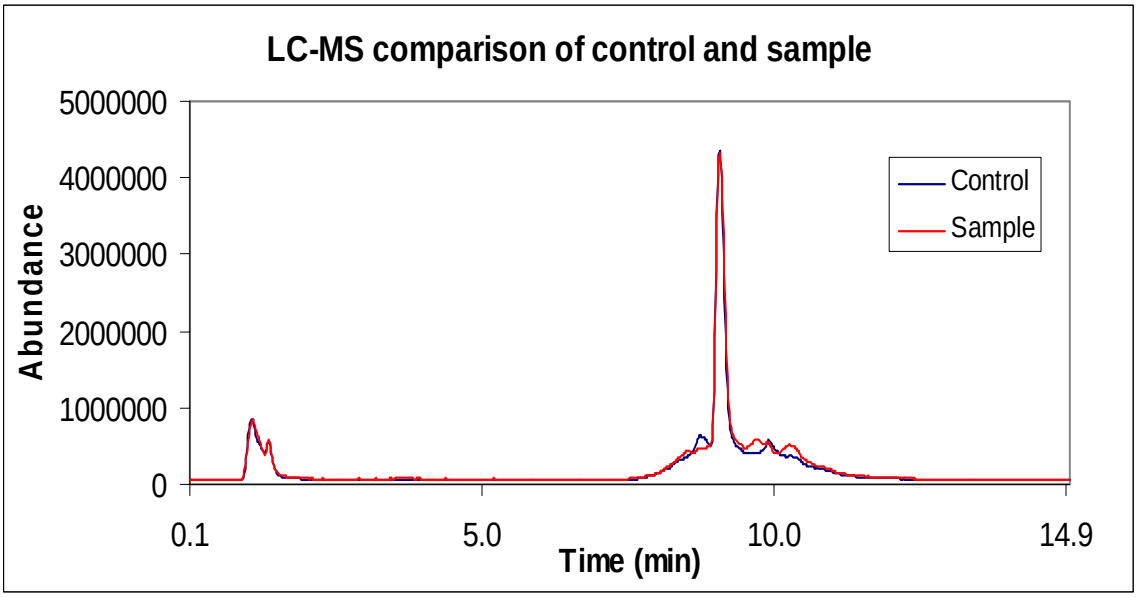

Figure 4.2 LC-MS chromatogram for phase I hepatic metabolism comparing control and sample

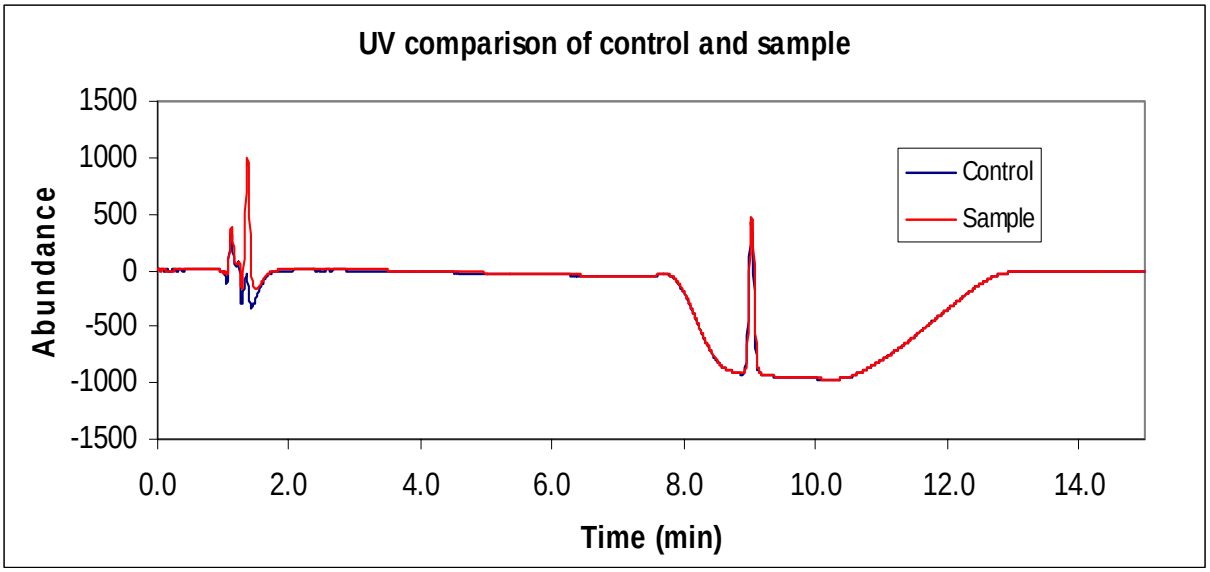

Figure 4.3 UV chromatogram for phase I hepatic metabolism comparing control and sample

4.3.4 In-vitro hepatic phase II metabolism

There was no apparent loss in parent compound concentration after incubations of MS-275 with human liver microsomes under the various conditions applied when assessed by UV and LC-MS detection. When patient plasma samples were digested with β-glucuronidase enzyme, there was no increase in parent peak area or total MS-275 concentration. This indicated that glucuronidation mediated by UDP glucuronosyltransferase mediated conjugation is not a preferred elimination pathway either. A potential drawback of using such an approach is that sensitivity of the assay may limit detecting very low levels glucuronidase-free MS-275 and that lower % change in peak concentrations may not be quantified accurately. These results taken together do not contribute substantially in explaining interindividual pharmacokinetic variability of

MS-275 and hence, additional experiments using cDNA expressed drug metabolizing enzymes were not considered.

4.3.5 Preliminary urinary excretion data

Table 4.4 Preliminary data from urine analysis from 3 patients taking MS-275 on 2 mg/m^2 dose level

Patient Urine	Matrix volume (µl)	β-glucuronidase (µl)	Final reaction volume	MS-275 Conc. (ng/ml)	Volume (ml) (after 24h)	Amount excreted (µg)
1	100	0	100	12.0	1820	21.92
2	100	0	100	8.8	2250	19.66
3	100	0	100	20.5	1150	23.56
DU1*	80	20	100	9.5		
DU2*	80	20	100	10.5		
DU3*	80	20	100	18.1		

* Digested urine samples from individual patients

As shown in Table 4.4, the results indicate that approximately 21.7 (±1.9) µg (overall mean) is excreted in urine. All patients (U) were at dose level 2 mg/m^2, who received an actual dose of 4 mg. Hence, approximately 0.5% of drug is excreted unchanged in urine. This suggests that renal elimination may not be a major pathway of elimination and/or MS-275 has poor oral bioavailability. Also, the ß-glucuronidase treated urine samples did not show any significant increase in parent MS-275 concentration, suggesting lack of presence of glucuronidated metabolites in urine.

4.3.6 Substrate specificity for efflux transporters

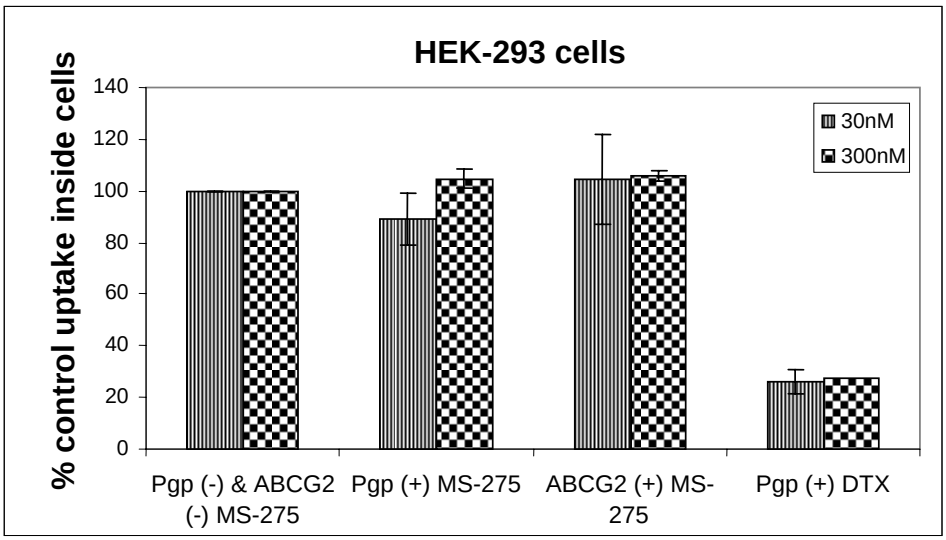

Figure 4.4 Substrate specificity of MS-275 to efflux transporters P-gp and ABCG2

Although there was some level of affinity seen for P-gp, expressed by lower % control uptake relative to P-gp-negative control, the difference was not statistically significant ($p=0.23$). There was higher variability at lower concentration for both P-gp and ABCG2 expressing cells treated with MS-275. At both the tested concentrations of 30nM and 300nM, MS-275 cannot be confirmed to be a substrate for neither P-gp nor ABCG2 efflux transporters. Under the same experimental conditions, docetaxel showed almost 3-fold stronger affinity towards P-gp compared to MS-275. These results were confirmed by both approaches described above. In conclusion, the variability in peak concentrations observed at higher dose levels cannot be correlated to inhibition of efflux proteins.

Even though the *in-vitro* transporter experiments incorporate the currently available strategy, there are potential pitfalls of using such approach for *in-vivo* predictions. For example, the concentrations selected in these experiments were based on a low and a high of the peak plasma concentration observed in humans. However, the differences in concentration of the drug in the gut to those used in *in-vitro* experiments may pose hinderences with accurately identifying extent of inhibition of the transporter. Also, the number and amount of transporter activity based on phenotypic differences in individuals varies and thus transporter efficiencies will be different. Although limited in a sense, these experiments provide some initial insight into substrate specificities of MS-275, but further experiments remain to be done in order to confirm these observations.

4.4 Discussion

The various processes mediating drug absorption and elimination, either through metabolic breakdown or active transepithelial secretion, are likely to impact substantially on variability in drug handling between individuals. For some drugs, strategies to individualize administration schedules based on patient differences in enzyme or protein expression or by co-administration of specific agents modulating side effects are being explored, which may ultimately lead to more selective chemotherapeutic use of those agents. The OATPs mediate the cellular uptake of a large number of structurally diverse endogenous compounds and xenobiotics [251]. Expression of two members of this family, namely OATP1B1 (formerly OATP-C, OATP2, or LST-1) and OATP1B3 (formerly OATP8, or LST-2) is restricted to the liver; due to their localization on the basolateral

membrane of hepatocytes, these proteins are likely to indirectly influence the hepatic metabolism and outward-directed transport of a wide variety of substrates [264]. Based on the peculiar concentration-time profile of MS-275 in humans [215], which is characterized by a peak concentration observed within 0.5 to 2 hours after drug intake, and which is followed by a very rapid decay in circulating concentrations, we speculated that MS-275 may be taken up actively into hepatocytes after gastrointestinal absorption and subsequently eliminated through hepatobiliary routes. In contrast, the *in-vitro* studies performed using *Xenopus laevis* oocytes expressing either OATP1B1 or OATP1B3 as a model system did not demonstrate any significant affinity of MS-275 for the liver-specific OATPs.

Cytochrome P450-mediated metabolism was also found not to be a major elimination pathway for MS-275, as evaluated using human liver microsomal preparations. This is not entirely surprising in view of prior work on similar agents that contain a benzamide moiety [265]. It is of note that the metabolism studies are somewhat limited by the fact that the rate of disappearance of the parent compound was assessed rather than the more analytically sensitive rate of formation of an unknown metabolite. However, it is unlikely that cytochrome P450-mediated oxidation is clinically relevant since no changes in the UV chromatogram were noted and hence, the primary pathways of elimination for MS-275 remain to be elucidated.

Based on above analysis, it cannot be entirely ruled out that MS-275 is sensitive to esterase-mediated cleavage and/or is conjugated by phase II enzymes. Indeed, consideration of the chemical structure of the drug suggests the potential for glucuronic

acid type of conjugation. Furthermore, the plasma concentration-time profile of MS-275 in several patients indicated the presence of a secondary peak, which is suggestive of enterohepatic circulation of the drug. Enterohepatic circulation is most commonly associated with the hydrolysis of drug secreted in the bile as a glucuronide conjugate by enzymatic activity originating from gastrointestinal microflora, followed by reabsorption of the liberated parent compound in the lower gastrointestinal tract. In contrast, no evidence for formation of glucuronic-acid conjugates of MS-275 was noted in our *in-vitro* experiments. The lack of any identifiable metabolite in these *in-vitro* studies does not necessarily mean that there are none *in-vivo*. However, under the experimental conditions applied, the contribution of metabolism to overall drug elimination is likely to be sufficiently small to conclude that this process does not cause a substantial interindividual difference in MS-275 pharmacokinetics.

4.5 Conclusion

In conclusion, these findings indicate that MS-275 is not a substrate for OATP1B1 and OATP1B3, and that inhibition of uptake by this transporter will not result in a clinically important, previously unrecognized type of pharmacokinetic interaction. Furthermore, hepatic phase I or phase II pathways do not seem to be relevant elimination routes for MS-275. The variability in MS-275 absorption noticed at higher dose levels is not an effect of inhibition of efflux transporters like P-gp or ABCG2. Future studies should focus on identifying possibilities of protease or esterase mediated cleavage of MS-275.

CHAPTER 5

Phase I Clinical Trial of Oral MS-275, in Patients with Advanced and Refractory Solid Tumors or Lymphoma

5.1 Introduction

Based on the promising preclinical data, a phase 1 trial of MS-275 was initially designed to use a daily schedule. This is an open label, single arm, and dose escalation, phase 1 study in advanced solid tumor and lymphoma patients.

Primary objectives of this phase I trial are:

1) To determine the dose-limiting toxicity (DLT) and maximum tolerated dose (MTD) in humans of MS-275 orally, initially given daily, once every two weeks, and subsequently on a once weekly schedule.

2) On the weekly schedule, to compare two formulations, one uncoated given in conjunction with a meal, and an uncoated formulation administered in the fasted state, with respect to toleration and preliminary pharmacology

3) To characterize the profile of adverse events, including changes in clinical chemistry and laboratory parameters.

3) To study the pharmacology and pharmacokinetics of MS-275.

4) To use the understanding of MS-275 pharmacology emerging from different schedules as a basis for designing possibly more frequent dose administration regimens.

Secondary objectives of this phase I trial are:

1) To look for evidence of antineoplastic activity in MS-275.

2) To measure the level of acetylation of histones H3 and H4 in peripheral blood mononuclear cells before and after MS-275 treatment.

3) To assess acetylation and specific gene expression in tumors, where readily accessible (skin or nodal metastasis).

a) Acetylation of histones H3 and H4

b) $p21^{WAF1/CIP1}$ and gelsolin gene expression by real-time RT-PCR

This is an open labeled single armed Phase I study of MS-275. As described before, MS-275 treatment produced DLT to the bone marrow (leucopenia and thrombocytopenia) and to the gastrointestinal systems in mice, rats, and dogs. Dose limiting toxicities were revealed early in the conduct of the daily schedule. Therefore, we focused our attention on a q14 day schedule without change of objectives.

5.2 Patients and Methods

5.2.1 Patient inclusion and exclusion criteria

Patients were eligible for this trial if they met the following criteria: Patients must have (1) a pathologically confirmed malignancy that is metastatic or unresectable, and for which standard curative or palliative measures do not exist or would likely not be effective; (2) an ECOG performance status $\leq$2, with no recent (within 2 months) weight loss of >10% of average body weight; (3) Life expectancy greater than 3 months; (4) age $\geq$ 18 years; (5) leukocytes $\geq$3000/µl, absolute neutrophil count $\geq$1500/µl, platelets

≥100,000/μl, creatinine within normal limits or measured creatinine clearance ≥ 60 ml/min/1.73m^2, total bilirubin ≤1.5 x upper limit of normal, AST /ALT ≤2.5 x upper limit of normal, adequate oral intake and serum albumin > 75% of lower limit normal; and (6) is able to give written consent, is willing to self administer and document the doses of MS 275 as needed, and is able to return to NCI for follow-up.

The following patients were excluded from the study: (1) those who had received prior anticancer therapy (chemotherapy, radiotherapy, vaccines and hormone therapy with the exception of GnRH agonists) within 4 weeks of study entry (6 weeks for nitrosoureas or mitomycin C, 8 weeks for UCN-01), or those who have not recovered from adverse events (reduced to grade 2 or less) due to agents administered more than 4 weeks earlier; (2) with known brain metastases; (3) history of allergic reactions attributed to compounds of similar chemical or biologic composition to MS-275; (4) uncontrolled intercurrent illness; (5) pregnant or lactating women; (6) men and women of reproductive potential without adequate contraception; (7) known HIV; (8) gastrointestinal conditions that might predispose for drug intolerability or poor drug absorption; and (9) major surgery within 21 days of study entry, intercurrent radiation, chemotherapy, immunotherapy or hormonal therapy (except for GnRH agonists).

This trial has been conducted under an IRB approved protocol of a NCI sponsored IND. The protocol design and conduct has followed all applicable regulations, guidance and local policies.

5.2.2 Dosage and dose escalation scheme

The initial human dosing design was a daily oral schedule for 28 days with an intended 14 day recovery period, constituting a 42 day cycle. The drug was administered with food, owing to preliminary evidence from animal studies of enhanced bioavailability in the fed state at a starting dose of 2 mg/m^2 (1/10th rat MTD) and an accelerated dose escalation scheme was planned at increments of 100% with single patient per dose level. [266] Due to unforeseen toxicities observed, the subsequent dosing schedule was changed to once orally every 2 weeks (q14 day schedule), constituting an approximately 14 day course. The drug administration and starting dose were the same as for the daily schedule, with a dose escalation increment of 2 mg/m^2, using a modified Fibonacci dose escalation scheme (3-6 patient cohorts). No intra-patient dose escalation was undertaken.

DLT was defined as 1st course adverse events $\geq$ grade 3 non-hematologic or $\geq$ grade 4 hematologic toxicity. The MTD was defined as one dose level below the dose at which $\geq$ 2/6 patients experience DLT. Dose reduction by one dose level was applied in the q14 day schedule for the occurrence of either grade 3 non-hematological toxicity, grade 4 hematological toxicity and persistent ($\geq$ 2 weeks) grade 2 non-hematological toxicity or per the investigator's assessment. There was no limitation for the number of dose reductions allowed. For dose reduction at dose level 1, 25%, 50%, and 75% decrease of starting does was the order of reduction.

5.2.3 Safety and efficacy measures

At study entry, a history, physical examination, laboratory studies (complete blood count, electrolytes, creatinine, BUN, total and direct bilirubin, ALT, AST, alkaline phosphatase, uric acid, prothrombin time, partial thromboplastin time, and urinalysis), CT scan, CXR and ECG were performed. Clinical assessments including a physical examination and adverse event evaluation were conducted at each follow up. Adverse events were graded by the NCI Common Toxicity Criteria, version 2.0. The CT scan and staging were performed every 6 weeks for the q14 day schedule. Disease specific staging techniques, such as bone marrow aspirate and biopsy, flow cytometry, cutaneous lesion photography or bone scan, were used as indicated. Responses were evaluated by the RECIST criteria [267] for solid tumors and the Cheson criteria [268] for lymphoma. Due to the daily schedule experience, MUGA scans were obtained on the q14 day schedule at base line, prior to course 2 and at each re-staging, in addition to ECG. Laboratory studies (CBC with differential, chemistry 20, PT and PTT) were performed at day 1, 3, 5, and 7 and then repeated weekly for the q14 day schedule. Twenty-four hour urine clearance, albumin, protein, uric acid and electrolytes were performed for q14 day schedule at baseline, and on days 3 and 13.

5.2.4 Pharmacokinetic studies

For pharmacokinetic analysis, 6 ml blood samples were taken on day 1 via an intravenous cannula inserted in the forearm prior to administration, at 2, 6, 12, 24, 36, 48, 60, 72, 84, and 96 hours post-dosing. Following initial pharmacokinetic evaluation of

data obtained from patients treated on the first 2 dose levels, the sampling protocol was amended to also include blood collection at 30 minutes and 1 hour. On the first day of pharmacokinetic sampling, patients were administered standardized meals immediately prior to drug administration. Blood samples were collected in sodium heparin tubes and were immediately centrifuged at 3000 g for 10 minutes at 4^{o}C, after which plasma was divided into 2 aliquots of at least 1 ml and frozen at –70^{o}C until the time of analysis. Plasma samples were assayed by the specific and sensitive high-performance liquid chromatographic assay with mass-spectrometric detection. [237] The lower limit of quantitation of this assay is 1 ng/mL, with values for precision and accuracy of $\leq$ 5.58 and $\leq$11.4% relative error, respectively.

Estimates of pharmacokinetic parameters for MS-275 were derived from individual concentration-time data sets by non-compartmental analysis using the software package WinNonlin v4.0 (Pharsight Corporation, Mountain View, CA). The peak plasma concentrations and the time to peak concentrations were the observed values. The area under the plasma concentration versus time curve (AUC) was calculated using the linear trapezoidal method from time zero to the time of the final quantifiable concentration ($AUC_{[tf]}$). The AUC was then extrapolated to infinity ($AUC_{[inf]}$) by dividing the last measured concentration by the rate constant of the terminal phase (k), which was determined by linear-regression analysis of the final 3 or 4 time points of the log-linear concentration-time plot. The apparent oral clearance of MS-275 (CL/F) was calculated by dividing the administered dose by the observed $AUC_{[inf]}$ and the terminal half-life ($T_{1/2}$) was calculated by dividing 0.693 by k.

5.2.5 Statistical analysis

All pharmacokinetic data are presented as mean $\pm$ SD except where otherwise indicated. Dose proportionality for MS-275 was assessed using a power model (i.e., AUC = α x dose$^{\beta}$) where an ideal proportional model corresponds to $\beta = 1$ (i.e., to a model of the form AUC = α x dose) and with the proportionality constant (α). Deviations of β from 1 correspond to deviations from ideal dose proportionality. Interindividual differences in pharmacokinetic parameters were assessed by the coefficient of variation (CV), expressed as the ratio of the standard deviation to the observed mean (SD/M). The apparent oral clearance and the terminal half-life were analyzed as a function of the MS-275 dose level using the Kruskal-Wallis' one-way analysis of ranks, followed by the Dunn's multiple comparison test for identifying statistically significantly different groups. Variability in parameter estimates for MS-275 between cohorts of patients that did or did not experience DLT was evaluated by a one-sided Mann-Whitney U test for differences in medians after testing for normality and heteroscedacsticity. A one way ANOVA was performed to compare mean values using two sided Dunnett's test. Statistical calculations were performed using the Number Cruncher Statistical System 2001 series (NCSS; J. L. Hintze, Kaysville, UT). The cut-off for statistical significance was considered at $p < 0.05$.

5.2.6 Pharmacodynamic analysis

Immunocytochemical analysis of acetylated histone H3 was performed on peripheral blood mononuclear cells (PBMCs) and data was provided to us for further analysis. PBMCs were isolated from whole blood by centrifugation on Ficoll-Paque Plus (Amersham, Little Chalfont, UK), pelleted onto glass slides by cytocentrifugation, fixed in 95% ethanol/5% glacial acetic acid for 1 min at room temperature, permeabilized with 0.2% Triton X-100 for 10 min at room temperature and nonspecific binding sites were blocked by incubating the cells with 1% bovine serum albumin in phosphate-buffered saline (PBS) for 1 hr at 4°C. Slides were incubated with polyclonal anti-acetylated histone H3 antibody (Upstate Biotechnology, Lake Placid, N.Y.) for 1 hr at 4°C. Each was washed two times for 2 min with PBS, then incubated at 4°C for 1 hr with Cy3-conjugated goat anti-rabbit immunoglobulin (Molecular Probes, Eugene, OR), and washed again with PBS. Finally, the slides were incubated with 4,6-diamidoino-2-phenylindole (DAPI, Sigma) for 10 min at room temperature, rinsed quickly with water, air-dried, mounted using SlowFade (Molecular Probes), and imaged using a Zeiss Axiophot microscope interfaced with a CCD camera (Optronics Engineering, Goleta, CA). Positive controls were prepared by exposing healthy donor PBMC to MS-275 *in-vitro*. For this analysis, buffy coats, provided anonymously as a byproduct of whole blood donations from paid healthy volunteer donors through an IRB approved protocol, were centrifuged on Ficoll-Paque Plus, mononuclear cells were depleted of monocytes by adherence to plastic for 2 hr at 37°C and incubated with MS-275 *in-vitro* for various times and at varying drug concentrations. Cells were then processed for histone

hyperacetylation in the same manner as the patient samples. Images of PBMC stained for acetylated histone H3 were imported into the Openlab image analysis program (Improvision, Coventry, UK), and of histone acetylation levels were assessed using the Openlab quantification software.

5.3 Results

5.3.1 General

The first subject was enrolled on April 5, 2001 and enrollment on the daily schedule finished after two patients and twenty-nine patients enrolled on the q14 day schedule until July 29, 2003. Of the total 31 enrolled patients, 30 patients received MS-275 and were evaluable for toxicity. One patient with melanoma was withdrawn before receiving treatment, because she developed bowel obstruction secondary to disease progression, requiring immediate surgical intervention. All patients had received prior therapy, 90% had surgical resection of the tumor, 97% had prior chemotherapy, 50% had radiotherapy and 50 % had immunotherapy. Patient demographics are summarized in Table 5.1. Patients were heavily pre-treated with a median of three prior therapies.

Table 5.1 Patient demographics

Patient characteristics	Number of patients, Mean or Median (range)
Total	31
Age (years)	57 (36-76)
Sex, male/female	19 / 12
ECOG performance status	1 (0-2)
0	7
1	21
2	3
Tumor type	
Melanoma	6
Renal cell carcinoma	6
NSCLC	4
Sarcoma	4
Breast	2
Colorectal	2
Lymphoma	2
Cervix	1
Mesothelioma	1
Prostate	1
Small bowel	1
Thyroid	1
Number of prior chemotherapy	3 (0-20)
0	1
1	6
2	10
≥ 3	14
Number of prior radiotherapy	
0	16
1	9
2	4
≥ 3	2
Number of prior immunotherapy	
0	16
1	9
2	6

5.3.2 Dose escalation and dose-limiting toxicity in daily and q14 day schedule

The dose escalation experience for both the MS-275 daily and the q14 day schedules are summarized in Table 5.2.

Daily schedule: Two male patients were enrolled in the daily x 28 schedule at dose level of 2 mg/m^2. Both experienced DLT before the completion of the first cycle. DLTs observed were abdominal/epigastric pain in one patient, and cardiac arrhythmia (SVT), elevated AST/ALT, hypotension, hypoalbuminemia, and hypophosphatemia in the second patient. All adverse events resolved within 2-3 weeks. Preliminary PK data from our initial 2 patients suggested that MS-275 had a substantially longer half-life in humans than initially predicted from the animal models. This may explain the unforeseen toxicity observed in these two patients during the daily MS-275 schedule. Assessment of histone H3 and H4 acetylation indicated HDAC inhibition occurred after one dose of MS-275. To ensure study patients' safety, we amended the dosing schedule to q14 days instead of pursuing the MTD on a reduced dose on daily schedule.

Q14 day schedule: A total of 28 patients have been treated on the q14 day schedule. As summarized in Table 5.2, the first patients with first course DLTs considered to be related to MS-275, anorexia, nausea and vomiting, were observed at dose level 3, or 6 mg/m^2. After 5 patients tolerated dose level 4 without DLT, dose escalation was continued up to level 5, or 10 mg/m^2. One patient experienced similar DLTs at level 5 as had been seen at level 3. At dose level 6 (12 mg/m^2), two patients experienced similar DLTs (Table 5.2). Therefore, the DLTs of MS-275 on a q14 day

schedule were recognized to include anorexia, nausea, vomiting and fatigue. We thus determined the MTD and RP2D of MS-275 for a q14 day schedule to be 10 mg/m^2.

First course adverse events observed, either probably or possibly related or unrelated to the MS-275 (based on the investigators assessment) are summarized in Table 5.3. There were no grade 4 adverse events probably or possibly related to MS-275 observed during the first course. The only first course grade 4 adverse event (dyspnea) observed during the study, which occurred at dose level 6 (12 mg/m^2), was considered unrelated to the MS-275 and likely due to progression of metastatic mesothelioma. MS275-induced fatigue, anorexia, nausea, and vomiting were observed as early as dose level 1 (2 mg/m^2), but were all tolerable. With dose escalation, intensity of these toxicities gradually increased. Other less frequent possible toxicities included taste change, headache, diarrhea, flatulence, bloating and reflux symptoms. Hematologic toxicities, such as thrombocytopenia and neutropenia became more apparent at these higher dose levels (Table 5.3). Anemia was frequently noticed during the first course and was thought to be induced by the frequent PK and laboratory sampling and not related to MS-275.

Table 5.2 Schedule, dose level and dose administration of MS-275

Dose level and schedule	Dose (mg/m^2)	Enrolled patient No.	Total number of courses (treated patients)	No. of patients with 1st course DLT	DLTs
QD x 28/42 day 1	2	2	2*	2	See text
Q 14 days					
1	2	3	22 (4)	0	0
2	4	3	16 (4)	0	0
3	6	6	51 (8)	1	3**
4	8	5	22 (9)	0	0
5	10	6	30 (8)	1	3**
6	12	5	16 (5)	2	7***

* Due to dose limiting toxicity, the treatment was terminated before the completion of the first course for both patients.
** Anorexia, nausea, and vomiting
*** Anorexia, nausea, vomiting, and fatigue

Table 5.3 Summary of first-course adverse events probably or possibly related to MS-275 at all dose levels (N=28)

Adverse Events	All grades (%)	Grade 3 (%)	Adverse Events	All grades (%)	Grade 3 (%)
Cardiovascular			**Hematological**		
Sinus Tachycardia	1 (3)	0	Anemia	8 (29)	0
Gastrointestinal			Leucopenia	6 (21)	0
Anorexia	10 (36)	4	Lymphopenia	5 (18)	0
Constipation	2 (7)	0	Neutropenia	7 (25)	0
Diarrhea	2 (7)	0	Thrombocytopenia	10 (36)	0
Dyspepsia	6 (21)	0	**Laboratory**		
Flatulence	3 (11)	0	Alk Phos	1 (4)	0
GI Other	2 (7)	0	Bilirubin	4 (14)	0

Nausea	18 (64)	4	Creatinine	2 (7)	0
Stomatitis	1 (4)	0	Hyperglycemia	3 (11)	0
Vomiting	11 (39)	4	Hypermagnesemia	2 (7)	0
General			Hypoalbuminemia	18 (64)	0
Allergic Reaction	1 (4)	0	Hypocalcaemia	6 (21)	0
Dehydration	3 (11)	0	Hypokalemia	1 (4)	0
Depression	1 (4)	0	Hyponatremia	7 (25)	0
Fatigue	15 (54)	1	Urinary electrolyte wasting	3 (11)	0
Fever	1 (4)	0	**Neurology**		
Headache	14 (50)	0	Neuro-Sensory deficits	2 (7)	0
Infection without Neutropenia	2 (7)	0	Tremors	1 (4)	0
Libido	1 (4)	0	**Pain**		
Middle Ear Infection	1 (4)	0	Abdominal pain	2 (7)	0
Muscle Weakness	1 (4)	0	Chest pain	2 (7)	0
Myalgia	1 (4)	0	Pain Other	1 (4)	0
Nail changes	1 (4)	0	Pleuretic Pain	1 (4)	0
Sweating	1 (4)	0	**Respiratory**		
Taste Disturbance	8 (29)	0	Cough	1 (4)	0
-	-	-	Rhinitis	1 (4)	0

Among possible drug-related biochemical abnormalities observed during the first-course hypoalbuminemia was observed most frequently, but it did not reach DLT on the q14 day schedule. Twenty-four hour urine analysis indicated there is no renal wasting of albumin, protein or electrolytes after MS-275 administration. No obvious gastrointestinal loss of albumin was observed clinically. The hypothesis that MS-275 may trigger inflammatory response, leading to decrease of albumin was examined by evaluating several patients' fibrinogen, C-reactive protein, and ferritin level at baseline and after

receiving MS-275. These inflammatory factors were only slightly elevated. The level of ACTH, Cortisol, Progestin and Estrogen was accessed on patients, who entered higher dose level of MS-275 (8, 10 and 12 mg/m^2), at the time of 0 and 24 hour of the first dose administered and no changes of these hormones were found. However, the level of pre-albumin was decreased after MS-275 administration, which suggests the possibility of production decline.

A total of 157 courses of MS-275 were administered on the q14 day schedule (Table 5.2). To assess potential adverse events during MS-275 chronic dosing, we noticed that with each course, some cumulating adverse events caused treatment interruption. For example, some grade 1-2 AEs occurred during early courses and occasionally progressed to higher grades during later courses, requiring reduction in dose or dosing frequency. The dose reductions were frequent on dose levels higher than 8 mg/m^2, as noted in Figure 5.1 and Table 5.4 (A).

Table 5.4 Dose reductions and summary of second course adverse events

(A) Number of patients who received dose reduction after course 1

Number of patients	2 mg/m^2	4 mg/m^2	6 mg/m^2	8 mg/m^2	10 mg/m^2	12 mg/m^2	Total
Course 1	3	3	6	5	6	5	28
Course 2	3	3	5	4	5	3	23
> Course 2 dose reduction	2	0	2	2	3	3	12

(B) Frequent (≥ 10%) Adverse Events Observed during ≥ Course 2, probably or possibly related to MS-275 (N = 23)

Adverse events	All Grade (%)	Grade 3	Grade 4	Adverse events	All Grade (%)	Grade 3	Grade 4
Cardiovascular				**Hematology**			
LVEF	3 (13)	0	0	Anemia	6 (26)	0	0
Gastrointestinal				Leucopenia	8 (35)	2	1
Abdominal Pain	5 (22)	0	0	Lymphopenia	4 (17)	0	0
Anorexia	13 (56)	1	0	Neutropenia	17 (74)	3	1
Constipation	3 (13)	0	0	Thrombocytopenia	14 (61)	1	0
Diarrhea	8 (35)	3	0	**Laboratory**			
Dyspepsia	6 (26)	0	0	Alk Phos	3 (13)	0	0
Flatulence	3 (13)	0	0	Creatinine elevation	3 (13)	0	0
Nausea	19 (83)	4	0	Hypercalcemia	4 (17)	0	0
Stomatitis	3 (13)	0	0	Hyperglycemia	5 (22)	0	0
Vomiting	7 (30)	1	0	Hypernatremia	1 (4)	0	0
General				Hypoalbuminemia	11 (48)	1	0
Arthalgia	4 (17)	0	0	Hypocalcemia	10 (43)	1	0
Chest Pain	4 (17)	0	0	Hypomagnesemia	6 (26)	0	0
Dehydration	5 (22)	0	0	Hyponatremia	8 (35)	2	0
Edema	4 (17)	0	0	Hypophosphatemia	6 (26)	4	0
Fatigue	23 (100)	3	0	SGPT (Alt)	3 (13)	0	0
Fever	5 (22)	0	0	Neuromuscular			
Headache	12 (52)	0	0	Muscle Weakness	3 (13)	0	0
Myalgia	7 (30)	0	0	Neuro-Sensory	3 (13)	0	0
Taste Disturbance	10 (43)	0	0	**Respiratory**			
Urine retention	2 (9)	0	0	Dyspnea	4 (22)	0	0

Frequent, cumulative drug-related AEs observed at or beyond course 2 were: anorexia, nausea, hypoalbuminemia, fatigue, headache, diarrhea, neutropenia, thrombocytopenia, leucopenia, and hypophosphatemia. Table 5.4 (B) summarizes all grade, grade 3, and grade 4 adverse events, occurring with a frequency of >10%during

the second course and beyond. Incidences of dose reduction after the second and subsequent courses of MS-275 are shown in Figure 5.1 and Table 5.4a. When MS-275 used on a q14 day schedule, the lowest (2 – 4 mg/m^2) doses are well tolerated, with ≤ 33% of patients going onto dose reduction, while in the 6 – 10 mg/m^2 dose range ≥ 50% of patients ultimately required dose reduction. One patient with metastatic NSCLC, who had stable disease at the first re-staging, withdrew himself from the study on the 7th day of course 4 and selected to receive standard chemotherapy (docetaxel 50 mg/m^2 q 3week). This patient developed a grade 4 neutropenia and leucopenia 8 days after receiving docetaxel, which was 16 days after the course 4 MS-275 dose. Taken together, the data of Table 5.4 and Figure 5.1 suggest that while 10 mg/m^2 every 14 days was the formal MTD according to the definition of the protocol, in practice titration of the tolerated dose to lower doses may be necessary during chronic or more frequent dosing.

Symptomatic cardiac adverse events were not observed in patients who received q14 day MS-275. There were 184 ECGs performed among 28 patients per protocol design. There were no ECG adverse events observed on q14 day schedule. The ECG intervals (HR, PR, QRS and QTc) only varied slightly at some follow up time points after baseline, but were of no statistical or clinical significance (data not shown). There were no ST–T wave changes from the baseline. MUGA (multiple gated acquisitions) scans were collected as per protocol design for all patients on the q14 day schedule. A total of 91 MUGA scans were performed and at baseline the mean LVEF in all 28 patients was 58.2% $\pm$ 1.62. Twenty-six of twenty-eight patients had both baseline MUGA and at least one follow up MUGA. At follow up, mean LVEF were 58.7% + 1.08 in 26 patients.

There were no statistically significant LVEF changes detected by the paired t-test in all 26 patients treated on q14 day schedule ($p = 0.526$) or per each dose level ($p = 0.106$ for 2 mg/m^2, $p = 0.350$ for 4 mg/m^2, $p = 0.133$ for 6 mg/m^2, $p = 0.951$ for 8 mg/m^2, 0.201 for 10 mg/m^2, and $p = 0.834$ for 12 mg/m^2).

With respect to the possibility of MS-275- induced immunosuppression, lymphopenia was observed through out the MS-275 courses. However, only three instances of HSV- positive stomatitis were apparent in patients receiving greater than one course. A CTCL patient who had stable disease for over 4 months experienced one episode of herpes zoster recurrence in conjunction with clinical worsening of a skin bacterial infection.

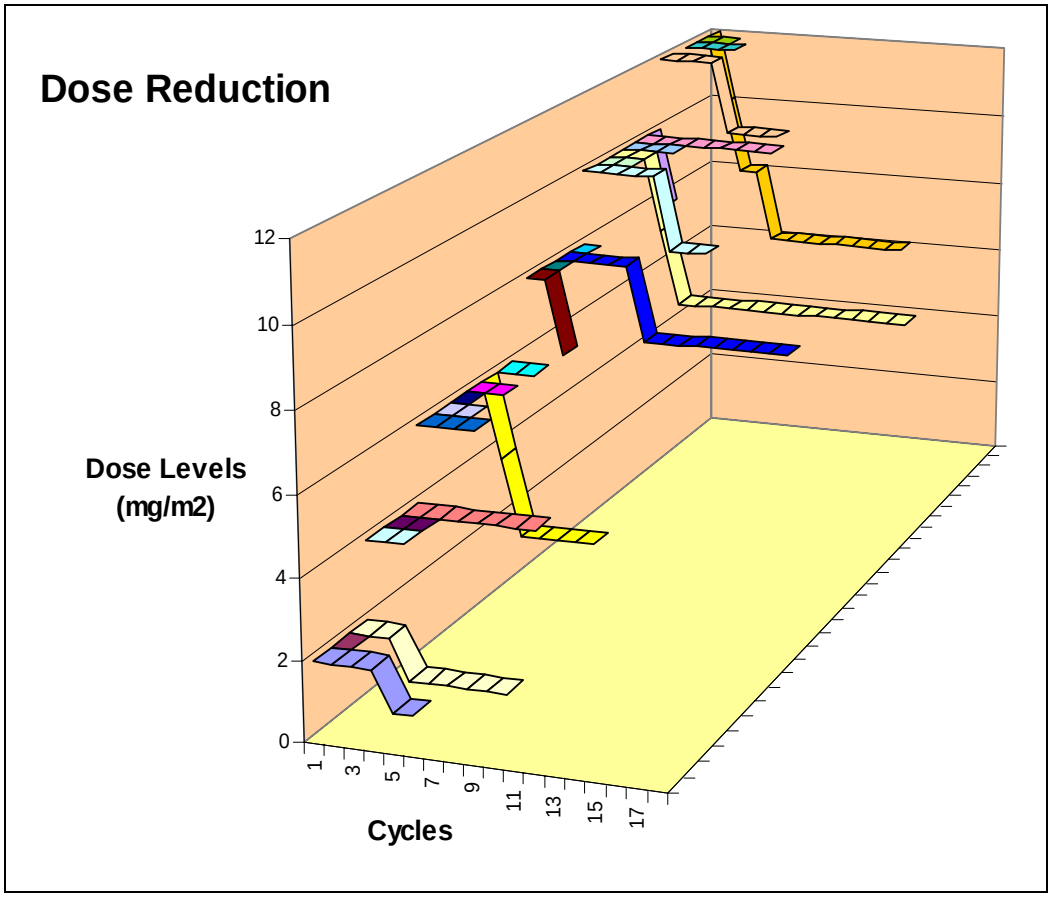

Each line represents a single patient started at his or her enrolled dose level and subsequent dose modification.

Figure 5.1 Dose reductions in patients on q14 day schedule at each dose level.

5.3.3 Responses

The treatment duration for each patient on the q14 day schedule is depicted in Figure 5.2. No CR or PR was observed on q14 day schedule. We observed 15 cases of stable disease with durations of 62 to 309 days. One patient with cervical cancer, treated at 12 mg/m^2 for the first course, 10 mg/m^2 for the second course, 8 mg/m^2 for the third

course and continued on 6 mg/m^2 every 3 weeks after the fourth course, sustained a 10 month period of stable disease. Another patient with NSCLC received the first course at 10 mg/m^2 and had two dose reductions to 6 mg/m^2, sustained a 9 month stable disease. Two melanoma patients initially treated at 8 mg/m^2 and continued on 6 mg/m^2, had 5 and 4 months stable disease.

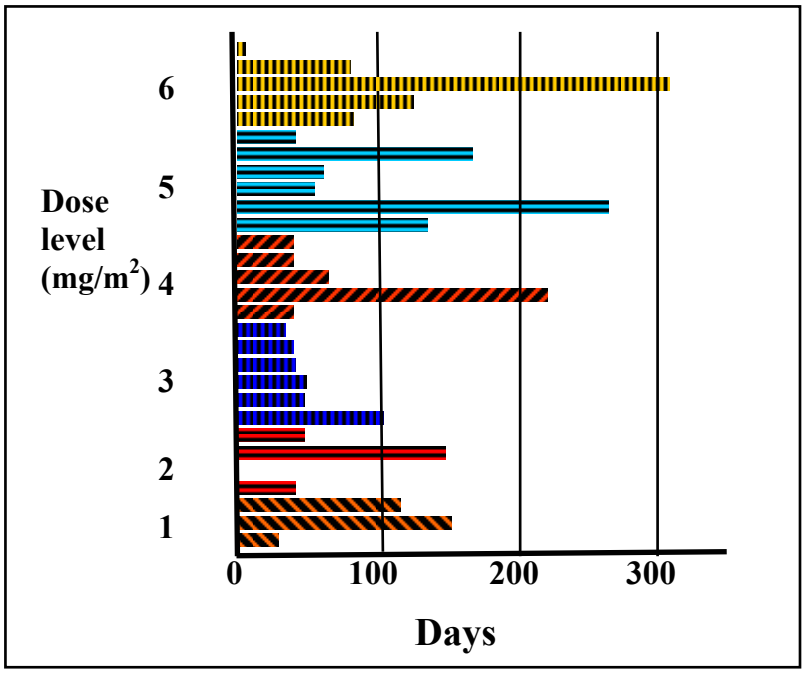

Figure 5.2 Treatment duration of patients receiving MS-275 on once every 14 days schedule

5.3.4 Pharmacokinetics

Pharmacokinetic studies were performed in 28 patients and complete concentration-time profiles were available for 27. The plasma concentration versus time

profiles of MS-275 were very similar for most patients studied, with mean curves obtained at each of the tested MS-275 dose levels (Figure 5.3). The mean non-compartmental pharmacokinetic parameters of MS-275 after doses ranging from 2 to 12 mg/m^2 are summarized in Table 5.5. Substantial interpatient variability in pharmacokinetic parameters was apparent at any dose level (CV for AUC, up to 53%). A similar degree in variability between patients was evident in the apparent oral clearance (CV = 38.8%), thereby influencing the actual systemic exposure to MS-275 during drug treatment. Furthermore, absorption of the drug was highly variable and yet the median peak plasma concentrations were reached 2 hours after drug intake. In 4 patients, the apparent gastro-intestinal uptake of MS-275 was very slow with peak plasma concentrations observed at 24 hours (n = 2), 48 hours (n = 1), and even 60 hours (n = 1) post dosing. In contrast, for 7 patients, peak plasma concentrations were observed already at the first sampling time point of 0.5 hours, suggesting very rapid absorption and a possible underestimation of the true extent of drug uptake in these individuals.

Table 5.5 Summary of MS-275 pharmacokinetic parameters using non-compartmental analysis

Dose (mg/m^2)	No. of patients (n)	Cmax (ng/ml)	AUC (ng*h/ml)	CL/F ($L/h/ m^2$)	$t_{1/2}$ (h)	Tmax (h)
2	3	1.7 (0.2)	196.3 (104.5)	13.8 (10.3)	80 (49)	6 (2-24)
4	3	4.8 (1.1)	391.7 (150.7)	11.3 (4.6)	51 (13)	6 (2-36)
6	6	9.6 (4.6)	492.8 (177.8)	13.1 (3.4)	53 (21)	2 (2-60)
8	5	15.5 (11.7)	357.7 (38.1)	22.6 (2.7)	40 (15)	2 (0.5-24)
10	6	45.1 (59.3)	528.9 (170.6)	20.5 5.9)	52 (11)	1.5 (0.5-2)
12	4	131.6 (128.3)	680.2 (262.0)	19.9 (8.1)	45 (7)	0.5 (0.5-2)
Grand Mean (SD)				17.4 (6.8)*	52 (22)**	
Grand Median (Range)						2 (0.5-60)

All values expressed as Mean (SD) except Tmax is in Median (Range)
*p-value for Kruskall-Wallis test (p = 0.071)
** p-value for Kruskall-Wallis test (p = 0.652)

Disappearance of MS-275 from the plasma compartment was characterized by elimination in an apparent bi-exponential fashion, with an overall very slow apparent oral clearance of 17.4 $\pm$ 6.8 $L/h/m^2$. The estimated apparent terminal disposition half-life was relatively consistent in all patients, exhibiting a mean value of 51.7 $\pm$ 21.6 hours (CV = 42%). As a result of the slow clearance, extended persistence of MS-275 was apparent, with detectable levels of the compound even 5 days after initial treatment in 19 of 27 patients.

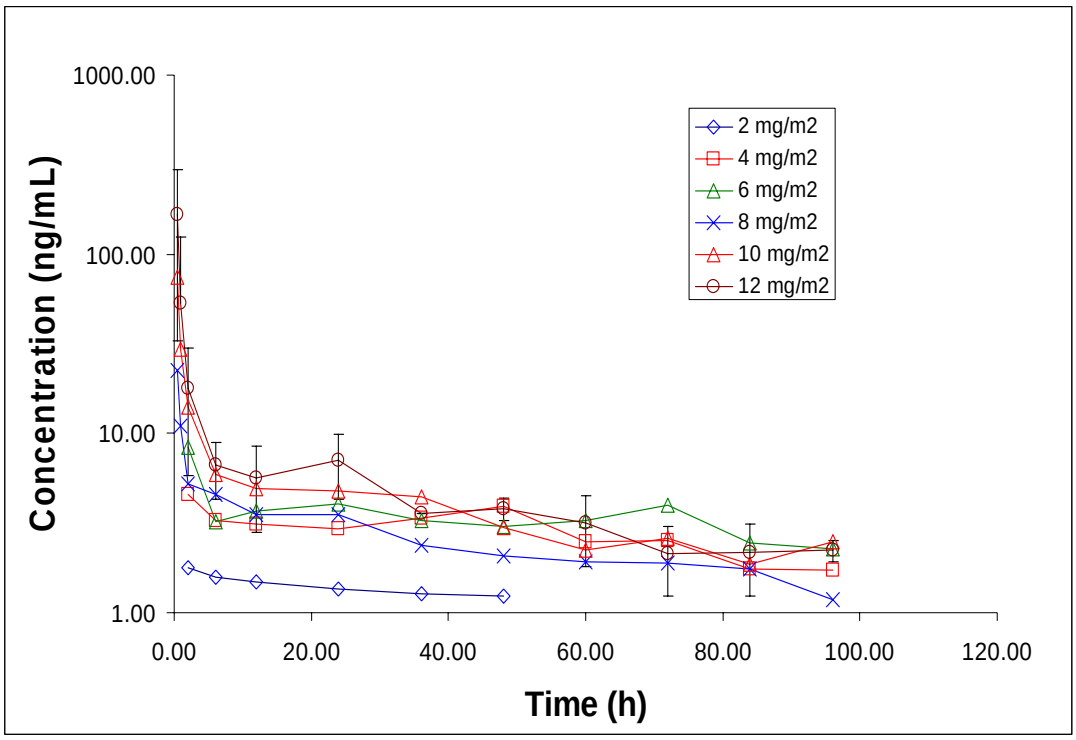

Data obtained from 31 cancer patients treated with MS-275 at dose levels ranging from 2.0 to 12 mg/m^2. Data from patients treated at the same dose levels were grouped and are presented as mean values (symbol) $\pm$ SE (error bar). The legend indicates each of the dose levels used.

Figure 5.3 Concentration-time profiles of MS-275 administered orally grouped by dose levels

The peak plasma concentrations as well as the AUCs increased in near proportion with the doses of MS-275 (Figure 5.4). The power model analysis indicated that the model poorly described the data, and that estimates of the parameter β was 0.517 $\pm$ 0.172 (r^2 = 0.323), while linear-regression analysis indicated near dose proportionality (r^2 = 0.556). The mean apparent oral clearance of MS-275 was not significantly dependent on

drug dose (p = 0.071), and the estimated terminal half-life was dose independent (p = 0.652) as well. A preliminary analysis of pharmacokinetic-pharmacodynamic relationships for MS-275 suggests that drug exposure is significantly higher in patients experiencing DLTs compared with patients that had no DLT (mean AUC, 517 $\pm$ 276 ng*h/mL, n = 4; versus 280 $\pm$ 121 ng*h/mL, n = 23 p = 0.048) (Figure 5.5).

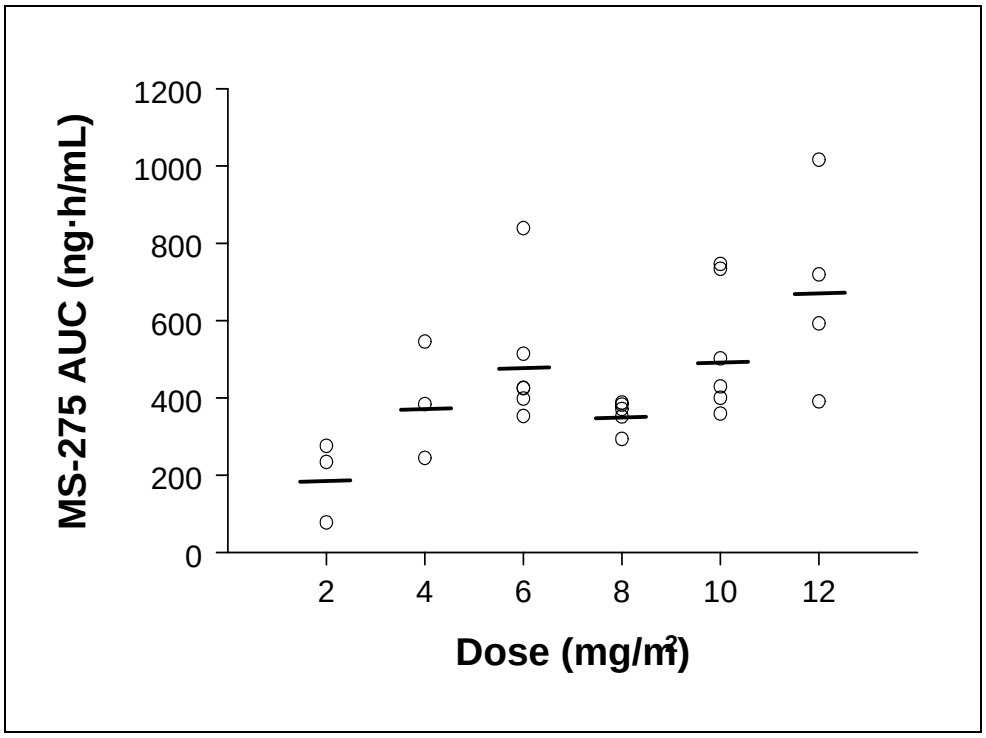

Thirty-one cancer patients were treated with MS-275 at dose levels ranging 2.0 to 12 mg/m^2. Each symbol represents data from an individual patient. Horizontal lines indicate the mean value for each dose group.

Figure 5.4 Effect of MS-275 dose on the area under the plasma concentration versus time curve (AUC)

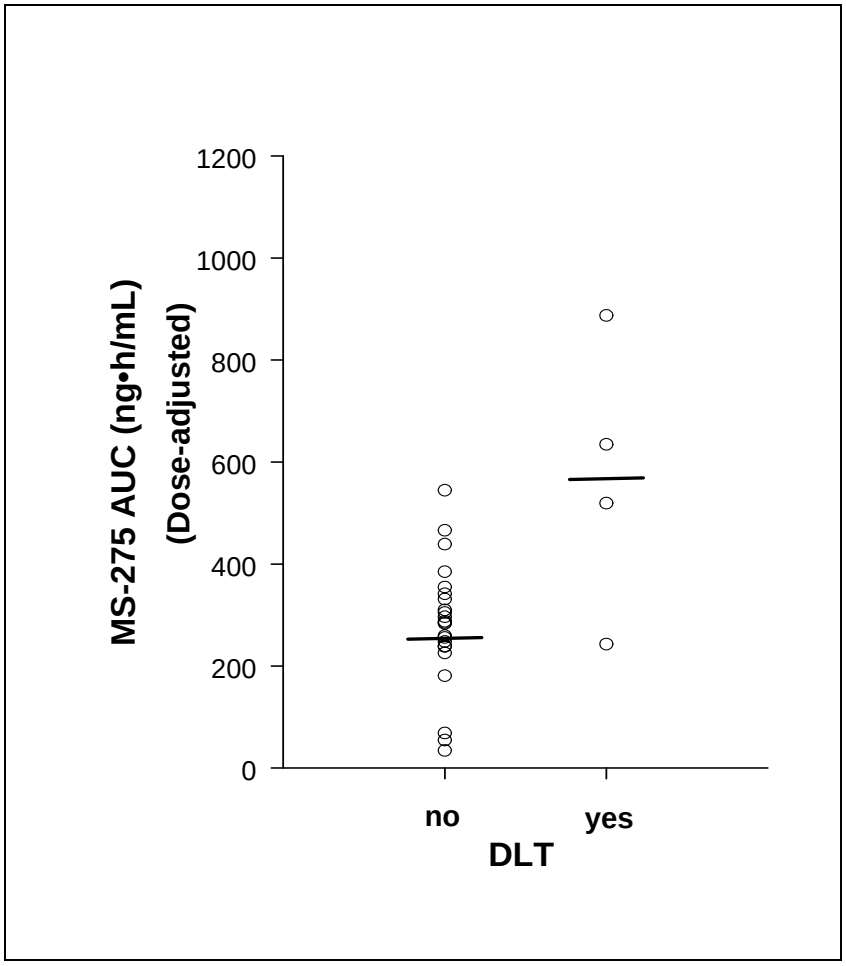

Each symbol represents data from an individual patient.

Figure 5.5 Comparative AUC of MS-275 from patients with and without dose-limiting toxicity (DLT).

5.3.5 Analysis of PBMC histone H3 acetylation

In-vitro incubation of healthy donor PBMCs with MS-275 induced hyperacetylation of histone H3 (Figure 5.6A, upper panel). Increased histone H3 acetylation could be seen in a concentration-dependent manner, as low as 30 nM MS-275 (data provided from collaborator). Patient PBMCs were collected pre-dosing and at

several time points post-dosing. Histone H3 hyperacetylation is shown for two patients at the 10 mg/m^2 level, one at 24 hr and one at 48 hr post treatment (Figure 5.6A, middle and lower panels). The level of histone hyperacetylation was quantified by image analysis software and displayed in graphical form for two series of patients. Figure 5.6B shows histone H3 acetylation in 7 patients treated at the 2 mg/m^2 level. Four of these patients never displayed H3 acetylation fluorescence above a two fold elevation from baseline, but three displayed greater than two fold elevation between 24 and 48 hr after their first dose of drug, and were showing evidence of deceased fluorescence staining by greater than 48 hr after drug. Figure 5.6C shows the histone H3 hyperacetylation response in a group of patients at the 10 mg/m^2 level. All of the patients treated at this dose level responded with differing intensities and kinetic profile. In the limited sample size studied in this protocol, there was no significant ($p < 0.05$; Number Cruncher Statistical System 2001 Series) correlation between the AUC, AUC/dose, CL/F, $C_{max,}$ C_{max}/dose and the normalized change in histone H3 acetylation at 24 hr after the initial dose (Table 5.6). However, these data emphasize that histone acetylation is apparent at doses well below 10 mg/m^2, raising the possibility that an optimal biological effect in causing histone acetylation may be achievable at less than the MTD defined by clinical toxicity.

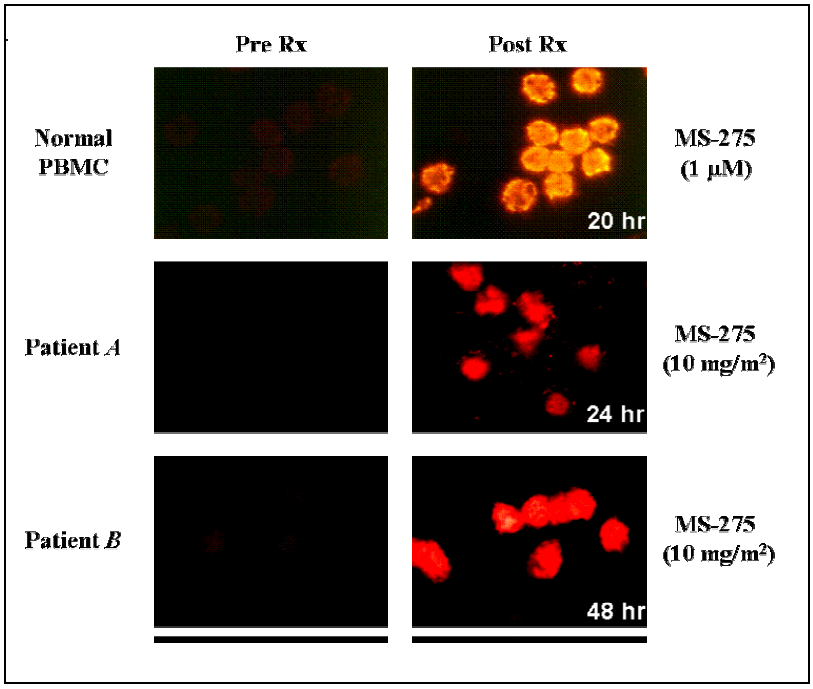

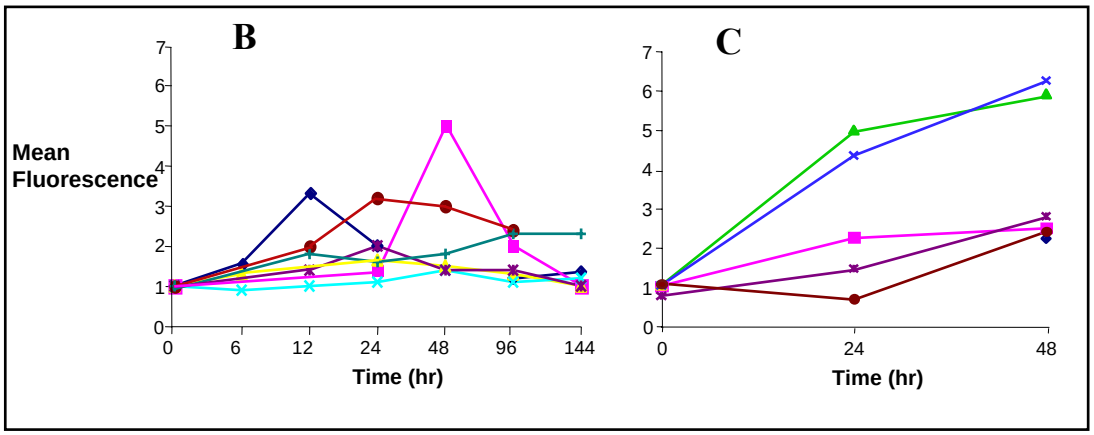

(A) Histone H3 hyperacetylation in response to MS-275 exposure in healthy donor PBMCs incubated *in-vitro* with 1 µM MS-275 for 20 hrs (upper panel). Shown in the middle and lower panels are PBMCs from two patients treated with 10 mg/m^2 MS-275. (B) Line graph of the mean fluorescence intensity of histone H3 acetylation in a group of patients treated at 2 mg/m^2 MS-275. (C) Line graph of the mean fluorescence intensity of histone H3 acetylation in a group of patients treated with 10 mg/m^2 MS-275.

Figure 5.6 Histone H3 hyper-acetylation in response to MS-275 treatment

Table 5.6 Correlation between PK parameters and % change in H3 acetylation after 24 hours

PK parameter	p-value	R-square
Cmax	0.8110	0.0054
Dose (mg)	0.7936	0.0035
Dose (mg/m^2)	0.7815	0.0035
Cmax/dose	0.8712	0.0025
AUC	0.7182	0.0123
AUC/dose	0.4513	0.0525
CL/F	0.6976	0.0143

Figures 5.34, 5.35, 5.36, 5.37 and 5.38 in the appendix depict actual plots.

5.4 Discussion

Different HDAC family members may target different promoters in controlling gene expression. Some of the transcriptional repressors recruit heterochromatin-like complexes that cause gene silencing mediated via specific repression pathways. These appear to involve HDAC and heterochromatin proteins that convert the gene region into a heterochromatic environment.[269] Non-histone proteins, including the activators p53 and GATA-1, and the general transcription factors, TFIIE and TFIIF, have also been reported to be acetylated by histone and acetyltransferases. This suggests that HDACs may regulate gene expression by deacetylation of non-histone proteins. [270-272] Very recently evidence has been gathered to show that even cell structural elements such as tubulin and

heat shock protein (hsp) 90 also can be acetylated after exposure to certain classes of HDAC inhibitors. Therefore a significant portion of anti-tumor and differentiating effect may arise through these additional mechanisms. HDACs may also participate in cell course regulation, since Rb/E2F mediated transcriptional repression involves recruitment of HDAC1 or HDAC2 by Rb. [273, 274] Therefore, the inhibitors of HDAC present an exciting, novel approach to the treatment of solid tumors, many of which are refractory to current therapies. Recent studies have emphasized that HDIs may be augmented in their gene-regulatory effects by co-administration with DNA methyltransferase inhibitors, and therefore understanding the pharmacologic profile of HDIs as single agents is a prelude to constructing regimens that would maximize ability to modulate gene expression. [44]

We conducted studies with MS-275 on two different dosing schedules. Initial experience with the MS-275 daily schedule revealed that the schedule with greatest antitumor activity predicted from animal studies was intolerable for humans. The human pharmacokinetic data suggested that MS-275 might have approximately 50 times longer half-life in humans relative to mice, rats and dogs. The implementation of the q14 day schedule allowed detailed assessment of human MS-275 adverse events and the 1st determination of the MS-275 pharmacokinetic and pharmacodynamic profile in humans. The q14 day schedule was relatively tolerable. The MTD was determined to be 10 mg/m^2. DLTs include generalized fatigue and gastrointestinal symptoms of nausea, vomiting, and anorexia. Similarly, frequent gastrointestinal adverse events related to MS-275 are dominant with gastrointestinal symptoms and also fatigue. Myelosuppression became apparent among cumulative adverse events related to MS-275.

Unlike the daily schedule, the q14 day schedule had neither symptomatic nor diagnostic cardiac adverse events observed. Compared to the published phase 1 studies of other histone deacetylase inhibitors such as SAHA IV q21days, depsipeptide (FK228), phenylbutyrate 120-hour IV and daily oral, neither grade 4 toxicity was observed on the MS-275 q14 day schedule, nor grade 2 or higher cardiac toxicity. [53, 119, 208, 210, 212, 275] On the other hand, frequent nausea, vomiting, and dyspepsia were a complication of depsipeptide, phenylbutyrate by the oral route, suggesting that the development of an oral HDAC inhibitor may prove to be a challenge. The grade 3 toxicities observed were all reversible. The tolerable adverse event profile observed in q14 day schedule encouraged the possibility that MS-275 might be a potentially well-tolerated chemotherapeutic agent. However, the q14 day schedule may not maintain a constant inhibition of HDAC activity. Therefore, based on our pharmacokinetic analysis a weekly dosing schedule is presently being tested for tolerability and possible tumor response.

The plasma concentration versus time profile of MS-275 after oral administration, and the subsequent long half-life justify the need for extended sampling, in this case up to 96 hours, coupled with sensitive analytical procedures for the accurate estimation of pharmacokinetic parameters. MS-275 was previously shown to be highly active in various animal models when administered orally. Most importantly, the recommended dose for further clinical studies using the current q 14 day oral dosing regimen provides peak plasma concentrations on average exceeding 75 ng/mL. This is above concentrations required *in-vitro* and *in-vivo* to induce significant growth inhibition in many models for various primary human tumors. [125, 126]

In the present study, MS-275 displays an apparent linear, dose-independent pharmacokinetic behavior over the dose range studied (2 - 12 mg/m^2). Overall, drug absorption was relatively rapid and, in some patients, the time to peak concentration was observed as early as 30 minutes, suggesting that MS-275 might undergo rapid gastric absorption prior to reaching the small intestine. The disappearance of MS-275 was characterized by a bi-exponential decline with a terminal half-life in plasma of approximately 50 hours, which is substantially longer than that observed for MS-275 in laboratory animals (Schering AG, data on file). The basis for this long half-life in humans may be related to enterohepatic recirculation processes; this is indicated by the appearance of a second MS-275 peak around 24-48 hours after initial drug intake in several patients. Furthermore, in one patient, the time to peak concentration was only observed at 60 hours, which is substantially longer than the normal gastrointestinal transit time. Any hypothetical recirculation is thus likely to mask the true disposition half-life of the free drug, as has been observed previously with many other agents. [276] In addition to enterohepatic recirculation, other factors which may influence the prolonged circulation of MS-275 could include binding of the compound to plasma proteins like human serum albumin and α_1-acid glycoprotein. However, we have found that MS-275 is only approximately 80% protein bound, and did not find any greater binding affinity to albumin than to other proteins. Therefore, there should be no significant clinical impact of protein binding on clearance. It has been well established that for drugs with extensive protein binding, prolonged sampling may demonstrate a relatively slow redistribution of drug into plasma and thus prolong the apparent half-life. It is also noteworthy that for

drugs undergoing enterohepatic recirculation, ingestion of food may impact plasma drug concentrations due to emptying of the gall bladder. However, although its potential impact on kinetics were not investigated here, the times that the patients under study took any food were noted and it thus unlikely that this alone explains the individual pharmacokinetic profiles.

The observed variability in the pharmacokinetic behavior of MS-275, with an interpatient variability in the apparent oral clearance of about 40%, is typical for cancer drugs administered orally. [277] As indicated, however, over the total dose range studied, the AUC of MS-275 demonstrated an apparent dose-independent behavior. Interestingly, body-surface area correction did not reduce the interpatient variability in the oral clearance (38.8% versus 39.5%), suggesting that body-surface area is not a significant predictor of MS-275 pharmacokinetics and that flat-dosing regimens might be applied in future studies without compromising overall safety profile.

H3 acetylation in PBMCs provided a surrogate measure of HDAC inhibition after MS-275 administration. While encouraging evidence of H3 acetylation was observed during this trial, it is clearly not an indicator of tumor response. Our data demonstrate interpatient variability in the magnitude and kinetics of histone H3 hyperacetylation. Although MS-275 can induce histone H3 hyperacetylation in PBMCs *in-vivo*, it is not clear whether histone H3 hyperacetylation is the most biologically relevant endpoint, nor is it known to what extent PBMCs reflect the MS-275 response in tumor cells *in-vivo*. These are critical questions which should continue to be examined in relation to MS-275 and other clinically-relevant histone deacetylase inhibitors.

In conclusion, our data indicate that MS-275 can be given safely on a once every 14 day schedule, but not on a daily schedule in the dose range explored. The DLTs were fatigue and gastrointestinal toxicities, including anorexia, nausea, vomiting. The recommended MS-275 q14 day dose for phase II studies is 10 mg/m^2. It is clear that for MS-275 used on a q14 day schedule, the low to median dose range of 2-4 mg/m^2 is well tolerated among patients. Although objective responses were not observed, 15 patients had stable disease while on q14 day schedule. An evaluation of pharmacokinetic-pharmacodynamic relations indicated a significant association between exposure to MS-275 and the occurrence of DLT. Evidence of drug target effect in a surrogate tissue, PBMCs, was observed. The relatively long half-life of MS-275 suggests that more frequent administration of low dose MS-275, but less frequent than daily administration, may be superior to the q14 day schedule. In addition, the actual influence of ingestion by humans in the fed or fasted state needs to be clarified and will be addressed in future studies. Further analysis of the absorption and disposition of MS-275 in individual patients with cancer, with respect to the current pharmacodynamic findings of HDAC inhibition, should be of great importance to identify the role of the various biological factors that may influence the compound's pharmacokinetic profile and pharmacological actions, as well as effects of other drug administered concomitantly. Therefore, further studies using a weekly schedule supported by these pharmacokinetic data are ongoing.

CHAPTER 6

Factors Affecting the Pharmacokinetic Profile of MS-275, in Patients with Cancer

6.1. Introduction

Data from a Phase I clinical trial with MS-275 administered orally revealed significant inter-individual pharmacokinetic variability, with the apparent oral clearance ranging approximately 4.3 fold between different patients, and with a coefficient of variation of 39%.[278] Although such high degree of variability is not unusual for anticancer drugs administered orally, it is an important issue to be addressed in relation to further development and optimization of dosing strategies for MS-275. This is particularly significant for MS-275, as variability in its oral exposure has been identified as an important determinant contributing to variability in toxicity.[278] Specifically, a preliminary analysis of pharmacokinetic-pharmacodynamic relationships for MS-275 suggests that drug exposure is significantly higher in the four patients experiencing dose-limiting toxicities compared to 23 patients that had no dose-limiting toxicity [mean (± SD) dose-normalized area under the curve, 517 ± 276 ng•h/mL *versus* 280 ± 121 ng•h/mL; p = .048].[278] Here, we evaluated potential sources of this pharmacokinetic variability by performing an exploratory analysis aimed at identifying predictors of drug exposure *in-vivo*.

6.2. Patients and methods

6.2.1 Patient Population

Records collected as part of two Phase I clinical trials with oral MS-275 performed at the National Cancer Institute (Trial I) and University of Maryland/Johns Hopkins University (Trial II) were examined prospectively. All patients had pathologically confirmed metastatic or unresectable malignant solid tumor or lymphoma (Trial I) or hematologic malignancy, predominantly acute myeloid leukemias (Trial II) for which standard curative or palliative measures did not exist or would likely be ineffective. All patients had adequate hematopoietic (absolute neutrophil count $\geq 1.5 \times 10^9$/liter; platelet count $\geq 100 \times 10^9$/liter, leucocytes $\geq 3 \times 10^9$/liter), hepatic and renal function at the time of entry in Trial I. Inclusion also required an Eastern Cooperative Oncology Group performance status of ≤ 2, age of ≥ 18 years, and a life expectancy of ≥ 3 months. All patients with complete information, consisting of sex, age, disease, height, weight, and first dose pharmacokinetic data, were included in the current analysis. Administration of all other concomitant drugs was avoided in order to reduce potential interactions. All patients showed willingness to self-administer and document doses of MS-275, and provided written informed consent for the pharmacologic analysis. The study protocols were approved by the respective local institutional review boards.

6.2.2 Drug Administration

MS-275 was provided by Schering AG (Berlin, Germany) as 1-, 5-, and 10-mg uncoated tablets. The drug was administered orally once a day at nominal dose levels

ranging between 2 to 12 mg/m^2 (Trial I) or 4 to10 mg/m^2 (Trial II) with dose increments of 2 mg/m^2 between subsequently evaluated dose levels. Tables in the appendix describe the dose administered, demographics, type of tumors, etc. for patients on both trials.

6.2.3 Pharmacokinetic Analysis

For pharmacokinetic analysis, 6-mL blood samples were collected in tubes containing sodium heparin prior to drug administration and at approximately 0.5, 1, 2, 6, 12, 24, 36, 48, 60, 72, 84, and 96 hours post-dose. The samples were immediately centrifuged at 3000 *g* for 10 minutes at 4° C, after which plasma was separated and then frozen at –70° C until the time of analysis. Plasma samples were assayed by high-performance liquid chromatography with mass-spectrometric detection, as described previously in Chapter 2.

Estimates of pharmacokinetic parameters for MS-275 were derived from individual concentration-time data sets by non-compartmental analysis using the software package WinNonlin v4.0 (Pharsight Corp., Mountain View, CA). The apparent oral clearance of MS-275 (CL/F) was calculated by dividing the administered nominal dose (mg/m^2) by the observed area under the plasma concentration versus time curve extrapolated to infinity (AUC). The percent contribution of the area extrapolated to calculate AUC was, on average (± SD), 32 ± 16%. Due to ethical constraints and in view of patient comfort, we could not extend the sampling time point beyond 96 hours. The CL/F of MS-275 in units of L/h was calculated by dividing the actual dose administered (in mg) by the observed AUC values. The CL/F in units of L/h/m^2 was calculated by

dividing the absolute clearance of MS-275 by a patient's individual body-surface area (BSA). A preliminary analysis indicated that the CL/F of MS-275 was not significantly dependent on drug dose, either in Trial I ($p = 0.232$, one-way analysis of variance test) or in Trial II ($p = 0.211$), suggesting that MS-275 displays a linear, dose-independent pharmacokinetic behavior over the studied dose range (2.0 to 12 mg/m^2). Therefore, the values of CL/F from patients treated on both trials at the various dose levels were combined without any further correction.

The various body size measures, including BSA (in m^2), lean body mass (LBM; in kg), ideal body weight (IBW; in kg), adjusted ideal body weight (AIBW; in kg; this parameter is often referred to as adjusted body weight or ABW in clinical practice), and body mass index (BMI in kg/m^2), were calculated using the following equations, with height expressed in meters and weight in kg [279-282]:

$$\text{BSA} = 0.007184 \times \text{weight}^{0.425} \times \text{height}^{0.725} \quad \text{(eq. 1)}$$

$$\text{LBM (men)} = 1.10 \times \text{weight} - 120 \times (\text{weight}/ (\text{height} \times 100))^2 \quad \text{(eq. 2)}$$

$$\text{LBM (women)} = 1.07 \times \text{weight} - 148 \times (\text{weight}/[\text{height} \times 100])^2 \quad \text{(eq. 3)}$$

$$\text{IBW (men)} = 50 + 0.91 \times ([\text{height} \times 100] - 152) \quad \text{(eq. 4)}$$

$$\text{IBW (women)} = 45 + 0.91 \times ([\text{height} \times 100] - 152) \quad \text{(eq. 5)}$$

$$\text{AIBW} = \text{IBW} + 0.25 \times (\text{weight} - \text{IBW}) \quad \text{(eq. 6)}$$

$$\text{BMI} = \text{weight} / (\text{height})^2 \quad \text{(eq. 7)}$$

BSA was also calculated using Mosteller's equation, $\sqrt{[(\text{height} \times \text{weight}) / 36]}$, which is also commonly used in clinical practice.[280] A preliminary analysis indicated that BSA values calculated using both equations were very similar; the mean ratio of BSA

calculated using one or the other method was 1.00 (range, 0.99 to 1.02; p = 0.99, unpaired Student's t-test), confirming the equivalence of both methods for the present pharmacokinetic analysis. All subsequent analyses were performed using individual BSA values as calculated using eq. 1. Patients were also classified into four BSA-groups: BSA <1.50 m^2, BSA between 1.51 and 1.70 m^2, BSA between 1.71 and 2.0 m^2, and BSA >2.0 m^2, respectively, and analyzed for differences in the observed CL/F as well as variability in CL/F.

6.2.4 Statistical analysis

All pharmacokinetic parameters are reported as mean values ± SD, unless stated otherwise. Inter-individual variability in parameters was evaluated by the coefficient of variation (%CV). Univariate linear-regression analysis was performed to evaluate potential relationships between MS-275 clearance and each of the studied body-size measures, sex, tumor type, and age. After testing for normality in parameter value distribution, absolute oral clearance (dependent variable) was plotted versus BSA, LBM, IBW, AIBW, BMI, weight, and height, respectively (independent variables). Adjusted r^2 and p-values were calculated and | r | values were used as a measurement for extent of correlation. The following categorization was applied for values for | r |, such that | r | > 0.70 indicates a strong association; 0.50 < | r | < 0.70 indicates moderately strong; 0.30 < | r | < 0.50 indicates weak to moderately strong, and | r | < 0.30 indicates a weak correlation. Differences in the %CV among BSA groups were determined by a modified-Levene equal-variance test. One-way analysis of variance (ANOVA) was used to

compare difference in body-size normalized CL/F values among different size categories and dose levels, followed by a *post-hoc* analysis using Dunnett's two-sided multiple-comparison test to determine group differences. All statistical calculations were performed using the NCSS package version 2001 (J. L. Hintze, Kaysville, UT). All p-values were two-sided and not adjusted for multiple comparisons.

6.3. Results

6.3.1 Patient population

The entire population studied consisted of 64 patients, of whom 36 were males and 28 females. A summary of patient demographic variables is provided in Table 6.1. The median age of patients was 57 years (range, 22-86 years). The patients received MS-275 orally on two independent trials (dose range Trial I, 2 to12 mg/m^2; dose range Trial II, 4 to10 mg/m^2). All patients had a pathologically confirmed metastatic or unresectable malignant solid tumor including lymphomas (Trial I) or relapsed or refractory acute leukemias (Trial II).

Table 6.1 Summary of patient demographic characteristics

Patient characteristic	Number of patients Mean (range)
Total number of patients	64
Age, years	58[a] (22-86)
Sex, male/female	36:28
Height, m	1.69[a] (1.30-1.85)
Weight, kg	77[a] (49-125)
BSA, m^2 (eq. 1)	1.88[a] (1.47-2.35)
LBM, kg (eq. 2, 3)	55[a] (28-76)
IBW, kg (eq. 4, 5)	63[a] (25-80)
AIBW, kg (eq. 6)	55[a] (32-84)
BMI (eq. 7)	27[a] (18-49)
Primary tumor site	
Bone marrow (hematologic)	25
Adrenal gland	1
Breast	3
Colorectal	6
Cervix	1
Oro-pharyngeal	1
Kidney	6
Liver	1
Lung	4
Head and neck	1
Lymph gland	3
Prostate	1
Sarcoma	3
Skin (melanoma)	8
MS-275 dose (mg/m^2)	
2	5
4	15
6	16
8	16
10	8
12	4

6.3.2 Evaluation of candidate covariates for CL/F of MS-275

The overall mean CL/F of MS-275 was 38.5 ± 18.7 L/h (range, 11.3 to 95.4 L/h), with a %CV of 48.7% (Table 6.2). After correction of CL/F for BSA, a mean value of 20.7 ± 10.4 L/h/m^2 was observed with a similar degree of variability (i.e., 50%). Likewise, after adjustment of MS-275 CL/F for individual differences in LBM, IBW, AIBW, BMI, weight, or height, the %CV was not reduced (Table 6.2). Using linear-regression analysis, it was found that the CL/F of MS-275 was not significantly related to any of the studied body-size estimates (Figures 6.1, 6.2, 6.3. 6.4 and 6.5). In a univariate analysis, including weight, height, sex, age, albumin, bilirubin, serum creatinine and tumor type as independent variables, no significant covariates were identified (P-value range, 0.06 to 0.99; adjusted r^2 range, <0.0001 and 0.082) (Table 6.3 and Figures 6.6, 6.7, 6.8, 6.11, 6.12, 6.13, 6.14, 6.15).

Table 6.2 Apparent oral clearance of MS-275 as a function of body-size measures

Body size measure	CV (%)	Mean clearance (Mean ± SD)	Units
None	49	38.5 ± 18.7	L/ h
BSA	50	20.7 ± 10.4	L/ h/ m^2
LBM	53	0.72 ± 0.38	L/ h/ kg
IBW	54	0.63 ± 0.34	L/ h/ kg
AIBW	47	0.71 ± 0.33	L/ h/ kg
BMI	55	1.48 ± 0.82	L/ h/ kg/ m^2
Weight	55	0.52 ± 0.28	L/ h/ kg
Length	49	22.8 ± 11.1	L/ h/ m

Table 6.3 Relationship between apparent oral clearance of MS-275 and patient characteristics

Variable	Significance P	r^2	Correlation | r |	Slope
BSA	0.88	0.0004	0.0199	1.9742
LBM	0.97	< 0.0001	0.0052	0.0101
IBW	0.69	0.0026	0.0512	0.0938
AIBW	**0.02**	**0.0822**	**0.2867**	**0.4466**
BMI	0.99	< 0.0001	0.0011	0.0035
Weight	0.89	0.0003	0.0178	0.0221
Length	0.75	0.0017	0.0407	8.1929
Dose (mg)	**0.04**	**0.0688**	**0.2622**	**0.9221**
Dose (mg/m^2)	**0.03**	**0.0748**	**0.2734**	**1.9102**
Gender	0.57	NA*	NA*	NA*
Age	0.06	0.0577	0.2402	0.3494
Tumor type	0.52	NA*	NA*	NA*
Albumin	0.26	0.0205	0.1430	-5.0317
Bilirubin*	0.83	0.0043	0.0656	-18.09
Creatinine*	0.19	0.0209	0.1446	-6.932

* Data available for n=26 patients on NCI trial

It is noteworthy that AIBW showed a statistically significant ($p = 0.02$; $r^2 = 0.082$), albeit weak correlation ($| r | = 0.29$) with CL/F of MS-275. Although a significant correlation between BSA-corrected dose (in mg/m^2) and CL/F was observed ($p = 0.03$), a *post-hoc* analysis indicated that this association was the result of high %CV observed in dose groups 6 mg/m^2 and 8 mg/m^2 without any obvious trends (Figures 6.9 and 6.10).

This is presumably an artifact due to the small sample sizes studied per dose group. Indeed, a multiple regression analysis did not result in any significant correlation of any of the studied covariates with the CL/F of MS-275 ($p = 0.22$, $|r| = 0.25$).

There were also no statistically significant gender differences in CL/F (males, 39.7 ± 17.4 L/h; females, 36.9 ± 20.5 L/h; $p = 0.57$), with similar %CV observed between sexes. Although minor differences in CL/F variability for the four studied BSA groups (i.e., ≤1.50, >1.50 and ≤1.70 m^2, >1.70 and ≤2.0 m^2, and >2.0 m^2) were found, these were not significantly different ($p = 0.51$); the %CV for these groups were 39% ($n = 3$), 35% ($n = 8$), 52% ($n = 39$), and 43% ($n = 14$), respectively. The corresponding mean CL/F values in these groups were 49.5 ± 19.1 L/h, 30.8 ± 10.9 L/h, 40.3 ± 20.8 L/h, and 35.5 ± 15.1 L/h, respectively ($p = 0.38$). Furthermore, correction with neither BSA nor any other body-size estimate could reduce variability (not shown).

6.4 Discussion

The dose of the majority of investigational agents evaluated in Phase I clinical trials is most commonly determined by using BSA as the only independent variable, and it has been shown that this approach nevertheless results in large inter-individual pharmacokinetic variability [277, 283]. Whilst this has been widely recognized for some agents, until recently its significance has not been fully appreciated, and it remains unstudied for most investigational anticancer drugs as well as those commonly used in today's clinical practice. The purpose of the present report was to assess the apparent oral clearance of the novel histone deacetylase inhibitor, MS-275, as a function of commonly

used body-size measures in adult cancer patients in an effort to explain the agent's substantial inter-individual pharmacokinetic variability [215].

As mentioned previously, and despite lacking evidence of its clinical relevance in adults, the use of BSA in drug dose calculations is widespread [284-286]. The most commonly used formula to estimate BSA originates from 1916, and during the last decade, several critical notes concerning this BSA-based dosing concept in oncology have been published [284, 286-289]. Indeed, it has been demonstrated that the clearance of most anticancer agents, including epirubicin, topotecan, cisplatin, and busulfan, is not related to BSA in adults [281, 290-294]. Various alternative body-size measures have been proposed in recent years, including ideal body weight, adjusted ideal body weight, body mass index, and lean body mass, which might be better predictors of drug clearance, although no clear rationale for their use has yet been described for any anticancer drug [277, 283].

In the present study we have also evaluated the relationships between the apparent oral clearance of MS-275 and several body-size measures in a group of 64 cancer patients. The coefficients of variation for the apparent oral clearance of MS-275 (expressed in L/h) or that expressed relative to BSA (expressed in $L/h/m^2$) when including all patients in this study were 49% and 50%, respectively. Thus, similar to most other chemotherapeutic agents, it was found that dose-adjustments based on BSA as done in both clinical trials did not reduce inter-individual pharmacokinetic variability of MS-275. In addition, using linear-regression analyses with body-size measures as the independent variable, no significant covariate for clearance could be identified. In

contrast, some estimates of body size (i.e., lean body mass, ideal body weight, and body-mass index) were shown to be even worse predictors of the apparent oral of MS-275 than BSA. It is noteworthy to point out that, although there was a statistically significant influence of adjusted-ideal body weight (AIBW) on the apparent oral clearance of MS-275, the correlation was weak and the data showed considerable scatter. Specifically, the apparent oral clearance of MS-275 increased by only 2.7 L/h per unit of AIBW and hence, a 1-kg increase in AIBW was associated with a mere 7.4% increase in apparent oral clearance. The interquartile range of AIBW values observed in our patient population was 46.0 to 63.8 kg, which suggests that, based on the regression model, a majority of treated adults will have a predicted oral CL/F of MS-275 in the range of 34.3 to 42.3 L/h. This range is clearly of minor relevance against a background of %CV in oral clearance. This suggests that dose adjustment of MS-275 for body-size measures is unnecessary in adult patients with cancer. As predicted by the regression model, typical patients with an AIBW of 32.5 kg and 84.1 kg would have apparent oral clearances of MS-275 of 28.3 and 51.4 L/h, respectively. These values are similar to the actually observed values of 32.3 and 60.6 L/h, respectively, and translate into an almost 2-fold difference in systemic exposure to MS-275 for a given oral dose. Further analysis is required to evaluate the clinical significance and the potential implications of this observation.

Albumin, bilirubin, serum creatinine, age and sex also had no significant influence on the apparent oral clearance of MS-275, suggesting that alterations of dosing regimens may not be required for the elderly. In addition to the processes mentioned, a

variety of other factors may influence MS-275 disposition, including binding of the compound to plasma proteins. For example, it has been well established that for drugs with very high protein binding, prolonged sampling may demonstrate a relatively slow redistribution of drug into plasma and thus prolong the apparent half-life and thereby change the apparent oral clearance. As shown in Chapter 3, the binding of MS-275 to human plasma proteins was concentration-independent, indicating a low affinity, possibly non-specific and non-saturable process, with overall a fraction unbound drug of approximately 19%.[295] Because this degree of binding can be considered relatively insignificant, it is likely that protein binding plays a negligible role in the context of the present study. This supposition is consistent with the observation in the current analysis that interindividual differences in albumin concentrations were not identified as an important contributing factor to pharmacokinetic variability of MS-275.

In order to further resolve the issue of attempting to individualize dosing strategies for MS-275, it will be imperative to determine which factors critically influence MS-275 absorption, elimination, and clinical outcomes (i.e., toxicity and efficacy). For example, as mentioned previously, the absolute oral bioavailability of MS-275 in humans is unknown, and it is likely that relatively small changes in the amount of drug absorbed have an increasingly greater impact on the apparent oral clearance for drugs with low bioavailability. Furthermore, there is a current lack of information regarding renal elimination pathways of MS-275 and unless renal excretion is negligible, which remains to be determined in subsequent investigations, its contribution to interpatient variability in the apparent oral clearance of MS-275 cannot be discounted.

Regardless, the concept of fixed-dosing rather than BSA-normalized dosing should be an area for fruitful clinical pharmacological studies with MS-275. Clearly, implementation of such concepts would have significant economic implications. The ability to rationally design unit doses has obvious benefits for the pharmaceutical company involved. Similarly, the availability of a fixed oral dose preparation without the need for subsequent individualization for patients' body size is in clinical practice more efficient and potentially more cost-effective than preparing individualized doses, and would eliminate a significant source of error in attempting to obtain precise dosing.[296]

6.5. Conclusion

In conclusion, the current pharmacokinetic analysis has eliminated a number of candidate covariates from further consideration as important determinants of MS-275 absorption and disposition. In view of the significant degree of variability in the apparent oral clearance of MS-275 and the relatively small range in observed BSA within the studied population, MS-275 can be added to the list of anticancer agents where BSA-based dosing does not appear to be more accurate and may suggest a false sense of accuracy. We are currently exploring the possible effects of food and differences in formulations of MS-275 that may help explain, in part, the high inter-individual pharmacokinetic variability. Better individual predictors of MS-275 pharmacokinetics and pharmacodynamics might be available in the future. However, further research into the exact relationships between these key factors and pharmacologic endpoints of MS-275 treatment is necessary before they can be implemented routinely. Unless such

predictors are identified, it is recommended to apply flat dosing regimens for MS-275 in future clinical trials involving adult cancer patients as the best and most cost effective alternative.

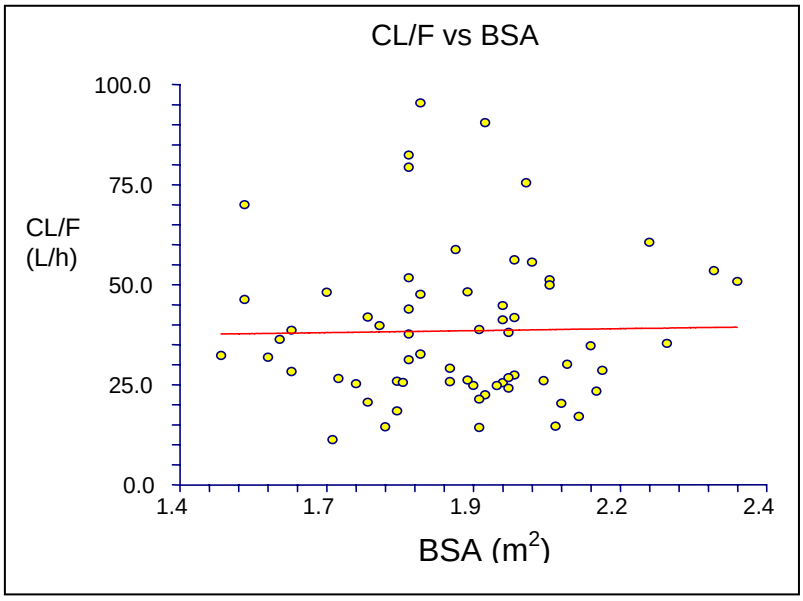

Figure 6.1 Relationship between apparent oral clearance of MS-275 and body surface area (BSA) (n = 64)

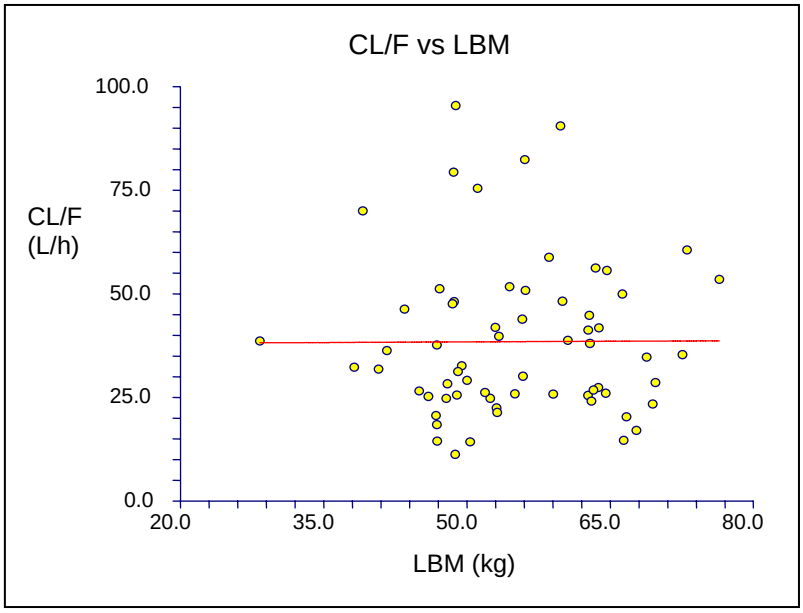

Figure 6.2 Relationship between apparent oral clearance of MS-275 and lean body mass (LBM) (n = 64)

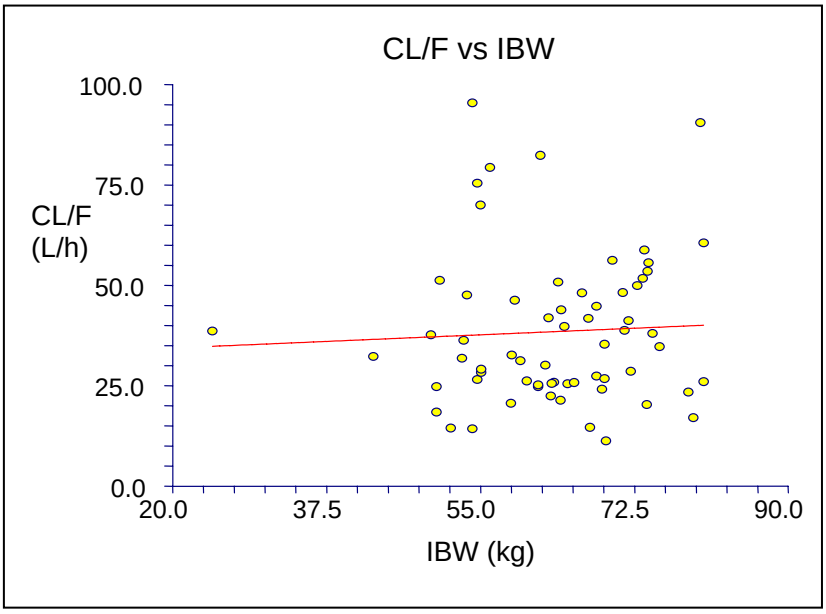

Figure 6.3 Relationship between apparent oral clearance of MS-275 and ideal body weight (IBW) (n = 64)

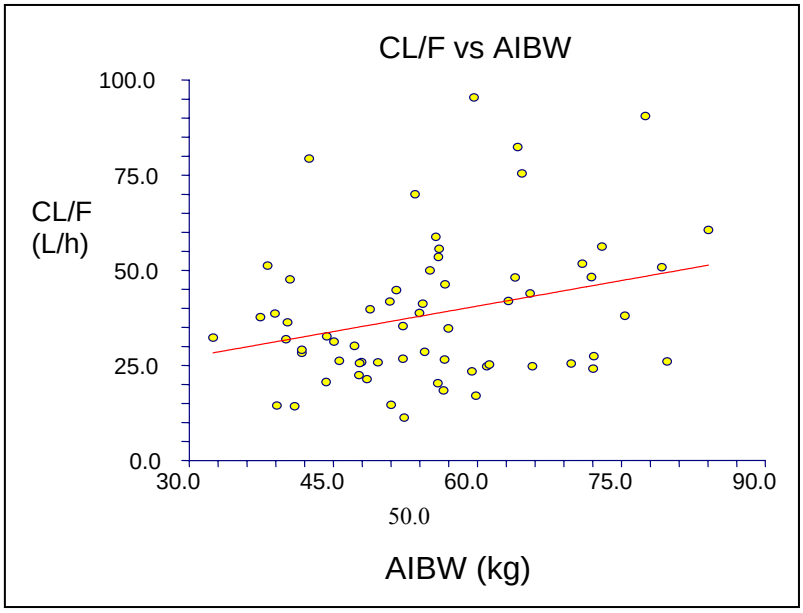

Figure 6.4 Relationship between apparent oral clearance of MS-275 and adjusted ideal body weight (AIBW) (n = 64)

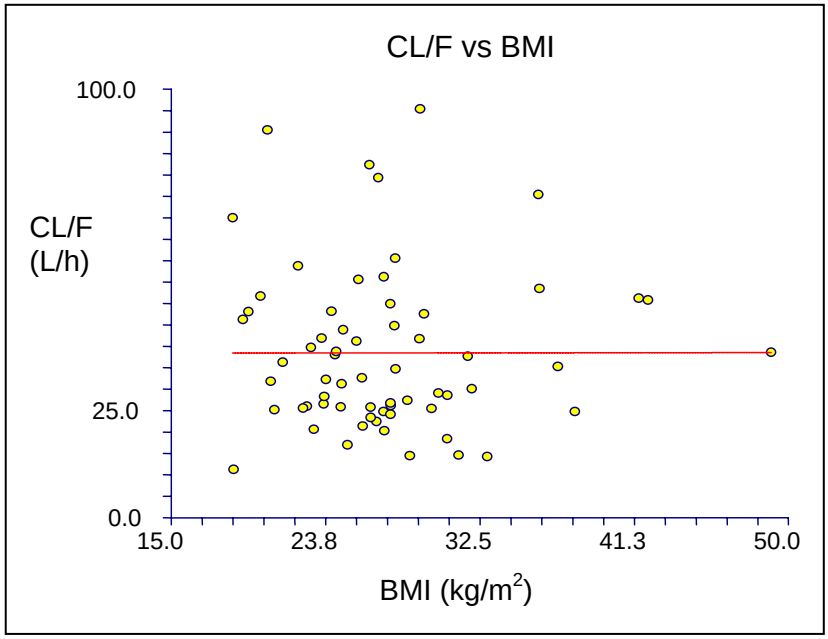

Figure 6.5 Relationship between apparent oral clearance of MS-275 and body mass index (BMI) (n = 64)

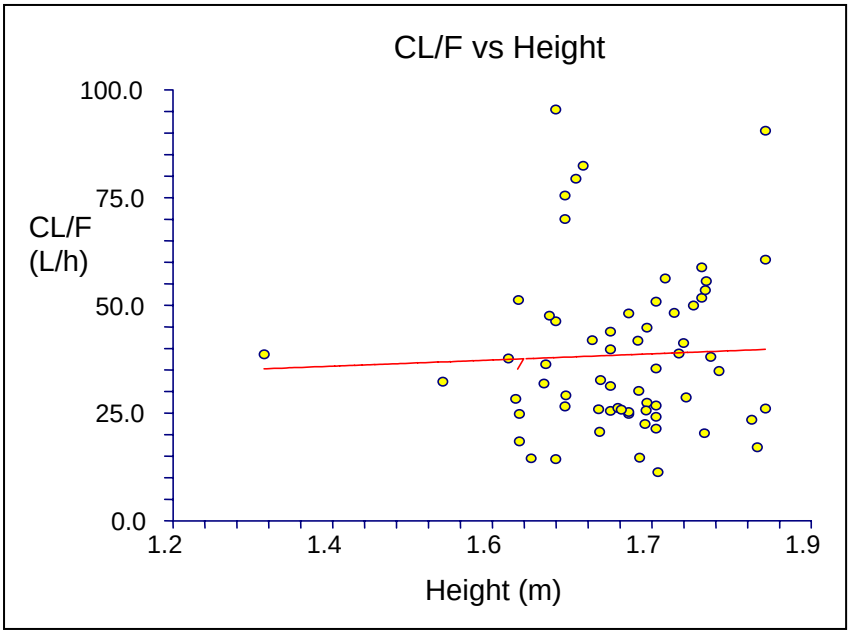

Figure 6.6 Relationship between apparent oral clearance of MS-275 and height (n = 64)

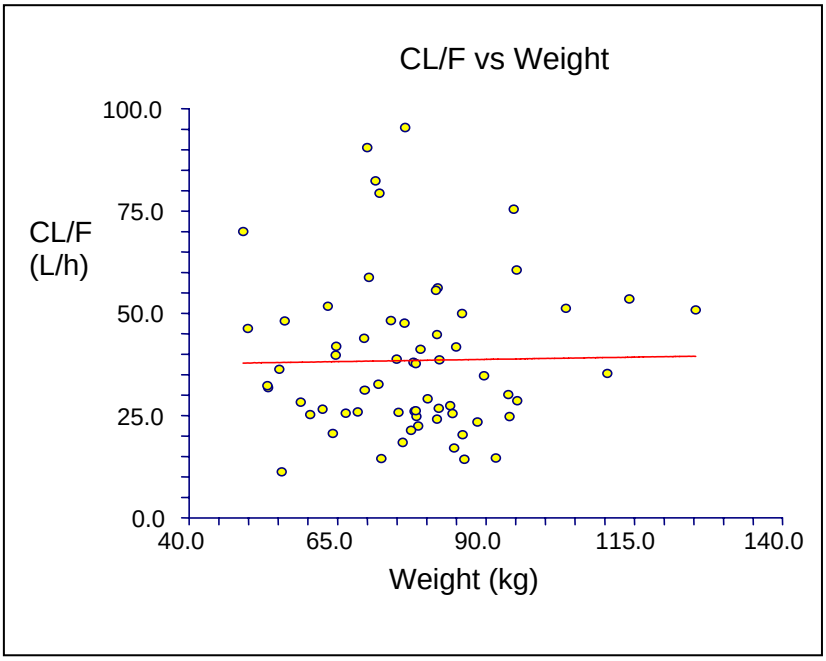

Figure 6.7 Relationship between apparent oral clearance of MS-275 and weight (n = 64)

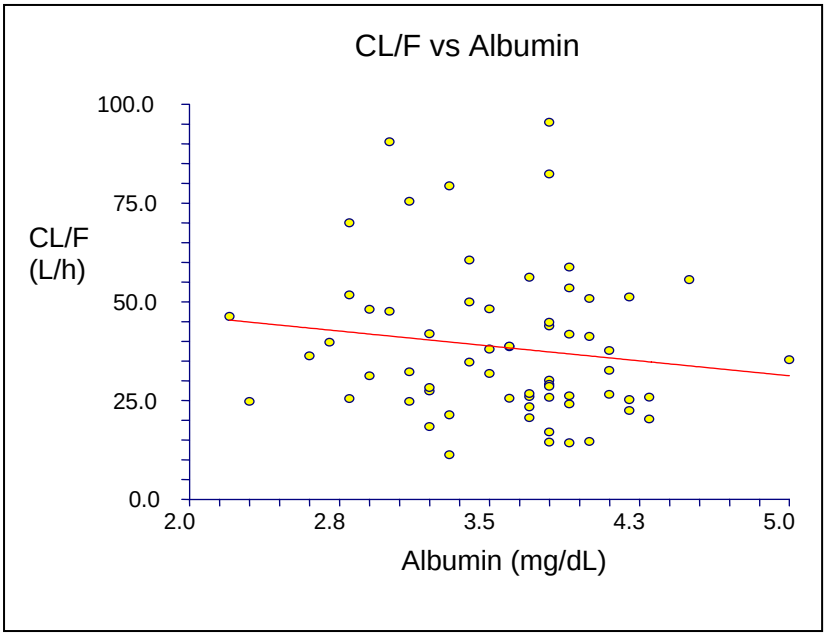

Figure 6.8 Relationship between apparent oral clearance of MS-275 and albumin (n = 64)

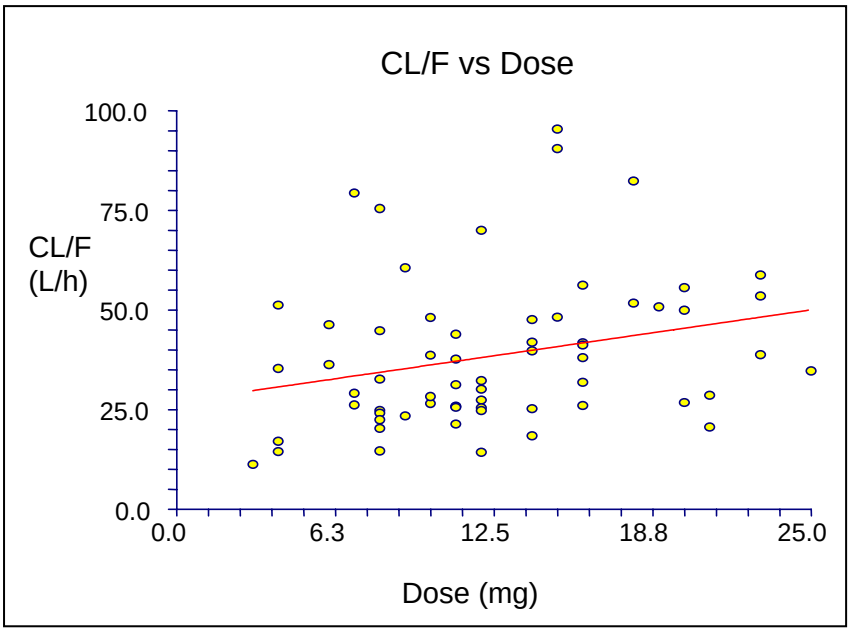

Figure 6.9 Relationship between apparent oral clearance of MS-275 and dose (mg) (n = 64)

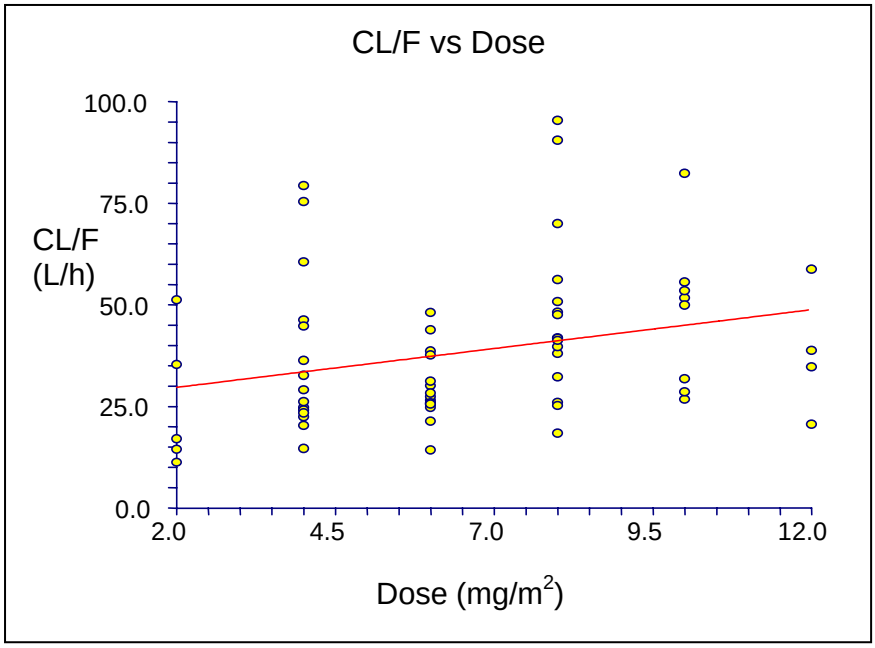

Figure 6.10 Relationship between apparent oral clearance of MS-275 and dose (mg/m^2) (n = 64)

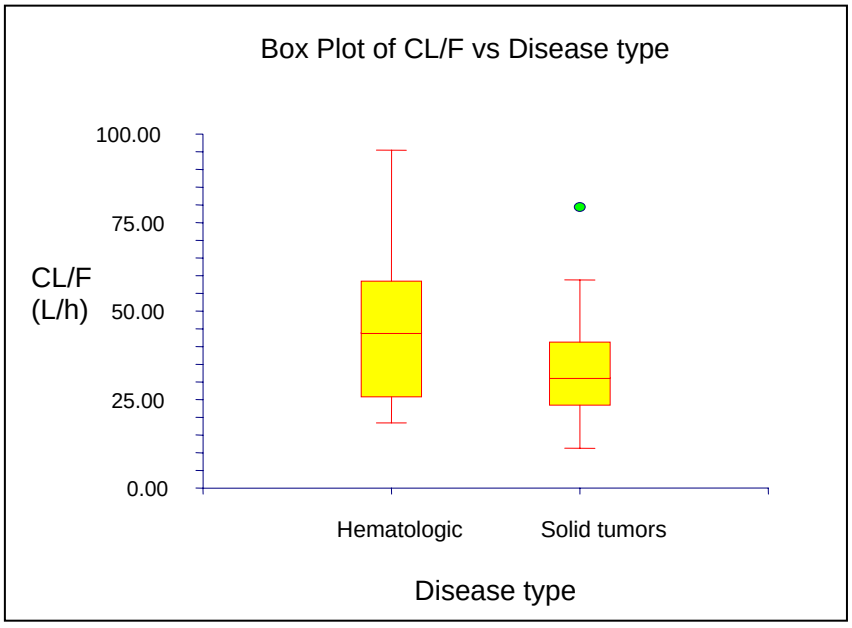

Figure 6.11 Disease type differences and correlation with oral apparent clearance of MS-275 (n = 64)

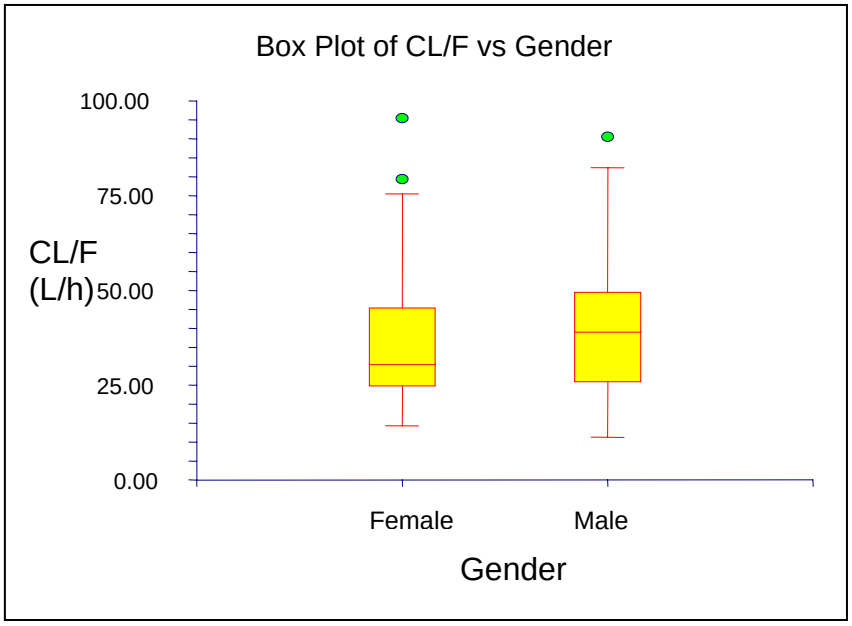

Figure 6.12 Gender differences and correlation with apparent oral clearance of MS-275 (n = 64)

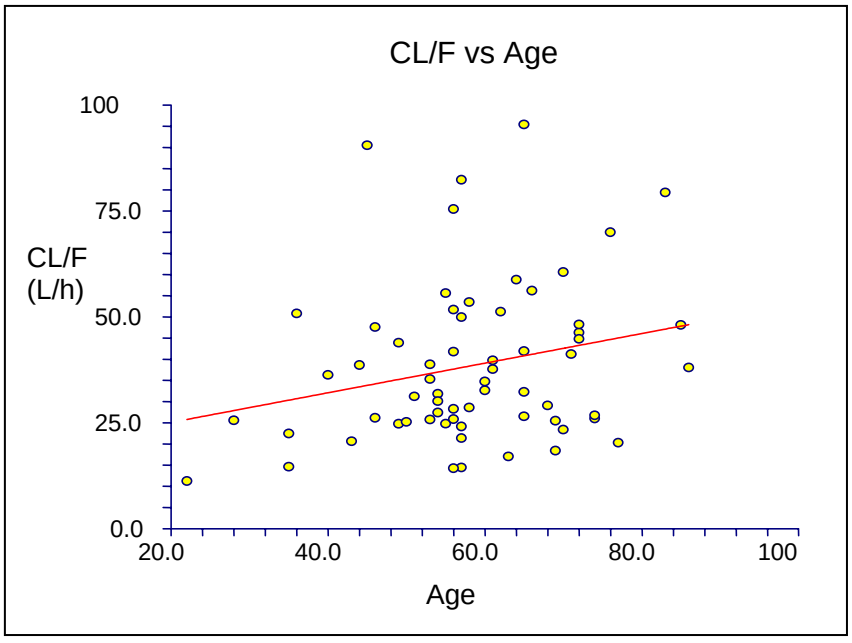

Figure 6.13 Relationship between apparent oral clearance of MS-275 and age (n = 64)

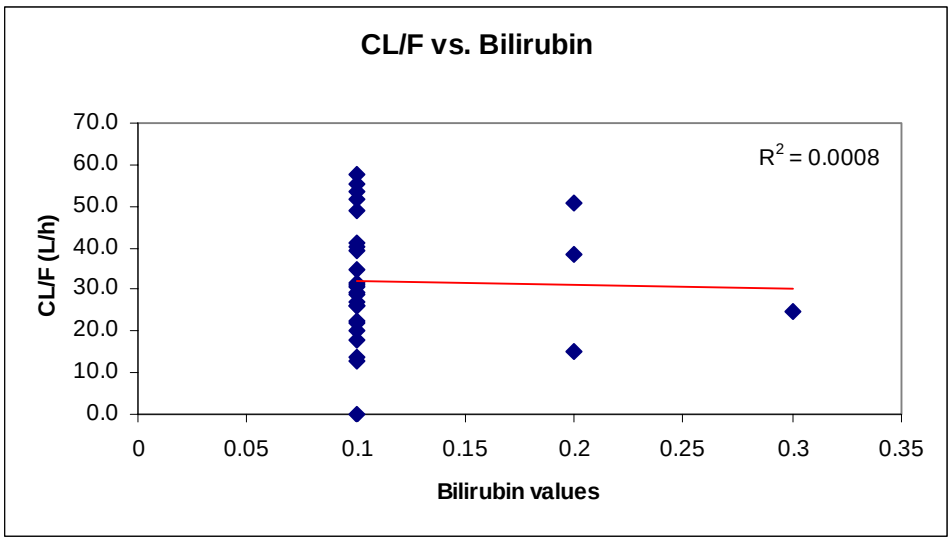

Figure 6.14 Relationship between apparent oral clearance of MS-275 and bilirubin levels from patients on NCI trial (n = 27)

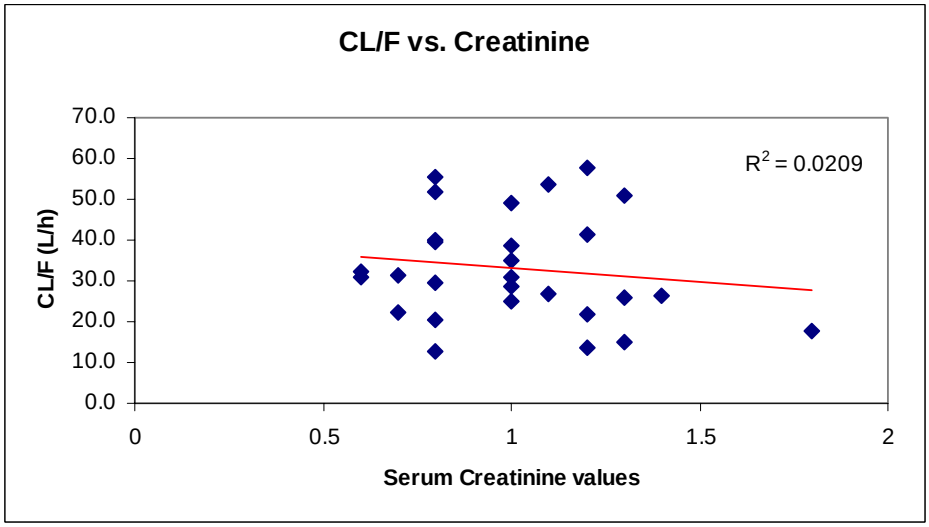

Figure 6.15 Relationship between apparent oral clearance of MS-275 and serum creatinine levels from patients on NCI trial (n = 27)

CHAPTER 7

Summary and Conclusions

MS-275 is a histone deacetylase inhibitor that is currently under clinical development for treatment of cancer. The work summarized here primarily focused on the clinical pharmacological aspects including pharmacokinetics and pharmacodynamics of MS-275 in patients with refractory solid tumors, lymphoma or advanced hematological malignancies.

The hypotheses that were tested and the objectives of the study were as follows:

1) Hypotheses

1. MS-275 will be well tolerated in the clinic when given orally at the proposed doses.
2. MS-275 will have quantifiable effects on the *in-vivo* biomarkers of anti-proliferation and apoptosis in the tumor cells.
3. The *in-vitro* and *ex-vivo* plasma protein binding will be extensive and linear in the clinically achievable concentration range.
4. Metabolism by transporters and phase II enzymes will be the major metabolic pathway for MS-275.
5. MS-275 will exhibit linear pharmacokinetics and single-dose pharmacokinetics will be useful in predicting steady state concentrations.

6. The relevant pharmacokinetic parameters of MS-275 absorption and disposition will be calculated, which may possibly explain inter-individual variability.

2) Objectives

1. To develop and validate an LC/MS assay that will quantitate MS-275 in human plasma or other matrix such as human liver microsomes.
2. To characterize the pharmacokinetics of oral MS-275 in plasma of patients with solid tumors and lymphomas.
3. To make pharmacodynamic correlations, if any, with the *in-vivo* anti-proliferative and apoptotic markers of biological effect and/toxicity.
4. To assess the *in-vitro* plasma protein binding of MS-275.
5. To characterize *in-vitro* the metabolic fate of MS-275.

The best anti-tumor activity of MS-275 in human tumor xenografts was observed on a 4-week long oral, once daily schedule. The drug was tolerable with acceptable toxicity profile at the highest dose. The drug was dosed based on body weight in preclinical species, while in humans the dosing was based on body-surface area. Based on *in-vitro* IC_{50} data, MS-275 has shown activity in cell-lines at micromolar concentration ranges (0.75 - 1.6 µg/ml or 2 - 4.8 µM). The peak concentrations in patients after single oral dose administration at the highest dose of 12 mg/m^2 were in the nanomolar range (29 - 320 ng/ml or 76 -848 nM), which were much lower in-vitro levels from preclinical species. The fraction unbound of MS-275 in *in-vitro* experiments with human plasma was found to be 19%. But it was significantly higher in five preclinical

species, namely rat, mice, dog, pig and rabbits (range 35 -45%). This difference in drug binding may be accounted due to lower proteins in plasma of all preclinical species compared to humans, and may in part explain the substantially longer half-life observed in humans. Although there was increase in acetylation of histone H3 seen in these patients at such low concentrations, the clinical activity cannot be translated into clinical efficacy of MS-275.

Initial experience with the first human dose levels of MS-275 on a once daily for 28 days schedule revealed that the drug was much less tolerated compared to rodents, with dose limiting thrombocytopenia and abdominal pain. Preliminary pharmacology studies pointed to a longer half-life in humans than the preclinical species (mouse, rat, dogs) (from Investigator's brochure). The preliminary PK data suggested that MS-275 might have a 40- to 50-fold longer half-life in humans. The MTD of MS-275 in rats was 18 mg/m^2/day and in dogs was >6 mg/m^2/day for 28 days dosing. A starting dose of 2 mg/m^2/day (about 1/10 of MTD in rats) was determined safe for human subjects as the initial dose of MS-275 in the phase I clinical trial administered daily for 28 days with an accelerated titration design. However, the initial human experience raised the possibility of abdominal pain, liver function and electrolyte abnormalities, and cardiac arrhythmia as potential adverse effects of the agent. Therefore, a more conservative dose escalation schedule, namely once every two weeks, was pursued with consideration of pharmacokinetic and pharmacodynamic endpoints as a basis for recommendation of dosing interval.

A total of 47 patients have been treated so far on three different administration schedules enrolled in the phase I clinical trial of orally administered MS-275. A minimum of 3 patients were accrued at each of the dose levels on each treatment arm. The daily x 28 schedule could not be pursued due to dose-limiting gastrointestinal toxicities in 2/2 patients treated. Hence, the biweekly schedule (q14 day) was evaluated. A total of 29 patients were treated, of which 28 were evaluable for toxicity and 27 were evaluable for pharmacokinetics. The DLTs on this schedule were grade 3 nausea, vomiting, fatigue and headache and the MTD was determined to be 10 mg/m^2. Based on this, a weekly schedule is currently being evaluated with a starting dose of 6 mg/m^2. On this schedule, the dose had to be de-escalated and the MTD has been determined to be 2 mg/m^2 and is in the final phase of completion. A food-effect study and a formulation effect study will be evaluated next on this weekly schedule. On all treatment schedules, single dose pharmacokinetics assessment were done in cycle 1 where blood samples were obtained before oral administration of the drug and 0.5, 1, 2, 6, 12, 24, 36, 48, 60, 72, 84 and 96 hours after drug administration. It was also observed that the group of patients who had a higher exposure to MS-275 had significantly higher occurrence of dose-limiting toxicities.

A sensitive, specific and rapid liquid chromatographic assay with mass spectrometric detection was developed and validated to quantitate MS-275 in plasma as well as pooled human liver microsomes. Calibration curves were constructed in the range of 1 to 100 ng/ml, and were analyzed using a weight factor proportional to the nominal concentration. Sample pretreatment involved a one-step protein precipitation with

acetonitrile of 0.1-ml samples. The analysis was performed on a column (75 × 4.6 mm I.D.) packed with 3.5-µm Phenyl-SB material, using methanol – 10 mM ammonium formate (55:45, vol/vol) as the mobile phase. The column effluent was monitored by mass spectrometry with positive electrospray ionization. The values for precision and accuracy were always ≤ 5.58% and < 11.4% relative error, respectively. Long term stability and freeze thaw stability of MS-275 were also evaluated. This method was successfully utilized to examine pharmacokinetics of MS-275 in cancer patients by assessing concentrations in various patient plasma samples. Assay characteristics were modified by using ultraviolet detection and using gradient elution when using human liver microsomal matrix.

The pharmacokinetic characterization was done for all patients by calculating all the non-compartmental parameters such as area under the curve (AUC), half life ($t_{1/2}$), apparent total clearance (Cl_t/F), apparent pseudo steady state volume of distribution (Vd_{pss}/F) and elimination rate constant (k_e) using specialized software WinNonlin (Pharsight Corp.). It was determined that MS-275 exhibits linear pharmacokinetics as the clearance was found to be independent of dose administered. The AUC and Cmax increased in near-proportions with increase in dose. The absorption was found to be very rapid in most patients with median Tmax of 2 h. The half-life was 50-fold longer than in pre-clinical species. Large interpatient variability was hypothesized to be due to variable absorption at gastrointestinal pH. To further explore and understand the factors affecting such interpatient variability of MS-275 *in-vivo*, *in-vitro* plasma protein binding and *in-vitro* drug metabolism were evaluated. Potential correlation of pharmacokinetic

parameters with *in-vivo* pharmacodynamic marker, histone acetylation was also addressed. Although there was an increase in acetylation of histones seen in PBMCs over time after exposure to MS-275, there was no significant correlation found when preliminary PK-PD analysis was performed between all relevant PK parameters such as exposure, peak concentration and apparent oral clearance with pharmacodynamic endpoint, % acetylation of histone H3 and H4 after 24 hours. Based on the pharmacokinetic data and adverse events observed from biweekly (q14day) schedule, another weekly (q7day) schedule is currently being tested. Preliminary data on the weekly schedule with starting dose of 6 mg/m^2 had to be de-escalated at further dose levels. This is not entirely surprising considering that half-life of MS-275 is 50 to 60 hours, there may be a 10-15% drug accumulation when dosing on a weekly schedule, which may in part be responsible for higher toxicity forcing dose de-escalation.

One of the early hypothesis for longer half life in humans was that MS-275 is extensively bound to plasma proteins, specifically to either albumin or alpha-acid glycoprotein. To explore this, we examined the role of protein binding as a possible determinant of the pharmacokinetic behavior of MS-275. The distribution of MS-275 in plasma was studied *in-vitro* using equilibrium dialysis and *ex vivo* in 5 cancer patients receiving the drug orally at a dose of 10 mg/m^2. The dialysis method uses a tracer amount of radiolabelled [*G*-^{3}H]MS-275 on a 96-well microdialysis plate with a 5-kDa cut-off membrane, and requires 250 µL sample. The time to equilibrium was established to be within 5 hours, and the mean unbound fraction of MS-275 (f_u) over a presumed therapeutic concentration range in human plasma was 0.188 ± 0.0075. The binding was

found to be concentration-independent, when tested over a clinically relevant concentration range, indicating a low affinity, possibly non-specific and non-saturable process. MS-275 was found to bind in decreasing order to plasma > α_1-acid glycoprotein > albumin. When displacement effect was tested among 19 commonly administered concomitant drugs, a slightly increased f_u was observed in the presence of only ibuprofen (f_u, 0.236 ± 0.001) and metoclopramide (f_u, 0.270 ± 0.042), suggesting weakly competitive displacement from protein-binding sites ($p < 0.01$). Compared to humans, significant species specific differences f_u was significantly higher in plasma from mouse (0.376), rat (0.393), rabbit (0.355), dog (0.436), and pig (0.439) ($p < 0.01$), which may explain, in part, the species-dependent pharmacokinetic profile of MS-275 observed previously. When fraction unbound was measured in 5 patient plasma samples, it was found that the total plasma concentrations were reflective of unbound concentration of MS-275 and that the fraction unbound does not change over time. Overall, MS-275 is 81% bound to plasma proteins and hence the clinical impact of binding on disposition would be minimal.

In an effort to identify transport and elimination pathways of MS-275, uptake studies were performed to identify substrate specificity for two liver-specific isoforms of organic anion transporting proteins OATP1B1 and OATP1B3. *In-vitro* hepatic phase I metabolism of MS-275 was evaluated by incubation of MS-275 with pooled human liver microsomes using appropriate co-factors like NADPH for CYP-450 enzymes and glucuronidation. *In-vitro* phase II metabolism studies involved using UDPGA as a co-factor or use of enzyme digestion technique using β-glucuronidase.

Accumulation of [*G*-^{3}H]MS-275 by oocytes expressing OATP1B1 or OATP1B3 was not significantly different from water-injected controls ($p = 0.82$). Furthermore, no metabolites could be detected after incubation of MS-275 in human liver microsomes, suggesting that hepatic metabolism is a minor pathway of elimination.

Elimination occurs by excretion and metabolism. Some drugs are excreted through bile and the more volatile substances through exhalation. Although, metabolism is the major mechanism for elimination of drugs, few drugs are eliminated entirely unchanged in urine. We have shown that for MS-275, hepatic phase I metabolic transformation is at best a minor pathway of elimination. Also, in related experiments with phase II metabolism, hepatic glucuronidation seems to be a minor pathway of elimination.

On the other hand, MS-275 has a substantially long half-life of approximately 52 hours in humans and we have confirmed that this is not due to extensive plasma protein binding. Currently, we believe that MS-275 may undergo enterohepatic recirculation (EHC) and may eventually be excreted in bile. Although this hypothesis has not been verified in individual experiments, the reason to believe of such a possibility is the presence of secondary peaks, observed in majority of patients' individual concentration-time profiles. The role of EHC can be identified by correlating the occurrence time of secondary peaks with the time of food intake. Unfortunately such information was not documented and is not available. Furthermore, there may be a correlation between bilirubin as a marker of biliary excretion and drug clearance. Bilirubin levels were measured over time and there was no trend observed. Using bilirubin as a covariate, there

was no correlation found with apparent oral clearance that may explain the wide inter-individual variability among patients. In addition, serum creatinine values also did not explain the high inter-individual variability and did not show any significant correlation with CL/F.

A correlative covariate analysis between apparent oral clearance and several covariates such as various demographic and body size measures was performed in an effort to explain the substantial interindividual pharmacokinetic variability of MS-275 in cancer patients. *In-vivo* pharmacokinetic data were obtained from 64 adult patients (36 male/28 female; median age, 57 years) receiving MS-275 orally (dose range, 2 to 12 mg/m^2) enrolled on two separate phase I clinical trials involving solid tumors, lymphomas and hematologic malignancies. The mean (± SD) apparent oral clearance of MS-275 was 38.5 ± 18.7 L/h, with a coefficient of variation (%CV) of 48.7%. When clearance was adjusted for body-surface area (BSA), the inter-individual variability was similar (%CV = 50.1%). In addition, in a linear-regression analysis, except for adjusted ideal body weight ($p = 0.02$, $|r| = 0.29$), none of the studied measures (BSA, lean-body mass, ideal body weight, body-mass index, height, weight, albumin, bilirubin, creatinine, age or sex) was a significant covariate ($P > 0.13$; $|r| < 0.11$) for oral clearance. This analysis eliminated a number of candidate covariates from further consideration as important determinants of MS-275 absorption and disposition. Furthermore, MS-275 can be added to the list of cancer drugs where BSA-based dosing is not more accurate than fixed dosing.

As per the guidelines suggested in the new proposed Biopharmaceutics Drug Disposition Classification System and available physicochemical data on MS-275, it can be predicted to fall under class 3 i.e. good GI solubility and poor permeability.[261] This classification system may be useful in predicting routes of elimination, effects of efflux and absorptive transporters on oral absorption, when transporter-enzyme interplay will yield clinically significant side-effects such as low bioavailability and drug-drug interactions, the direction and importance of food effects, and transporter effects on post-absorption systemic levels following oral and intravenous dosing. BDDCS suggests that Class 3 compounds are primarily eliminated unchanged in urine or bile. In preliminary data from urine samples of patients taking MS-275, we notice that less than 1% of drug is eliminated unchanged in urine. Also, the lower permeability profile may be affecting limited access to metabolizing enzymes within the hepatocytes. Based on our *in-vitro* studies with human liver microsomes, we have shown that phase I metabolism is a minor pathway of elimination. In light of all these observations, we speculate strongly that biliary excretion is a major pathway of elimination for MS-275.

For Class 3 compounds, sufficient drug will be available in gut lumen due to good solubility, but an absorptive transporter may be necessary to overcome the poor permeability characteristics of these compounds. However, intestinal apical efflux transporters may also be important for the absorption of such compounds when sufficient enterocyte penetration is achieved via an uptake transporter. It is also possible that drug formulation excipients can affect uptake transporters and modify bioavailability. The outcome from the formulation-effect sub-study will shed more light on this issue. Food

can also influence drug bioavailability and the rate of availability. There is a speculation that high-fat meals may inhibit drug transporters, both influx and efflux. For Class 3 compounds, high-fat will decrease the extent of bioavailability as shown recently (effect of fruit juices on fexofenadine) by decreased uptake due to inhibition of organic anion transporting polypeptides. We conducted studies involving liver-specific OATPs, and even though we found that MS-275 is neither a substrate for OATP1B1 and OATP1B3 nor P-gp and ABCG2, effects of other intestinal OATPs cannot be ruled out. Renal elimination of may be affected by uptake and efflux transporters and may be important where a kidney-specific uptake transporter is involved. Further studies may substantiate our findings and shed more light onto the transporter-enzyme interplay related to drug absorption and disposition.

Considering all the results from this project together, there is a lot of potential for further exploration of MS-275, specifically to identify enzymes involved in elimination and metabolism. Also, as data becomes available from parallel clinical trials elsewhere, a more robust covariate analysis can be performed using modeling approaches. The outcome from the currently ongoing formulation-effect and food-effect sub-studies would be critical in understanding the absorption differences as well as explaining the wide interindividual variability of MS-275. Furthermore, it will be worthwhile to perform a bioavailability study as and when an IV formulation becomes available.

BIBLIOGRAPHY

1. Marks PA, Richon VM, Miller T, Kelly WK. Histone deacetylase inhibitors. Adv Cancer Res 2004; 91:137-68.
2. Marks PA, Miller T, Richon VM. Histone deacetylases. Curr Opin Pharmacol 2003; 3:344-51.
3. Marks PA, Richon VM, Rifkind RA. Histone deacetylase inhibitors: inducers of differentiation or apoptosis of transformed cells. J Natl Cancer Inst 2000; 92:1210-6.
4. Marks P, Rifkind RA, Richon VM, et al. Histone deacetylases and cancer: causes and therapies. Nat Rev Cancer 2001; 1:194-202.
5. Thiagalingam S, Cheng KH, Lee HJ, et al. Histone deacetylases: unique players in shaping the epigenetic histone code. Ann N Y Acad Sci 2003; 983:84-100.
6. Grozinger CM, Schreiber SL. Deacetylase enzymes: biological functions and the use of small-molecule inhibitors. Chem Biol 2002; 9:3-16.
7. Gregory PD, Wagner K, Horz W. Histone acetylation and chromatin remodeling. Exp Cell Res 2001; 265:195-202.
8. Schreiber SL, Bernstein BE. Signaling network model of chromatin. Cell 2002; 111:771-8.
9. Nakatani Y. Histone acetylases--versatile players. Genes Cells 2001; 6:79-86.
10. Chen H, Tini M, Evans RM. HATs on and beyond chromatin. Curr Opin Cell Biol 2001; 13:218-24.
11. Annunziato AT, Hansen JC. Role of histone acetylation in the assembly and modulation of chromatin structures. Gene Expr 2000; 9:37-61.
12. Roth SY, Denu JM, Allis CD. Histone acetyltransferases. Annu Rev Biochem 2001; 70:81-120.
13. Gregoretti IV, Lee YM, Goodson HV. Molecular evolution of the histone deacetylase family: functional implications of phylogenetic analysis. J Mol Biol 2004; 338:17-31.
14. Timmermann S, Lehrmann H, Polesskaya A, Harel-Bellan A. Histone acetylation and disease. Cell Mol Life Sci 2001; 58:728-36.
15. Mahlknecht U, Hoelzer D. Histone acetylation modifiers in the pathogenesis of malignant disease. Mol Med 2000; 6:623-44.
16. Johnstone RW, Licht JD. Histone deacetylase inhibitors in cancer therapy: is transcription the primary target? Cancer Cell 2003; 4:13-8.
17. Pandolfi PP. Histone deacetylases and transcriptional therapy with their inhibitors. Cancer Chemother Pharmacol 2001; 48 Suppl 1:S17-9.
18. Fenrick R, Hiebert SW. Role of histone deacetylases in acute leukemia. J Cell Biochem Suppl 1998; 30-31:194-202.

19. Gray SG, Ekstrom TJ. The human histone deacetylase family. Exp Cell Res 2001; 262:75-83.
20. Imai S, Armstrong CM, Kaeberlein M, Guarente L. Transcriptional silencing and longevity protein Sir2 is an NAD-dependent histone deacetylase. Nature 2000; 403:795-800.
21. Kao HY, Verdel A, Tsai CC, et al. Mechanism for nucleocytoplasmic shuttling of histone deacetylase 7. J Biol Chem 2001; 276:47496-507.
22. Guardiola AR, Yao TP. Molecular cloning and characterization of a novel histone deacetylase HDAC10. J Biol Chem 2002; 277:3350-6.
23. de Ruijter AJ, van Gennip AH, Caron HN, et al. Histone deacetylases (HDACs): characterization of the classical HDAC family. Biochem J 2003; 370:737-49.
24. Jung M. Inhibitors of histone deacetylase as new anticancer agents. Curr Med Chem 2001; 8:1505-11.
25. Heltweg B, Dequiedt F, Marshall BL, et al. Subtype selective substrates for histone deacetylases. J Med Chem 2004; 47:5235-43.
26. Miller TA, Witter DJ, Belvedere S. Histone deacetylase inhibitors. J Med Chem 2003; 46:5097-116.
27. Zhou Y, Santoro R, Grummt I. The chromatin remodeling complex NoRC targets HDAC1 to the ribosomal gene promoter and represses RNA polymerase I transcription. Embo J 2002; 21:4632-40.
28. Frye RA. Phylogenetic classification of prokaryotic and eukaryotic Sir2-like proteins. Biochem Biophys Res Commun 2000; 273:793-8.
29. Jones PA, Baylin SB. The fundamental role of epigenetic events in cancer. Nat Rev Genet 2002; 3:415-28.
30. Wade PA. Transcriptional control at regulatory checkpoints by histone deacetylases: molecular connections between cancer and chromatin. Hum Mol Genet 2001; 10:693-8.
31. Davis PK, Brackmann RK. Chromatin remodeling and cancer. Cancer Biol Ther 2003; 2:22-9.
32. Bhalla K, List A. Histone deacetylase inhibitors in myelodysplastic syndrome. Best Pract Res Clin Haematol 2004; 17:595-611.
33. Kristeleit R, Stimson L, Workman P, Aherne W. Histone modification enzymes: novel targets for cancer drugs. Expert Opin Emerg Drugs 2004; 9:135-54.
34. Bouchain G, Leit S, Frechette S, et al. Development of potential antitumor agents. Synthesis and biological evaluation of a new set of sulfonamide derivatives as histone deacetylase inhibitors. J Med Chem 2003; 46:820-30.
35. Bouchain G, Delorme D. Novel hydroxamate and anilide derivatives as potent histone deacetylase inhibitors: synthesis and antiproliferative evaluation. Curr Med Chem 2003; 10:2359-72.
36. Curtin ML, Garland RB, Heyman HR, et al. Succinimide hydroxamic acids as potent inhibitors of histone deacetylase (HDAC). Bioorg Med Chem Lett 2002; 12:2919-23.
37. Curtin M, Glaser K. Histone deacetylase inhibitors: the Abbott experience. Curr Med Chem 2003; 10:2373-92.

38. Remiszewski SW. The discovery of NVP-LAQ824: from concept to clinic. Curr Med Chem 2003; 10:2393-402.
39. Remiszewski SW, Sambucetti LC, Atadja P, et al. Inhibitors of human histone deacetylase: synthesis and enzyme and cellular activity of straight chain hydroxamates. J Med Chem 2002; 45:753-7.
40. Arts J, de Schepper S, Van Emelen K. Histone deacetylase inhibitors: from chromatin remodeling to experimental cancer therapeutics. Curr Med Chem 2003; 10:2343-50.
41. Kouraklis G, Theocharis S. Histone deacetylase inhibitors and anticancer therapy. Curr Med Chem Anti-Canc Agents 2002; 2:477-84.
42. Remiszewski SW. Recent advances in the discovery of small molecule histone deacetylase inhibitors. Curr Opin Drug Discov Devel 2002; 5:487-99.
43. Kim DH, Kim M, Kwon HJ. Histone deacetylase in carcinogenesis and its inhibitors as anti-cancer agents. J Biochem Mol Biol 2003; 36:110-9.
44. Plumb JA, Steele N, Finn PW, Brown R. Epigenetic approaches to cancer therapy. Biochem Soc Trans 2004; 32:1095-7.
45. Drummond DC, Noble CO, Kirpotin DB, et al. Clinical Development of Histone Deacetylase Inhibitors As Anticancer Agents. Annu Rev Pharmacol Toxicol 2004.
46. Eyal S, Yagen B, Sobol E, et al. The activity of antiepileptic drugs as histone deacetylase inhibitors. Epilepsia 2004; 45:737-44.
47. Kramer OH, Zhu P, Ostendorff HP, et al. The histone deacetylase inhibitor valproic acid selectively induces proteasomal degradation of HDAC2. Embo J 2003; 22:3411-20.
48. Michaelis M, Michaelis UR, Fleming I, et al. Valproic acid inhibits angiogenesis in vitro and in vivo. Mol Pharmacol 2004; 65:520-7.
49. Tang R, Faussat AM, Majdak P, et al. Valproic acid inhibits proliferation and induces apoptosis in acute myeloid leukemia cells expressing P-gp and MRP1. Leukemia 2004; 18:1246-51.
50. Takai N, Desmond JC, Kumagai T, et al. Histone deacetylase inhibitors have a profound antigrowth activity in endometrial cancer cells. Clin Cancer Res 2004; 10:1141-9.
51. Gurvich N, Tsygankova OM, Meinkoth JL, Klein PS. Histone deacetylase is a target of valproic acid-mediated cellular differentiation. Cancer Res 2004; 64:1079-86.
52. Thelen P, Schweyer S, Hemmerlein B, et al. Expressional changes after histone deacetylase inhibition by valproic acid in LNCaP human prostate cancer cells. Int J Oncol 2004; 24:25-31.
53. Carducci MA, Nelson JB, Chan-Tack KM, et al. Phenylbutyrate induces apoptosis in human prostate cancer and is more potent than phenylacetate. Clin Cancer Res 1996; 2:379-87.
54. Piscitelli SC, Thibault A, Figg WD, et al. Disposition of phenylbutyrate and its metabolites, phenylacetate and phenylacetylglutamine. J Clin Pharmacol 1995; 35:368-73.

55. Gore SD, Carducci MA. Modifying histones to tame cancer: clinical development of sodium phenylbutyrate and other histone deacetylase inhibitors. Expert Opin Investig Drugs 2000; 9:2923-34.
56. Johnstone RW. Histone-deacetylase inhibitors: novel drugs for the treatment of cancer. Nat Rev Drug Discov 2002; 1:287-99.
57. Bernhard D, Ausserlechner MJ, Tonko M, et al. Apoptosis induced by the histone deacetylase inhibitor sodium butyrate in human leukemic lymphoblasts. Faseb J 1999; 13:1991-2001.
58. Gozzini A, Rovida E, Dello Sbarba P, et al. Butyrates, as a single drug, induce histone acetylation and granulocytic maturation: possible selectivity on core binding factor-acute myeloid leukemia blasts. Cancer Res 2003; 63:8955-61.
59. Kuefer R, Hofer MD, Altug V, et al. Sodium butyrate and tributyrin induce in vivo growth inhibition and apoptosis in human prostate cancer. Br J Cancer 2004; 90:535-41.
60. Finzer P, Stohr M, Seibert N, Rosl F. Phenylbutyrate inhibits growth of cervical carcinoma cells independent of HPV type and copy number. J Cancer Res Clin Oncol 2003; 129:107-13.
61. Batova A, Shao LE, Diccianni MB, et al. The histone deacetylase inhibitor AN-9 has selective toxicity to acute leukemia and drug-resistant primary leukemia and cancer cell lines. Blood 2002; 100:3319-24.
62. Patnaik A, Rowinsky EK, Villalona MA, et al. A phase I study of pivaloyloxymethyl butyrate, a prodrug of the differentiating agent butyric acid, in patients with advanced solid malignancies. Clin Cancer Res 2002; 8:2142-8.
63. Reid T, Valone F, Lipera W, et al. Phase II trial of the histone deacetylase inhibitor pivaloyloxymethyl butyrate (Pivanex, AN-9) in advanced non-small cell lung cancer. Lung Cancer 2004; 45:381-6.
64. Zimra Y, Nudelman A, Zhuk R, et al. Uptake of pivaloyloxymethyl butyrate into leukemic cells and its intracellular esterase-catalyzed hydrolysis. J Cancer Res Clin Oncol 2000; 126:693-8.
65. Zimra Y, Wasserman L, Maron L, et al. Butyric acid and pivaloyloxymethyl butyrate, AN-9, a novel butyric acid derivative, induce apoptosis in HL-60 cells. J Cancer Res Clin Oncol 1997; 123:152-60.
66. Gore SD, Weng LJ, Figg WD, et al. Impact of prolonged infusions of the putative differentiating agent sodium phenylbutyrate on myelodysplastic syndromes and acute myeloid leukemia. Clin Cancer Res 2002; 8:963-70.
67. Gore SD, Weng LJ, Zhai S, et al. Impact of the putative differentiating agent sodium phenylbutyrate on myelodysplastic syndromes and acute myeloid leukemia. Clin Cancer Res 2001; 7:2330-9.
68. Melchior SW, Brown LG, Figg WD, et al. Effects of phenylbutyrate on proliferation and apoptosis in human prostate cancer cells in vitro and in vivo. Int J Oncol 1999; 14:501-8.
69. Finnin MS, Donigian JR, Cohen A, et al. Structures of a histone deacetylase homologue bound to the TSA and SAHA inhibitors. Nature 1999; 401:188-93.

70. Yoshida M, Horinouchi S, Beppu T. Trichostatin A and trapoxin: novel chemical probes for the role of histone acetylation in chromatin structure and function. Bioessays 1995; 17:423-30.
71. Yoshida M, Furumai R, Nishiyama M, et al. Histone deacetylase as a new target for cancer chemotherapy. Cancer Chemother Pharmacol 2001; 48 Suppl 1:S20-6.
72. Jung M, Brosch G, Kolle D, et al. Amide analogues of trichostatin A as inhibitors of histone deacetylase and inducers of terminal cell differentiation. J Med Chem 1999; 42:4669-79.
73. Herold C, Ganslmayer M, Ocker M, et al. The histone-deacetylase inhibitor Trichostatin A blocks proliferation and triggers apoptotic programs in hepatoma cells. J Hepatol 2002; 36:233-40.
74. Hoshikawa Y, Kwon HJ, Yoshida M, et al. Trichostatin A induces morphological changes and gelsolin expression by inhibiting histone deacetylase in human carcinoma cell lines. Exp Cell Res 1994; 214:189-97.
75. Strait KA, Dabbas B, Hammond EH, et al. Cell cycle blockade and differentiation of ovarian cancer cells by the histone deacetylase inhibitor trichostatin A are associated with changes in p21, Rb, and Id proteins. Mol Cancer Ther 2002; 1:1181-90.
76. Donadelli M, Costanzo C, Faggioli L, et al. Trichostatin A, an inhibitor of histone deacetylases, strongly suppresses growth of pancreatic adenocarcinoma cells. Mol Carcinog 2003; 38:59-69.
77. Park WH, Jung CW, Park JO, et al. Trichostatin inhibits the growth of ACHN renal cell carcinoma cells via cell cycle arrest in association with p27, or apoptosis. Int J Oncol 2003; 22:1129-34.
78. Margueron R, Licznar A, Lazennec G, et al. Oestrogen receptor alpha increases p21(WAF1/CIP1) gene expression and the antiproliferative activity of histone deacetylase inhibitors in human breast cancer cells. J Endocrinol 2003; 179:41-53.
79. Richon VM, Zhou X, Rifkind RA, Marks PA. Histone deacetylase inhibitors: development of suberoylanilide hydroxamic acid (SAHA) for the treatment of cancers. Blood Cells Mol Dis 2001; 27:260-4.
80. Richon VM, Emiliani S, Verdin E, et al. A class of hybrid polar inducers of transformed cell differentiation inhibits histone deacetylases. Proc Natl Acad Sci U S A 1998; 95:3003-7.
81. Marks PA. The mechanism of the anti-tumor activity of the histone deacetylase inhibitor, suberoylanilide hydroxamic acid (SAHA). Cell Cycle 2004; 3:534-5.
82. Richon VM, Webb Y, Merger R, et al. Second generation hybrid polar compounds are potent inducers of transformed cell differentiation. Proc Natl Acad Sci U S A 1996; 93:5705-8.
83. Coffey DC, Kutko MC, Glick RD, et al. Histone deacetylase inhibitors and retinoic acids inhibit growth of human neuroblastoma in vitro. Med Pediatr Oncol 2000; 35:577-81.
84. Munster PN, Troso-Sandoval T, Rosen N, et al. The histone deacetylase inhibitor suberoylanilide hydroxamic acid induces differentiation of human breast cancer cells. Cancer Res 2001; 61:8492-7.

85. Huang L, Pardee AB. Suberoylanilide hydroxamic acid as a potential therapeutic agent for human breast cancer treatment. Mol Med 2000; 6:849-66.
86. Vrana JA, Decker RH, Johnson CR, et al. Induction of apoptosis in U937 human leukemia cells by suberoylanilide hydroxamic acid (SAHA) proceeds through pathways that are regulated by Bcl-2/Bcl-XL, c-Jun, and p21CIP1, but independent of p53. Oncogene 1999; 18:7016-25.
87. Cohen LA, Marks PA, Rifkind RA, et al. Suberoylanilide hydroxamic acid (SAHA), a histone deacetylase inhibitor, suppresses the growth of carcinogen-induced mammary tumors. Anticancer Res 2002; 22:1497-504.
88. Butler LM, Agus DB, Scher HI, et al. Suberoylanilide hydroxamic acid, an inhibitor of histone deacetylase, suppresses the growth of prostate cancer cells in vitro and in vivo. Cancer Res 2000; 60:5165-70.
89. Richon VM, Sandhoff TW, Rifkind RA, Marks PA. Histone deacetylase inhibitor selectively induces p21WAF1 expression and gene-associated histone acetylation. Proc Natl Acad Sci U S A 2000; 97:10014-9.
90. Butler LM, Zhou X, Xu WS, et al. The histone deacetylase inhibitor SAHA arrests cancer cell growth, up-regulates thioredoxin-binding protein-2, and down-regulates thioredoxin. Proc Natl Acad Sci U S A 2002; 99:11700-5.
91. Gui CY, Ngo L, Xu WS, et al. Histone deacetylase (HDAC) inhibitor activation of p21WAF1 involves changes in promoter-associated proteins, including HDAC1. Proc Natl Acad Sci U S A 2004; 101:1241-6.
92. Kutko MC, Glick RD, Butler LM, et al. Histone deacetylase inhibitors induce growth suppression and cell death in human rhabdomyosarcoma in vitro. Clin Cancer Res 2003; 9:5749-55.
93. Butler LM, Webb Y, Agus DB, et al. Inhibition of transformed cell growth and induction of cellular differentiation by pyroxamide, an inhibitor of histone deacetylase. Clin Cancer Res 2001; 7:962-70.
94. Yu C, Subler M, Rahmani M, et al. Induction of apoptosis in BCR/ABL+ cells by histone deacetylase inhibitors involves reciprocal effects on the RAF/MEK/ERK and JNK pathways. Cancer Biol Ther 2003; 2:544-51.
95. Kim YB, Lee KH, Sugita K, et al. Oxamflatin is a novel antitumor compound that inhibits mammalian histone deacetylase. Oncogene 1999; 18:2461-70.
96. Su GH, Sohn TA, Ryu B, Kern SE. A novel histone deacetylase inhibitor identified by high-throughput transcriptional screening of a compound library. Cancer Res 2000; 60:3137-42.
97. Catley L, Weisberg E, Tai YT, et al. NVP-LAQ824 is a potent novel histone deacetylase inhibitor with significant activity against multiple myeloma. Blood 2003; 102:2615-22.
98. Atadja P, Gao L, Kwon P, et al. Selective growth inhibition of tumor cells by a novel histone deacetylase inhibitor, NVP-LAQ824. Cancer Res 2004; 64:689-95.
99. Zhang XD, Gillespie SK, Borrow JM, Hersey P. The histone deacetylase inhibitor suberic bishydroxamate regulates the expression of multiple apoptotic mediators and induces mitochondria-dependent apoptosis of melanoma cells. Mol Cancer Ther 2004; 3:425-35.

100. Plumb JA, Finn PW, Williams RJ, et al. Pharmacodynamic response and inhibition of growth of human tumor xenografts by the novel histone deacetylase inhibitor PXD101. Mol Cancer Ther 2003; 2:721-8.
101. Furumai R, Komatsu Y, Nishino N, et al. Potent histone deacetylase inhibitors built from trichostatin A and cyclic tetrapeptide antibiotics including trapoxin. Proc Natl Acad Sci U S A 2001; 98:87-92.
102. Nishino N, Jose B, Okamura S, et al. Cyclic tetrapeptides bearing a sulfhydryl group potently inhibit histone deacetylases. Org Lett 2003; 5:5079-82.
103. Komatsu Y, Tomizaki KY, Tsukamoto M, et al. Cyclic hydroxamic-acid-containing peptide 31, a potent synthetic histone deacetylase inhibitor with antitumor activity. Cancer Res 2001; 61:4459-66.
104. Kijima M, Yoshida M, Sugita K, et al. Trapoxin, an antitumor cyclic tetrapeptide, is an irreversible inhibitor of mammalian histone deacetylase. J Biol Chem 1993; 268:22429-35.
105. Kosugi H, Towatari M, Hatano S, et al. Histone deacetylase inhibitors are the potent inducer/enhancer of differentiation in acute myeloid leukemia: a new approach to anti-leukemia therapy. Leukemia 1999; 13:1316-24.
106. Han JW, Ahn SH, Park SH, et al. Apicidin, a histone deacetylase inhibitor, inhibits proliferation of tumor cells via induction of p21WAF1/Cip1 and gelsolin. Cancer Res 2000; 60:6068-74.
107. Singh SB, Zink DL, Liesch JM, et al. Structure, histone deacetylase, and antiprotozoal activities of apicidins B and C, congeners of apicidin with proline and valine substitutions. Org Lett 2001; 3:2815-8.
108. Meinke PT, Colletti SL, Doss G, et al. Synthesis of apicidin-derived quinolone derivatives: parasite-selective histone deacetylase inhibitors and antiproliferative agents. J Med Chem 2000; 43:4919-22.
109. Singh SB, Zink DL, Liesch JM, et al. Structure and chemistry of apicidins, a class of novel cyclic tetrapeptides without a terminal alpha-keto epoxide as inhibitors of histone deacetylase with potent antiprotozoal activities. J Org Chem 2002; 67:815-25.
110. Kim SH, Ahn S, Han JW, et al. Apicidin is a histone deacetylase inhibitor with anti-invasive and anti-angiogenic potentials. Biochem Biophys Res Commun 2004; 315:964-70.
111. Hong J, Ishihara K, Yamaki K, et al. Apicidin, a histone deacetylase inhibitor, induces differentiation of HL-60 cells. Cancer Lett 2003; 189:197-206.
112. Piekarz R, Bates S. A review of depsipeptide and other histone deacetylase inhibitors in clinical trials. Curr Pharm Des 2004; 10:2289-98.
113. Sasakawa Y, Naoe Y, Inoue T, et al. Effects of FK228, a novel histone deacetylase inhibitor, on human lymphoma U-937 cells in vitro and in vivo. Biochem Pharmacol 2002; 64:1079-90.
114. Sasakawa Y, Naoe Y, Inoue T, et al. Effects of FK228, a novel histone deacetylase inhibitor, on tumor growth and expression of p21 and c-myc genes in vivo. Cancer Lett 2003; 195:161-8.

115. Sasakawa Y, Naoe Y, Noto T, et al. Antitumor efficacy of FK228, a novel histone deacetylase inhibitor, depends on the effect on expression of angiogenesis factors. Biochem Pharmacol 2003; 66:897-906.
116. Byrd JC, Shinn C, Ravi R, et al. Depsipeptide (FR901228): a novel therapeutic agent with selective, in vitro activity against human B-cell chronic lymphocytic leukemia cells. Blood 1999; 94:1401-8.
117. Kwon HJ, Kim MS, Kim MJ, et al. Histone deacetylase inhibitor FK228 inhibits tumor angiogenesis. Int J Cancer 2002; 97:290-6.
118. Marshall JL, Rizvi N, Kauh J, et al. A phase I trial of depsipeptide (FR901228) in patients with advanced cancer. J Exp Ther Oncol 2002; 2:325-32.
119. Sandor V, Bakke S, Robey RW, et al. Phase I trial of the histone deacetylase inhibitor, depsipeptide (FR901228, NSC 630176), in patients with refractory neoplasms. Clin Cancer Res 2002; 8:718-28.
120. Byrd JC, Marcucci G, Parthun MR, et al. A phase I and pharmacodynamic study of depsipeptide (FK228) in chronic lymphocytic leukemia and acute myeloid leukemia. Blood 2004.
121. LoRusso PM, Demchik L, Foster B, et al. Preclinical antitumor activity of CI-994. Invest New Drugs 1996; 14:349-56.
122. Graziano MJ, Pilcher GD, Walsh KM, et al. Preclinical toxicity of a new oral anticancer drug, CI-994 (acetyldinaline), in rats and dogs. Invest New Drugs 1997; 15:295-310.
123. Prakash S, Foster BJ, Meyer M, et al. Chronic oral administration of CI-994: a phase 1 study. Invest New Drugs 2001; 19:1-11.
124. Suzuki T, Ando T, Tsuchiya K, et al. Synthesis and histone deacetylase inhibitory activity of new benzamide derivatives. J Med Chem 1999; 42:3001-3.
125. Saito A, Yamashita T, Mariko Y, et al. A synthetic inhibitor of histone deacetylase, MS-27-275, with marked in vivo antitumor activity against human tumors. Proc Natl Acad Sci U S A 1999; 96:4592-7.
126. Jaboin J, Wild J, Hamidi H, et al. MS-27-275, an inhibitor of histone deacetylase, has marked in vitro and in vivo antitumor activity against pediatric solid tumors. Cancer Res 2002; 62:6108-15.
127. Fournel M, Trachy-Bourget MC, Yan PT, et al. Sulfonamide anilides, a novel class of histone deacetylase inhibitors, are antiproliferative against human tumors. Cancer Res 2002; 62:4325-30.
128. Cheng HL, Mostoslavsky R, Saito S, et al. Developmental defects and p53 hyperacetylation in Sir2 homolog (SIRT1)-deficient mice. Proc Natl Acad Sci U S A 2003; 100:10794-9.
129. McLaughlin F, La Thangue NB. Histone deacetylase inhibitors open new doors in cancer therapy. Biochem Pharmacol 2004; 68:1139-44.
130. Rosato RR, Grant S. Histone deacetylase inhibitors in cancer therapy. Cancer Biol Ther 2003; 2:30-7.
131. Zhu WG, Dai Z, Ding H, et al. Increased expression of unmethylated CDKN2D by 5-aza-2'-deoxycytidine in human lung cancer cells. Oncogene 2001; 20:7787-96.

132. Warrener R, Beamish H, Burgess A, et al. Tumor cell-selective cytotoxicity by targeting cell cycle checkpoints. Faseb J 2003; 17:1550-2.
133. Archer SY, Meng S, Shei A, Hodin RA. p21(WAF1) is required for butyrate-mediated growth inhibition of human colon cancer cells. Proc Natl Acad Sci U S A 1998; 95:6791-6.
134. Sowa Y, Orita T, Hiranabe-Minamikawa S, et al. Histone deacetylase inhibitor activates the p21/WAF1/Cip1 gene promoter through the Sp1 sites. Ann N Y Acad Sci 1999; 886:195-9.
135. Sowa Y, Orita T, Minamikawa-Hiranabe S, et al. Sp3, but not Sp1, mediates the transcriptional activation of the p21/WAF1/Cip1 gene promoter by histone deacetylase inhibitor. Cancer Res 1999; 59:4266-70.
136. Chai F, Evdokiou A, Young GP, Zalewski PD. Involvement of p21(Waf1/Cip1) and its cleavage by DEVD-caspase during apoptosis of colorectal cancer cells induced by butyrate. Carcinogenesis 2000; 21:7-14.
137. Huang L, Sowa Y, Sakai T, Pardee AB. Activation of the p21WAF1/CIP1 promoter independent of p53 by the histone deacetylase inhibitor suberoylanilide hydroxamic acid (SAHA) through the Sp1 sites. Oncogene 2000; 19:5712-9.
138. Sandor V, Senderowicz A, Mertins S, et al. P21-dependent g(1)arrest with downregulation of cyclin D1 and upregulation of cyclin E by the histone deacetylase inhibitor FR901228. Br J Cancer 2000; 83:817-25.
139. Siavoshian S, Segain JP, Kornprobst M, et al. Butyrate and trichostatin A effects on the proliferation/differentiation of human intestinal epithelial cells: induction of cyclin D3 and p21 expression. Gut 2000; 46:507-14.
140. Lavelle D, Chen YH, Hankewych M, DeSimone J. Histone deacetylase inhibitors increase p21(WAF1) and induce apoptosis of human myeloma cell lines independent of decreased IL-6 receptor expression. Am J Hematol 2001; 68:170-8.
141. Blagosklonny MV, Robey R, Sackett DL, et al. Histone deacetylase inhibitors all induce p21 but differentially cause tubulin acetylation, mitotic arrest, and cytotoxicity. Mol Cancer Ther 2002; 1:937-41.
142. Wang ZM, Hu J, Zhou D, et al. Trichostatin A inhibits proliferation and induces expression of p21WAF and p27 in human brain tumor cell lines. Ai Zheng 2002; 21:1100-5.
143. Chiba T, Yokosuka O, Arai M, et al. Identification of genes up-regulated by histone deacetylase inhibition with cDNA microarray and exploration of epigenetic alterations on hepatoma cells. J Hepatol 2004; 41:436-45.
144. Chiba T, Yokosuka O, Fukai K, et al. Cell growth inhibition and gene expression induced by the histone deacetylase inhibitor, trichostatin A, on human hepatoma cells. Oncology 2004; 66:481-91.
145. Mitsiades N, Mitsiades CS, Richardson PG, et al. Molecular sequelae of histone deacetylase inhibition in human malignant B cells. Blood 2003; 101:4055-62.
146. Kim YB, Ki SW, Yoshida M, Horinouchi S. Mechanism of cell cycle arrest caused by histone deacetylase inhibitors in human carcinoma cells. J Antibiot (Tokyo) 2000; 53:1191-200.

147. Yokota T, Matsuzaki Y, Miyazawa K, et al. Histone deacetylase inhibitors activate INK4d gene through Sp1 site in its promoter. Oncogene 2004; 23:5340-9.
148. Li H, Wu X. Histone deacetylase inhibitor, Trichostatin A, activates p21(WAF1/CIP1) expression through downregulation of c-myc and release of the repression of c-myc from the promoter in human cervical cancer cells. Biochem Biophys Res Commun 2004; 324:860-7.
149. Aron JL, Parthun MR, Marcucci G, et al. Depsipeptide (FR901228) induces histone acetylation and inhibition of histone deacetylase in chronic lymphocytic leukemia cells concurrent with activation of caspase 8-mediated apoptosis and down-regulation of c-FLIP protein. Blood 2003; 102:652-8.
150. Rosato RR, Wang Z, Gopalkrishnan RV, et al. Evidence of a functional role for the cyclin-dependent kinase-inhibitor p21WAF1/CIP1/MDA6 in promoting differentiation and preventing mitochondrial dysfunction and apoptosis induced by sodium butyrate in human myelomonocytic leukemia cells (U937). Int J Oncol 2001; 19:181-91.
151. Nguyen DM, Schrump WD, Tsai WS, et al. Enhancement of depsipeptide-mediated apoptosis of lung or esophageal cancer cells by flavopiridol: activation of the mitochondria-dependent death-signaling pathway. J Thorac Cardiovasc Surg 2003; 125:1132-42.
152. Guo F, Sigua C, Tao J, et al. Cotreatment with histone deacetylase inhibitor LAQ824 enhances Apo-2L/tumor necrosis factor-related apoptosis inducing ligand-induced death inducing signaling complex activity and apoptosis of human acute leukemia cells. Cancer Res 2004; 64:2580-9.
153. Ruefli AA, Ausserlechner MJ, Bernhard D, et al. The histone deacetylase inhibitor and chemotherapeutic agent suberoylanilide hydroxamic acid (SAHA) induces a cell-death pathway characterized by cleavage of Bid and production of reactive oxygen species. Proc Natl Acad Sci U S A 2001; 98:10833-8.
154. Lucas DM, Davis ME, Parthun MR, et al. The histone deacetylase inhibitor MS-275 induces caspase-dependent apoptosis in B-cell chronic lymphocytic leukemia cells. Leukemia 2004; 18:1207-14.
155. Rosato RR, Almenara JA, Grant S. The histone deacetylase inhibitor MS-275 promotes differentiation or apoptosis in human leukemia cells through a process regulated by generation of reactive oxygen species and induction of p21CIP1/WAF1 1. Cancer Res 2003; 63:3637-45.
156. Yao Q, Nishiuchi R, Li Q, et al. FLT3 expressing leukemias are selectively sensitive to inhibitors of the molecular chaperone heat shock protein 90 through destabilization of signal transduction-associated kinases. Clin Cancer Res 2003; 9:4483-93.
157. Atadja P, Hsu M, Kwon P, et al. Molecular and cellular basis for the anti-proliferative effects of the HDAC inhibitor LAQ824. Novartis Found Symp 2004; 259:249-66; discussion 266-8, 285-8.
158. Peart MJ, Tainton KM, Ruefli AA, et al. Novel mechanisms of apoptosis induced by histone deacetylase inhibitors. Cancer Res 2003; 63:4460-71.

159. Kamitani H, Taniura S, Watanabe K, et al. Histone acetylation may suppress human glioma cell proliferation when p21 WAF/Cip1 and gelsolin are induced. Neuro-oncol 2002; 4:95-101.
160. Mielnicki LM, Ying AM, Head KL, et al. Epigenetic regulation of gelsolin expression in human breast cancer cells. Exp Cell Res 1999; 249:161-76.
161. Mie Lee Y, Kim SH, Kim HS, et al. Inhibition of hypoxia-induced angiogenesis by FK228, a specific histone deacetylase inhibitor, via suppression of HIF-1alpha activity. Biochem Biophys Res Commun 2003; 300:241-6.
162. Qian DZ, Wang X, Kachhap SK, et al. The histone deacetylase inhibitor NVP-LAQ824 inhibits angiogenesis and has a greater antitumor effect in combination with the vascular endothelial growth factor receptor tyrosine kinase inhibitor PTK787/ZK222584. Cancer Res 2004; 64:6626-34.
163. Williams RJ. Trichostatin A, an inhibitor of histone deacetylase, inhibits hypoxia-induced angiogenesis. Expert Opin Investig Drugs 2001; 10:1571-3.
164. Sawa H, Murakami H, Ohshima Y, et al. Histone deacetylase inhibitors such as sodium butyrate and trichostatin A inhibit vascular endothelial growth factor (VEGF) secretion from human glioblastoma cells. Brain Tumor Pathol 2002; 19:77-81.
165. Baylin SB, Esteller M, Rountree MR, et al. Aberrant patterns of DNA methylation, chromatin formation and gene expression in cancer. Hum Mol Genet 2001; 10:687-92.
166. Herman JG, Baylin SB. Gene silencing in cancer in association with promoter hypermethylation. N Engl J Med 2003; 349:2042-54.
167. Cameron EE, Bachman KE, Myohanen S, et al. Synergy of demethylation and histone deacetylase inhibition in the re-expression of genes silenced in cancer. Nat Genet 1999; 21:103-7.
168. Zhu WG, Lakshmanan RR, Beal MD, Otterson GA. DNA methyltransferase inhibition enhances apoptosis induced by histone deacetylase inhibitors. Cancer Res 2001; 61:1327-33.
169. Zhu WG, Otterson GA. The interaction of histone deacetylase inhibitors and DNA methyltransferase inhibitors in the treatment of human cancer cells. Curr Med Chem Anti-Canc Agents 2003; 3:187-99.
170. Yang X, Phillips DL, Ferguson AT, et al. Synergistic activation of functional estrogen receptor (ER)-alpha by DNA methyltransferase and histone deacetylase inhibition in human ER-alpha-negative breast cancer cells. Cancer Res 2001; 61:7025-9.
171. Keen JC, Yan L, Mack KM, et al. A novel histone deacetylase inhibitor, scriptaid, enhances expression of functional estrogen receptor alpha (ER) in ER negative human breast cancer cells in combination with 5-aza 2'-deoxycytidine. Breast Cancer Res Treat 2003; 81:177-86.
172. Jang ER, Lim SJ, Lee ES, et al. The histone deacetylase inhibitor trichostatin A sensitizes estrogen receptor alpha-negative breast cancer cells to tamoxifen. Oncogene 2004; 23:1724-36.

173. Shaker S, Bernstein M, Momparler LF, Momparler RL. Preclinical evaluation of antineoplastic activity of inhibitors of DNA methylation (5-aza-2'-deoxycytidine) and histone deacetylation (trichostatin A, depsipeptide) in combination against myeloid leukemic cells. Leuk Res 2003; 27:437-44.
174. Lemaire M, Momparler LF, Farinha NJ, et al. Enhancement of antineoplastic action of 5-aza-2'-deoxycytidine by phenylbutyrate on L1210 leukemic cells. Leuk Lymphoma 2004; 45:147-54.
175. Belinsky SA, Klinge DM, Stidley CA, et al. Inhibition of DNA methylation and histone deacetylation prevents murine lung cancer. Cancer Res 2003; 63:7089-93.
176. Kim MS, Blake M, Baek JH, et al. Inhibition of histone deacetylase increases cytotoxicity to anticancer drugs targeting DNA. Cancer Res 2003; 63:7291-300.
177. Marchion DC, Bicaku E, Daud AI, et al. Sequence-specific potentiation of topoisomerase II inhibitors by the histone deacetylase inhibitor suberoylanilide hydroxamic acid. J Cell Biochem 2004; 92:223-37.
178. Nimmanapalli R, Bhalla K. Mechanisms of resistance to imatinib mesylate in Bcr-Abl-positive leukemias. Curr Opin Oncol 2002; 14:616-20.
179. Yu C, Rahmani M, Almenara J, et al. Histone deacetylase inhibitors promote STI571-mediated apoptosis in STI571-sensitive and -resistant Bcr/Abl+ human myeloid leukemia cells. Cancer Res 2003; 63:2118-26.
180. Nimmanapalli R, Fuino L, Stobaugh C, et al. Cotreatment with the histone deacetylase inhibitor suberoylanilide hydroxamic acid (SAHA) enhances imatinib-induced apoptosis of Bcr-Abl-positive human acute leukemia cells. Blood 2003; 101:3236-9.
181. Rahmani M, Yu C, Dai Y, et al. Coadministration of the heat shock protein 90 antagonist 17-allylamino- 17-demethoxygeldanamycin with suberoylanilide hydroxamic acid or sodium butyrate synergistically induces apoptosis in human leukemia cells. Cancer Res 2003; 63:8420-7.
182. Rosato RR, Almenara JA, Yu C, Grant S. Evidence of a functional role for p21WAF1/CIP1 down-regulation in synergistic antileukemic interactions between the histone deacetylase inhibitor sodium butyrate and flavopiridol. Mol Pharmacol 2004; 65:571-81.
183. Rosato RR, Almenara JA, Cartee L, et al. The cyclin-dependent kinase inhibitor flavopiridol disrupts sodium butyrate-induced p21WAF1/CIP1 expression and maturation while reciprocally potentiating apoptosis in human leukemia cells. Mol Cancer Ther 2002; 1:253-66.
184. Maggio SC, Rosato RR, Kramer LB, et al. The histone deacetylase inhibitor MS-275 interacts synergistically with fludarabine to induce apoptosis in human leukemia cells. Cancer Res 2004; 64:2590-600.
185. Pei XY, Dai Y, Grant S. Synergistic induction of oxidative injury and apoptosis in human multiple myeloma cells by the proteasome inhibitor bortezomib and histone deacetylase inhibitors. Clin Cancer Res 2004; 10:3839-52.
186. Yu C, Rahmani M, Conrad D, et al. The proteasome inhibitor bortezomib interacts synergistically with histone deacetylase inhibitors to induce apoptosis in Bcr/Abl+ cells sensitive and resistant to STI571. Blood 2003; 102:3765-74.

187. Nimmanapalli R, Fuino L, Bali P, et al. Histone deacetylase inhibitor LAQ824 both lowers expression and promotes proteasomal degradation of Bcr-Abl and induces apoptosis of imatinib mesylate-sensitive or -refractory chronic myelogenous leukemia-blast crisis cells. Cancer Res 2003; 63:5126-35.
188. Bali P, George P, Cohen P, et al. Superior activity of the combination of histone deacetylase inhibitor LAQ824 and the FLT-3 kinase inhibitor PKC412 against human acute myelogenous leukemia cells with mutant FLT-3. Clin Cancer Res 2004; 10:4991-7.
189. Huang Y, Horvath CM, Waxman S. Regrowth of 5-fluorouracil-treated human colon cancer cells is prevented by the combination of interferon gamma, indomethacin, and phenylbutyrate. Cancer Res 2000; 60:3200-6.
190. Huang Y, Waxman S. Enhanced growth inhibition and differentiation of fluorodeoxyuridine-treated human colon carcinoma cells by phenylbutyrate. Clin Cancer Res 1998; 4:2503-9.
191. Fuino L, Bali P, Wittmann S, et al. Histone deacetylase inhibitor LAQ824 down-regulates Her-2 and sensitizes human breast cancer cells to trastuzumab, taxotere, gemcitabine, and epothilone B. Mol Cancer Ther 2003; 2:971-84.
192. Rosato RR, Almenara JA, Dai Y, Grant S. Simultaneous activation of the intrinsic and extrinsic pathways by histone deacetylase (HDAC) inhibitors and tumor necrosis factor-related apoptosis-inducing ligand (TRAIL) synergistically induces mitochondrial damage and apoptosis in human leukemia cells. Mol Cancer Ther 2003; 2:1273-84.
193. Zhang XD, Gillespie SK, Borrow JM, Hersey P. The histone deacetylase inhibitor suberic bishydroxamate: a potential sensitizer of melanoma to TNF-related apoptosis-inducing ligand (TRAIL) induced apoptosis. Biochem Pharmacol 2003; 66:1537-45.
194. Jansen MS, Nagel SC, Miranda PJ, et al. Short-chain fatty acids enhance nuclear receptor activity through mitogen-activated protein kinase activation and histone deacetylase inhibition. Proc Natl Acad Sci U S A 2004; 101:7199-204.
195. Liu LT, Chang HC, Chiang LC, Hung WC. Histone deacetylase inhibitor up-regulates RECK to inhibit MMP-2 activation and cancer cell invasion. Cancer Res 2003; 63:3069-72.
196. Chung YL, Wang AJ, Yao LF. Antitumor histone deacetylase inhibitors suppress cutaneous radiation syndrome: Implications for increasing therapeutic gain in cancer radiotherapy. Mol Cancer Ther 2004; 3:317-25.
197. Zhang Y, Adachi M, Zhao X, et al. Histone deacetylase inhibitors FK228, N-(2-aminophenyl)-4-[N-(pyridin-3-yl-methoxycarbonyl)amino- methyl]benzamide and m-carboxycinnamic acid bis-hydroxamide augment radiation-induced cell death in gastrointestinal adenocarcinoma cells. Int J Cancer 2004; 110:301-8.
198. Coffey DC, Kutko MC, Glick RD, et al. The histone deacetylase inhibitor, CBHA, inhibits growth of human neuroblastoma xenografts in vivo, alone and synergistically with all-trans retinoic acid. Cancer Res 2001; 61:3591-4.

199. He LZ, Tolentino T, Grayson P, et al. Histone deacetylase inhibitors induce remission in transgenic models of therapy-resistant acute promyelocytic leukemia. J Clin Invest 2001; 108:1321-30.
200. Hu E, Dul E, Sung CM, et al. Identification of novel isoform-selective inhibitors within class I histone deacetylases. J Pharmacol Exp Ther 2003; 307:720-8.
201. Furumai R, Matsuyama A, Kobashi N, et al. FK228 (depsipeptide) as a natural prodrug that inhibits class I histone deacetylases. Cancer Res 2002; 62:4916-21.
202. Hanahan D, Weinberg RA. The hallmarks of cancer. Cell 2000; 100:57-70.
203. Thibault A, Cooper MR, Figg WD, et al. A phase I and pharmacokinetic study of intravenous phenylacetate in patients with cancer. Cancer Res 1994; 54:1690-4.
204. Thibault A, Samid D, Cooper MR, et al. Phase I study of phenylacetate administered twice daily to patients with cancer. Cancer 1995; 75:2932-8.
205. Chang SM, Kuhn JG, Robins HI, et al. Phase II study of phenylacetate in patients with recurrent malignant glioma: a North American Brain Tumor Consortium report. J Clin Oncol 1999; 17:984-90.
206. Chang SM, Kuhn JG, Ian Robins H, et al. A study of a different dose-intense infusion schedule of phenylacetate in patients with recurrent primary brain tumors consortium report. Invest New Drugs 2003; 21:429-33.
207. Carducci MA, Gilbert J, Bowling MK, et al. A Phase I clinical and pharmacological evaluation of sodium phenylbutyrate on an 120-h infusion schedule. Clin Cancer Res 2001; 7:3047-55.
208. Gilbert J, Baker SD, Bowling MK, et al. A phase I dose escalation and bioavailability study of oral sodium phenylbutyrate in patients with refractory solid tumor malignancies. Clin Cancer Res 2001; 7:2292-300.
209. A. Atmaca AM, T. Heinzel, M. Göttlicher, A. Neumann, S.-E. Al-Batran, E. Martin, I. Bartsch, A. Knuth, E. Jaeger. A dose-escalating phase I study with valproic acid (VPA) in patients (pts) with advanced cancer. Journal of Clinical Oncology, 2004 ASCO Annual Meeting Proceedings (Post-Meeting Edition). 2004; 22:3169.
210. Kelly WK, Richon VM, O'Connor O, et al. Phase I clinical trial of histone deacetylase inhibitor: suberoylanilide hydroxamic acid administered intravenously. Clin Cancer Res 2003; 9:3578-88.
211. G. Garcia-Manero J-PI, J. Cortes, C. Koller, S. O´brien, E. Estey, A. A. Canalli, J. Chiao, V. Richon, H. Kantarjian. Phase I study of oral suberoylanilide hydroxamic acid (SAHA), a histone deacetylase inhibitor, in patients (pts) with advanced leukemias or myelodysplastic syndromes (MDS). Journal of Clinical Oncology, ASCO Annual Meeting Proceedings 2004; Vol 22:3027.
212. Kelly WK OCO, Richon VM, et. al. A Phase I clinical trial of an oral formulation of the histone deacetylase inhibitor of suberoylanilide hydroxamic acid (SAHA). 14th EORTC-NCI-AACR meeting, Frankfurt 2002; 286.
213. G. Blumenschein CL, M. Kies, B. Glisson, V. Papadimitrakopoulou, R. Zinner, E. Kim, A. Gillenwater, J. Chiao, W. Hong. Phase II clinical trial of suberoylanilide hydroxamic acid (SAHA) in patients (pts) with recurrent and/or metastatic head

and neck cancer(SCCHN). Journal of Clinical Oncology, ASCO Annual Meeting Proceedings. 2004; Vol 22:5578.
214. Piekarz RL, Robey R, Sandor V, et al. Inhibitor of histone deacetylation, depsipeptide (FR901228), in the treatment of peripheral and cutaneous T-cell lymphoma: a case report. Blood 2001; 98:2865-8.
215. Ryan Q, Headlee D, Sparreboom A, Figg W, Zhai S, Trepel J, Murgo A, Elsayed Y, Karp J and Sausville E. A phase I trial of an oral histone deacetylase inhibitor, MS-275, in advanced solid tumor and lymphoma patients. Proc Am Soc Clin Oncol 2003; 22:200.
216. L. Gore SNH, M. Basche, S. K. S. Raj, I. Arnold, C. O'Bryant, S. Witta, B. Rohde, C. McCoy, S. G. Eckhardt. Updated results from a phase I trial of the histone deacetylase (HDAC) inhibitor MS-275 in patients with refractory solid tumors. Journal of Clinical Oncology, ASCO Annual Meeting Proceedings 2004; Vol 22:3026.
217. O. G. Ottmann DJD, R. M. Stone, H. Pfeifer, B. Lowenberg, P. Atadja, B. Peng, J. W. Scott, M. Dugan, P. Sonneveld. A Phase I, pharmacokinetic (PK) and pharmacodynamic (PD) study of a novel histone deacetylase inhibitor LAQ824 in patients with hematologic malignancies. Journal of Clinical Oncology, ASCO Annual Meeting Proceedings 2004; Vol 22:3024.
218. E. K. Rowinsky SP, A. Patnaik, A. O'Donnell, M. M. Mita, P. Atadja, B. Peng, M. Dugan, J. W. Scott, J. S. De Bono. A phase I, pharmacokinetic (PK) and pharmacodynamic (PD) study of a novel histone deacetylase (HDAC) inhibitor LAQ824 in patients with advanced solid tumors. Journal of Clinical Oncology, ASCO Annual Meeting Proceedings 2004; Vol 22:3022.
219. J. Beck TF, E. Rowinsky, C. Huber, M. Mita, P. Atadja, B. Peng, C. Kwong, M. Dugan, A. Patnaik. Phase I pharmacokinetic (PK) and pharmacodynamic (PD) study of LBH589A: A novel histone deacetylase inhibitor. Journal of Clinical Oncology, ASCO Annual Meeting Proceedings. 2004; Vol 22:3025.
220. Nemunaitis JJ, Orr D, Eager R, et al. Phase I study of oral CI-994 in combination with gemcitabine in treatment of patients with advanced cancer. Cancer J 2003; 9:58-66.
221. Undevia SD, Kindler HL, Janisch L, et al. A phase I study of the oral combination of CI-994, a putative histone deacetylase inhibitor, and capecitabine. Ann Oncol 2004; 15:1705-11.
222. A Wozniak JOS, J Fiorica, W Grove. Phase II Trial of CI-994 in Patients (pts) with Advanced Nonsmall Cell Lung Cancer (NSCLC). Proc Am Soc Clin Oncol 1999; Abstract No: 1878.
223. J O'Shaughnessy LF, J Fiorica, W Grove. Phase II Trial of CI-994 in Patients (pts) with Metastatic Renal Cell Carcinoma (RCC). Proc Am Soc Clin Oncol 1999; Abstract No: 1346.
224. Mark Zalupski JOS, Svetislava Vukelja, Anthony Shields, Kathy Diener, William Grove. Phase II Trial of II-994 in Patients (PTS) with Advanced Pancreatic Cancer (APC). Proc Am Soc Clin Oncol 2000; Abstract No: 1115.

225. Jairo Olivares AW, Stephen Olson, Lynne R Pauer, William Grove, John Nemunaitis. Phase I Pharmacokinetic (PK) Study of CI-994 in Combination with Carboplatin (C) and Paclitaxel (T) in Patients (pts) with Advanced Solid Tumors. Proc Am Soc Clin Oncol 2001; Abstract No. 346.
226. T. Reid AW, M. Vakil, T. Cosgriff, T. Harper, F. Valone, D. Magnuson, A. Bhatnagar. Dose escalation study of pivanex (a histone deacetylase inhibitor) in combination with docetaxel for advanced non-small cell lung cancer. Journal of Clinical Oncology, ASCO Annual Meeting Proceedings 2004; 22:7279.
227. Park JH, Jung Y, Kim TY, et al. Class I histone deacetylase-selective novel synthetic inhibitors potently inhibit human tumor proliferation. Clin Cancer Res 2004; 10:5271-81.
228. Lee BI, Park SH, Kim JW, et al. MS-275, a histone deacetylase inhibitor, selectively induces transforming growth factor beta type II receptor expression in human breast cancer cells. Cancer Res 2001; 61:931-4.
229. Haggarty SJ, Koeller KM, Wong JC, et al. Domain-selective small-molecule inhibitor of histone deacetylase 6 (HDAC6)-mediated tubulin deacetylation. Proc Natl Acad Sci U S A 2003; 100:4389-94.
230. Sausville EA, Alley MC, Pacula-Cox CM, al. e. Pharmacologic evaluations of MS-275(NSC7069950), a novel benzamide strcuture with a unique spectrum of antitumor activity. Proc Am Ass. Cancer Research 2001; 42:927 (#4976).
231. Park SH, Lee SR, Kim BC, et al. Transcriptional regulation of the transforming growth factor beta type II receptor gene by histone acetyltransferase and deacetylase is mediated by NF-Y in human breast cancer cells. J Biol Chem 2002; 277:5168-74.
232. Mullauer L, Fujita H, Ishizaki A, Kuzumaki N. Tumor-suppressive function of mutated gelsolin in ras-transformed cells. Oncogene 1993; 8:2531-6.
233. Shah VP, Midha KK, Dighe S, et al. Analytical methods validation: bioavailability, bioequivalence and pharmacokinetic studies. Conference report. Eur J Drug Metab Pharmacokinet 1991; 16:249-55.
234. Sparreboom A, Loos WJ. Protein binding of anticancer drugs. In: Figg WD, McLeod HL, eds. Handbook of Anticancer Pharmacokinetics and Pharmacodynamics. Totawa, NJ: Humana Press, 2004:169-188.
235. Acharya MR, Baker SD, Verweij J, et al. Determination of fraction unbound docetaxel using micro-equilibrium dialysis. Anal Biochem 2004; 331:192-94.
236. Ryan Q, Headlee D, Elsayed Y, et al. A first in human trial of an oral histone deacetylase inhibitor, MS-275, in advanced solid tumor and lymphoma patients. Proc Am Assoc Cancer Res 2004; 45:199 (abstract).
237. Hwang K, Acharya MR, Sausville EA, et al. Determination of MS-275, a novel histone deacetylase inhibitor, in human plasma by liquid chromatography-electrospray mass spectrometry. J Chromatogr B Analyt Technol Biomed Life Sci 2004; 804:289-94.
238. Rossing N. Albumin metabolism in neoplastic diseases. Scand J Clin Lab Invest 1968; 22:211-6.
239. Bacchus H. Serum glycoproteins in cancer. Prog Clin Pathol 1975; 6:111-35.

240. Duche JC, Urien S, Simon N, et al. Expression of the genetic variants of human alpha-1-acid glycoprotein in cancer. Clin Biochem 2000; 33:197-202.
241. Loos WJ, Baker SD, Verweij J, et al. Clinical pharmacokinetics of unbound docetaxel: role of polysorbate 80 and serum proteins. Clin Pharmacol Ther 2003; 74:364-71.
242. Ten Tije AJ, Loos WJ, Verweij J, et al. Disposition of polyoxyethylated excipients in humans: implications for drug safety and formulation approaches. Clin Pharmacol Ther 2003; 74:509-10.
243. Whitlam JB, Crooks MJ, Brown KF, Pedersen PV. Binding of nonsteroidal anti-inflammatory agents to proteins--I. Ibuprofen-serum albumin interaction. Biochem Pharmacol 1979; 28:675-8.
244. Dasgupta A. Clinical utility of free drug monitoring. Clin Chem Lab Med 2002; 40:986-93.
245. Benet LZ, Hoener BA. Changes in plasma protein binding have little clinical relevance. Clin Pharmacol Ther 2002; 71:115-21.
246. Webb D, Buss DC, Fifield R, et al. The plasma protein binding of metoclopramide in health and renal disease. Br J Clin Pharmacol 1986; 21:334-6.
247. Fuse E, Tanii H, Kurata N, et al. Unpredicted clinical pharmacology of UCN-01 caused by specific binding to human alpha1-acid glycoprotein. Cancer Res 1998; 58:3248-53.
248. Wilkinson GR. Plasma and tissue binding considerations in drug disposition. Drug Metab Rev 1983; 14:427-65.
249. Benet LZ, Cummins CL, Wu CY. Unmasking the dynamic interplay between efflux transporters and metabolic enzymes. Int J Pharm 2004; 277:3-9.
250. Kim RB. Organic anion-transporting polypeptide (OATP) transporter family and drug disposition. Eur J Clin Invest 2003; 33 Suppl 2:1-5.
251. Marzolini C, Tirona RG, Kim RB. Pharmacogenomics of the OATP and OAT families. Pharmacogenomics 2004; 5:273-82.
252. Konig J, Cui Y, Nies AT, Keppler D. A novel human organic anion transporting polypeptide localized to the basolateral hepatocyte membrane. Am J Physiol Gastrointest Liver Physiol 2000; 278:G156-64.
253. Konig J, Cui Y, Nies AT, Keppler D. Localization and genomic organization of a new hepatocellular organic anion transporting polypeptide. J Biol Chem 2000; 275:23161-8.
254. Nishizato Y, Ieiri I, Suzuki H, et al. Polymorphisms of OATP-C (SLC21A6) and OAT3 (SLC22A8) genes: consequences for pravastatin pharmacokinetics. Clin Pharmacol Ther 2003; 73:554-65.
255. Niemi M, Schaeffeler E, Lang T, et al. High plasma pravastatin concentrations are associated with single nucleotide polymorphisms and haplotypes of organic anion transporting polypeptide-C (OATP-C, SLCO1B1). Pharmacogenetics 2004; 14:429-40.
256. Mwinyi J, Johne A, Bauer S, et al. Evidence for inverse effects of OATP-C (SLC21A6) 5 and 1b haplotypes on pravastatin kinetics. Clin Pharmacol Ther 2004; 75:415-21.

257. Van Asperen J, Van Tellingen O, Beijnen JH. The pharmacological role of P-glycoprotein in the intestinal epithelium. Pharmacol Res 1998; 37:429-35.
258. Dresser GK, Bailey DG. The effects of fruit juices on drug disposition: a new model for drug interactions. Eur J Clin Invest 2003; 33 Suppl 2:10-6.
259. Kharasch ED, Walker A, Hoffer C, Sheffels P. Evaluation of first-pass cytochrome P4503A (CYP3A) and P-glycoprotein activities using alfentanil and fexofenadine in combination. J Clin Pharmacol 2005; 45:79-88.
260. Baron JM, Goh LB, Yao D, et al. Modulation of P450 CYP3A4-dependent metabolism by P-glycoprotein: implications for P450 phenotyping. J Pharmacol Exp Ther 2001; 296:351-8.
261. Wu CY, Benet LZ. Predicting drug disposition via application of BCS: transport/absorption/ elimination interplay and development of a biopharmaceutics drug disposition classification system. Pharm Res 2005; 22:11-23.
262. Kemper EM, Boogerd W, Thuis I, et al. Modulation of the blood-brain barrier in oncology: therapeutic opportunities for the treatment of brain tumours? Cancer Treat Rev 2004; 30:415-23.
263. Kemper EM, Verheij M, Boogerd W, et al. Improved penetration of docetaxel into the brain by co-administration of inhibitors of P-glycoprotein. Eur J Cancer 2004; 40:1269-74.
264. Shitara Y, Sato H, Sugiyama Y. Evaluation of Drug-Drug Interaction in the Hepatobiliary and Renal Transport of Drugs. Annu Rev Pharmacol Toxicol 2004.
265. Karanam BV, Hop CE, Liu DQ, et al. In vitro metabolism of MK-0767 [(+/-)-5-[(2,4-dioxothiazolidin-5-yl)methyl]-2-methoxy-N-[[(4-trifluoromet hyl) phenyl]methyl]benzamide], a peroxisome proliferator-activated receptor alpha/gamma agonist. I. Role of cytochrome P450, methyltransferases, flavin monooxygenases, and esterases. Drug Metab Dispos 2004; 32:1015-22.
266. Simon R, Freidlin B, Rubinstein L, et al. Accelerated titration designs for phase I clinical trials in oncology. J Natl Cancer Inst 1997; 89:1138-47.
267. Gehan EA, Tefft MC. Will there be resistance to the RECIST (Response Evaluation Criteria in Solid Tumors)? J Natl Cancer Inst 2000; 92:179-81.
268. Cheson BD, Horning SJ, Coiffier B, et al. Report of an international workshop to standardize response criteria for non-Hodgkin's lymphomas. NCI Sponsored International Working Group. J Clin Oncol 1999; 17:1244.
269. Ryan RF, Schultz DC, Ayyanathan K, et al. KAP-1 corepressor protein interacts and colocalizes with heterochromatic and euchromatic HP1 proteins: a potential role for Kruppel-associated box-zinc finger proteins in heterochromatin-mediated gene silencing. Mol Cell Biol 1999; 19:4366-78.
270. Imhof A, Yang XJ, Ogryzko VV, et al. Acetylation of general transcription factors by histone acetyltransferases. Curr Biol 1997; 7:689-92.
271. Gu W, Roeder RG. Activation of p53 sequence-specific DNA binding by acetylation of the p53 C-terminal domain. Cell 1997; 90:595-606.
272. Boyes J, Byfield P, Nakatani Y, Ogryzko V. Regulation of activity of the transcription factor GATA-1 by acetylation. Nature 1998; 396:594-8.

273. Brehm A, Miska EA, McCance DJ, et al. Retinoblastoma protein recruits histone deacetylase to repress transcription. Nature 1998; 391:597-601.
274. Luo RX, Postigo AA, Dean DC. Rb interacts with histone deacetylase to repress transcription. Cell 1998; 92:463-73.
275. Gilmour PS, Rahman I, Donaldson K, MacNee W. Histone acetylation regulates epithelial IL-8 release mediated by oxidative stress from environmental particles. Am J Physiol Lung Cell Mol Physiol 2003; 284:L533-40.
276. Sparreboom A, Loos W. Protein binding of anticancer drugs. in Figg Wd, McLeod HL (eds): Handbook of Anticancer Pharmacokinetics and Pharmacodynamics, Totowa, NJ, Humana Press 2004; Chapter 12:pp 169-188.
277. Baker SD, Verweij J, Rowinsky EK, et al. Role of body surface area in dosing of investigational anticancer agents in adults, 1991-2001. J Natl Cancer Inst 2002; 94:1883-8.
278. Ryan Q, Headlee D, Sparreboom A, et al. A phase I trial of an oral histone deacetylase inhibitor, MS-275, in advanced solid tumor and lymphoma patients. Proc Am Soc Clin Oncol 2003; 22:200.
279. Du Bois D, Du Bois EF. A formula to estimate the approximate surface area if height and weight be known. Nutrition 1916; 5:303-11; discussion 312-3.
280. Mosteller RD. Simplified calculation of body-surface area. N Engl J Med 1987; 317:1098.
281. Gibbs JP, Gooley T, Corneau B, et al. The impact of obesity and disease on busulfan oral clearance in adults. Blood 1999; 93:4436-40.
282. Morgan DJ, Bray KM. Lean body mass as a predictor of drug dosage. Implications for drug therapy. Clin Pharmacokinet 1994; 26:292-307.
283. Felici A, Verweij J, Sparreboom A. Dosing strategies for anticancer drugs: the good, the bad and body-surface area. Eur J Cancer 2002; 38:1677-84.
284. Gurney H. How to calculate the dose of chemotherapy. Br J Cancer 2002; 86:1297-302.
285. Gurney H. Dose calculation of anticancer drugs: a review of the current practice and introduction of an alternative. J Clin Oncol 1996; 14:2590-611.
286. Ratain MJ. Body-surface area as a basis for dosing of anticancer agents: science, myth, or habit? J Clin Oncol 1998; 16:2297-8.
287. Du Bois D, Du Bois EF. A formula to estimate the approximate surface area if height and weight be known. 1916. Nutrition 1989; 5:303-11; discussion 312-3.
288. Grochow LB, Baraldi C, Noe D. Is dose normalization to weight or body surface area useful in adults? J Natl Cancer Inst 1990; 82:323-5.
289. Sawyer M, Ratain MJ. Body surface area as a determinant of pharmacokinetics and drug dosing. Invest New Drugs 2001; 19:171-7.
290. Bruno R, Vivier N, Veyrat-Follet C, et al. Population pharmacokinetics and pharmacokinetic-pharmacodynamic relationships for docetaxel. Invest New Drugs 2001; 19:163-9.
291. Gurney HP, Ackland S, Gebski V, Farrell G. Factors affecting epirubicin pharmacokinetics and toxicity: evidence against using body-surface area for dose calculation. J Clin Oncol 1998; 16:2299-304.

292. Cosolo WC, Morgan DJ, Seeman E, et al. Lean body mass, body surface area and epirubicin kinetics. Anticancer Drugs 1994; 5:293-7.
293. Dobbs NA, Twelves CJ. What is the effect of adjusting epirubicin doses for body surface area? Br J Cancer 1998; 78:662-6.
294. de Jongh FE, Verweij J, Loos WJ, et al. Body-surface area-based dosing does not increase accuracy of predicting cisplatin exposure. J Clin Oncol 2001; 19:3733-9.
295. Acharya MR, Sparreboom A, Sausville EA, et al. Interspecies differences in plasma protein binding of MS-275, a histone deacetylase inhibitor. Proc Am Asc of Cancer Res 2005; (in press).
296. Egorin MJ. Overview of recent topics in clinical pharmacology of anticancer agents. Cancer Chemother Pharmacol 1998; 42 Suppl:S22-30.

Appendix 1

Supplemental in vivo pharmacokinetic data tables and figures

Table 5.7 Summary of non-compartmental pharmacokinetic parameters for all patients on biweekly schedule receiving MS-275 orally with food

Pat #	Patient Initials	Dose (mg/m^2)	Dose (mg)	Dose Group	R-sq	Lambda_z	$t_{1/2}$ (h)	Tmax (h)	Cmax (ng/mL)	T_{last} (h)
1	HJ	2	4	1	1	0.0281	24.7	2	1.85	24
2	DU	2	4	1	0.9894	0.006	115.5	6	1.85	48
3	BH	2	4	1	1	0.0069	100.4	24	1.45	48
4	BA	4	8	2	0.8129	0.0195	35.5	2	4.01	96
5	LD	4	8	2	0.9596	0.012	57.8	36	6.09	96
6	RR	4	9	2	0.9603	0.0119	58.2	6	4.41	96
7	HR	6	11	3	0.8972	0.0119	58.2	12	4.83	96
8	ML	6	12	3	0.7744	0.0208	33.3	2	11.16	96
9	TJ	6	10	3	0.9821	0.0108	64.2	2	8.1	96
10	SL	6	12	3	0.9243	0.0218	31.8	60	10.49	96
11	HP	6	11	3	0.2921	0.0155	44.7	2	5.6	96
12	JC	6	11	3	0.434	0.0082	84.5	2	17.36	96
13	WB	8	16	4	0.9086	0.0125	55.4	2	5.33	96
14	PR	8	14	4	0.8837	0.0135	51.3	0.5	19.07	96
15	RP	8	14	4	0.9402	0.0301	23.0	24	4.53	96
16	TB	8	12	4	0.9831	0.0155	44.7	0.5	33.01	96
17	TL	8	16	4	0.7966	0.0287	24.1	2	15.53	96
18	BD	10	20	5	0.8547	0.0115	60.3	0.5	44.85	84

19	WC	10	21	5	0.6608	0.0105	66.0	2	17.43	96
20	LJ	10	20	5	0.7804	0.0133	52.1	0.5	163.21	96
21	TC	10	16	5	0.8613	0.0176	39.4	1	25.43	84
22	WR	10	20	5	0.9248	0.017	40.8	2	10.07	72
23	CJ	10	23	5	0.9686	0.0136	51.0	2	9.41	96
24	HJ	12	23	6	0.8089	0.0171	40.5	2	29.19	96
25	CC	12	23	6	0.7613	0.0173	40.1	0.5	96.3	84
26	TD	12	21	6	0.7417	0.0153	45.3	0.5	319.12	96
27	ED	12	25	6	0.8569	0.0128	54.1	0.5	81.91	96
Median					**0.8837**	**0.0136**	**50.96**	**2**	**10.49**	**96**
Mean					**0.8429**	**0.0155**	**51.74**	**7.278**	**35.244**	**87.56**
SD					**0.1663**	**0.0062**	**21.52**	**13.71**	**67.198**	**18.48**
%CV					**19.728**	**39.695**	**41.66**	**188.3**	**190.67**	**21.10**
Min					**0.2921**	**0.006**	**23.02**	**0.5**	**1.45**	**24**
Max					**1**	**0.0301**	**115.5**	**60**	**319.12**	**96**

*Patients #'s 10, 22, 26 and 27 (highlighted boxes) experienced dose limiting toxicities.

Table 5.8 Summary of non-compartmental pharmacokinetic parameters for all patients on biweekly schedule receiving drug orally with food

Pat #	Patient Initials	Dose (mg/m^2)	Dose (mg)	Dose Group	AUC last (ng.h/mL)	AUC inf (ng.h/mL)	AUC % extrap	Vz/F	CL/F ($L/h/m^2$)
1	HJ	2	4	1	34.71	78.07	55.54	0.91	25.60
2	DU	2	4	1	69.01	276.18	75.01	1.20	7.20
3	BH	2	4	1	55.14	234.54	76.49	1.24	8.50
4	BA	4	8	2	181.34	244.93	25.96	0.84	16.30
5	LD	4	8	2	355.05	546.06	34.98	0.61	7.30
6	RR	4	9	2	248.37	384.05	35.33	0.88	10.40
7	HR	6	11	3	285.51	426.21	33.01	1.18	14.10
8	ML	6	12	3	331.47	398.31	16.78	0.72	15.10
9	TJ	6	10	3	225.89	353.30	36.06	1.57	17.00
10	SL	6	12	3	634.86	839.45	24.37	0.33	7.10
11	HP	6	11	3	238.62	425.25	43.89	0.91	14.10
12	JC	6	11	3	283.79	514.34	44.82	1.42	11.70
13	WB	8	16	4	287.99	388.02	25.78	1.65	20.60
14	PR	8	14	4	256.20	352.08	27.23	1.69	22.70
15	RP	8	14	4	259.86	294.11	11.64	0.90	27.20
16	TB	8	12	4	296.78	371.47	20.11	1.39	21.50
17	TL	8	16	4	341.82	382.88	10.72	0.73	20.90
18	BD	10	20	5	239.60	400.39	40.16	2.17	25.00
19	WC	10	21	5	439.20	734.38	40.19	1.29	13.60
20	LJ	10	20	5	544.82	746.87	27.05	1.01	13.40
21	TC	10	16	5	385.20	502.20	23.30	1.13	19.90

22	WR	10	20	5	243.31	359.53	32.33	1.63	27.80
23	CJ	10	23	5	310.37	429.81	27.79	1.72	23.30
24	HJ	12	23	6	466.34	592.97	21.35	1.19	20.20
25	CC	12	23	6	305.16	391.17	21.99	1.77	30.70
26	TD	12	21	6	887.62	1016.67	12.69	0.77	11.80
27	ED	12	25	6	519.57	719.82	27.82	1.30	16.70
Median					**287.99**	**398.31**	**27.79**	**1.186**	**16.70**
Mean					**323.24**	**459.37**	**32.31**	**1.190**	**17.40**
SD					**178.88**	**204.39**	**16.38**	**0.424**	**6.75**
%CV					**55.338**	**44.495**	**50.69**	**35.63**	**38.82**
Min					**34.71**	**78.07**	**10.72**	**0.329**	**7.1**
Max					**887.62**	**1016.67**	**76.49**	**2.171**	**30.7**

*Patients #'s 10, 22, 26 and 27 (highlighted boxes) experienced dose limiting toxicities.

Table 5.9 Details of pharmacokinetic parameters per dose level

Pat #	Dose (mg/m^2)	Dose Group	Cmax (ng/mL)	AUC inf (ng.h/mL)	Vz/F	CL/F ($L/h/m^2$)	Cmax/Dose	AUC/Dose	$t_{1/2}$ (h)
1	2	1	1.85	78.07	0.91	25.6	0.93	39.03	24.7
2	2	1	1.85	276.18	1.20	7.2	0.93	138.09	115.5
3	2	1	1.45	234.54	1.24	8.5	0.73	117.27	100.4
		Mean	**1.72**	**196.26**	**1.12**	**0.01**	**13.77**	**0.86**	**98.13**
		SD	**0.23**	**104.45**	**0.18**	**0.01**	**10.27**	**0.12**	**52.23**
		%CV	**13.45**	**53.22**	**16.20**	**74.59**	**74.59**	**13.45**	**53.22**
		Min	**1.45**	**78.07**	**0.91**	**0.01**	**7.20**	**0.73**	**39.03**
		Max	**1.85**	**276.18**	**1.24**	**0.03**	**25.60**	**0.93**	**138.09**
4	4	2	4.01	244.93	0.84	16.3	1.00	61.23	35.5
5	4	2	6.09	546.06	0.61	7.3	1.52	136.52	57.8
6	4	2	4.41	384.05	0.88	10.4	1.10	96.01	58.2
		Mean	**4.84**	**391.68**	**0.77**	**0.01**	**11.33**	**1.21**	**97.92**
		SD	**1.10**	**150.71**	**0.15**	**0.00**	**4.57**	**0.28**	**37.68**
		%CV	**22.82**	**38.48**	**18.76**	**40.34**	**40.34**	**22.82**	**38.48**
		Min	**4.01**	**244.93**	**0.61**	**0.01**	**7.30**	**1.00**	**61.23**
		Max	**6.09**	**546.06**	**0.88**	**0.02**	**16.30**	**1.52**	**136.52**
7	6	3	4.83	426.21	1.18	14.1	0.81	71.04	58.2

8	6	3	11.16	398.31	0.72	15.1	1.86	66.38	33.3
9	6	3	8.1	353.30	1.57	17.0	1.35	58.88	64.2
10	6	3	10.49	839.45	0.33	7.1	1.75	139.91	31.8
11	6	3	5.6	425.25	0.91	14.1	0.93	70.88	44.7
12	6	3	17.36	514.34	1.42	11.7	2.89	85.72	84.5
		Mean	**9.59**	**492.81**	**1.02**	**0.01**	**13.18**	**1.60**	**82.13**
		SD	**4.57**	**177.77**	**0.46**	**0.00**	**3.44**	**0.76**	**29.63**
		%CV	**47.66**	**36.07**	**45.19**	**26.08**	**26.08**	**47.66**	**36.07**
		Min	**4.83**	**353.30**	**0.33**	**0.01**	**7.10**	**0.81**	**58.88**
		Max	**17.36**	**839.45**	**1.57**	**0.02**	**17.00**	**2.89**	**139.91**
13	8	4	5.33	388.02	1.65	20.6	0.67	48.50	55.4
14	8	4	19.07	352.08	1.69	22.7	2.38	44.01	51.3
15	8	4	4.53	294.11	0.90	27.2	0.57	36.76	23.0
16	8	4	33.01	371.47	1.39	21.5	4.13	46.43	44.7
17	8	4	15.53	382.88	0.73	20.9	1.94	47.86	24.1
		Mean	**15.49**	**357.71**	**1.27**	**0.02**	**22.58**	**1.94**	**44.71**
		SD	**11.65**	**38.14**	**0.44**	**0.00**	**2.70**	**1.46**	**4.77**
		%CV	**75.21**	**10.66**	**34.33**	**11.98**	**11.98**	**75.21**	**10.66**
		Min	**4.53**	**294.11**	**0.73**	**0.02**	**20.60**	**0.57**	**36.76**
		Max	**33.01**	**388.02**	**1.69**	**0.03**	**27.20**	**4.13**	**48.50**
18	10	5	44.85	400.39	2.17	25.00	4.49	40.04	60.3
19	10	5	17.43	734.38	1.29	13.60	1.74	73.44	66.0
20	10	5	163.21	746.87	1.01	13.4	16.32	74.69	52.1
21	10	5	25.43	502.20	1.13	19.9	2.54	50.22	39.4
22	10	5	10.07	359.53	1.63	27.8	1.01	35.95	40.8
23	10	5	9.41	429.81	1.72	23.3	0.94	42.98	51.0

		Mean	**45.07**	**528.87**	**1.49**	**0.02**	**20.50**	**4.51**	**52.89**
		SD	**59.34**	**170.57**	**0.43**	**0.01**	**6.00**	**5.93**	**17.06**
		%CV	**131.66**	**32.25**	**28.96**	**29.25**	**29.25**	**131.66**	**32.25**
		Min	**9.41**	**359.53**	**1.01**	**0.01**	**13.40**	**0.94**	**35.95**
		Max	**163.21**	**746.87**	**2.17**	**0.03**	**27.80**	**16.32**	**74.69**
24	12	6	29.19	592.97	1.19	20.2	2.43	49.41	40.5
25	12	6	96.3	391.17	1.77	30.7	8.03	32.60	40.1
26	12	6	319.12	1016.67	0.77	11.8	26.59	84.72	45.3
27	12	6	81.91	719.82	1.30	16.7	6.83	59.99	54.1
		Mean	**131.63**	**680.16**	**1.26**	**0.02**	**19.85**	**10.97**	**56.68**
		SD	**128.28**	**262.00**	**0.41**	**0.01**	**8.01**	**10.69**	**21.83**
		%CV	**97.45**	**38.52**	**32.77**	**40.36**	**40.36**	**97.45**	**38.52**
		Min	**29.19**	**391.17**	**0.77**	**0.01**	**11.80**	**2.43**	**32.60**
		Max	**319.12**	**1016.67**	**1.77**	**0.03**	**30.70**	**26.59**	**84.72**

Table 6.4 Patient demographics

Pat #	Age (yr)	Dose mg/m^2	Dose mg	Sex	Weight kg	Height (m)	Albumin	HISTOLOGY	Primary Site
1	65	6	10	F	62.5	1.63	4.1	ACUTE MYELOGENOUS LEUKEMIA	Bone marrow
2	54	6	12	M	84.0	1.72	3.2	ACUTE LEUKEMIA	Bone marrow
3	85	6	10	M	56.1	1.70	2.9	ACUTE MYELOGENOUS LEUKEMIA	Bone marrow
4	69	6	12	M	84.4	1.68	2.8	ACUTE MYELOID LEUKEMIA	Bone marrow
5	74	8	16	M	78.0	1.85	3.7	ACUTE MYELOGENOUS LEUKEMIA	Bone marrow
6	56	10	18	M	63.4	1.78	2.8	ACUTE MYELOGENOUS LEUKEMIA	Bone marrow
7	65	8	15	F	76.4	1.62	3.8	PERSISTENT ACUTE MYELOID LEUKEMIA	Bone marrow
8	57	10	18	M	71.4	1.65	3.8	RESIDUAL ACUTE MYELOID LEUKEMIA	Bone marrow
9	44	6	10	F	82.2	1.30	3.6	ACUTE MYELOGENOUS LEUKEMIA	Bone marrow
10	66	8	16	M	81.9	1.74	3.7	PERSISTENT ACUTE MYELOID LEUKEMIA	Bone marrow
11	36	8	19	F	125.4	1.73	4	ACUTE MYELOGENOUS LEUKEMIA RELAPSE	Bone marrow
12	55	4	8	F	78.3	1.70	2.3	MULTIPLE LYELOMA	Bone marrow
13	72	4	6	M	49.9	1.62	2.2	MYELODYSPLASTIC SYNDROME	Bone marrow
14	76	8	12	F	49.1	1.63	2.8	ACUTE MYELOID LEUKEMIA	Bone marrow
15	70	4	9	M	95.2	1.85	3.4	RELAPSED ACUTE LEUKEMIA	Bone marrow
16	49	6	12	F	94.0	1.58	3.1	RESIDUAL ACUTE LEUKEMIA	Bone marrow
17	45	8	15	M	70.0	1.85	3.0	PERSISTENT ACUTE MYELOID LEUKEMIA	Bone marrow
18	86	8	16	M	77.8	1.79	3.5	RESIDUAL ACUTE LEUKEMIA	Bone marrow
19	56	4	8	F	94.7	1.63	3.1	ACUTE LEUKEMIA	Bone marrow
20	50	8	14	F	60.4	1.70	4.2	RELAPSE ACUTE MYELOGENOUS LEUKEMIA	Bone marrow
21	69	8	14	F	76.0	1.58	3.2	ACUTE LEUKEMIA	Bone marrow
22	49	6	11	M	69.5	1.68	3.8	CML WIH NUMEROUS EARLY PRECURSORS	Bone marrow

23	72	8	15	M	74.0	1.75	3.5	RELAPSED ACUTE LEUKEMIA	Bone marrow
24	65	8	14	M	64.8	1.66	3.2	RESIDUAL ACUTE MYELOID LEUKEMIA	Bone marrow
25	57	4	8	M	81.8	1.73	3.9	RELAPSED MULTIPLE MYELOMA	Bone marrow
26	35	4	8	F	78.6	1.718	4.2	Adrenal Cortical Carcinoma	Adrenocortical Cancer
27	57	2	4	F	72.4	1.593	3.8	Poorly Diff Adenoca	Breast
28	40	4	6	F	55.2	1.609	2.6	Infiltrating poorly different ductal CA	Breast
29	57	6	11	F	77.4	1.73	3.3	Adenocarcinoma	Breast
30	43	12	21	F	64.2	1.668	3.7	mod diff adenoca	Cervix
31	53	12	23	M	75	1.755	3.6	Poorly Diff Adenoca	Colon
32	46	4	7	F	78.2	1.688	3.9	mod diff adenoca	Colon
33	54	10	16	F	53.3	1.607	3.5	mod diff invasive adenoca	Colon
34	83	4	7	F	72.1	1.642	3.3	Poorly to mod diff Adeno Ca	Colon
35	22	2	3	M	55.6	1.732	3.3	Nasopharyngeal Carcinoma	Head and Neck
36	63	2	4	M	84.7	1.841	3.8	Renal Cell Clear Cell	Kidney
37	53	6	11	M	75.3	1.692	3.8	Renal Cell Carcinoma	Kidney
38	35	4	8	M	91.7	1.712	4.0	Renal Cell Carcinoma	Kidney
39	54	6	12	F	93.8	1.711	3.8	Renal Cell CA, Clear cell type.	Kidney
40	46	8	14	F	76.3	1.613	3.0	Renal Cell Clear Cell	Kidney
41	56	6	10	M	58.8	1.576	3.2	Renal Cell Clear Cell	Kidney
42	60	4	8	F	71.9	1.669	4.1	Spindle cell sarcoma, Leromyosarcoma	Leiomyosarcoma
43	68	4	7	F	80.2	1.631	3.8	Adenocarcinoma	Liver
44	56	6	11	M	68.4	1.667	4.3	Poorly different. adenocarcinoma of lung	Lung
45	74	10	20	M	82.1	1.73	3.7	Bronchoalveolar CA	Lung
46	61	8	14	M	64.7	1.68	2.7	Squamous Cell Carcino	Lung
47	65	8	12	F	53.2	1.496	3.1	Non Small Cell	Lung
48	64	12	23	M	70.3	1.78	3.9	Peripheral T cell lymphoma	Lymphoma
49	51	6	11	F	69.6	1.68	2.9	Cutaneous T-cell Lymphoma	Lymphoma
50	62	2	4	F	103.5	1.579	4.2	Follicular	Lymphoma
51	58	10	23	M	114.2	1.784	3.9	Melanoma	Melanoma
52	61	6	11	F	78.2	1.568	4.1	Metastatic Malignant Melanoma	Melanoma

53	70	4	9	M	88.6	1.835	3.7	Melanoma	Melanoma
54	56	6	12	F	86.4	1.62	3.9	Melanoma	Melanoma
55	56	8	16	M	85	1.71	3.9	Melanoma NOS	Melanoma
56	58	10	21	M	95.3	1.763	3.8	Cutaneous	Melanoma
57	60	12	25	M	89.7	1.799	3.4	Mesothelioma NOS	Mesothelioma
58	77	4	8	M	86.1	1.783	4.3	Poorly Differentiated	Oral-Pharyngeal
59	71	8	16	M	79	1.76	4.0	Adenocarcinoma	Prostate
60	28	6	11	F	66.4	1.719	3.6	mod diff adenoca	Rectum
61	55	10	20	M	81.6	1.785	4.5	mod to poorly diff colonic adenoca	Rectum
62	57	10	20	M	86	1.771	3.4	Sarcoma NOS	Sarcoma
63	53	2	4	M	110.5	1.73	5	Mycosis Fungoides	Skin
64	72	4	8	M	81.8	1.72	3.8	Atypical lymphoid infiltrate consistant	Skin
Mean	**58**	**6.6**	**12.4**		**77.4**	**1.69**	**3.56**		
SD	**13**	**2.7**	**5.3**		**15.0**	**0.09**	**0.51**		
%CV	**22**	**40.7**	**43.0**		**19.4**	**5.55**	**14.46**		
Min	**22**	**2.0**	**3.0**		**49.1**	**1.30**	**2.20**		
Max	**86**	**12.0**	**25.0**		**125.4**	**1.85**	**4.50**		
Median	**57**	**6.0**	**11.7**		**77.9**	**1.70**	**3.70**		

Table 6.5 Patient demographics and adjusted CL/F with body measures

Pat #	BSA 1 (m2)	BSA 2 (m2)	Ratio BSA 1 / BSA 2	LBM (kg)	IBW (kg)	AIBW (kg)	BMI	CL/F (L/h)	CL/F (L/h/m2) BSA 2	CL/F (L/h/kg) LBM	CL/F (L/h/kg) IBW	CL/F (L/h/kg) AIBW	CL/F (L/h/kg) BMI	CL/F (L/h/kg) Weight	CL/F (L/h/m) Length
1	1.68	1.67	0.99	45.01	54.65	56.61	23.64	26.56	15.90	0.59	0.49	0.47	1.12	0.42	16.33
2	2.00	1.97	0.98	63.78	68.20	72.15	28.39	27.41	13.90	0.43	0.40	0.38	0.97	0.33	15.94
3	1.63	1.65	1.01	48.67	66.56	63.95	19.37	48.12	29.19	0.99	0.72	0.75	2.48	0.86	28.27
4	1.99	1.95	0.98	62.70	64.92	69.79	29.76	25.50	13.10	0.41	0.39	0.37	0.86	0.30	15.14
5	2.00	2.02	1.01	64.56	80.39	79.80	22.69	26.03	12.90	0.40	0.32	0.33	1.15	0.33	14.04
6	1.77	1.79	1.01	54.48	73.48	70.96	20.06	51.74	28.87	0.95	0.70	0.73	2.58	0.82	29.10
7	1.85	1.81	0.98	48.83	54.10	59.68	29.11	95.43	52.61	1.95	1.76	1.60	3.28	1.25	58.91
8	1.81	1.79	0.99	56.07	61.83	64.22	26.23	82.37	46.12	1.47	1.33	1.28	3.14	1.15	49.92
9	1.72	1.59	0.93	28.32	24.53	38.94	49.02	38.64	24.29	1.36	1.58	0.99	0.79	0.47	29.84
10	1.99	1.97	0.99	63.50	70.02	72.99	27.05	56.23	28.58	0.89	0.80	0.77	2.08	0.69	32.32
11	2.45	2.35	0.96	56.15	63.84	79.23	42.04	50.83	21.67	0.91	0.80	0.64	1.21	0.41	29.43
12	1.92	1.90	0.99	52.46	61.56	65.75	27.03	24.79	13.05	0.47	0.40	0.38	0.92	0.32	14.56
13	1.50	1.51	1.01	43.48	58.92	56.66	19.06	46.30	30.62	1.06	0.79	0.82	2.43	0.93	28.61
14	1.49	1.51	1.01	39.11	55.01	53.53	18.48	70.00	46.37	1.79	1.27	1.31	3.79	1.43	42.95
15	2.21	2.20	0.99	73.08	80.39	84.10	27.70	60.58	27.58	0.83	0.75	0.72	2.19	0.64	32.68
16	2.03	1.94	0.96	47.86	50.01	61.00	37.89	24.78	12.77	0.52	0.50	0.41	0.65	0.26	15.73
17	1.90	1.92	1.01	59.82	80.03	77.52	20.45	90.51	47.04	1.51	1.13	1.17	4.43	1.29	48.92
18	1.97	1.96	1.00	62.91	74.57	75.38	24.28	38.04	19.36	0.60	0.51	0.50	1.57	0.49	21.25
19	2.07	1.99	0.96	51.13	54.65	64.66	35.82	75.46	37.87	1.48	1.38	1.17	2.11	0.80	46.41
20	1.69	1.70	1.01	45.99	61.56	61.27	20.85	25.24	14.84	0.55	0.41	0.41	1.21	0.42	14.83
21	1.82	1.77	0.97	46.86	50.01	56.50	30.64	18.44	10.40	0.39	0.37	0.33	0.60	0.24	11.71

22	1.80	1.79	0.99	55.82	64.20	65.52	24.74	43.90	24.59	0.79	0.68	0.67	1.77	0.63	26.19
23	1.90	1.89	1.00	60.02	71.20	71.90	24.08	48.21	25.45	0.80	0.68	0.67	2.00	0.65	27.50
24	1.73	1.72	1.00	52.99	62.74	63.26	23.52	41.92	24.35	0.79	0.67	0.66	1.78	0.65	25.25
25	1.98	1.96	0.99	63.06	68.84	72.08	27.43	24.14	12.34	0.38	0.35	0.33	0.88	0.30	13.98
26	1.94	1.92	0.99	53.12	63.02	47.69	26.63	22.47	11.73	0.42	0.36	0.47	0.84	0.29	13.08
27	1.79	1.75	0.98	46.90	51.64	39.13	28.53	14.48	8.27	0.31	0.28	0.37	0.51	0.20	9.09
28	1.57	1.57	1.00	41.64	53.10	40.23	21.32	36.32	23.11	0.87	0.68	0.90	1.70	0.66	22.58
29	1.93	1.91	0.99	53.19	64.11	48.52	25.86	21.39	11.18	0.40	0.33	0.44	0.83	0.28	12.36
30	1.72	1.72	1.00	46.77	58.47	44.27	23.08	20.66	12.01	0.44	0.35	0.47	0.90	0.32	12.38
31	1.91	1.91	1.00	60.58	71.39	53.98	24.35	38.79	20.34	0.64	0.54	0.72	1.59	0.52	22.10
32	1.91	1.89	0.99	51.91	60.29	45.64	27.44	26.19	13.88	0.50	0.43	0.57	0.95	0.33	15.52
33	1.54	1.55	1.00	40.75	52.92	40.09	20.64	31.86	20.59	0.78	0.60	0.79	1.54	0.60	19.83
34	1.81	1.79	0.99	48.61	56.10	42.49	26.74	79.36	44.41	1.63	1.41	1.87	2.97	1.10	48.33
35	1.64	1.66	1.02	48.79	69.29	52.40	18.53	11.28	6.78	0.23	0.16	0.22	0.61	0.20	6.51
36	2.08	2.08	1.00	67.77	79.21	59.87	24.99	17.05	8.20	0.25	0.22	0.28	0.68	0.20	9.26
37	1.88	1.86	0.99	59.06	65.65	49.66	26.30	25.81	13.87	0.44	0.39	0.52	0.98	0.34	15.25
38	2.09	2.04	0.98	66.44	67.47	51.03	31.29	14.65	7.18	0.22	0.22	0.29	0.47	0.16	8.56
39	2.11	2.06	0.98	55.89	62.38	47.21	32.04	30.13	14.63	0.54	0.48	0.64	0.94	0.32	17.61
40	1.85	1.81	0.98	48.52	53.46	40.50	29.33	47.60	26.34	0.98	0.89	1.18	1.62	0.62	29.51
41	1.60	1.59	0.99	47.98	55.10	41.72	23.67	28.30	17.79	0.59	0.51	0.68	1.20	0.48	17.96
42	1.83	1.81	0.99	49.47	58.56	44.34	25.81	32.66	18.08	0.66	0.56	0.74	1.27	0.45	19.57
43	1.91	1.86	0.98	50.03	55.10	41.73	30.15	29.11	15.65	0.58	0.53	0.70	0.97	0.36	17.85
44	1.78	1.77	0.99	55.04	63.38	47.95	24.61	25.87	14.64	0.47	0.41	0.54	1.05	0.38	15.52
45	1.99	1.96	0.99	63.28	69.11	52.27	27.43	26.78	13.65	0.42	0.39	0.51	0.98	0.33	15.48
46	1.74	1.74	1.00	53.37	64.56	48.84	22.92	39.76	22.92	0.75	0.62	0.81	1.73	0.61	23.67
47	1.49	1.47	0.99	38.21	42.82	32.49	23.77	32.30	22.01	0.85	0.75	0.99	1.36	0.61	21.59
48	1.86	1.87	1.01	58.61	73.66	55.69	22.19	58.80	31.37	1.00	0.80	1.06	2.65	0.84	33.03
49	1.80	1.79	0.99	49.07	59.56	45.09	24.66	31.25	17.46	0.64	0.52	0.69	1.27	0.45	18.60
50	2.13	2.03	0.95	47.16	50.37	38.17	41.51	51.24	25.30	1.09	1.02	1.34	1.23	0.50	32.45
51	2.38	2.31	0.97	76.45	74.02	55.96	35.88	53.51	23.19	0.70	0.72	0.96	1.49	0.47	30.00
52	1.85	1.79	0.97	46.86	49.37	37.42	31.81	37.69	21.07	0.80	0.76	1.01	1.18	0.48	24.03

53	2.13	2.11	0.99	69.48	78.67	59.46	26.31	23.43	11.08	0.34	0.30	0.39	0.89	0.26	12.77
54	1.97	1.91	0.97	50.35	54.10	40.98	32.92	14.30	7.48	0.28	0.26	0.35	0.43	0.17	8.82
55	2.01	1.97	0.98	63.85	67.29	50.90	29.07	41.79	21.17	0.65	0.62	0.82	1.44	0.49	24.44
56	2.16	2.12	0.98	69.77	72.11	54.53	30.66	28.60	13.50	0.41	0.40	0.52	0.93	0.30	16.22
57	2.12	2.10	0.99	68.84	75.39	56.99	27.72	34.73	16.58	0.50	0.46	0.61	1.25	0.39	19.31
58	2.07	2.05	0.99	66.73	73.93	55.90	27.08	20.32	9.93	0.30	0.27	0.36	0.75	0.24	11.39
59	1.97	1.95	0.99	62.72	71.84	54.32	25.50	41.23	21.11	0.66	0.57	0.76	1.62	0.52	23.43
60	1.78	1.78	1.00	48.97	63.11	47.76	22.47	25.58	14.34	0.52	0.41	0.54	1.14	0.39	14.88
61	2.01	2.00	0.99	64.68	74.12	56.03	25.61	55.63	27.80	0.86	0.75	0.99	2.17	0.68	31.16
62	2.06	2.03	0.99	66.30	72.84	55.07	27.42	49.95	24.55	0.75	0.69	0.91	1.82	0.58	28.21
63	2.30	2.23	0.97	72.59	69.11	52.27	36.92	35.33	15.88	0.49	0.51	0.68	0.96	0.32	20.42
64	1.98	1.95	0.99	62.84	68.20	51.58	27.65	44.81	22.98	0.71	0.66	0.87	1.62	0.55	26.05
Mean	**1.90**	**1.88**	**0.99**	**55**	**63**	**55**	**27**	**38.5**	**20.7**	**0.72**	**0.63**	**0.71**	**1.48**	**0.52**	**22.79**
SD	**0.20**	**0.19**	**0.02**	**10**	**10**	**12**	**6**	**18.7**	**10.4**	**0.38**	**0.34**	**0.33**	**0.82**	**0.28**	**11.14**
CV%	**10.73**	**10.06**	**1.66**	**18**	**16**	**22**	**21**	**48.7**	**50.1**	**53.40**	**53.87**	**47.12**	**55.25**	**54.46**	**48.86**
Min	**1.49**	**1.47**	**0.93**	**28**	**25**	**32**	**18**	**11.3**	**6.8**	**0.22**	**0.16**	**0.22**	**0.43**	**0.16**	**6.51**
Max	**2.45**	**2.35**	**1.02**	**76**	**80**	**84**	**49**	**95.4**	**52.6**	**1.95**	**1.76**	**1.87**	**4.43**	**1.43**	**58.91**
Median	**1.91**	**1.90**	**0.99**	**54**	**64**	**54**	**26**	**33.7**	**18.7**	**0.64**	**0.54**	**0.67**	**1.22**	**0.46**	**20.12**

Figure 4.5 **Relationship between mean peak concentration (C_{max}) and dose for patients on biweekly schedule of MS-275**

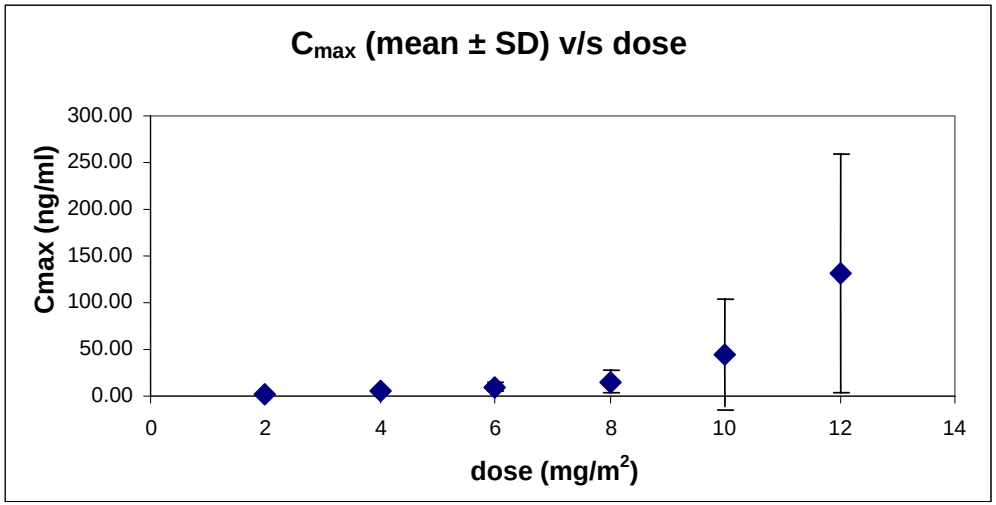

Figure 4.5 Relationship between median peak concentration (C_{max}) and dose for patients on biweekly schedule of MS-275

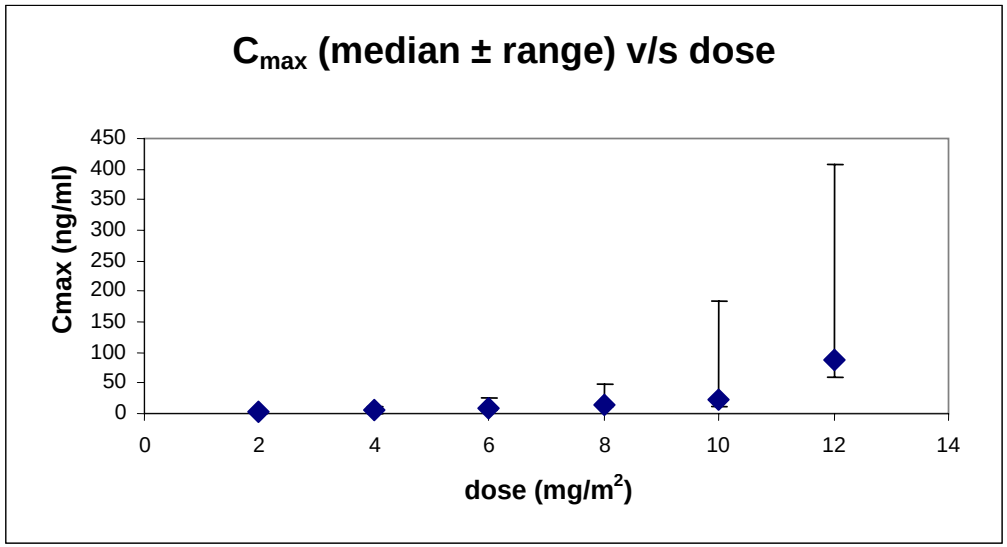

Figure 5.7 Semi-logarithmic plot of concentration versus time profile for patient no. 1 (dose=2 mg/m^2)

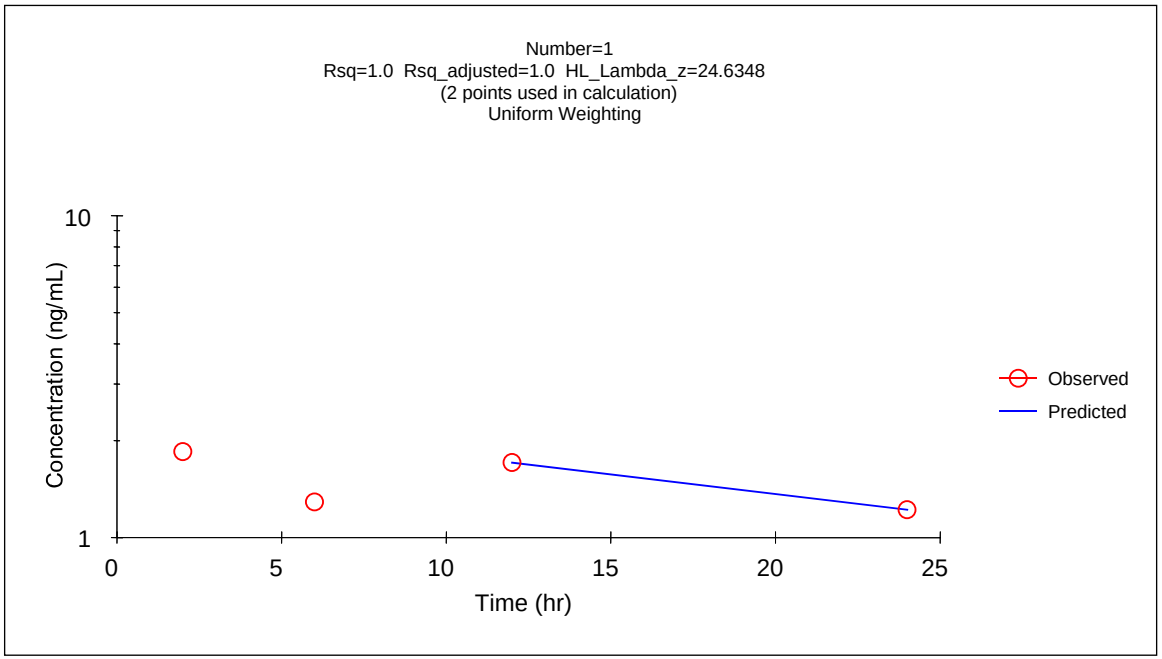

X vs. Observed Y and Predicted Y

Figure 5.8 Semi-logarithmic plot of concentration versus time profile for patient no. 2 (dose=2 mg/m^2)

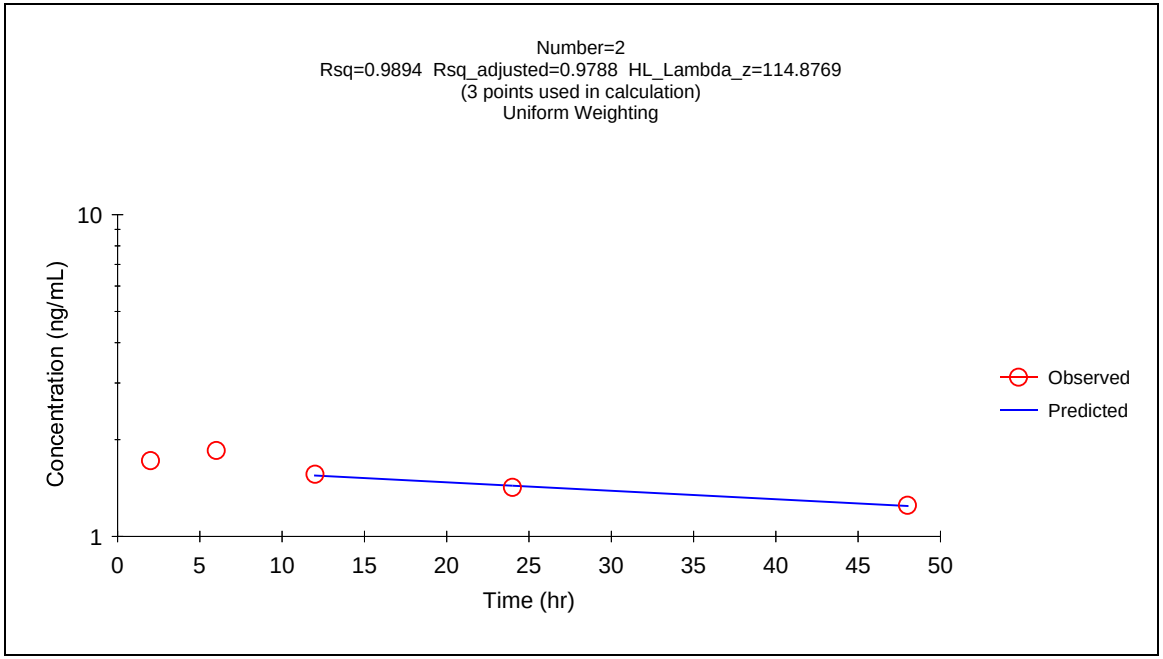

X vs. Observed Y and Predicted Y

Figure 5.9 Semi-logarithmic plot of concentration versus time profile for patient no. 3 (dose=2 mg/m^2)

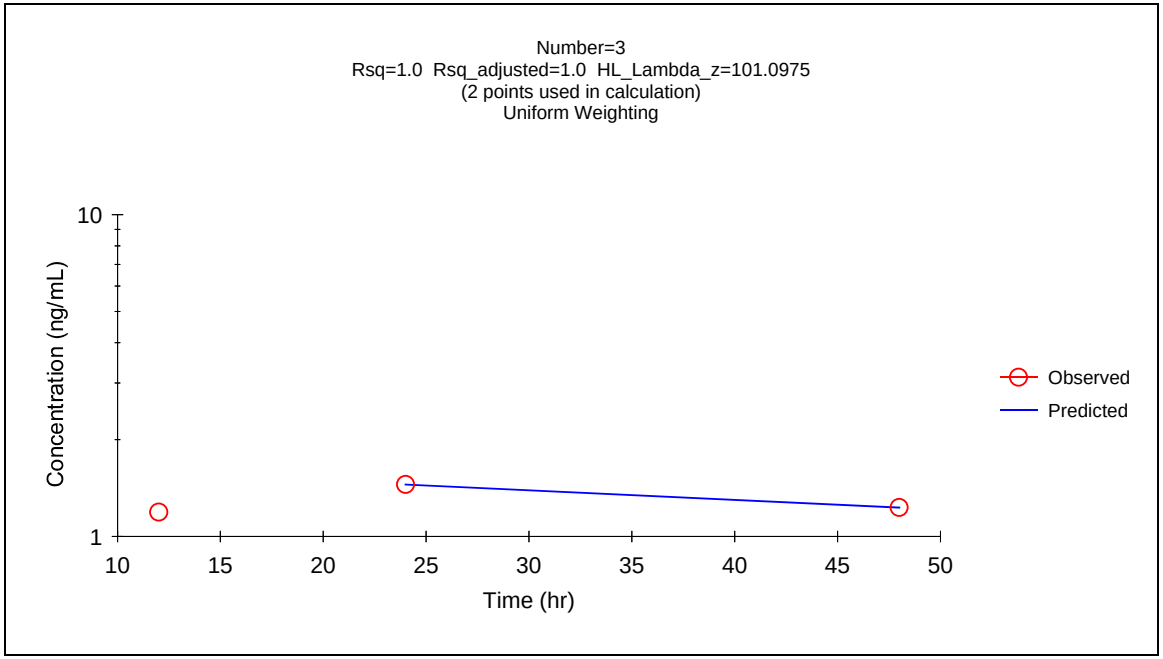

X vs. Observed Y and Predicted Y

Figure 5.10 Semi-logarithmic plot of concentration versus time profile for patient no. 4 (dose=4 mg/m^2)

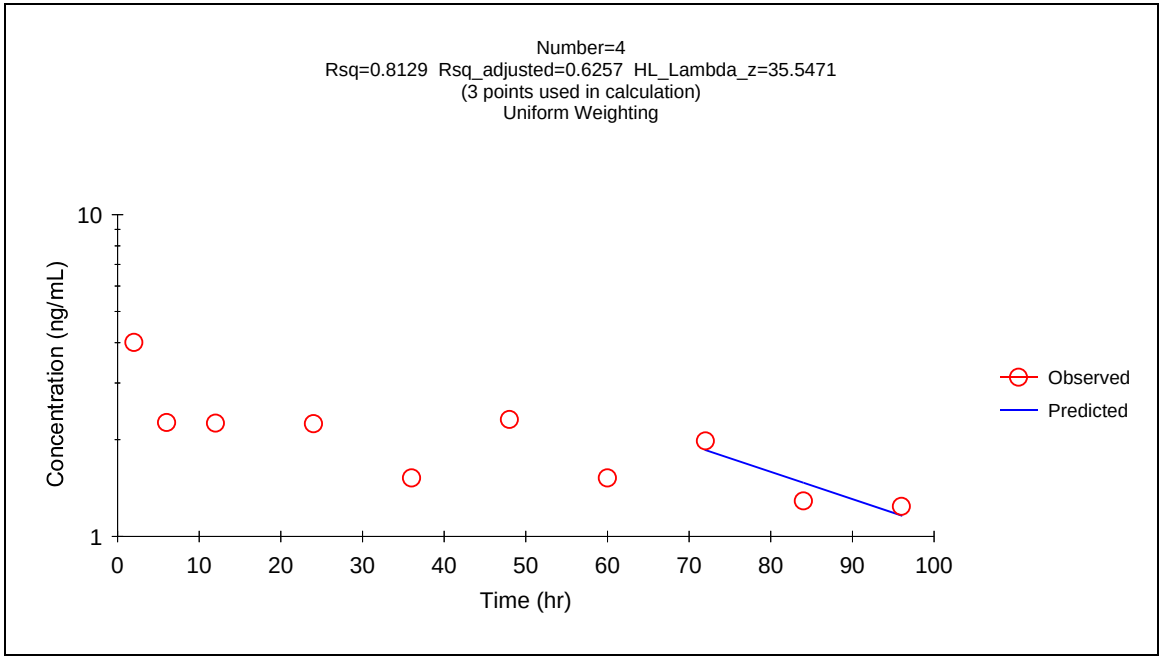

X vs. Observed Y and Predicted Y

Figure 5.11 Semi-logarithmic plot of concentration versus time profile for patient no. 5 (dose=4 mg/m^2)

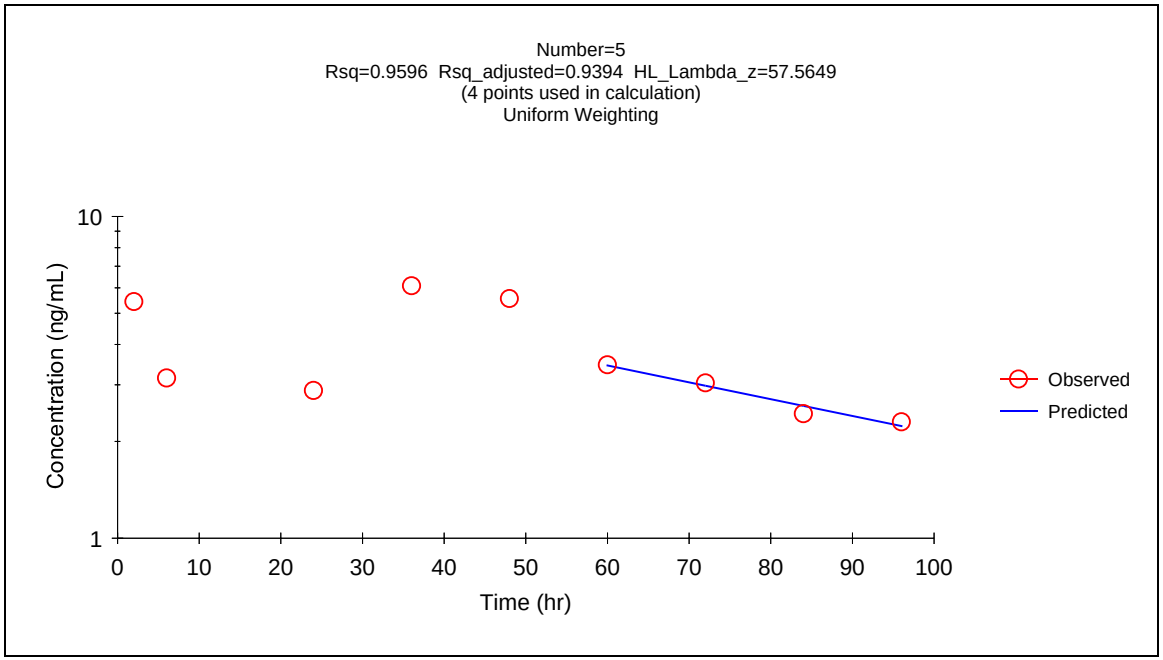

X vs. Observed Y and Predicted Y

Figure 5.12 Semi-logarithmic plot of concentration versus time profile for patient no. 6 (dose=4 mg/m^2)

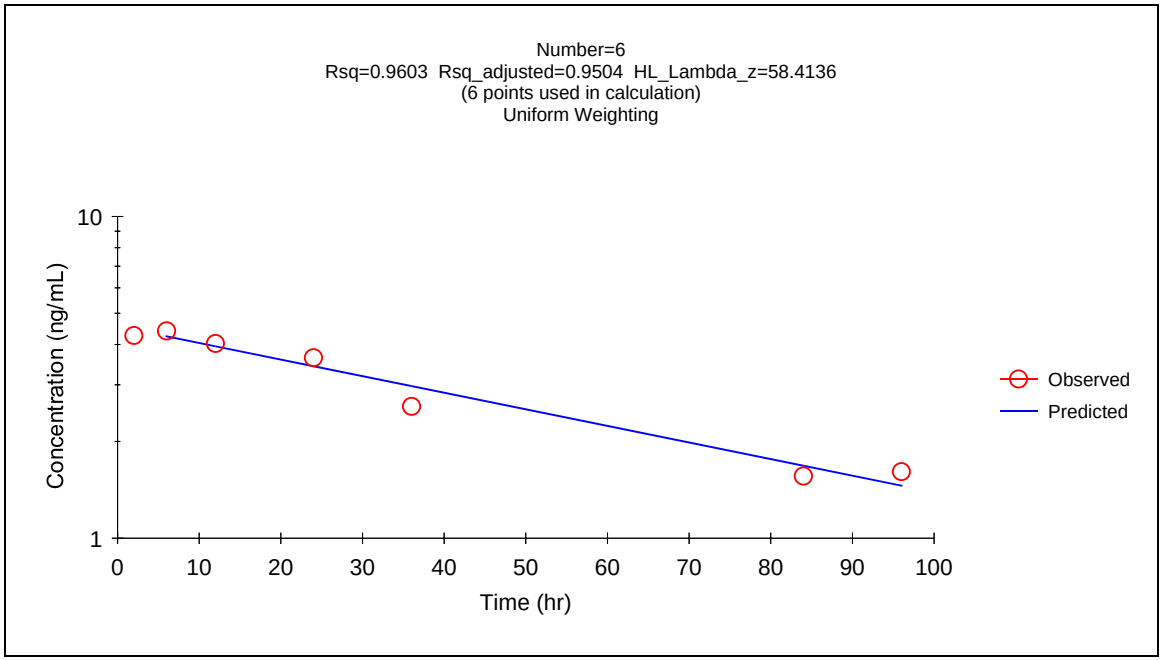

X vs. Observed Y and Predicted Y

Figure 5.13 Semi-logarithmic plot of concentration versus time profile for patient no. 7 (dose=6 mg/m^2)

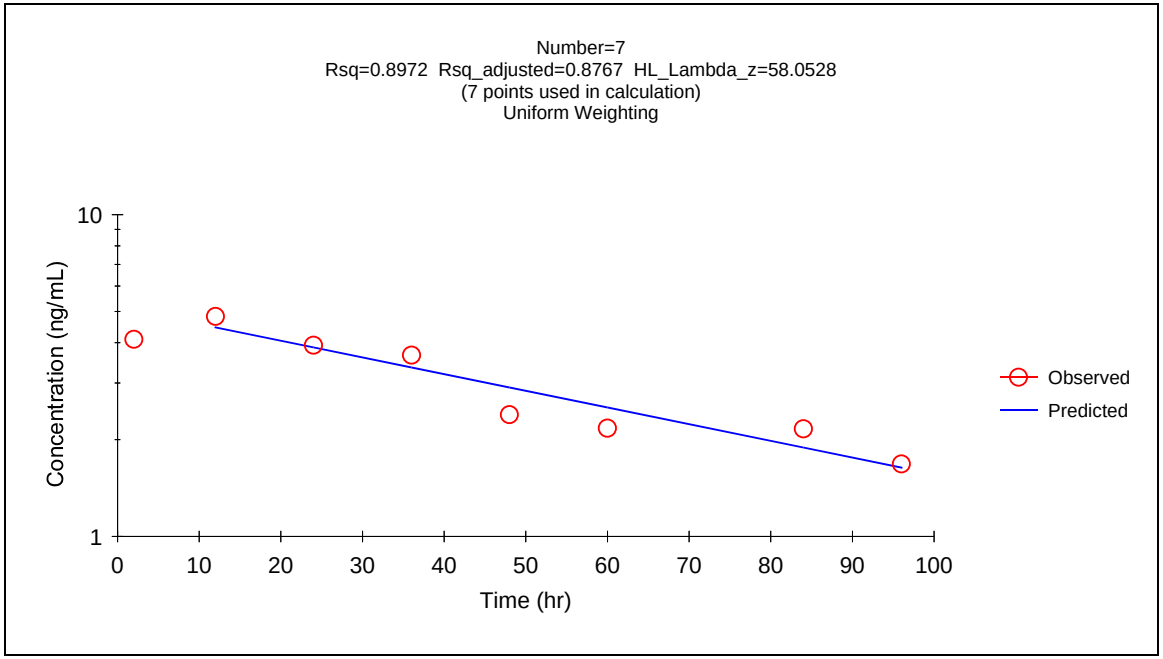

X vs. Observed Y and Predicted Y
:

Figure 5.14 Semi-logarithmic plot of concentration versus time profile for patient no. 8 (dose=6 mg/m^2)

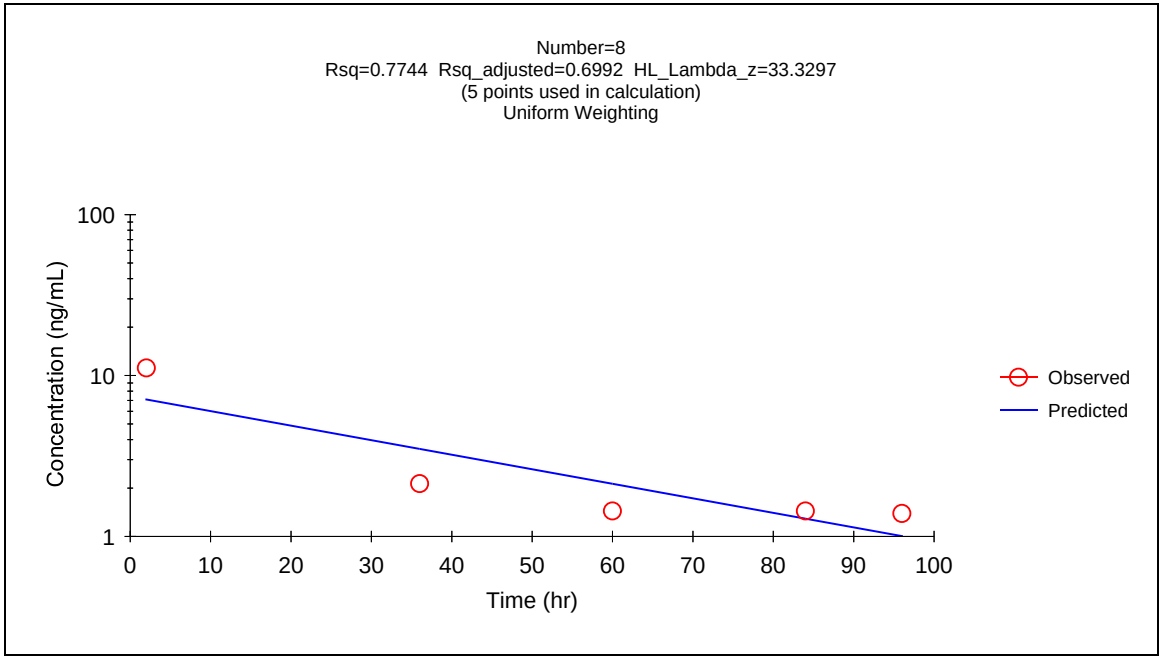

X vs. Observed Y and Predicted Y

Figure 5.15 Semi-logarithmic plot of concentration versus time profile for patient no. 9 (dose=6 mg/m^2)

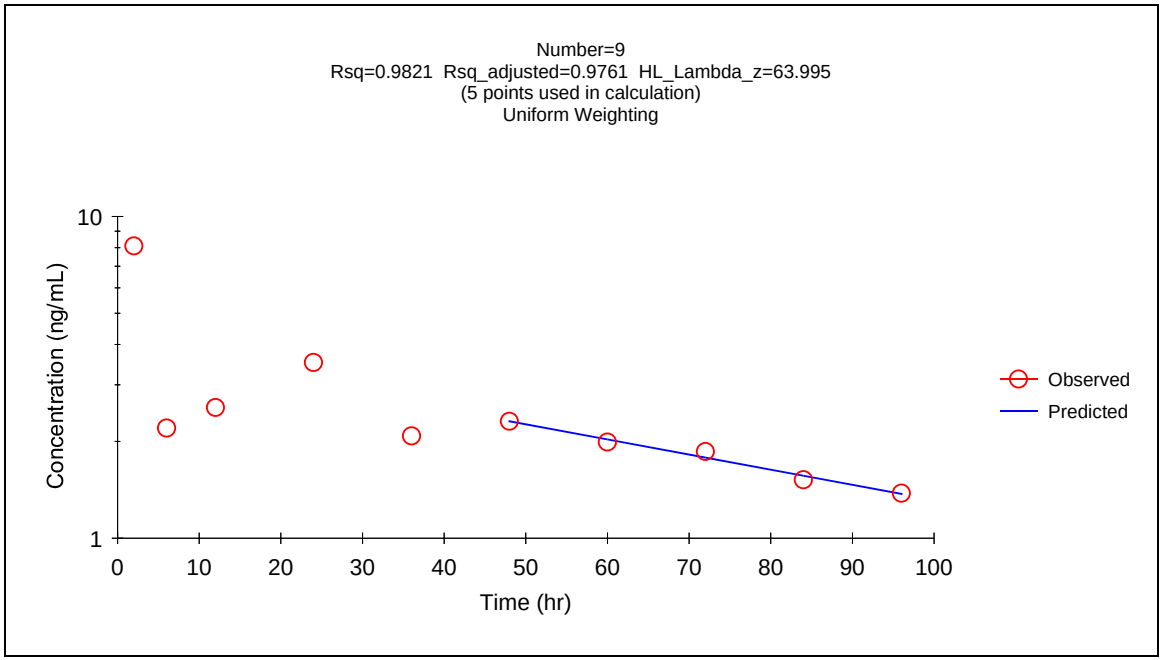

X vs. Observed Y and Predicted Y

Figure 5.16 Semi-logarithmic plot of concentration versus time profile for patient no. 10 (dose=6 mg/m^2)

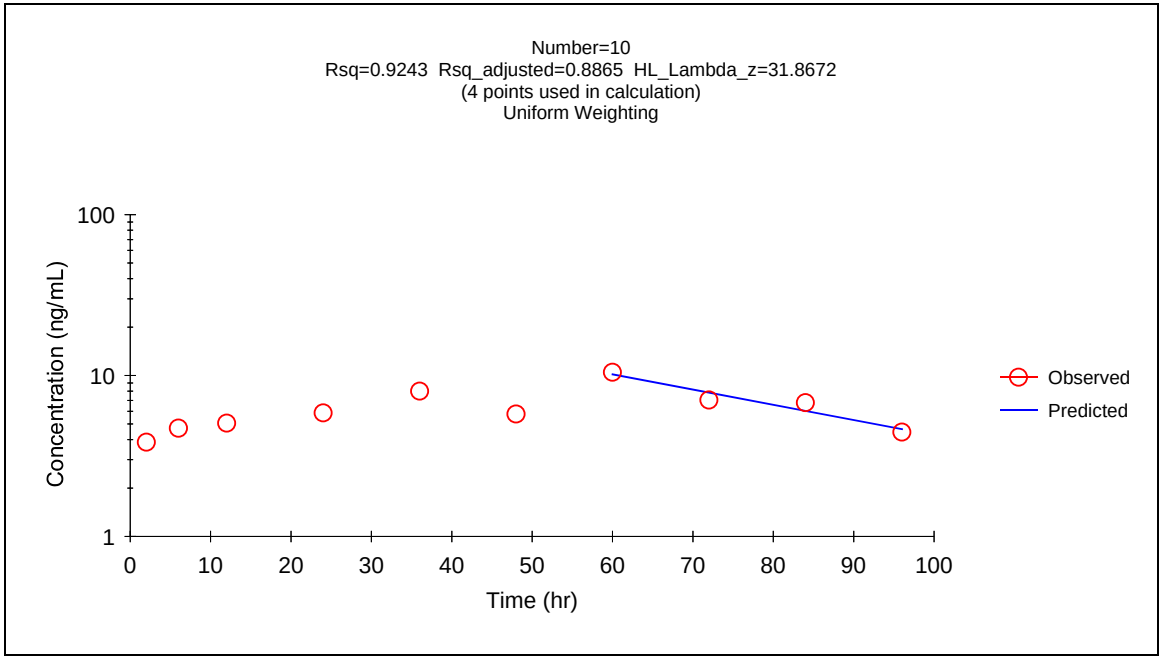

X vs. Observed Y and Predicted Y

Figure 5.17 Semi-logarithmic plot of concentration versus time profile for patient no. 11 (dose=6 mg/m^2)

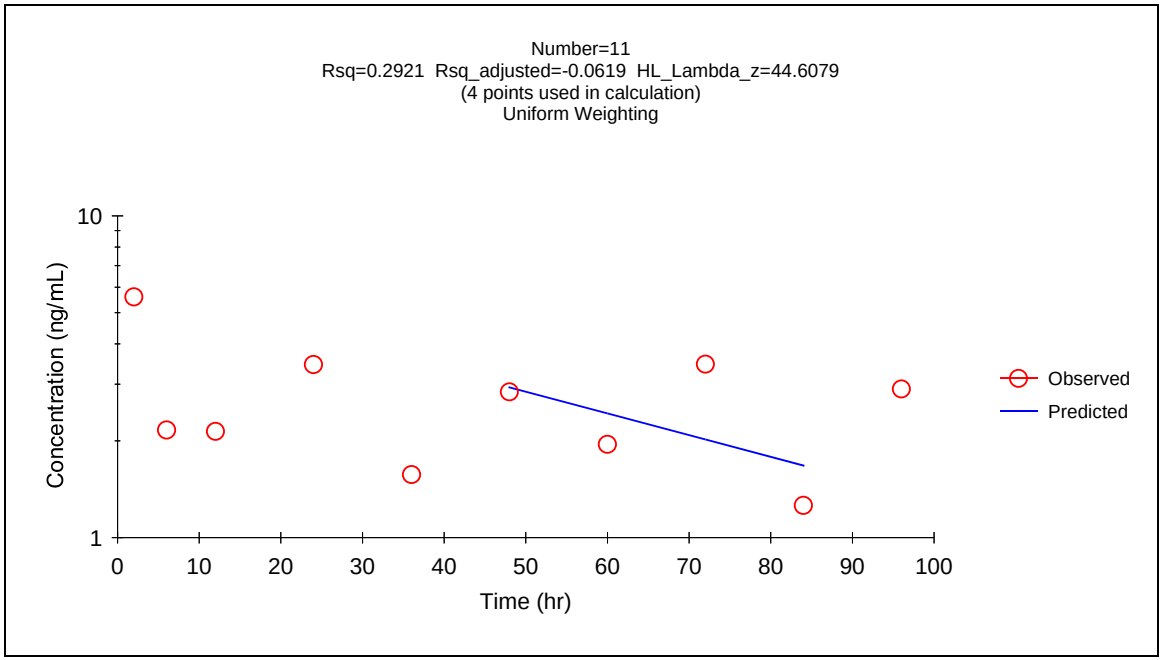

X vs. Observed Y and Predicted Y

Figure 5.18 Semi-logarithmic plot of concentration versus time profile for patient no. 12 (dose=6 mg/m^2)

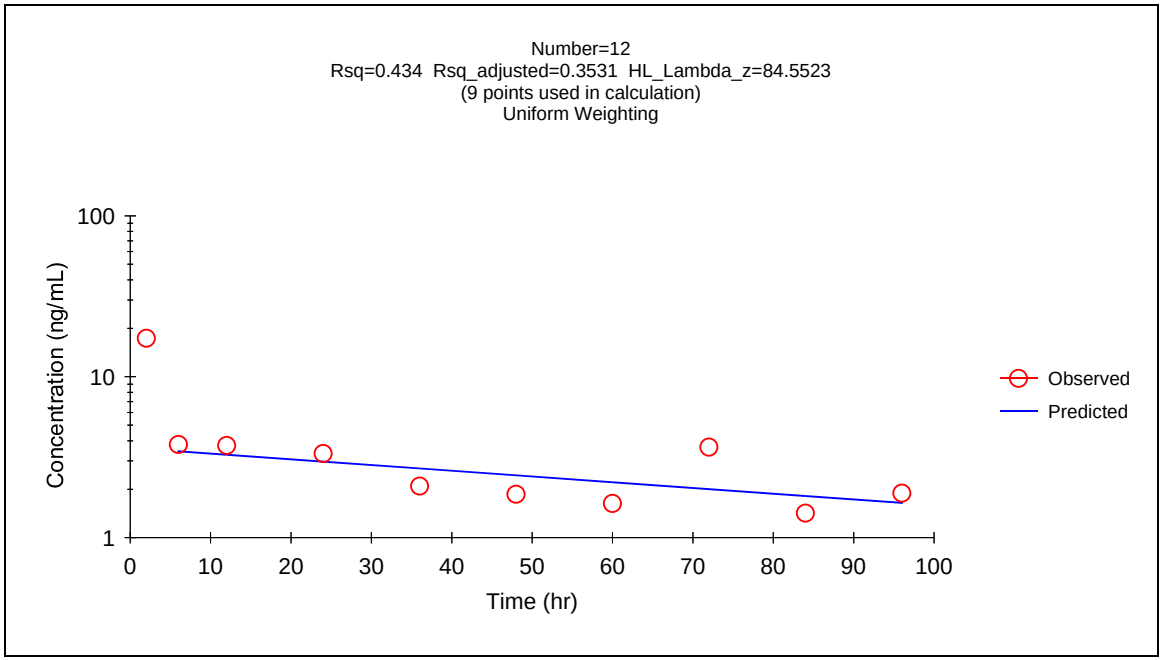

X vs. Observed Y and Predicted Y

Figure 5.19 Semi-logarithmic plot of concentration versus time profile for patient no. 13 (dose=8 mg/m^2)

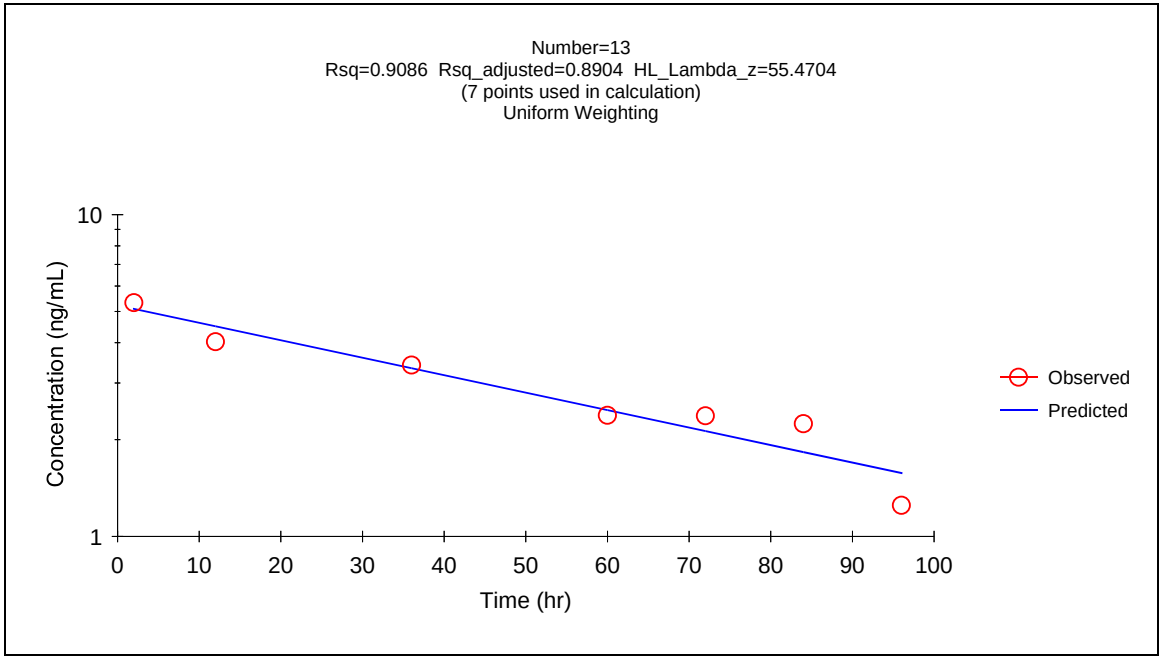

X vs. Observed Y and Predicted Y

Figure 5.20 Semi-logarithmic plot of concentration versus time profile for patient no. 14 (dose=8 mg/m^2)

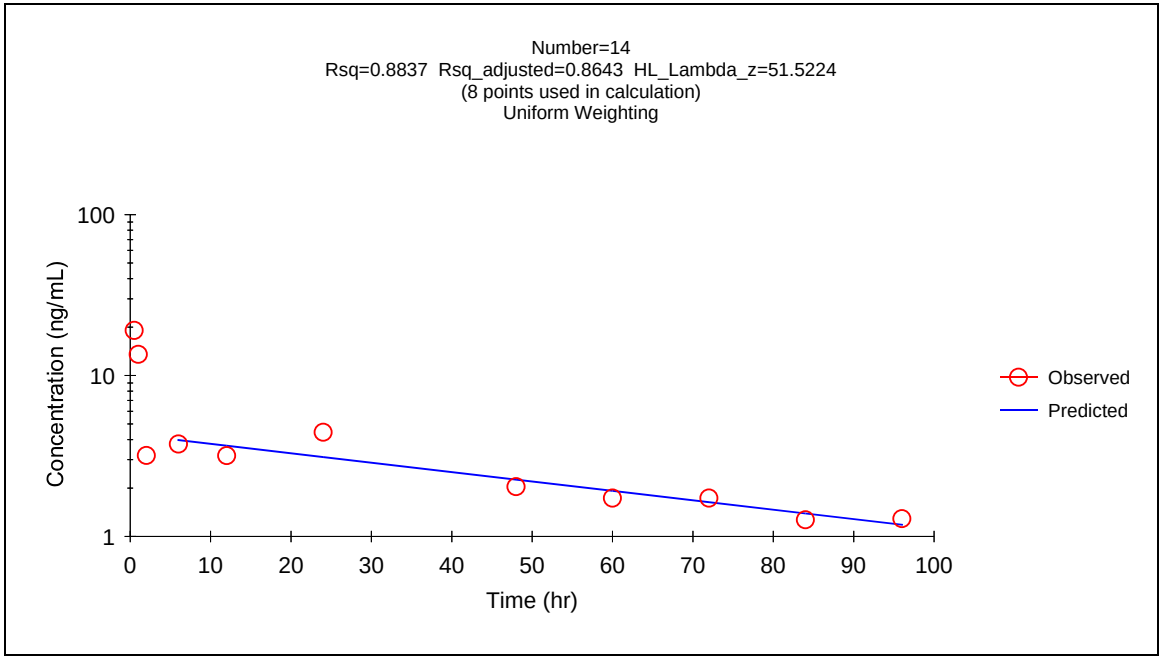

X vs. Observed Y and Predicted Y

Figure 5.21 Semi-logarithmic plot of concentration versus time profile for patient no. 15 (dose=8 mg/m^2)

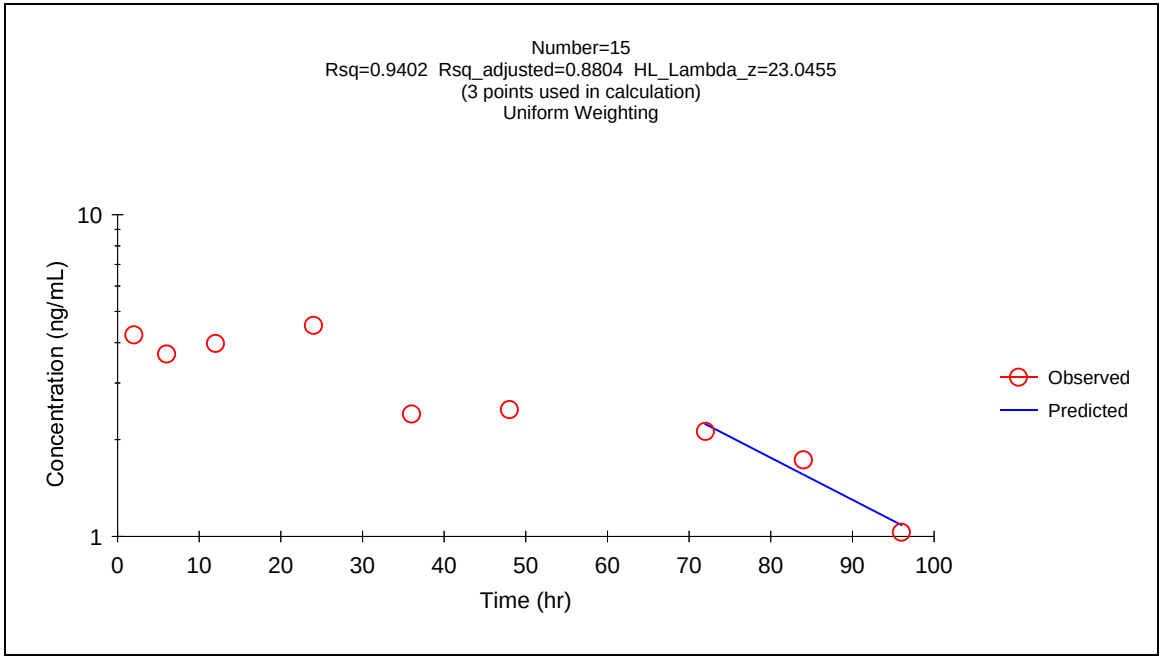

X vs. Observed Y and Predicted Y

Figure 5.22 Semi-logarithmic plot of concentration versus time profile for patient no. 16 (dose=8 mg/m^2)

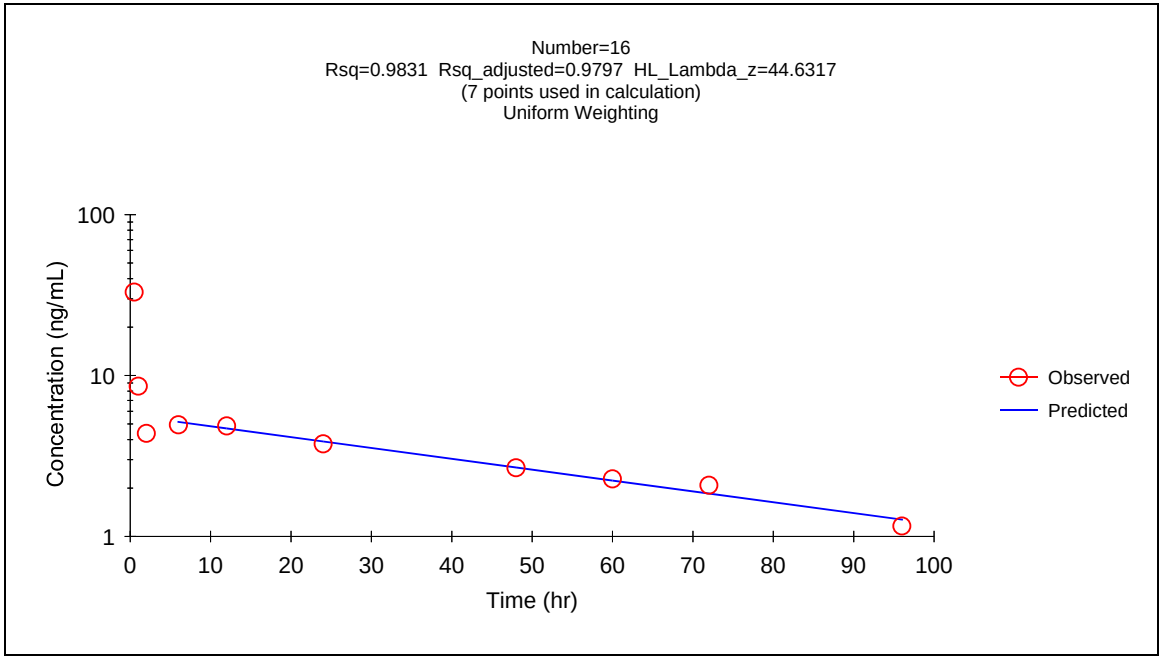

X vs. Observed Y and Predicted Y

Figure 5.23 Semi-logarithmic plot of concentration versus time profile for patient no. 17 (dose=8 mg/m^2)

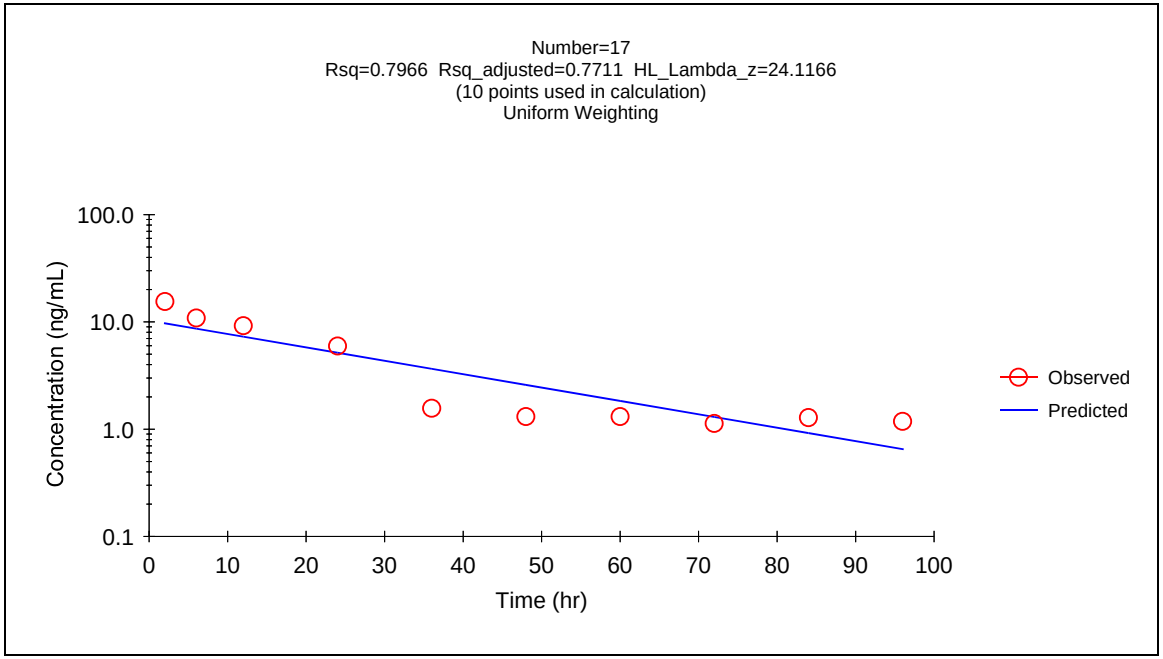

X vs. Observed Y and Predicted Y

Figure 5.24 Semi-logarithmic plot of concentration versus time profile for patient no. 18 (dose=10 mg/m^2)

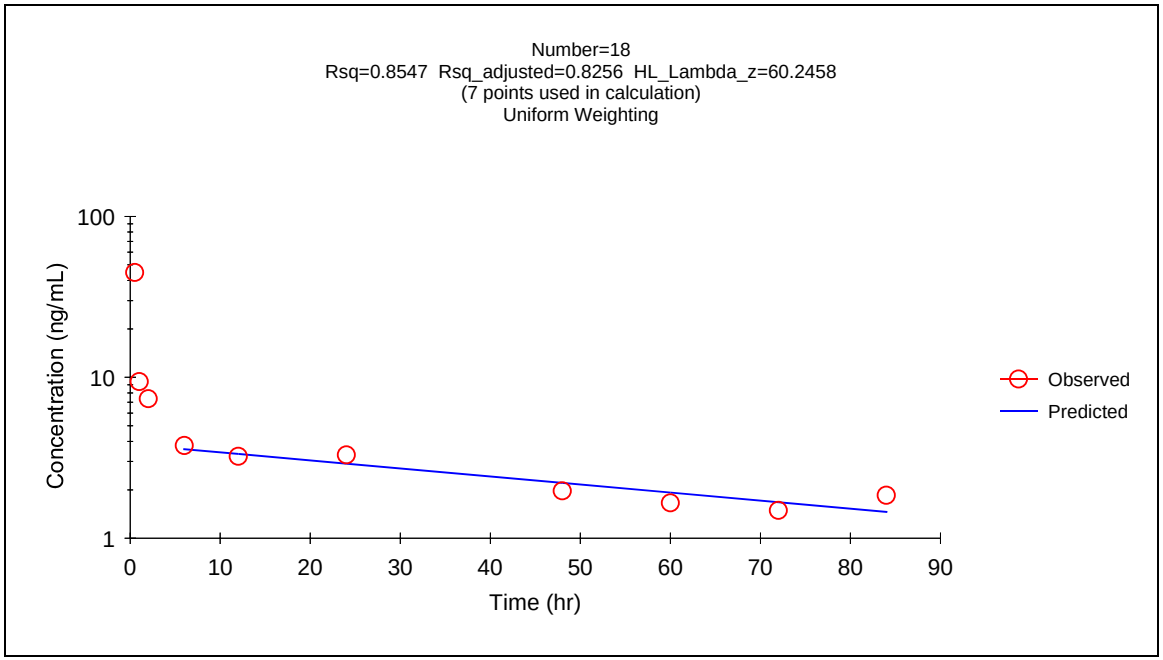

X vs. Observed Y and Predicted Y

Figure 5.25 Semi-logarithmic plot of concentration versus time profile for patient no. 19 (dose=10 mg/m^2)

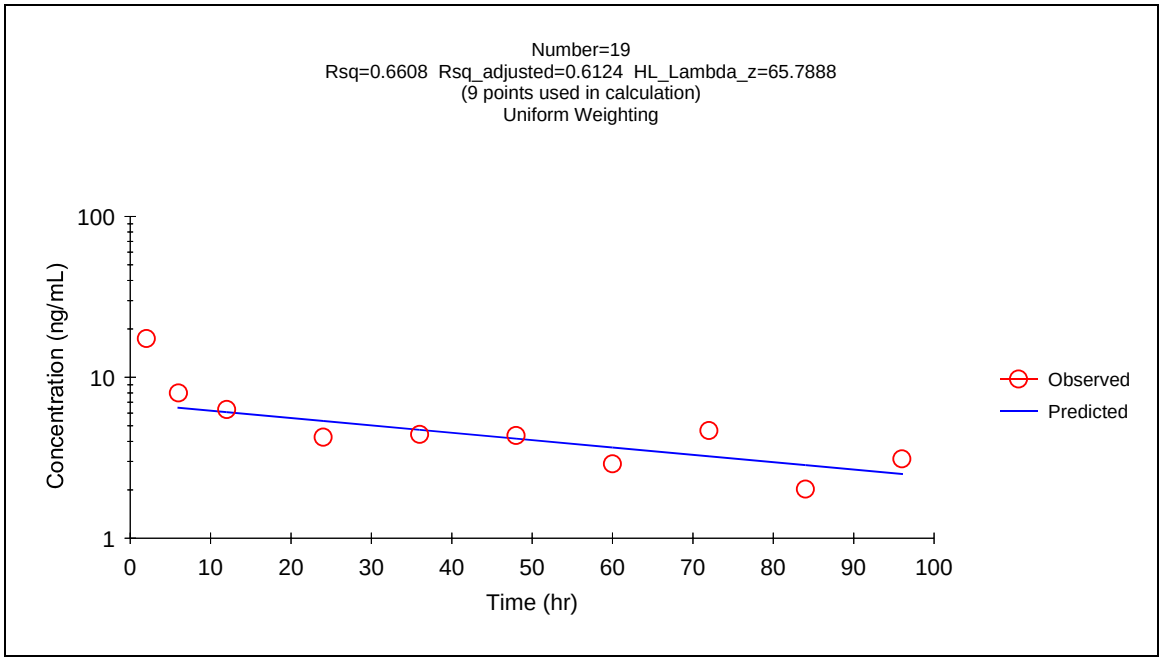

X vs. Observed Y and Predicted Y

Figure 5.26 Semi-logarithmic plot of concentration versus time profile for patient no. 20 (dose=10 mg/m^2)

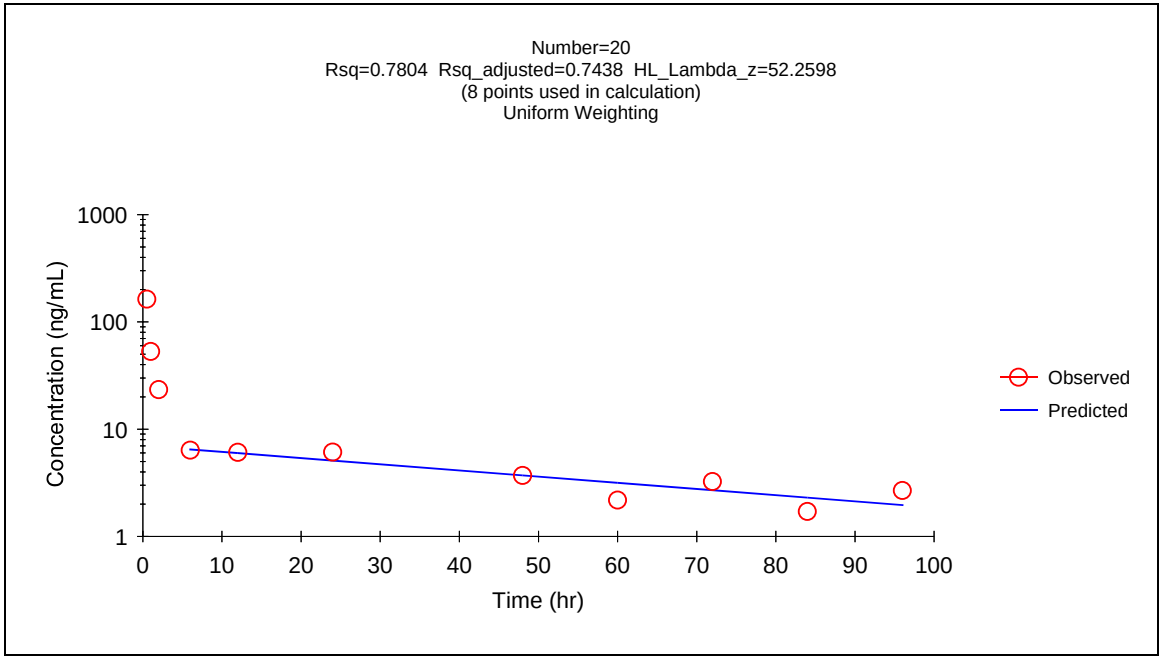

X vs. Observed Y and Predicted Y

Figure 5.27 Semi-logarithmic plot of concentration versus time profile for patient no. 21 (dose=10 mg/m^2)

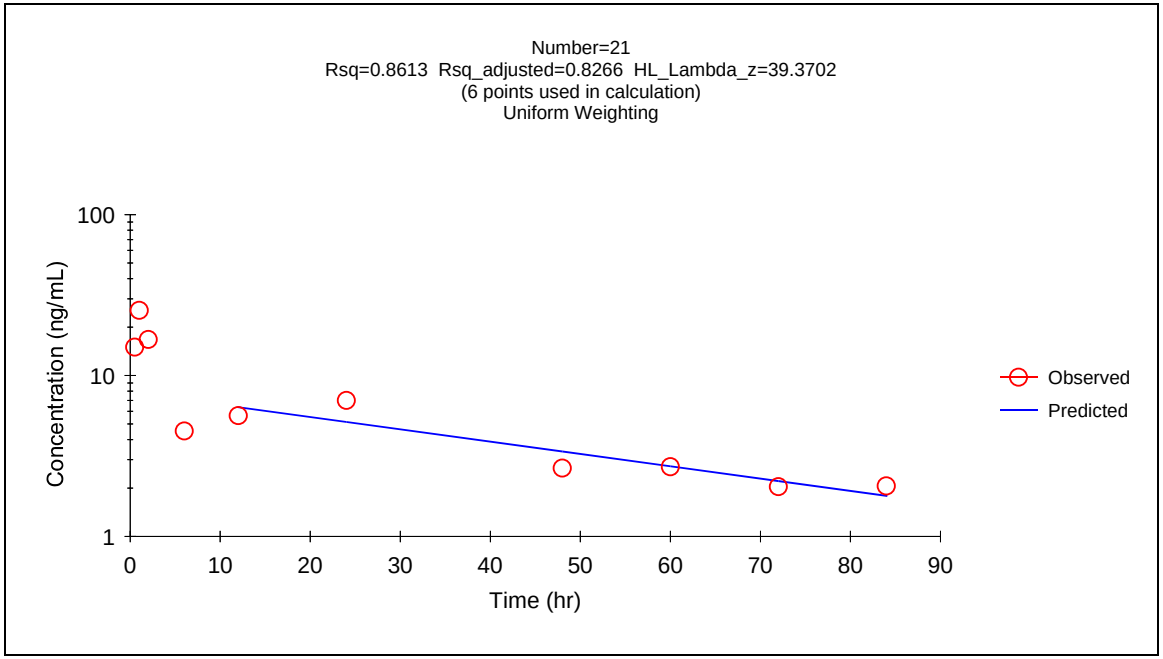

X vs. Observed Y and Predicted Y

Figure 5.28 Semi-logarithmic plot of concentration versus time profile for patient no. 22 (dose=10 mg/m^2)

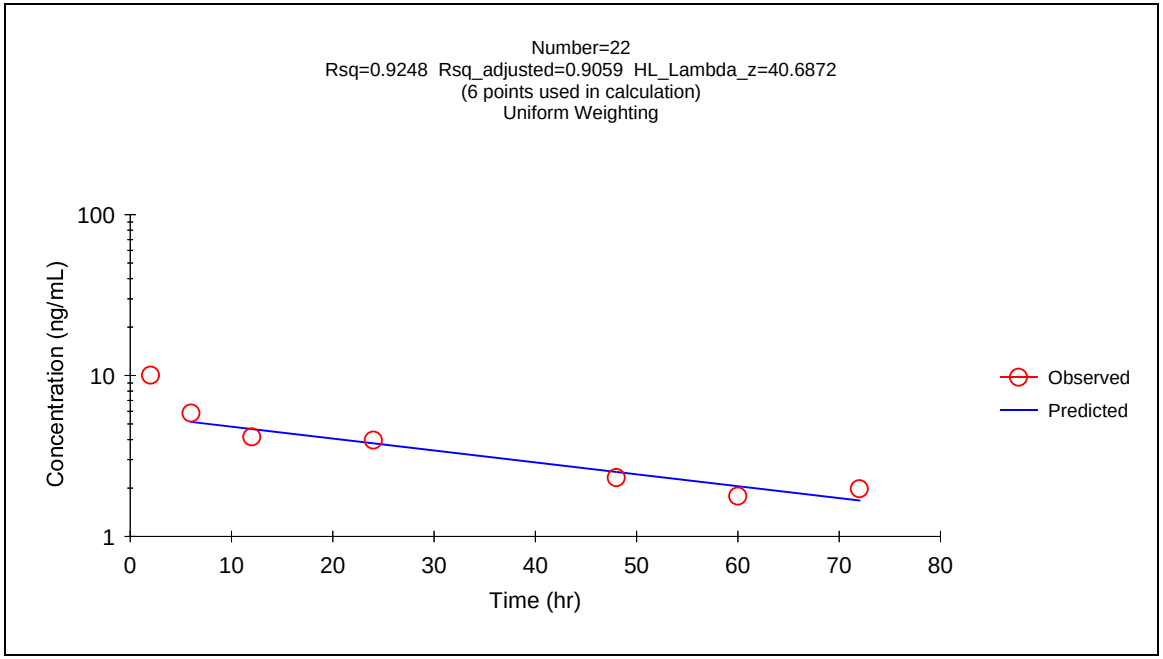

X vs. Observed Y and Predicted Y

Figure 5.29 Semi-logarithmic plot of concentration versus time profile for patient no. 23 (dose=10 mg/m^2)

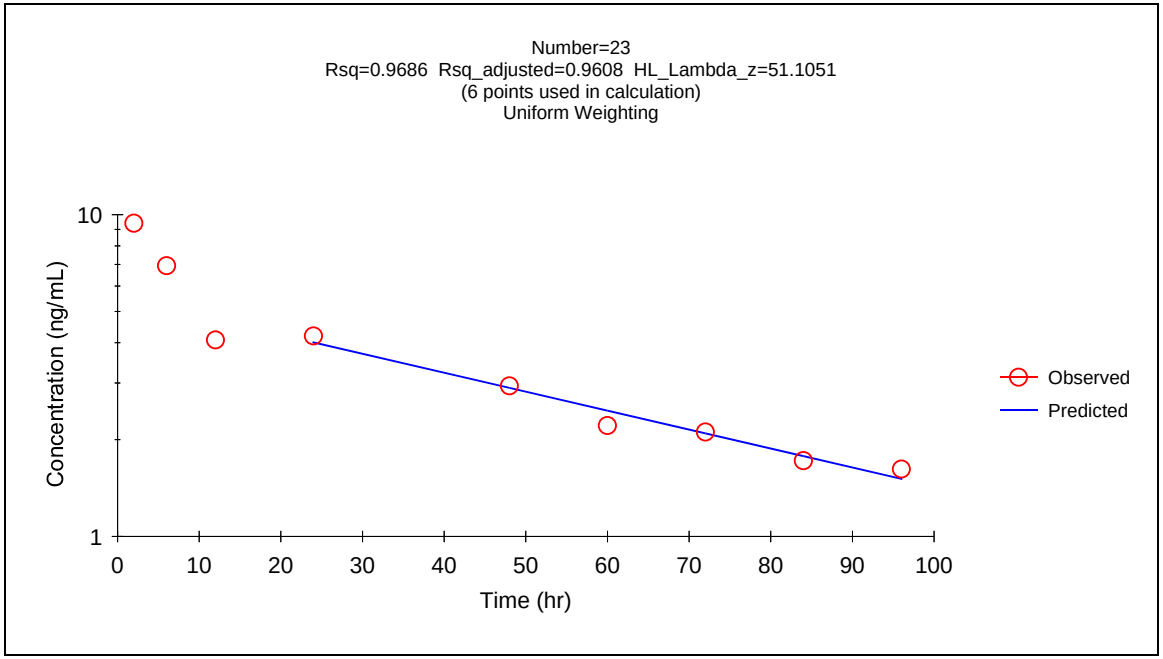

X vs. Observed Y and Predicted Y

Figure 5.30 Semi-logarithmic plot of concentration versus time profile for patient no. 24 (dose=12 mg/m^2)

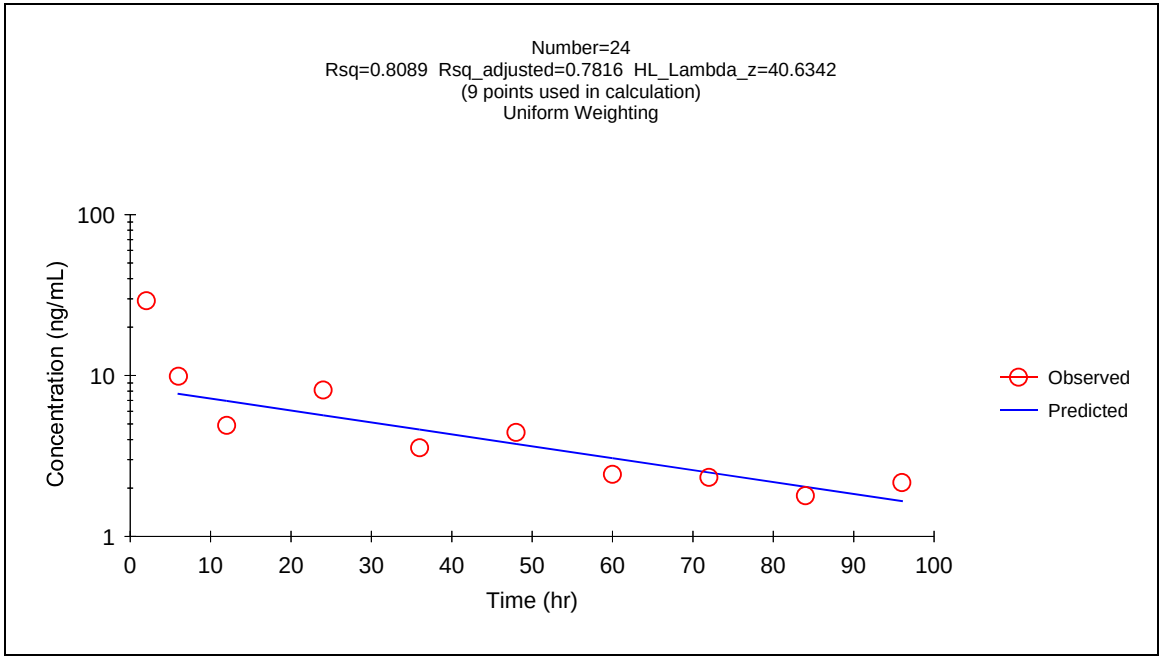

X vs. Observed Y and Predicted Y

Figure 5.31 Semi-logarithmic plot of concentration versus time profile for patient no. 25 (dose=12 mg/m^2)

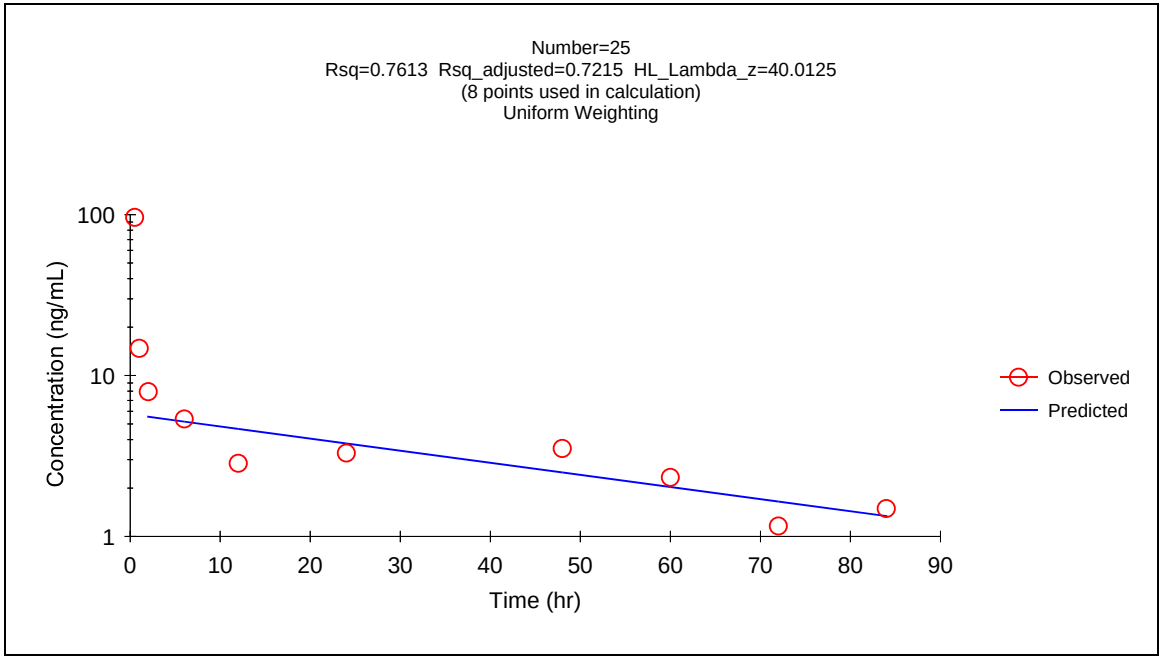

X vs. Observed Y and Predicted Y

Figure 5.32 Semi-logarithmic plot of concentration versus time profile for patient no. 26 (dose=12 mg/m^2)

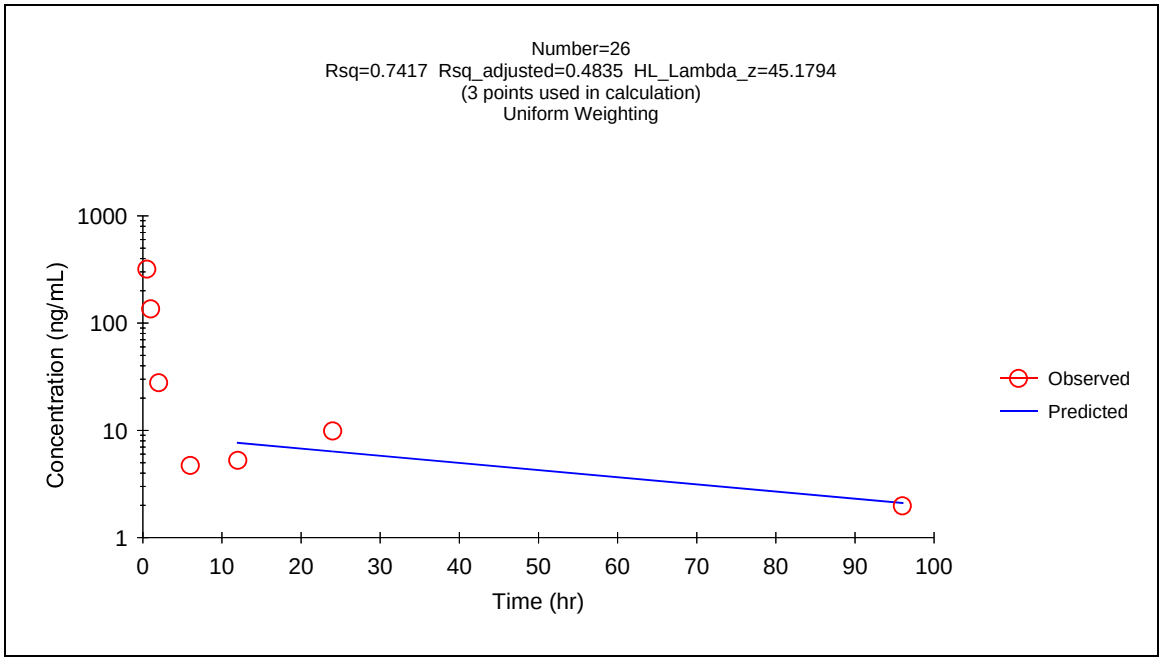

X vs. Observed Y and Predicted Y

Figure 5.33 Semi-logarithmic plot of concentration versus time profile for patient no. 27 (dose=12 mg/m^2)

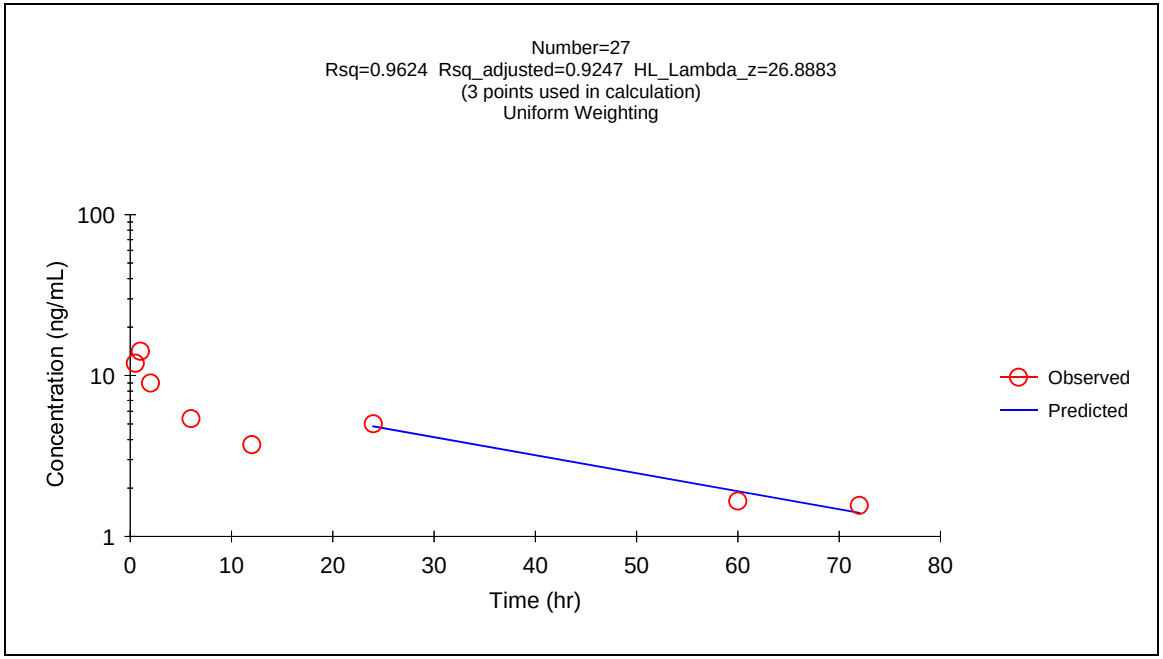

X vs. Observed Y and Predicted Y

Figure 5.34 Correlation between peak concentration (Cmax) and % change in histone H3 acetylation after 24 hours in patients taking MS-275 on biweekly schedule

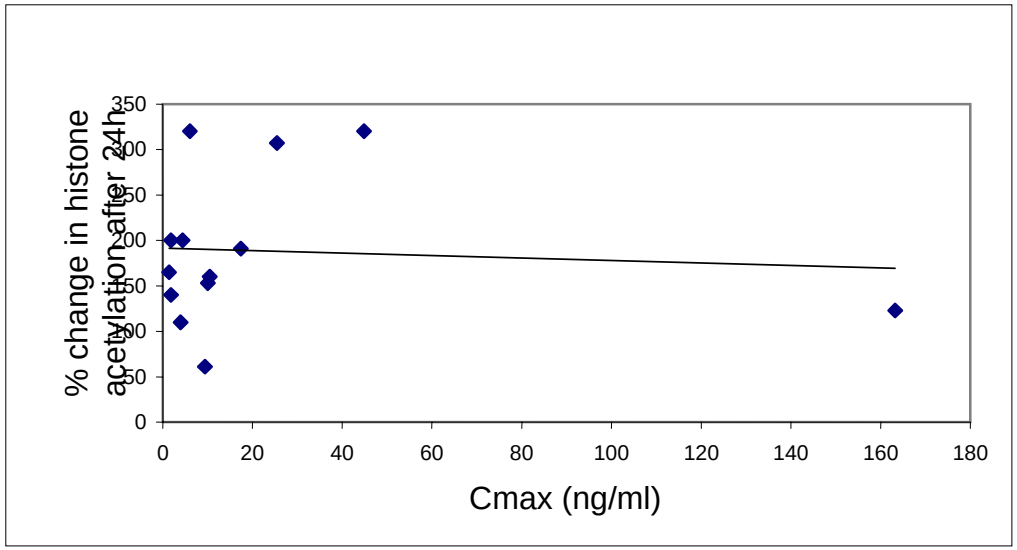

Figure 5.35 Correlation between dose administered (mg/m^2) and % change in histone H3 acetylation after 24 hours in patients taking MS-275 on biweekly schedule

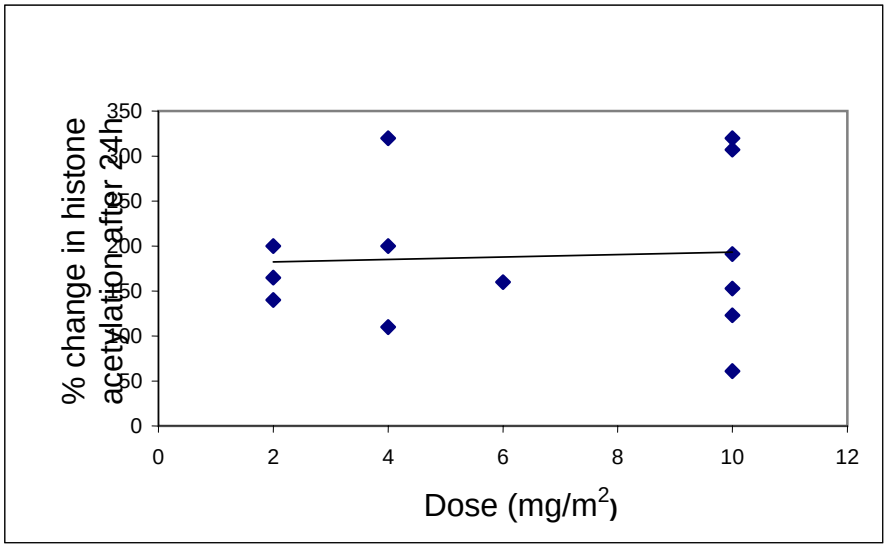

Figure 5.36 Correlation between dose administered (mg) and % change in histone H3 acetylation after 24 hours in patients taking MS-275 on biweekly schedule

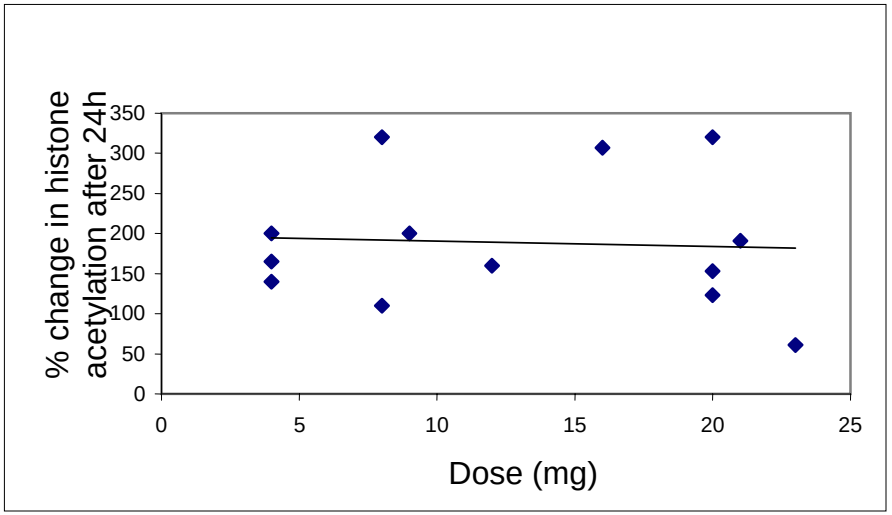

Figure 5.37 Correlation between exposure (AUC) and % change in histone H3 acetylation after 24 hours in patients taking MS-275 on biweekly schedule

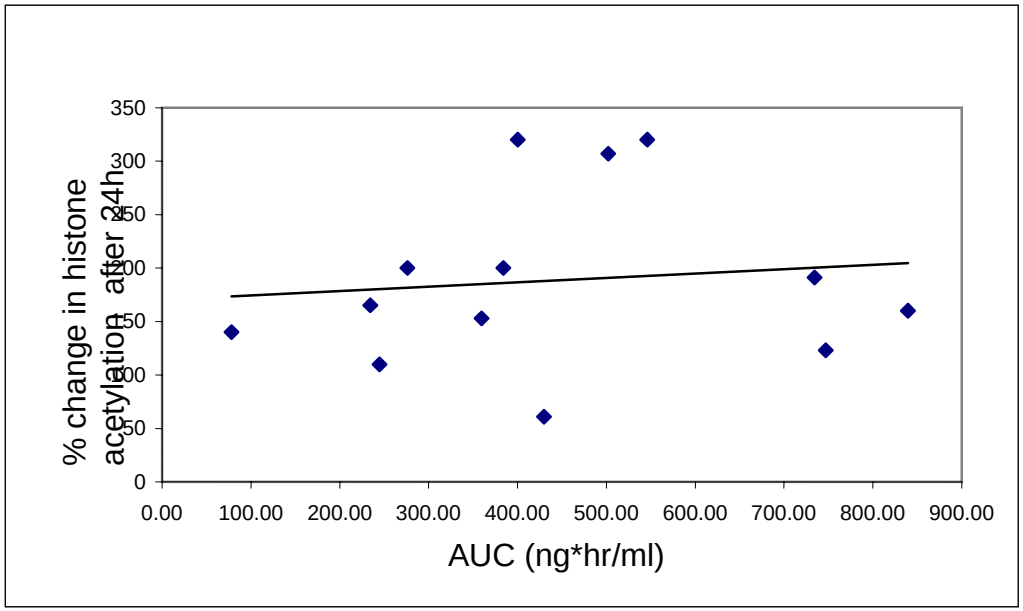

Figure 5.38 Correlation between apparent oral clearance and % change in histone H3 acetylation after 24 hours in patients taking MS-275 on biweekly schedule

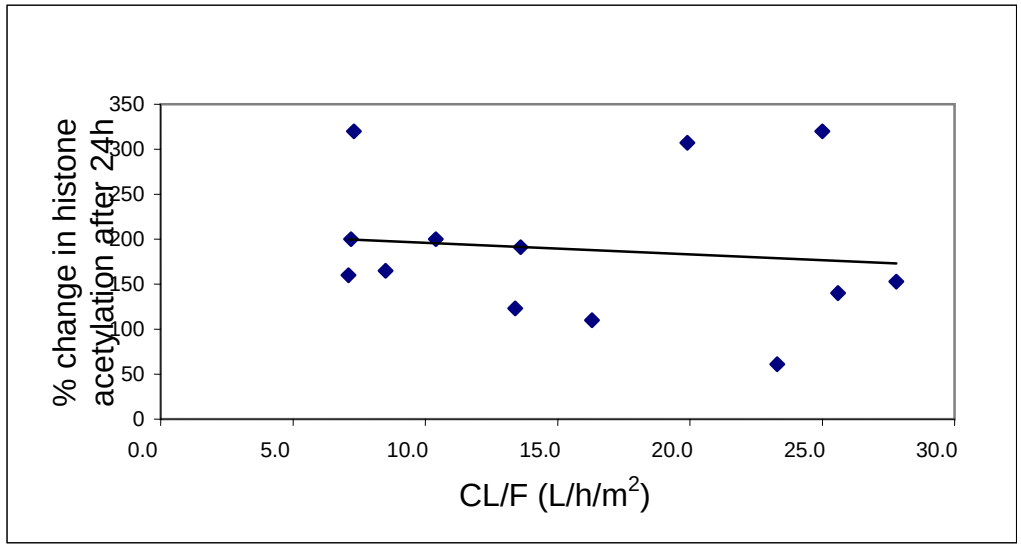

Vita

Milin R. Acharya was born in 1975 in Ahmedabad, India and is an Indian citizen with permanent residence in United States of America. He holds a Bachelor's degree in Biochemistry from St. Xavier's College, India completed in 1995. He received a Master's degree in Biochemistry from University of Scranton, Scranton, Pennsylvania in 1999. He received his Doctoral degree in Pharmaceutical Sciences from Virginia Commonwealth University, Richmond, Virginia in 2005.

The current list of his publications is as follows:

1) Acharya M.R., Figg W.D., Venitz J and Sparreboom A. *Chemically Modified Tetracyclines as Matrix Metalloproteinase Inhibitors in Anti-Cancer Drug Development* Book Chapter in **Research Advances in Cancer**, Part II, 2003, Vol 3: 247-260. Mohan R.M. (editor), Publishers: Global Research Network, Kerala, India

2) Acharya M.R. and Figg W.D. *Book Review: Handbook of Pharmaceutical Biotechnology* **Ann Pharmacother** 2004 Jan, Vol 38: 178

3) Sparreboom A, Cox M., Acharya M. and Figg W. *Herbal Remedies: Potential Adverse Interactions with Anticancer Agents* **J Clin Oncol** 2004 Jun 15; 22(12): 2489-2503.

4) Hwang K, Acharya M.R., Sausville E.A., Zhai S., Woo E.W., Figg W.D. and Sparreboom A. *Determination of MS-275, a novel histone deacetylase inhibitor, in human plasma by liquid chromatography-electrospray mass spectrometry* **J Chromatogr B Analyt Technol Biomed Life Sci** 2004 May 25; 804 (2):289-294.

5) Acharya M.R., Venitz J and Figg W.D. *What dose do you start with and how quickly do you increase that dose?* **American Pharmaceutical Outsourcing** 2004 Sep/Oct; Vol 5 (5): 26-31

6) Acharya M.R., Baker S.D., Verweij J., Figg W.D. and Sparreboom A. *Determination of fraction unbound docetaxel using semi-high throughput micro-equilibrium dialysis* **Anal Biochem** 2004 Aug 1; 331(1):192-194

7) Acharya M.R., Venitz J., Figg W.D. and Sparreboom A. *Chemically modified tetracyclines as inhibitors of matrix metalloproteinase* **Drug Resist Updat** 2004, Vol 7 (3): 195-208

8) Sparreboom A, Chen H., Acharya M.R., Senderowicz A.M., Messmann R.A., Kuwabara T., Venzon D.J., Murgo A., Headlee D., Sausville E.A. and Figg W.D. *Effects of α1-Acid Glycoprotein on the Clinical Pharmacokinetics of UCN-01* **Clin Cancer Res** 2004 Oct 15, 10(20): 6840-6846.

9) Acharya M.R. and Figg W.D. *Histone deacetylase inhibitor enhances the antileukemic activity of an established nucleoside analogue* **Cancer Biol Ther** 2004 Aug; 3(8): 719-720

10) Acharya M.R., Sparreboom A., Sausville E.A., Conley B.A., Doroshow J.H., Venitz J. and Figg W.D. *Interspecies differences in protein binding of MS-275, a novel histone deacetylase inhibitor* **Cancer Chemother Pharmacol (in press)**

11) Ryan Q., Headlee D., Acharya M., Sparreboom A., Trepel J., Ye J., Hwang K., Figg W., Chung E., Murgo A., Millelo G., Elsayed Y., Monga M., Kanitsky M., Zwiebel J. and Sausville E. *A Phase I trial of MS-275, a Histone Deacetylase Inhibitor in Oral Formulation, on a Daily or Q14 Day Schedule, in Patients with Advanced Solid Tumor or Lymphoma* **J Clin Oncol** 2005 Jun 10; 23(17): 3912-22

12) Lepper E.R., Nooter K., Verweij J., Acharya M.R., Figg W.D. and Sparreboom A. *Mechanisms of Resistance to Anticancer Drugs: the Role of Polymorphic ABC Transporters ABCB1 and ABCG2* **Pharmacogenomics** March 2005, Vol. 6, No. 2, 115-138

13) Acharya M.R., Sparreboom A., Sausville E.A., Venitz J. and Figg W.D. *Rational Development of Histone Deacetylase Inhibitors as Anticancer Agents: A Review* **Mol Pharmacol (in press)**

14) Acharya M., Karp J., Sausville E., Hwang K., Ryan Q., Gojo I., Venitz J., Figg W. and Sparreboom A. *Factors affecting the pharmacokinetic profile of MS-275, a histone deacetylase inhibitor, in patients with cancer* **(submitted)**

15) Smith N.F., Acharya M.R., Desai N., Figg W.D. and Sparreboom A. *Identification of OATP1B3 as a high-affinity hepatocellular transporter of paclitaxel* **Cancer Biol Ther (in press)**